

**UNIVERSITA' DEGLI STUDI DI MILANO**

Department of Medical Biotechnology and Translational Medicine

PhD Course in Experimental Medicine and Medical Biotechnologies (XXXIII cycle)



**HDAC8 and cohesin: "omics" analyses for the identification  
and functional validation of their targets using zebrafish  
(*Danio rerio*) and *in vitro* model systems**

(BIO/13-Applied Biology)

PhD thesis of  
Marco SPREAFICO  
R11854

Tutor: Prof. Anna PISTOCCHI

Supervisor: Prof. Elena BATTAGLIOLI

PhD coordinator: Prof. Massimo LOCATI

A.Y. 2019-2020

# SUMMARY

ABSTRACT .....	1
1. INTRODUCTION .....	3
1.1 HDAC8.....	3
1.1.1 An overview on histone deacetylases.....	3
1.1.2 HDAC8: structure and substrates .....	4
1.1.3 HDAC8 and cohesin.....	6
1.1.4 HDAC8 and disorders .....	7
1.2 HDAC inhibitors .....	11
1.2.1 HDACi: pros and cons .....	11
1.2.2 HDAC8 specific inhibition.....	12
1.3 The zebrafish model .....	14
1.3.1 Zebrafish use in research .....	14
1.3.2 Zebrafish as a model to study HDAC8.....	16
2. AIM .....	19
3. RESULTS: PUBLISHED PAPERS .....	20
3.1 Modeling Cornelia de Lange syndrome <i>in vitro</i> and <i>in vivo</i> reveals a role for cohesin complex in neuronal survival and differentiation .....	20
3.2 HDAC8 regulates canonical Wnt pathway to promote differentiation in skeletal muscle.....	31
3.3 HDAC8: a promising therapeutic target for acute myeloid leukemia .....	46
4. RESULTS: SUBMITTED PAPERS .....	69
4.1 Targeting HDAC8 to ameliorate skeletal muscle differentiation in Duchenne muscular dystrophy	69
4.2 The genome-wide impact of <i>nipblb</i> loss-of-function on zebrafish gene expression .....	93
5. DISCUSSION .....	112
6. CONCLUSIONS .....	120
REFERENCES.....	121

## ABSTRACT

The use of pan-HDACi for disease treatment has gained an interest in recent years, albeit exhibiting low specificity, variable efficacy and side effects. Each HDAC with its own activity could be considered as an independent pharmacological target to develop an effective therapy that circumvents the adverse effects of pan-HDACi treatment. HDAC8 belongs to class I HDAC and is known to modulate cohesin complex activity through deacetylation of SMC3. It possesses a unique structure among HDACs, which allowed the development of highly specific inhibitors, such as the PCI-34051. However, HDAC8 function and its involvement in pathological conditions is still largely unknown. To examine in depth HDAC8 physiological and pathological roles and assess whether it can represent a valuable pharmacological target, we analysed its function and the effect of its inhibition by using both *in vitro* (cell lines) and *in vivo* (zebrafish) models. In particular, we assessed HDAC8 function in three different tissues and related disorders: i) haematopoietic stem and progenitor cells (HSPC) and acute myeloid leukemia (AML); ii) neural stem cells (NSC) and Cornelia de Lange syndrome (CdLS); iii) skeletal muscle and Duchenne muscular dystrophy (DMD). We found that HDAC8 overexpression increased the proliferation of HSPCs in zebrafish and that its inhibition with PCI treatment restored normal phenotype, favouring cell cycle arrest, and induced apoptosis of AML cells. By contrast, HDAC8 knockdown lead to impairment of both central nervous system development and skeletal muscle differentiation. Furthermore, we found that HDAC8 overexpression is also associated with DMD phenotype and demonstrated that treatment with PCI inhibitor almost restored normal condition. Such positive effects were underlined by multiple mechanisms, which included cell cycle arrest, apoptosis induction and modulation of canonical Wnt pathway. Moreover, by acetylome profiling

we identified  $\alpha$ -tubulin as HDAC8 target thus revealing HDAC8 involvement in regulation of microtubule structure.

Additionally, to confirm the involvement of HDAC8 in the aforementioned pathologies, we investigated also the role of its partner NIPBL. By RNA-seq analysis we assessed the effect of NIPBL knockdown on gene expression revealing a number of differentially expressed genes linked to pathways altered in CdLS or AML.



# 1. INTRODUCTION

## 1.1 HDACs

### 1.1.1 An overview on histone deacetylases

Histone deacetylases (HDACs) are a highly conserved family of enzymes that are responsible for the removal of acetyl moieties from lysine residues. Since their discovery, 18 human HDAC isoforms were characterized and classified on the basis on their structure, function, sub-cellular localization and homology to yeast HDACs. According to these criteria, four classes were identified: class I, which comprises HDAC1,2,3 and 8; class II, which is further subdivided into class IIa, including HDAC4,5,7 and 9, and class IIb, composed by HDAC6 and HDAC10; class III, which is the class of the sirtuins family (SIRT1-7); class IV, with a unique member HDAC11. Classes I, II and IV HDACs are  $Zn^{2+}$ -dependent enzymes sharing a conserved catalytic domain. By contrast, class III sirtuins are  $NAD^+$ -dependent deacetylases and present a different catalytic domain compared to other HDACs (Parbin et al. 2014). Class I HDACs are mainly nuclear, whereas other classes members are able to shuttle from the nucleus to the cytoplasm and sirtuins were found to localize also in mitochondria (Banerjee et al. 2019).

HDACs were initially identified as negative regulators of gene expression: deacetylation of lysines on histone tails by HDACs increases the positive charge of tails, which in turn bind to the negative charged DNA, causing chromatin condensation and preventing transcription. Since HDACs lack DNA-binding capability, they require association with protein complexes to execute their gene expression modulation activity (Patra et al. 2019). In addition to this well-known function, studies revealed that HDACs are also involved in post-translational modification of non-histone proteins, regulating diverse cellular processes such as cell cycle progression, apoptosis and cytoskeleton dynamics. For example, class I HDACs were reported to deacetylate several transcription factors

(Banerjee et al. 2019), whereas HDAC6 was demonstrated to deacetylate tubulin (Hubbert et al. 2002).

### **1.1.2 HDAC8: structure and substrates**

Histone deacetylase 8 (HDAC8) is the last characterized class I HDAC. It is a ubiquitously expressed  $Zn^{2+}$ -dependent HDAC mapped on human chromosome X (Buggy et al. 2000; Hu et al. 2000; Van Den Wyngaert et al. 2000). HDAC8 is the smallest class I HDAC and studies revealed that it is characterized by unique features compared to other members of its class. Structurally, HDAC8 is a 42 kDa protein (377 amino acids) consisting of a N-terminal serine binding domain and a HDAC catalytic domain, which also contains the nuclear localization signal. Like other class I members, HDAC8 possesses a catalytic tyrosine Y306, which is preceded by a class I HDAC specific tetra-glycine motif (G302GGGY) (Porter et al. 2016). These glycine residues were proven to play a crucial role in deacetylation reaction, as single amino acid substitutions cause loss of Y306 catalytic activity (Porter et al. 2016). The active site of the enzyme is constituted by a tunnel that leads to a cavity in which the catalytic site resides. According to crystallography studies, the tunnel is formed by amino acids F152, F208, H180, G151, M274 and Y306, which are conserved among class I HDACs, except for methionine 274, which is a leucine in all other class I members instead (Somoza et al. 2004). As for the catalytic domain, it presents 7 loops (L1-L7) and the  $Zn^{2+}$  ion is located between L4 and L7 (Lombardi et al. 2011). Compared to other class I HDACs, HDAC8 lacks the C-terminal protein binding domain, which is required for the recruitment to complexes regulating HDACs function, thus suggesting either its activity might not require co-complexes or it might use different recruitment mechanisms (Somoza et al. 2004). Also, in proximity of the active site HDAC8 possesses a peculiar N-terminal L1 loop, in terms of size and composition as well as of flexibility. In fact, the L1 loop is highly flexible and capable of undergoing conformational changes to accommodate different substrates (Somoza et al. 2004). Additionally, HDAC8 differs from other class I HDACs due to its unique regulation by cAMP-

dependent protein kinase (PKA), which negatively modulates its deacetylase activity by phosphorylation of serine S39 (H. Lee, Rezai-Zadeh, and Seto 2004).

Despite belonging to class I, HDAC8 was shown to localize both in the nucleus and in the cytoplasm (Waltregny et al. 2005; J. Li et al. 2014). Whether histones can be considered HDAC8 targets is still debated. In fact, while *in vitro* deacetylase assays indicated HDAC8 activity over histones and histone tail-derived peptides (Buggy et al. 2000; Hu et al. 2000; Van Den Wyngaert et al. 2000; H. Lee, Rezai-Zadeh, and Seto 2004), successive acetylome studies failed in identifying acetylation changes of histones following HDAC8 modulation (Olson et al. 2014; Schölz et al. 2015). On the contrary, among nuclear substrates, several proteins involved in transcription regulation and mRNA processing were identified. The first evidence of deacetylation of transcription factors by HDAC8 was reported by Wilson and colleagues, who showed that HDAC8 positively modulates estrogen-related receptor  $\alpha$  (ERR $\alpha$ ) binding to DNA, both *in vitro* and *in vivo* (Wilson et al. 2010). More recently, an acetylome study identified other transcription factors and mRNA processing modulators as candidate HDAC8 targets, such as retinoic acid induced 1 (RAI1), AT-rich interactive domain-containing protein 1A (ARID1A), zinc finger Ran-binding domain-containing protein 2 (ZRANB2) and nuclear receptor co-activator 3 (NCOA3) (Olson et al. 2014). Interestingly, HDAC8 was shown to negatively modulate p53 function. Wu and colleagues demonstrated that HDAC8 not only suppresses p53 activity through deacetylation of Lys382, but also downregulates its expression, thus promoting cell cycle progression and inhibiting intrinsic apoptotic pathway (Wu et al. 2013). Importantly, p53 deacetylation by HDAC8 was demonstrated to play a pivotal role in favouring long-term hematopoietic stem cell (LT-HSC) survival under hematopoietic stress, as conditional *Hdac8<sup>gd/d</sup>* mice showed a progressive loss of HSC repopulating capability over time (Hua et al. 2017). Another well-known HDAC8 nuclear substrate is the cohesin complex protein structural maintenance of chromosome 3 (SMC3), which acetylation/deacetylation modulate cohesin recycling (see **paragraph 1.1.3**) (Deardorff, Bando, et al. 2012; Schölz et al. 2015).

As for cytoplasmic substrates, HDAC8 seems to be mainly involved in the deacetylation of targets associated with cytoskeleton dynamics. Li and colleagues demonstrated that HDAC8 is responsible for cortactin deacetylation in smooth muscle tissue in response to acetylcholine stimulation, thus strongly affecting smooth muscle contraction as deacetylated cortactin is able to induce actin polymerization (J. Li et al. 2014). Also, HDAC8 was shown to associate with smooth muscle  $\alpha$ -actin (Waltregny et al. 2005; Saito et al. 2019). Similarly, HDAC8 inhibition was reported to negatively affect TGF $\beta$ 1-induced contraction in human lung fibroblasts (Saito et al. 2019). Moreover, a recent paper highlighted a new role for HDAC8 as an  $\alpha$ -tubulin deacetylase in HeLa cells (Vanaja, Ramulu, and Kalle 2018).

In addition to its canonical deacetylase activity, a scaffolding function has been proposed for HDAC8. Evidence supporting this hypothesis came from Gao and colleagues, who showed that HDAC8 binds both cAMP response element-binding protein (CREB) and protein phosphatase 1 (PP1), thus favouring CREB dephosphorylation by PP1 and reducing CREB-mediated gene expression (J. Gao et al. 2009).

### **1.1.3 HDAC8 and cohesin**

Cohesin is a ring-shaped multiprotein complex which is highly conserved among species. It favours DNA encircling and mediate diverse functions, such as modulation of sister chromatid cohesion during cell cycle (Michaelis, Ciosk, and Nasmyth 1997; Watrin and Peters 2009; Jeppsson et al. 2014) and transcriptional regulation by both mediating chromatin architecture modification (Wendt et al. 2008; Kagey et al. 2010; Seitan et al. 2013; Lyu, Rowley, and Corces 2018; Bernardi 2018) and interacting with RNA polymerase II.

The core structure of the complex in human is composed by structural maintenance of chromosome 1 and 3 (SMC1 and SMC3), by the  $\alpha$ -kleisin subunit RAD21 (homologue of yeast Scc1) (Nasmyth 2011) and by either stromal antigen 1 or 2 (SA1 and SA2, also known as STAG1 and STAG2) (Canudas and Smith 2009). In addition, several other factors associate with cohesin to modulate

its function, such as the Nipped B-like (NIPBL) and MAU2 proteins, which are responsible for loading the complex onto DNA (Ciosk et al. 2000; Krantz et al. 2004).

Cohesin operates in a cyclic manner (**Figure 1**): it is loaded onto DNA, performs its function and then is removed from the chromosome to start a new cycle. For the proper occurrence of this cycle, the acetylation of SMC3 is crucial, as it makes the complex cohesive. In human acetylation of SMC3 occurs on K105/K106 and is performed by ESCO1 or ESCO2 acetyltransferase (Hou and Zou 2005; Vega et al. 2005), whereas HDAC8 deacetylates the subunit to mediate recycling of the complex (Deardorff, Bando, et al. 2012).

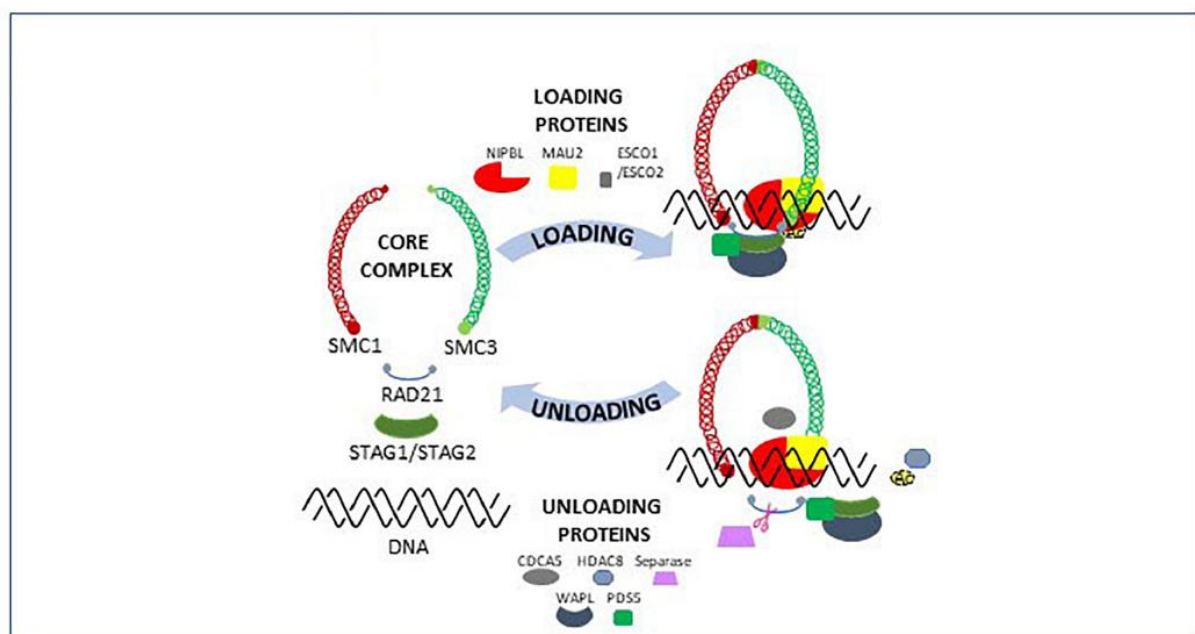


*Figure 1: Cohesin complex and accessory factors. Adapted from (Pezzotta et al. 2019)*

### 1.1.4 HDAC8 and disorders

In the last years some studies revealed increasing evidence of HDAC8 involvement in several diseases, ranging from cancer to viral infections (**Figure 2**). The first description of HDAC8 involvement in human disorders was in patients affected by Cornelia de Lange Syndrome (CdLS) (Deardorff, Bando, et al. 2012; Kaiser et al. 2014; Feng et al. 2014; X. Gao et al. 2018), a multiorgan disorder characterized by intellectual disability, facial dysmorphism, growth

retardation, limb defects and cardiac anomalies (Kline et al. 2018) and associated to mutation of cohesin members (Tonkin et al. 2004; Krantz et al. 2004; Musio et al. 2006; Deardorff et al. 2007; Deardorff, Wilde, et al. 2012). In these patients *HDAC8* mutations are mainly *de novo* missense mutations causing complete or partial loss of deacetylase activity and they were reported to associate with severely skewed X inactivation, thus suggesting a strong negative selection for the mutant allele (Deardorff, Bando, et al. 2012; Decroos et al. 2014; Kaiser et al. 2014). How *HDAC8* or other cohesin subunits mutations cause CdLS is still debated. Sister chromatid cohesion was unaffected in CdLS patients (Castronovo et al. 2009), but recent works highlighted dysregulation of multiple vital biological processes in mutant cohesin cell lines (Liu et al. 2009; Yuen et al. 2016; Mills et al. 2018), thus suggesting that the mechanism underlying the syndrome may be a genome-wide gene expression dysregulation. Indeed, *HDAC8* mutations cause dysregulation of gene expression in a lymphoblastoid cell line (LCL) derived from a CdLS patient and the genome alteration strongly correlated with those found in cell lines carrying mutation of *NIPBL* (Deardorff, Bando, et al. 2012).

Differently from CdLS, no *HDAC8* mutation has been associated to cancer so far. Conversely, *HDAC8* dysregulation or overexpression was reported. A study by Nakagawa and colleagues identified *HDAC8* overexpression in several cancers, including lung, gastric, pancreas and colon cancers (Nakagawa et al. 2007). In hepatocellular carcinoma *HDAC8* upregulation was associated to increased proliferation and inhibition of apoptosis (Wu et al. 2013), whereas in a model of non-alcoholic fatty liver disease-associated hepatocellular carcinoma (NAFLD-associated HCC) it was demonstrated to both sustain NAFLD by inducing insulin resistance and promote tumour growth by positively modulating the canonical WNT pathway (Tian et al. 2015). In breast cancer cells *HDAC8* was reported to promote invasion through induction of metalloproteinase 9 (Park et al. 2011) and its high expression was correlated with advanced stage neuroblastoma and poor outcome (Oehme et al. 2009). *HDAC8* was associated to haematological malignancies as well. In a study by Moreno and colleagues, an increase in *HDAC8* expression was found in a group of 94

childhood acute lymphoblastic leukemia (ALL) patients (Moreno et al. 2010). Its overexpression was reported also in adult T cell leukemia/lymphoma (TLL) (Higuchi et al. 2013) and in human myeloma cell lines (Mithraprabhu et al. 2014). Interestingly, in a particular subset of acute myeloid leukemia (AML) patients carrying an inversion on chromosome 16 (inv(16)), HDAC8 was demonstrated to interact with the resulting fusion protein, CBF $\beta$ -SMMHC, consisting of the RUNX1 binding interface of core-binding factor  $\beta$  (CBF $\beta$ ) and the coiled-coil rod region of smooth muscle myosin heavy chain (SMMHC) (Durst et al. 2003). More recently, Qi and colleagues showed that the inv(16) fusion protein leads to increased deacetylation of p53 by HDAC8, thus causing p53 inhibition and promoting survival and proliferation of inv(16)<sup>+</sup> AML CD34<sup>+</sup> cells. Interestingly, they identified an increased HDAC8 expression not only in inv(16)<sup>+</sup> AML CD34<sup>+</sup> cells, but also in non-inv(16)<sup>+</sup> CD34<sup>+</sup> cells deriving from AML patients (Qi et al. 2015), suggesting that a specific HDAC8 inhibition could be a promising therapeutic treatment for several types of AML. In addition to the negative modulation of p53 activity, HDAC8 was proposed to contribute to tumour progression through interaction with ever-shorter telomerase 1B (EST1B), which prevents ubiquitin-mediated EST1B degradation and increases telomerase activity in HeLa cells (Heehyoung Lee et al. 2006).

Besides CdLS and cancer, HDAC8 was also associated to infections. In fact, the HDAC8 ortholog of *Schistosoma mansoni* was demonstrated to be crucial for the survival of the parasite worm (Marek et al. 2013) and human HDAC8 was shown to promote penetration of Influenza A and Uukuniemi virus into cells (Yamauchi et al. 2011).

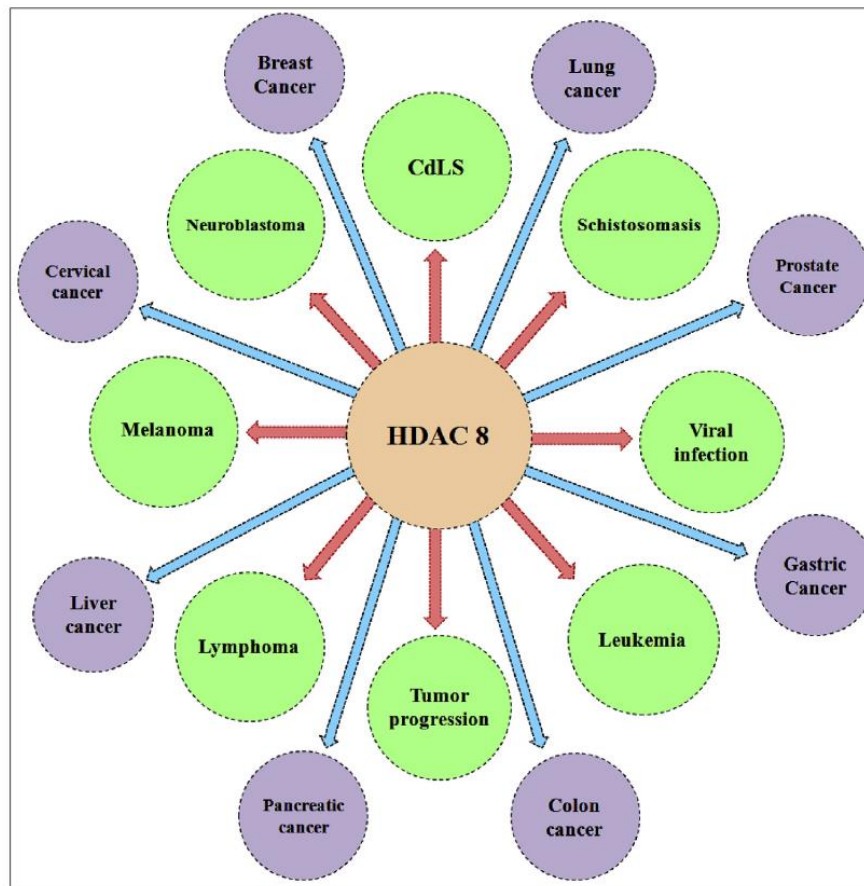


*Figure 2: HDAC8 is associated to several diseases. From (Banerjee et al. 2019)*



## 1.2 HDAC inhibitors

### 1.2.1 HDACi: pros and cons

HDAC inhibitors (HDACi) are drugs that block the activity of histone deacetylases, thus restoring or increasing acetylation levels of histones and other non-histone target proteins. HDACi mainly comprise four classes of molecules: short chain fatty acids, hydroxamic acids, benzamides and cyclic tetrapeptides (Fischer et al. 2010).

HDACi are now widely used as anti-cancer drugs because different tumours show a global decrease of acetylation levels due to HDACs overexpression (Parbin et al. 2014). Studies involving HDACi showed their potential in inhibiting tumours survival and progression in both solid and haematological malignancies (Ceccacci and Minucci 2016; Imai, Maru, and Tanaka 2016; Eckschlager et al. 2017). This anti-cancer activity is related to multiple mechanisms of action of HDACi, which include cell cycle arrest, modulation of pro- and anti-proliferative factors such as proliferating cell nuclear antigen (PCNA) and p21, apoptosis induction and inhibition of angiogenesis (Kuefer et al. 2004; X. N. Li et al. 2005; Shabbeer et al. 2007; Sun et al. 2009). In the wake of these promising results, several HDACi are currently under pre-clinical study or clinical trials as anti-cancer treatment and the Food and Drug Administration (FDA) already approved clinical use for four of them, namely vorinostat, romidepsin, belinostat and panobinostat. In particular, vorinostat (also known as suberoylanilide hydroxamic acid, SAHA) and romidepsin are currently used in the treatment of cutaneous T-cell lymphoma (CTCL), whereas belinostat and panobinostat were approved for the treatment of peripheral T-cell lymphoma and multiple myeloma, respectively (Eckschlager et al. 2017). In addition to their anti-cancer effects, HDACi have emerged as a potential therapeutic approach also for other pathologies, such as neurodegenerative and psychiatric disorders (reviewed by (Qiu et al. 2017)). Interestingly, HDACs inhibition has recently emerged as an attractive pharmacological approach for the treatment of Duchenne muscular dystrophy (DMD), a X-linked skeletal muscle disorder caused by mutations in the *DMD* gene encoding for dystrophin (Hoffman, Brown, and Kunkel 1987). In fact, several

works revealed a crucial role for HDACs in the epigenetic regulation of myogenesis (Sincennes, Brun, and Rudnicki 2016) and their inhibition was proven to favour myoblasts fusion and myogenic differentiation by promoting skeletal muscle differentiation and regeneration (Iezzi et al. 2002; 2004; Kobayashi et al. 2007; Saccone et al. 2014). In this regard, HDACi efficacy in *in vivo* DMD models has already been proven (Minetti et al. 2006; Colussi et al. 2008; Johnson, Farr, and Maves 2013) and HDACi Givinostat is currently in phase III clinical trial.

Despite displaying a promising potential, HDACi use is still limited by safety issues, which are likely due to the lack of specificity. In fact, due to structure conservation among HDACs, most of the HDACi are nonselective and act as pan-HDACi, thus conditioning a number of cellular processes as a result of inhibition of all HDAC proteins, causing a number of side effects, including nausea, anorexia, thrombocytopenia and metabolic dysfunctions (Subramanian et al. 2010). As a consequence, many HDACi failed to pass clinical trials. Thus, current efforts focus on better understand the role of single HDACs in pathologies and develop more selective inhibitors in order to improve therapy outcome.

### **1.2.2 HDAC8 specific inhibition**

The peculiar structure of HDAC8 (Somoza et al. 2004) allowed the development of highly specific inhibitors, even though none of them has been approved for clinical use yet (Banerjee et al. 2019). To date, more than 20 HDACi showed HDAC8 inhibition capability, including pan-HDACi and HDAC8 selective inhibitors. Several compounds that exhibit HDAC8 inhibition specificity were identified, such as hydroxamic acids (KrennHrubec et al. 2007), triazoles (Suzuki et al. 2014) and *meta*-sulfamoyl *N*-hydroxybenzamides (Zhao et al. 2018). Most potent HDAC8 selective inhibitors include tetrapeptide derivatives (Vaidya et al. 2012), aryl hydroxamate derivative PCI-34051 (Balasubramanian et al. 2008) and triazole analogue OJI-1 (Ingham et al. 2016). Interestingly, PCI-34051 (hereafter PCI) showed a >200-fold specificity for HDAC8 than other HDAC isoforms (Balasubramanian et al. 2008).

HDAC8 inhibition was extensively assessed as an anti-cancer approach and it was reported to mediate several anti-tumoral mechanisms. In *in vitro* and *in vivo* models of neuroblastoma, treatment with HDAC8 specific inhibitors induced apoptosis and retinoic acid-mediated differentiation together with growth arrest through upregulation of p21 (Rettig et al. 2015). Similar results were reported by Lopez and colleagues, who observed S-phase cell cycle arrest and apoptosis in human and mouse malignant peripheral nerve sheath tumour (MPNST) cell lines following treatment with HDAC8 inhibitors (Lopez et al. 2015). Consistently, PCI treatment determined cell cycle arrest and apoptosis in BEL-7404 and PLC5 liver cancer cells but not in LO2 and HepG2 cell lines, which expressed low HDAC8 levels (Tian et al. 2015). Also, in *inv(16)*<sup>+</sup> CD34<sup>+</sup> AML HSCs inhibition of HDAC8 restored p53 acetylation, causing p53-dependent apoptosis and abrogating AML survival and progression (Qi et al. 2015). Differently, in T-cell lymphoma cell lines PCI treatment induced caspase-mediated apoptosis by PLC $\gamma$ 1-dependent calcium mobilization (Balasubramanian et al. 2008). In colon cancer cells HDAC8 inhibition by methylselenocysteine (MSC) induced activation of Bcl2-modifying factor (BMF)-mediated apoptotic pathway (Kang et al. 2014). In breast cancer cell lines, PCI treatment inhibited proliferation and reduced migration (An et al. 2019). Interestingly, Dasgupta and colleagues suggested that alteration of cohesin transcriptional activity might not be one of anti-tumoral mechanisms underlying HDAC8 inhibitors efficacy, as one could expect due to HDAC8 regulation of SMC3 acetylation status (Dasgupta et al. 2016).

## **1.3 The zebrafish model**

### **1.3.1 Zebrafish use in research**

Zebrafish (*Danio rerio*) is a small (3-4 cm) freshwater teleost belonging to the *Cyprinidae* family and hailing from Asia (India, Pakistan, Bangladesh and Nepal). Zebrafish use as a research model is rapidly catching on as it confers a number of advantages in comparison to other animal models, such as mouse or rat. These advantages include: relative low cost of maintenance; easy manipulation; external fertilization, which avoids the sacrifice of mothers to study embryonic development; high numbers of fertilized eggs from a single mating, which guarantee samples numerousness; possibility of directly observe organ development due to optical transparency of embryos within the first 24 hours post fertilization (hpf), a window which can be further expanded by preventing pigmentation through addition of 1-phenyl 2-thiourea (PTU) to fish water (Karlsson, Von Hofsten, and Olsson 2001). Zebrafish is widely used as a tool to study gene functions in biological processes and their involvement in disease insurgence. It is a good tool to model human diseases by either inducing a transient dysregulation of specific gene expression or by generating mutant lines carrying disease-associated mutations.

To transiently modulate gene expression, in terms of gene knockdown or gene overexpression, the most applied method is to inject specific gene sequences in zebrafish embryos at 1-cell stage of development (Rosen, Sweeney, and Mably 2009). A specific gene knockdown can be obtained by injection of a specific modified antisense oligonucleotide sequence, called morpholino (MO), which can bind mRNA at the level of either ATG transcription start site, or a specific splicing site. In the first case, protein synthesis is completely blocked (Nasevicius and Ekker 2000); in the second case, exon skipping or intron retention leads to the synthesis of a defective protein (Draper, Morcos, and Kimmel 2001). Overexpression of a specific gene can be performed by injecting the relative full-length mRNA sequence. The main limitations of this technique are the transient activity of morpholino, which maximum effect is reached at 3 days post-fertilization (dpf) by

totally disappearing at 6 dpf (Nasevicius and Ekker 2000), and transient expression of mRNA which undergoes a rapid degradation.

To overcome these limits, it would be possible to generate zebrafish mutants, carrying specific gene mutations. Generation of mutant lines can be achieved by multiple systems such as N-ethyl-N-nitrosurea (ENU) (Mullins et al. 1994), a method consisting in adult zebrafish males exposure to ENU in order to mutagenize their sperm before mating with adult females, thus giving birth to a spawn carrying heterozygous mutations. This technique is highly efficient but it is limited by the randomness of induced mutations (Moens et al. 2008). In recent years generation of mutant zebrafish lines improved both in terms of efficiency and specificity due to introduction of genome engineering techniques which allow precise gene editing, such as zinc-finger nuclease (ZFN), TALEN and CRISPR/Cas9 technology (Porteus and Carroll 2005; Sander et al. 2011; M. Li et al. 2016).

Zebrafish genome editing is also widely used to generate transgenic reporter lines that express a fluorescent reporter gene, such as GFP or mCherry, in specific cells or tissues in different conditions. To generate a transgenic zebrafish line using gene editing technologies a knock-in should be performed to insert the coding sequence of a reporter gene in a specific gene locus, downstream the promoter sequence which can control the tissue specific expression of reporter gene in different conditions. For example, the *Tg(CD41:GFP)* line expresses GFP in haematopoietic stem and progenitors cells (HSPCs) (Lin et al. 2005; Ma et al. 2011), while in the *Tg(TOPdGFP)* line GFP expression is under control of canonical WNT pathway activity (Dorsky, Sheldahl, and Moon 2002).

In addition to genetic studies, zebrafish also represents a good model for drug testing, as it offers several advantages in drug screening compared to other *in vitro* and *in vivo* models (MacRae and Peterson 2015). In fact, the large number of embryos obtained by a single mating allows to test several molecules or different doses of a specific drug at once. Also, treatment with drugs is easy to perform, as embryos can adsorb small compounds directly from fish water. Additionally, the

transparency of embryos permits direct observation of organs development, thus giving an immediate read-out of specific and side effects of tested drugs.

### **1.3.2 Zebrafish as a model to study HDAC8**

Several molecular mechanisms and developmental processes are highly conserved between zebrafish and mammals. Therefore, the zebrafish is a valuable model to study HDAC8 functions in physiological processes and related disorders. These include haematopoiesis and AML, neurogenesis and CdLS, skeletal muscle development and DMD. Zebrafish is widely adopted as a model to study haematopoiesis and haematological disorders. In zebrafish two haematopoietic waves occur, primitive and definitive, which are temporarily separated by a transient intermediate wave (Bertrand et al. 2007; Paik and Zon 2010). Primitive haematopoiesis begins at the 2-somite (around 10.5 hpf) stage of embryo development and gives rise to erythroid and myeloid lineages cells (Detrich et al. 1995; Bennett et al. 2001; Lieschke et al. 2002). In definitive haematopoiesis, which begins at around 30 hpf, self-renewing haematopoietic cells (HSCs), which differentiate in all blood cell types and sustain haematopoiesis throughout adulthood (Bertrand et al. 2010), arise. Zebrafish represents a useful model to study haematopoiesis as oxygen exchange in zebrafish embryos can entirely rely on passive diffusion until 7 dpf, thus making possible to use it as a powerful tool to study haematopoiesis-related mutations that would be lethal in other models, such as mouse (Gore et al. 2018). Furthermore, despite haematopoiesis takes place in different sites compared to mammals, genes and molecular mechanisms regulating this process are highly conserved (Potts and Bowman 2017). This knowledge led to the generation of several transgenic lines for specific blood populations, which allow an easy and rapid read-out of perturbation of haematopoietic processes and represent a powerful tool to study haematopoietic disorders. In particular, zebrafish is extensively used to study AML, both by employing mutant lines carrying AML-specific mutation or chromosomal rearrangements, such as AML1-ETO (Yeh et al. 2008), or by taking advantage of transgenic lines to assess the effect of dysregulation of specific genes,

such as nucleophosmin (NMP1) (Barbieri et al. 2016; Mazzola et al. 2019), on haematopoietic progenitor self-renewal and differentiation capability. In this regard, the *Tg(CD41:GFP)* line (Lin et al. 2005; Ma et al. 2011) is a useful tool to study HDAC8 activity in HSPCs and its implication with AML.

Analogously to haematopoiesis, also myogenesis occurs in two waves in zebrafish. The primary myogenic wave takes place after somites formation and gives rise to a functional myotome by 24 hpf; the secondary myogenesis occurs between 48 and 72 hpf and is characterized by differentiation of secondary muscle fibers (Rossi and Messina 2014). Despite some differences, such as the stage of skeletal muscle commitment and existence of a myogenic presomitic cell population (known as adaxial cells) in zebrafish (Stickney, Barresi, and Devoto 2000), molecular basis underlying skeletal muscle development are well conserved between zebrafish and mammals. These includes, for example, Myf5 and MyoD transcription factors (Rescan 2001). Importantly, studies demonstrated that zebrafish is a useful system to model DMD. In fact, by either generation of mutant lines (Bassett et al. 2003; Jeffrey R. Guyon et al. 2009), or by morpholino injection (J. R. Guyon et al. 2003), it is possible to obtain a severe DMD phenotype which better recapitulates human DMD phenotype than *Mdx* mouse (Maves 2014). Therefore, zebrafish represents a suitable model to study HDAC8 role in skeletal muscle development and its possible involvement in DMD.

Zebrafish is a widely adopted tool to study neurogenesis, as its neurons show a degree of proliferation potentially higher than mammals during adulthood (Schmidt, Strähle, and Scholpp 2013). Zebrafish embryonic neurogenesis begins as soon as gastrulation occurs and is regulated by factors and signaling pathways which are highly conserved in higher vertebrates. Some examples are Fgf and Wnt signaling (Schmidt, Strähle, and Scholpp 2013). Noticeably, the canonical Wnt signaling, in addition to neurogenesis (Zwamborn et al. 2018), is involved in skeletal muscle development (Rudnicki and Williams 2015), HSC self-renewal (Richter, Traver, and Willert 2017) and AML (Gruszka, Valli, and Alcalay 2019) and was demonstrated to be

modulated by HDAC8 (Tian et al. 2015). Indeed, zebrafish is widely adopted to study the canonical Wnt signaling (Dorsky, Sheldahl, and Moon 2002; Pistocchi et al. 2013; Barbieri et al. 2016; Mazzola et al. 2019). Thus, it represents a suitable model to investigate HDAC8 role in the aforementioned processes.



## 2. AIM

Pan-HDACi are rapidly gaining interest for the treatment of diverse diseases, such as cancer. However, the use of pan-HDACi is still hampered by low specificity and safety issues, as several side effects are associated with them. More effective therapies which circumvent the adverse effects of pan-HDACi treatment might be developed by pharmacologically targeting single HDACs with their own activity. Since HDAC8 possesses a unique structure among HDACs it is possible to develop highly specific inhibitors, such as the PCI-34051. A more extensive knowledge of HDAC8 physiological function and involvement in diseases would make it possible to employ such specific inhibitors in order to improve the outcome of therapy for disorders involving HDAC8 dysregulation. On this basis, the aim of this thesis is to study more in depth HDAC8 physiological and pathological functions and to evaluate its inhibition by the highly selective inhibitor PCI-34051 by using both cell lines and the zebrafish (*Danio rerio*) model. Since HDAC8 is strictly associated to the cohesin complex, another objective of this thesis is to indirectly validate and expand our findings on HDAC8 function by assessing the role of another modulator of the cohesin complex: NIPBL.

### **3. RESULTS: PUBLISHED PAPERS**

#### **3.1 Modeling Cornelia de Lange syndrome *in vitro* and *in vivo* reveals a role for cohesin complex in neuronal survival and differentiation**

Cornelia de Lange syndrome (CdLS) is a multiorgan disorder which is associated to mutation in gene encoding for cohesin complex proteins, including *HDAC8* loss-of-function mutations. A typical feature of CdLS is a severe intellectual disability, likely due to defects of central nervous system development. To assess the effect of *HDAC8* deficiency in nervous system, in this work we downregulated the expression of *HDAC8* in neural stem cells (NSCs) and evaluated their proliferation and differentiation capability. In parallel, we assessed the impact of *HDAC8* deficiency on nervous system development also *in vivo* performing *hdac8* knockdown in the zebrafish model.

## GENERAL ARTICLE

## Modeling Cornelia de Lange syndrome *in vitro* and *in vivo* reveals a role for cohesin complex in neuronal survival and differentiation

Daniele Bottai<sup>1,‡</sup>, Marco Spreafico<sup>2,‡</sup>, Anna Pistocchi<sup>2</sup>, Grazia Fazio<sup>3</sup>, Raffaella Adami<sup>1</sup>, Paolo Grazioli<sup>1</sup>, Adriana Canu<sup>2</sup>, Cinzia Bragato<sup>4,5</sup>, Silvia Rigamonti<sup>1,3</sup>, Chiara Parodi<sup>1</sup>, Gianni Cazzaniga<sup>3</sup>, Andrea Biondi<sup>6</sup>, Franco Cotelli<sup>7</sup>, Angelo Selicorni<sup>8</sup> and Valentina Massa<sup>1,\*,†</sup>

<sup>1</sup>Dipartimento di Scienze della Salute, Università degli Studi di Milano, Milan 20142, Italy, <sup>2</sup>Dipartimento di Biotecnologie Mediche e Medicina Traslazionale, Università degli Studi di Milano, Milan 20090, Italy, <sup>3</sup>Centro Ricerca Tettamanti, Clinica Pediatrica, Università degli Studi di Milano-Bicocca, Fondazione MBBM/Ospedale S. Gerardo, Monza 20900, Italy, <sup>4</sup>Fondazione IRCCS Istituto Neurologico C. Besta, Milano 20131, Italy, <sup>5</sup>PhD program in Neuroscience, University of Milano-Bicocca, Monza, Italy, <sup>6</sup>Clinica Pediatrica, Università degli Studi di Milano-Bicocca, Fondazione MBBM/Ospedale S. Gerardo, Monza 20900, Italy, <sup>7</sup>Dipartimento di Bioscienze, Università degli Studi di Milano, Milan 20131, Italy and <sup>8</sup>UOC Pediatria, ASST Lariana, Como 22042, Italy

\*To whom correspondence should be addressed at: Dipartimento di Scienze della Salute, Università degli Studi di Milano, via A. Di Rudini, 8, Milano 20142, Italy. Tel/Fax: +39 0250323207; Email: Valentina.Massa@unimi.it

### Abstract

Cornelia de Lange syndrome (CdLS), which is reported to affect ~1 in 10 000 to 30 000 newborns, is a multisystem organ developmental disorder with relatively mild to severe effects. Among others, intellectual disability represents an important feature of this condition. CdLS can result from mutations in at least five genes: nipped-B-like protein, structural maintenance of chromosomes 1A, structural maintenance of chromosomes 3, RAD21 cohesin complex component and histone deacetylase 8 (HDAC8). It is believed that mutations in these genes cause CdLS by impairing the function of the cohesin complex (to which all the aforementioned genes contribute to the structure or function), disrupting gene regulation during critical stages of early development. Since intellectual disorder might result from alterations in neural development, in this work, we studied the role of *Hdac8* gene in mouse neural stem cells (NSCs) and in vertebrate (*Danio rerio*) brain development by knockdown and chemical inhibition experiments. Underlying features of *Hdac8* deficiency is an increased cell death in the developing neural tissues, either in mouse NSCs or in zebrafish embryos.

<sup>†</sup>Valentina Massa, <http://orcid.org/0000-0003-2246-9515>

<sup>‡</sup>These authors should be regarded as joint first authors.

Received: July 31, 2018. Revised: September 11, 2018. Accepted: September 12, 2018

© The Author(s) 2018. Published by Oxford University Press. All rights reserved.  
For Permissions, please email: [journals.permissions@oup.com](mailto:journals.permissions@oup.com)

## Introduction

During embryonic development and, in mouse, up to 4 weeks after birth, the brain is shaped by immature neurons generated in excessive number that die before maturation is completed. This process is fundamental for achieving optimal brain connectivity, and a number of brain disorders have been associated with altered neuronal cell death (1,2). It has also been shown that disturbing this finely tuned developmental process exerts detrimental effects on cell composition and global brain activity impacting on cognition (3). Signals involved in this balance are numerous and vary both during developmental stages and within involved brain areas. Some signals are considered 'core', thereby inhibiting cell death allowing for proliferation and differentiation, others are 'neuron-type specific' reflecting differences in receptors expressed on the cell membrane (4,5). Neurogenesis during embryonic development, hence, envisages excessive differentiated neurons that will be removed if not fully integrated, starting from a pool of progenitor cells named neural stem cells (NSCs). In lower mammals such as mice primitive NSCs are present from embryonic day 5.5 (E5.5). At E7.5, neural induction begins and the forming neural tube gives rise to the brain and the spinal cord. The cell population composing the neural tube consists of a relatively homogenous population of neuroepithelial cells that proliferate and expand through symmetric division. In the developing embryo, radial glial cells comprise NSCs that divide symmetrically to increase pool size and originate progenitors that migrate away from the periventricular germinal zone (6). In adults, the subventricular zone (SVZ), which extends along the length of the lateral wall of the lateral ventricles, and the dentate gyrus of the hippocampus represent the two most important reservoirs of NSCs (7). NSCs' self-renewal, expansion, division and differentiation are controlled by a number of factors, both extrinsic (such as morphogens) and intrinsic (such as epigenetic modifications). Among these, hierarchically prominent role has been shown for chromatin remodeling, including accessibility and histone modifications (8). Interestingly, Cornelia de Lange syndrome (CdLS) is a genetic disorder caused by mutations in genes codifying for proteins regulating both chromatin features (CdLS1 MIM Mendelian Inheritance in Man 122470, CdLS2 MIM 300590, CdLS3 MIM 610759, CdLS4 MIM614701, CdLS5 MIM 300882). Indeed, 80% of CdLS patients present mutations in one of five genes: NIPBL Nipped-B-like protein, structural maintenance of chromo-

somes 1A (SMC1A), structural maintenance of chromosomes 3 (SMC3), RAD21 cohesin complex component (RAD21) and histone deacetylase 8 (HDAC8) (9). The first four genes are part of the cohesin complex, a multimeric structure controlling chromosomal cohesion in all eukaryotic cells (10). The fifth gene, HDAC8, encodes for a class I histone deacetylase, hence considered an 'eraser' in the epigenetic machinery components (11) with a known target (SMC3) in the cohesin complex (12). The present study sought to ascertain HDAC8 role in mammalian NSCs' capabilities and during vertebrate embryonic brain development, with a particular emphasis on cell death as previous studies have shown the fundamental role of cohesin complex to maintain viable cells during embryonic development in neural tissues and given the importance of HDAC8 in regulating a master regulator of cell death (i.e. p53) (13–18).

## Results

### HDAC8 inhibition reduces murine NSCs' proliferation rate, inducing apoptosis and differentiating capabilities

During the proliferative phase, cells continuously treated with a specific inhibitor of HDAC8 activity N-hydroxy-1-[[4-methoxyphenyl]methyl]-1H-indole-6-carboxamide showed a lower proliferative capability. The proliferation of PCI34051-treated NSCs was significantly lower compared to controls, as shown in Figure 1A, in which the average of three experiments for each culture is shown. The slopes of the growth curves are significantly different ( $P < 0.044$ ) and the overall number of cells treated with PCI34051 decreased during culture whereas the number of the cells treated with dimethyl sulfoxide (DMSO) (CTR) Control exponentially increased during the experiment. Analysis of cell death revealed a significant increase in apoptosis following treatment with the inhibitor (Fig. 1B).

Treatment with HDAC8 inhibitor caused a change in differentiation capabilities significantly reducing the levels of expression of  $\beta$ -tubulin III  $P < 0.01$  (Fig. 2) of ~50% at both time points (Fig. 2B and C).

### Hdac8 silencing reduces murine NSCs' proliferation rate and differentiating capabilities

The knockdown of *Hdac8* transcript in NSCs using specific small interfering ribonucleic acids (siRNAs) induced a significant reduction of the proliferative capability. siRNAs effects were synergist, although of less impact compared to inhibitor

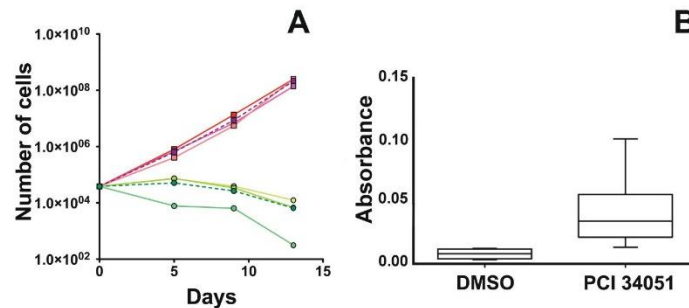


**Figure 1.** Growth curve and apoptosis of the PCI34051 treated cells. Reddish colors represent the controls, greenish colors represent PCI34051 treated cells. (A) In red #A DMSO, in purple #B DMSO, in pink #C DMSO, in light green #A PCI34051, in green #B PCI34051, in bright green #C PCI34051; in purple with dashed line represents the mean of the three samples treated with DMSO, in green with dashed line represents the mean of the samples treated with PCI34051. (B) Apoptosis levels induced by PCI34051 treatment expressed as absorbance (Y axis) per samples (x axis).

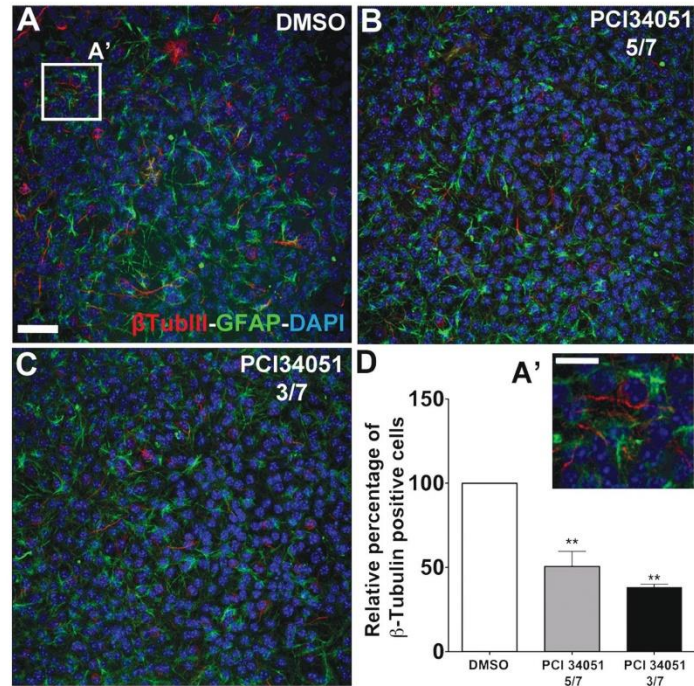


**Figure 2.** Immunofluorescence analysis of NSCs differentiation. (A) DMSO-treated sample (controls). (B) PCI34051-treated sample for 3 days. (C) PCI34051-treated sample for 5 days. (A') Magnification of white box in A showing  $\beta$ -tubulin III and GFAP positive cells. (D) White column CTR (DMSO-treated), gray column PCI34051-treated cell between days 5 and 7 of the differentiation, black column PCI34051-treated cell between days 3 and 7 of the differentiation. \*\* =  $P < 0.0017$ . Scale bar indicates in A = 25  $\mu$ m, in A' = 10  $\mu$ m, Blue DAPI, green GFAP, red  $\beta$ -tubulin III.

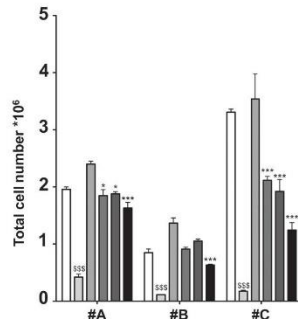


**Figure 3.** Proliferative changes induced in NSCs by the knockdown of *Hdac8* NSCs. The knockdown of *Hdac8* transcript causes a significant reduction of NSCs proliferation in all three analyzed cultures. The analysis was performed comparing also PCI34051 effects. Bars represent from left to right, for each dataset, CTR, PCI34051, CTR siRNA, HDAC8.1, HDAC8.2 and HDAC8.1 + HDAC8.2.

treatment (Fig. 3). The knockdown of *Hdac8* transcript in NSCs induced a significant reduction of proliferation in all analyzed samples, with a stronger effect upon using a combination of HDAC8.1 and HDAC8.2 siRNA (10 nM each). Nevertheless, even

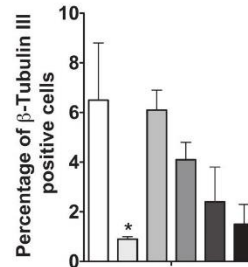


**Figure 4.** Changes in differentiation induced in NSCs by the knockdown of *Hdac8* NSCs. The knockdown of *Hdac8* transcript causes an alteration of NSCs' differentiation. The analysis was performed comparing also PCI34051 effects. Bars represent from left to right CTR (3/7), PCI34051 (3/7), CTR siRNA (3/7), HDAC8.1 + HDAC8.2 (3/7), CTR siRNA (5/7) and HDAC8.1 + HDAC8.2 (5/7).

the single treatments were able to induce a significant ( $P < 0.05$ ; sample A) or highly significant ( $P < 0.001$ ; sample C) reduction of NSCs' proliferation. The knockdown of *Hdac8* transcript in differentiating NSCs reduces, ~30%, in a not significant fashion the expression of  $\beta$ -tubulin III (Fig. 4), supporting the outcome observed following chemical inhibition.



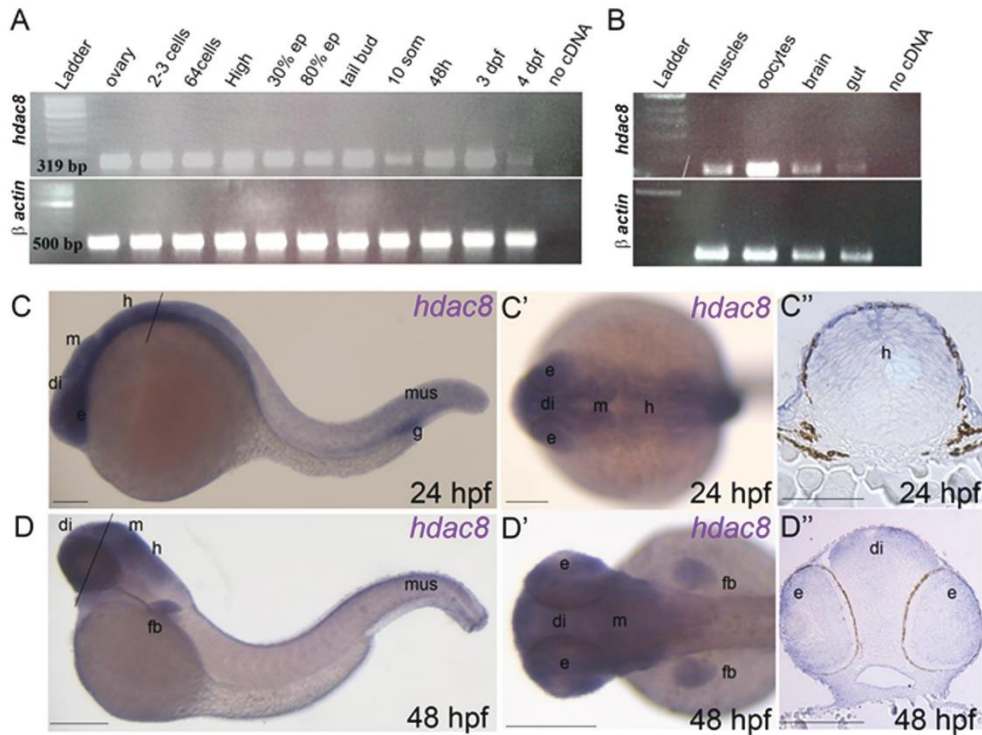


**Figure 5.** Expression analysis of *hdac8* in zebrafish. (A and B) RT-PCR performed on different embryonic stages: *hdac8* and  $\beta$ -actin expression are shown. (C–D) *hdac8* WISH analyses on zebrafish embryos at 24 and 48 hpf developmental stages. (C) 24 hpf embryo showing *hdac8* expression in different regions of the CNS (eyes, diencephalon, mesencephalon, hindbrain), in muscles and in the gut. (C') Dorsal view (anterior to the left) of the different regions of *hdac8* expression in the CNS. (C'') Transverse histological sections (section level is indicated in C with black line) of a previously hybridized embryo at 24 hpf. *hdac8* was expressed in the hindbrain. (D–D') *hdac8* WISH at 48 hpf. The transcript persisted in the eyes, diencephalon, mesencephalon, hindbrain and muscles. *hdac8* expression was present also in the fin buds at 48 hpf. (D'') Transverse sections of the head at 48 hpf (section level is indicated in D with black line). ep, epiboly; e, eye; di, diencephalon; m, midbrain; h, hindbrain; fb, fin bud; mus, muscles; g, gut. Scale bars indicate 100  $\mu$ m.

#### Zebrafish *hdac8* identification and expression analyses

The human HDAC8 amino acid sequence was used as a query for identifying *in silico* the zebrafish *hdac8* gene. NCBI (<http://www.ncbi.nlm.nih.gov/BLAST/>), ClustalW (<http://www.ebi.ac.uk/Tools/clustalw/>) and SMART (<http://smart.embl-heidelberg.de/>) tools were used for basic handling and analyses of the nucleotide and protein sequences. Zebrafish *hdac8* is present in a single copy on chromosome 7 (nucleotide position: 51 710 354–51 749 895).

Characterization of zebrafish *hdac8* expression, using reverse transcription-Polymerase Chain Reaction assays (RT-PCR) techniques, revealed that the transcript was present from the first stages of development up to 4 days post-fertilization (dpf), thus including maternal and zygotic transcription (Fig. 5A). Moreover, zebrafish *hdac8* was found to be expressed through development and in adult organs such as muscles, oocytes, brain and gut (Fig. 5B).

Whole-mount *in situ* hybridization (WISH) expression analyses in embryos at 24 h post-fertilization (hpf) with a specific probe for zebrafish *hdac8* showed the presence of the transcript

in the central nervous system (CNS), specifically in the dorsal part and eyes (Fig. 5C–C'). Moreover, in line with the expression in adult organs, *hdac8* was expressed in muscles and gut (Fig. 5C). At 48 hpf, *hdac8* was expressed in the CNS, eyes, muscles and fin buds (Fig. 5D–D').

#### *hdac8* loss-of-function results in increased cell death in the CNS

Loss-of-function studies were carried out by injecting a morpholino (*hdac8*-MO; Gene Tools LLC, Philomath, OR, USA), a modified antisense oligonucleotide which binds specifically to *hdac8* messenger RNA (mRNA) blocking the production of protein. Embryos were initially injected with different concentrations of ATG- or splice-*hdac8*-MO (0.5, 1 and 1.5 pmol per embryo) in order to assess the dose-dependent effect. One picomole per embryo was identified as the dose capable of generating the greatest number of embryos with typical phenotypic defects without causing global or drastic alterations in the body plane development. Embryos injected with 1 pmole per embryo of ATG- or splice-*hdac8*-MOs were developmentally abnormal with defects in the cephalic structures

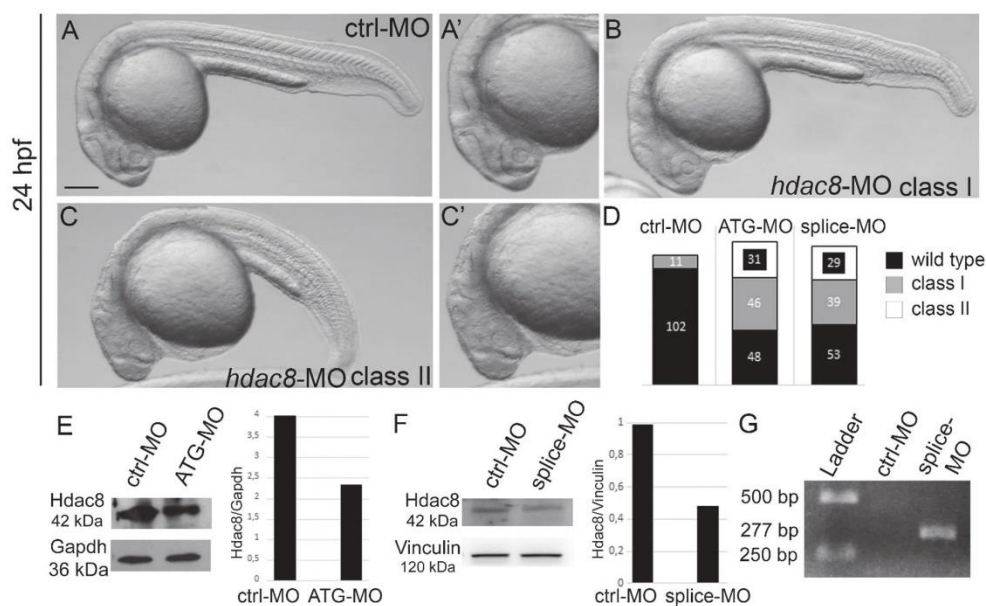


**Figure 6.** Phenotypical analysis of embryos with *hdac8* loss of function. (A–D) Phenotypical analysis of embryos at 24 hpf microinjected with *hdac8*-MO. (B and C) compared to control embryos (A). (A', C') higher magnification of the cephalic region of the embryo in A and C. (D) Quantification of embryos microinjected with *hdac8*-MO presenting phenotypes with different degree of severity classified as: class I mild phenotype and class II severe phenotype. (E and F) Western blot analyses showed reduced levels of Hdac8 (42 kDa) in the 24 hpf ATG-*hdac8*-MO injected embryos compared to controls at the same developmental stage (E) and in splice-*hdac8*-MO injected embryos compared to controls at the same developmental stage (F). Gapdh (36 kDa) housekeeping in (E) and Vinculin (120 kDa) in (F). (G) RT-PCR performed on control and splice-*hdac8*-MO injected embryos at 24 hpf. RT-PCR primers were designed in exon1 and intron1. The amplification product was 277 bp and comprehended the intron1 in splice-*hdac8*-MO injected embryos, while in ctrl-MO there was no amplification as the intron1 was removed. Scale bars indicate 100  $\mu$ m.

(eye size, structure of the CNS) and in the formation of the tail (curved tail). Similar morphological phenotypes were obtained with the injection of the two different morpholinos directed against *hdac8*. These defects were used as benchmark to classify *hdac8*-MO into two phenotypic classes (class I mild phenotype and class II severe phenotype) (Fig. 6A–C'). The distribution of the phenotypic classes was comparable between the ATG- and splice-*hdac8*-MOs, strongly suggesting that the morphological defects were caused by *hdac8* loss of function (Fig. 6D). To further validate the *hdac8*-MO efficiency, we analyzed Hdac8 protein levels in 24 hpf embryos injected with ATG- or splice-*hdac8*-MOs. Quantification analyses indicated that, at this concentration, the efficiency of Hdac8 reduction was ~50% (Fig. 6E–F). Since splice-*hdac8*-MO was designed against the *hdac8* exon1–intron1 junction, the retention of intron1 in morphant embryos was verified by PCR technique (Fig. 6G).

#### CNS malformations are caused by augmented apoptosis rescued by WNT pathway activation

The abnormal development of cephalic CNS was associated with the presence of apoptotic/necrotic tissues. Hence, TUNEL assays were conducted in *hdac8*-loss-of-function embryos at 24 hpf for evaluating rate of programmed cell death. Analysis showed increased apoptosis at the level of the midbrain, hind-brain optic vesicles and spinal cord in embryos injected with

*hdac8*-MO compared to the control embryos (Fig. 7A–B). As we have previously shown in zebrafish models of cohesinopathies (13,14) that augmented apoptosis was caused by altered canonical WNT pathway, *hdac8*-loss-of-function embryos were treated with lithium chloride (LiCl) for activating the WNT pathway. Following treatment with LiCl, TUNEL assay showed significantly reduced levels of apoptosis compared to control embryos (83.3%;  $N = 42$ ; Fig. 7C). Moreover, injecting an *in vitro* synthesized zebrafish *hdac8*-mRNA a rescue of the apoptotic phenotype caused by the splice-*hdac8*-MO was observed, confirming the role for *hdac8* in preventing apoptosis (Fig. 7D). For these experiments, the splice-*hdac8*-MO was utilized for avoiding the possible direct impact of the ATG-*hdac8*-MO against the injected *hdac8*-mRNA.

The efficacy and specificity of the *hdac8* loss of function were extensively tested with the two *hdac8* morpholinos as shown in Fig. 8. Increased apoptosis was obtained with the injection of the ATG or splice-*hdac8*-MO (Fig. 8B–C) in comparison to controls (A); the levels of apoptotic cells were increased in class II embryos with more severe phenotype than class I (Fig. 8B'–C'). Moreover, to address a synergistic effect of the two morpholinos, we injected subcritical doses of ATG-*hdac8*-MO (0,5 pmol/embryo) or splice-*hdac8*-MO (0,5 pmol/embryo) that singularly did not cause any effects on cell death. When co-injected with subcritical doses of each MO, the typical apoptotic phenotype previously observed by means of full doses injections was found (Fig. 8D).

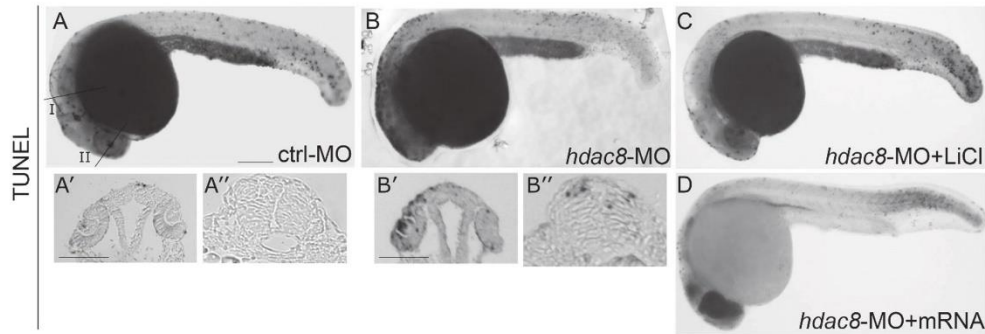


**Figure 7.** Apoptosis is increased in *hdac8*-MO-injected embryos and rescued by LiCl treatment or *hdac8*-mRNA injection. (A-C) Analysis of the apoptotic cells by visual TUNEL staining in embryos at 24 hpf microinjected with *hdac8*-MO (B) compared to control embryos (A). Dying cells were present in particular at the level of the CNS (arrows in brain and spinal cord) and in optic vesicles as shown by transverse histological sections carried out at the level of the black line (I and II) in A and B (A<sup>I</sup>, A<sup>II</sup>, B<sup>I</sup>, B<sup>II</sup>). (C) Reduced apoptosis in *hdac8*-MO injected embryos upon LiCl treatment. (D) Reduced apoptosis was also observed in embryos co-injected with splice-*hdac8*-MO and *hdac8*/mRNA. Scale bar indicates 100  $\mu$ m.

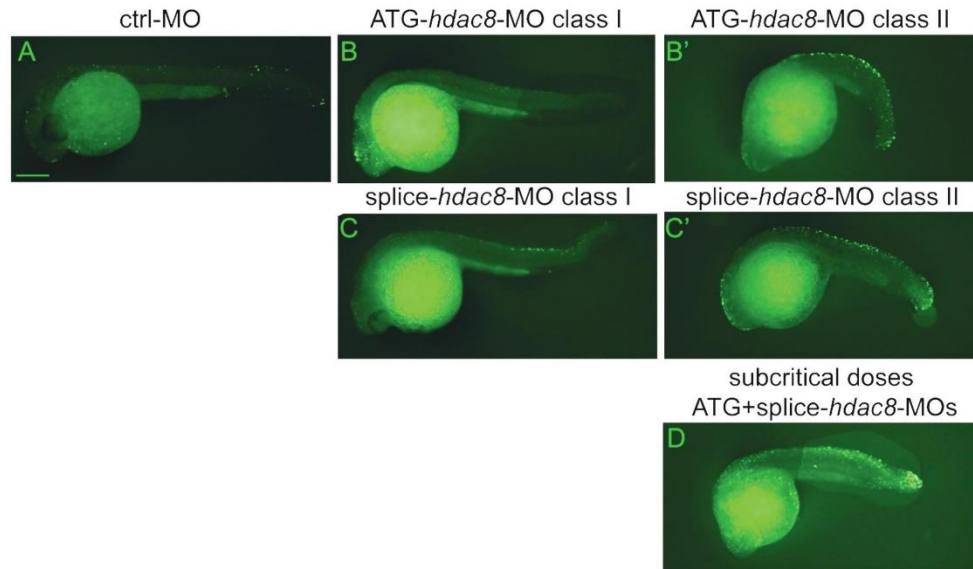


**Figure 8.** Specificity of the apoptotic phenotype observed following *hdac8* haploinsufficiency. The increased apoptosis was specifically due to the *hdac8* haploinsufficiency as it was obtained by injecting of the two different ATG and splice-*hdac8*-MO. (A-C) Specificity of the apoptotic phenotype following *hdac8* loss of function. The increased apoptotic levels were present in both ATG- and splice-*hdac8*-MO-injected embryos (B and C) in comparison to controls (A). Fluorescent TUNEL staining in embryos injected with different morpholinos confirmed the specificity of the phenotype. The class II embryos (B'-C') presented more apoptotic cells than embryos of class I (B and C). (D) Injection of subcritical doses of ATG- and splice-*hdac8*-MO that singularly did not generate apoptosis demonstrated a synergistic effect on apoptotic levels. SC, spinal cord; di, diencephalon; h, hindbrain; n, notocord. Scale bar indicates 100  $\mu$ m.

## Discussion

Regulation of neuronal cell death is a fundamental process during both embryonic and adult life (19). During embryonic development, neurons are produced in excess number probably to ensure an adequate number of nerve cells at birth (20). Increased apoptosis during brain development has been associated to abnormal morphology and to adult behavioral abnormalities

(21). In the present study, inhibition of HDAC8 enzymatic activity leads to an excessive apoptosis both in murine NSCs and in the developing vertebrate brain. HDAC8 is a histone deacetylase known to act on SMC3 availability; hence, it is considered a player in the cohesin complex (12). Indeed, deacetylation of SMC3 is a critical step for protein recycling in cells. Cohesins and condensins are protein complexes acting prominently as



regulators of cell division, controlling deoxyribonucleic acid (DNA) content separation in daughter cells. Intriguingly, germ line mutations in both complexes are associated with human conditions affecting brain development. Biallelic mutations in condensin components *NCAPD2*, *NCAPH*, or *NCAPD3* cause microcephaly in humans (22). Dominant autosomal or X-linked mutations in cohesin complex genes cause CdLS, a congenital multiorgan syndrome that presents microcephaly and autistic self-aggressive behaviors (9). Previous studies on models of CdLS have reported increased cell death in the developing brain (13,14,23) associated to an impaired activation of the canonical WNT pathway or mitotic imbalance in the *rad21* model, in which molecular analyses have shown both by array and RNA sequencing deregulation of the WNT pathway (24,25). Canonical WNT pathway is mediated by activation of  $\beta$ -catenin, reduced in CdLS models, that translocates in the cell nucleus where it binds to DNA for gene expression regulation (26,27). Among known targets, Cyclin D1 (*CCND1*) is extensively described (28). Notably, *CCND1* is known to play a pivotal role during neurogenesis. Indeed, it has been shown that overexpression of the cyclin-dependent kinase 4 (*cdk4*)–cyclinD1 complex, positive regulators of cell cycle progression, induces NSCs' expansion (29). Moreover, several studies indicated that shortening of NSCs' cell cycle in embryonic and adult brain is sufficient for inhibiting neuronal differentiation (30,31). Hence, we sought to evaluate a model of CdLS NSCs. We inhibited HDAC8 using PCI34051, a chemical compound known to specifically act on HDAC8 deacetylase activity (12) in proliferating and differentiating murine NSCs. Our results clearly showed that upon HDAC8 inhibition NSCs reduce their capability of proliferating, confirming recent findings shown in cell lines (32). Likely, this is because of the observed increased apoptosis and it does not translate into an augmented differentiation as expected in physiological condition in smooth muscle (33) and brain (34). It was already demonstrated, in cellular model of glioblastomas, that the knockdown of another cohesin, *SMC1A*, led to the significant decrease in proliferation of U251 and U87MG cells (35). These results are on line with our *in vitro* analysis of the role of HDAC8 in NSCs. Importantly, we found a significant reduction in cells positive for the neuronal marker  $\beta$ -tubulin III, indicating that their neurogenic differentiating capabilities are hampered. Importantly, it has been recently shown that retinoic pathway response is impaired in CdLS patients fibroblasts, suggesting a weakened activation following exposure to a master player in neuronal differentiation (36). A neuronal reduction in CdLS patients could explain part of the behavioral and morphological features often reported after birth [as reviewed in (37,38)]. Hence, a detailed analysis in mammals should be conducted for better dissecting this possibility. To note, a consistently high expression of CdLS–cohesins in the developing mouse embryos and human adult CNS, especially in hindbrain and hindbrain-derived structures (39), notwithstanding the non-proliferative characteristics of such organs, has been recently reported. In the present study, *Danio rerio* models of *hdac8* deficiency obtained by morpholino antisense injections confirmed an increased apoptosis in the developing CNS associated with altered canonical WNT pathway. Molecular and morphological alterations could be rescued upon chemical activation by LiCl treatment as previously shown in other CdLS models (13).

In conclusion, we report an association between HDAC8 inhibition—model of CdLS—and increased cell death in the developing neural tissues, both *in vitro* and *in vivo* with a consequent reduction in neuronal differentiation capabilities, which could be involved in the severe mental retardation observed in CdLS.

## Materials and Methods

### Neural stem cells

NSCs obtained from SVZ of 4 months old C57BL/6 male mice were used. Cells were cultivated in a medium containing epidermal growth factor (EGF) and fibroblast growth factor (FGF) (40–42). Three different cultures from three mice were used for the experiments.

### PCI34051 treatment

Cells were firstly grown in a large culture flask and then plated in a 12 wells tissue culture plate at the concentration of 10 000 cell/cm<sup>2</sup>. Experiments were performed in triplicate for each culture. For proliferating cells experiments, cultures were treated either with PCI34051 25  $\mu$ M, a known HDAC8 inhibitor (12), or with DMSO 1:1000, a concentration that does not alter NSCs' properties, such as proliferation and differentiation. After 5 days of culture, spheres were harvested and mechanically dissociated to single cells and counted. The fold change was determined dividing the total number of cells by the initial number of plated cells. Differentiation was achieved by plating cells in presence of adhesion molecules Cultrex (Tema Ricerca, Italy) and in absence of growth factors. In a 48 well plate, round sterile coverslip of the diameter of 1 cm was inserted. Wells were coated with 150  $\mu$ l of Cultrex for 1 h and 40 000 cells were loaded with 500  $\mu$ l of medium containing FGF but not EGF (40–42) for 2 days. Following growth factor removal, treatment with HDAC8 inhibitor was started. Two different time points (from day 3 to day 7 and from day 5 to day 7) were used. As control, treated cells with DMSO 1:1000 for days 3 to 7 were used. At the end of the treatment, the medium was removed, the cells washed once with Phosphate-Buffered Saline (PBS) and fixed with 4% paraformaldehyde for 10 min. Cells were then washed once with PBS and either used for immunocytochemistry or stored at 4°C. Experiments were run in duplicates.

### Silencing NSCs

A 48 multiwell plate was coated with laminin (Synthetic Laminin Peptide, Sigma SCR127, Darmstadt, Germany) using a concentration of 150  $\mu$ g/ml as suggested by the supplier. Two siRNAs (Qiagen, Germantown, MD, USA) expected to anneal different regions of the HDAC8 transcript (Flexitube siRNA 5 nmol cat nr SI01063895 and catalogue number SI01063902) were used. As negative control AllStars Negative Control siRNA (cat nr 1027280) with no homology to any known mammalian genes and minimal non-specific effects was selected. HiPerFect Transfection Reagent (Qiagen) was used for siRNAs delivery. Four different cultures of NSCs were used, and experiments were run in triplicates. We first plated dissociated cells (10 000 cells per well) on laminin-coated wells as a monolayer in 500  $\mu$ l of proliferative medium (PM) for 1 day. The following day, incubation medium (with siRNAs and Transfection Reagent prepared following the manufacturer instruction) was added drop-wise onto the attached cells that were incubated under their normal growth conditions for 3 h before adding the PM medium. The medium was changed after 24 h and cells were cultured for 2–3 days. The cells were then harvested, dissociated and counted. siRNAs concentrations were selected in pilot studies, choosing 20 nM as experimental concentration. For analyses of *Hdac8* silencing in differentiating NSCs, three different cultures were used.

### Immunostaining of differentiated NSC

Differentiation capabilities were assayed by means of immunostaining. For this purpose, antibodies against glial fibrillary acidic protein (GFAP; 1:250, Immunological Sciences AB-10635) and  $\beta$ -tubulin III (1:250, Immunological Sciences AB-10288) were used. Briefly, fixed cells were permeabilized with 0.1% Triton-X in PBS for 10 min at room temperature, then the primary antibodies were added overnight at 4°C in PBS with 10% normal goat serum NGS. Secondary antibodies conjugated with fluorophores were used: Alexa-fluor 488 (Goat anti mouse Immunological Sciences IS20010) and Alexa-fluor 555 (Goat anti rabbit Immunological Sciences IS20012). Nuclei were stained with 4', 6-Diamidino-2-phenylindole dihydrochloride (DAPI) 300 nM (43). Images were acquired using a Leica SP2 microscope, Buccinasco, Milan, Italy with Helium/Neon and Argon/Krypton lasers. The number of positive cells was counted and compared within treatments. Experiments were repeated twice. A minimum of 1400 cells for each sample and for each treatment were counted.

### Apoptosis assay

Apoptosis in NSCs was quantified using a Caspase-3/CPP32 Colorimetric Assay (BioVision, Milpitas, CA, USA) following manufacturer's protocol. Briefly, NSCs were harvested after 5 days of culture, resuspended in chilled lysis buffer and centrifuged and supernatant (representing cytosolic extract) was used. Following protein concentration measurement, spectrophotometric detection of the chromophore p-nitroaniline (pNA) after cleavage from the labeled substrate DEVD-pNA allowed for cell death assessment. Samples were run as experimental triplicates and technical duplicates.

### Animals

Breeding wild-type fish (zebrafish, *D. rerio*) of the AB strain were maintained at 28°C on a 14 h light/10 h dark cycle. Embryos were collected by natural spawning, staged according to Kimmel and colleagues (44) and raised at 28°C in fish water (Instant Ocean, Blacksburg, VA, USA, 0.1% methylene blue) in Petri dishes, according to established techniques. Zebrafish embryos were raised and maintained under standard conditions and national guidelines (Italian decree 4 March 2014, n. 26). All experimental procedures were approved by Institutional Animal Care and Use Committee, N. OPBA\_93\_2017. Embryonic ages are expressed in hpf and dpf.

LiCl was added to fish water for 30 min at the 10–12 somite stages at a concentration of 0.3 M at 28°C as previously described (13). Treated embryos were then washed three times with water and allowed to develop to 24 hpf.

### Reverse transcription-PCR assays

Total RNA from 12 samples (an average of 30 embryos per sample) was extracted with the TOTALLY RNA isolation kit (Ambion, Life Technologies, Paisley UK), treated with RQ1 RNase-Free DNase (Promega Madison WI, USA) and oligo(dT)-reverse transcribed using SuperScript II RT (Invitrogen, Carlsbad, CA, USA), according to manufacturers' instructions. PCR products were loaded and resolved onto 1% agarose gels. The  $\beta$ -actin expression was tested in parallel with the gene of interest as a housekeeping gene control for the complementary DNA loaded.

The following primers were used:

*hdac8pr\_sense* 5'-ACATGAGGGTCGTGAAGCCT-3'  
*hdac8pr\_antisense* 5'-ACCGGTCATTACATAACA-3'  
*hdac8fl\_sense* 5'-ATGAGTGAAAAAGCGACAG-3'  
*hdac8fl\_antisense* 5'-CGATCCTAAACTACATTCTTC-3'  
*hdac8E1\_sense* 5'-GTCCAAAGTCAGCAGACT-3'  
*hdac8I2\_antisense* 5'-GTGAGATGAACTGCACTCT-3'

### In situ hybridization and histological analysis

WISH experiments were carried out as described by Thisse and colleagues (45). For each experiment a minimum of 30 controls and MO-injected embryos were analyzed. *hdac8* probe was cloned using RT-PCR primers. For histological sections, stained embryos were refixed in 4% PFA Paraformaldehyde, dehydrated and stored in methanol, wax embedded and sectioned (5  $\mu$ m). Images of embryos and sections were acquired using a microscope equipped with digital camera with LAS Leica Imaging software (Leica, Wetzlar, Germany). Images were processed using Adobe Photoshop software and, when necessary, different focal planes of the same image have been taken separately and later merged in a single image.

### TUNEL staining

For (Terminal deoxynucleotidyl transferase dUTP nick end labeling) assay, a minimum of 24 embryos (per experimental group) were fixed in 4% PFA for 2 h at room temperature. Embryos were washed with methanol at -20°C and then twice with PBC Phosphate-Buffered Saline with Citrate (0.001% Triton X-100; 0.1% sodium citrate in PBS) for 10 min. Staining for apoptotic cells was performed using the AP-*In situ* Cell Death Detection Kit (Roche Diagnostics, Penzberg, Germany) carefully leaving labeling reagents to react for the same length of time for all experiments. Embryos were incubated at 37°C for 1 h and fluorescent apoptotic cells were detected under a fluorescent microscope (Leica). For the visual staining, embryos were then washed, stained and mounted for microscopic imaging.

### Injections

To repress *hdac8* mRNA translations, two morpholinos were synthesized (Gene Tools LLC) targeting *hdac8*-ATG and exon1-intron1 junction (splice-*hdac8*-MO) (46),

ATG-*hdac8*-MO: 5'-CATTACTGTCGGTTTTTCACTCAT-3'  
 splice-*hdac8*-MO: 5'-TGCAGAGTGCACTTCATCTACCCG-3',

and used at the concentration of 1 pmole per embryo in 1x Danieau buffer (pH 7.6). A standard control morpholino oligonucleotide (ctrl-MO) was injected in parallel (47). When co-injected, ATG- and splice-*hdac8*-MOs were used at subcritical doses of 0.5 pmole per embryo in 1x Danieau buffer (pH 7.6). In all experiments, *hdac8*-MO-injected embryos were compared to embryos injected with the same amount of ctrl-MO at the same developmental stage. For the *in vivo* test of the specificity of morpholino-mediated knockdown, the rescue of morphants phenotype was evaluated by co-injecting zebrafish *hdac8*-mRNA at the concentration of 500 pg per embryo.

### Western blot

Fish embryos (minimum 30 per experimental group) were lysated in RIPA buffer (5  $\mu$ l for each embryo) and homogenized.



Samples were boiled for 10 min at 95°C. A total of 20 µl of protein sample was size-fractionated by gel Pre-cast (Invitrogen) and transferred with iBlot (Invitrogen). The nitrocellulose membranes were blocked with 5% non-fat dry milk in PBST (PBS containing 0.1% Tween 20) for 30 min at room temperature and subsequently incubated with the primary antibody: rabbit anti-Hdac8 [1:1000, HDAC8 (H-145) sc-11405, Santa Cruz Biotechnology, Santa Cruz, CA, USA and mouse anti-GAPDH (1:2500, Developmental Studies Hybridoma bank)] and mouse anti-Vinculin (1:6000, Sigma), diluted in 4% milk/PBST over night at 4°C. Horseradish peroxidase-conjugated secondary antibody (Sigma Aldrich, St Louis MO, USA) was used for 1 h at room temperature. The antigen signal was detected with the ECL chemiluminescence detection system (Amersham, Piscataway, NJ, USA) as specified by the manufacturer.

#### Data analysis

Proliferation statistical analysis was performed using Student's t-test. NSC immunostaining analysis was performed using the one-way analysis of variance followed by Bonferroni's multiple comparison test. Apoptosis assay was analyzed using student's t-test.  $P \leq 0.05$  was set as statistically significant. For graphs, Graphpad Prism software was used; for figures, Adobe Photoshop was used.

#### Acknowledgements

The authors are grateful to the Italian National Association of Volunteers Cornelia de Lange for support and inspiration. The authors want to express their deepest gratitude to Dr Julia Horsfield for manuscript commenting.

*Conflict of Interest statement.* None declared.

#### Funding

Fondazione Cariplo (2015-0783 to V.M.); Dipartimento DISS, Linea B, Università degli Studi di Milano (to V.M.); Dipartimento BIOMETRA, Linea B, Università degli Studi di Milano (to A.P.); Fondazione Mariani (Como, Italy) (to A.S.); Molecular and Translational Science-Università degli Studi di Milano scholarship (to P.G.).

#### References


- Ribe, E.M., Serrano-Saiz, E., Akpan, N. and Troy, C.M. (2008) Mechanisms of neuronal death in disease: defining the models and the players. *Biochem. J.*, **415**, 165–182.
- Martin, L.J. (2001) Neuronal cell death in nervous system development, disease, and injury (Review). *Int. J. Mol. Med.*, **7**, 455–478.
- Pfisterer, U. and Khodosevich, K. (2017) Neuronal survival in the brain: neuron type-specific mechanisms. *Cell Death Dis.*, **8**, e2643.
- Temple, S. (2001) The development of neural stem cells. *Nature*, **414**, 112–117.
- Gage, F.H. (2000) Mammalian neural stem cells. *Science*, **287**, 1433–1438.
- Xu, W., Lakshman, N. and Morshead, C.M. (2017) Building a central nervous system: the neural stem cell lineage revealed. *Neurogenesis (Austin)*, **4**, e1300037.
- Daniela, F., Vescovi, A.L. and Bottai, D. (2007) The stem cells as a potential treatment for neurodegeneration. *Methods Mol. Biol.*, **399**, 199–213.
- Gaspar-Maia, A., Alajem, A., Meshorer, E. and Ramalho-Santos, M. (2011) Open chromatin in pluripotency and reprogramming. *Nat. Rev. Mol. Cell Biol.*, **12**, 36–47.
- Deardorff, M.A., Noon, S.E. and Krantz, I.D. (1993) Cornelia de Lange syndrome. In *Gene Reviews*, University of Washington: Seattle (WA).
- Hagstrom, K.A. and Meyer, B.J. (2003) Condensin and cohesin: more than chromosome compactor and glue. *Nat. Rev. Genet.*, **4**, 520–534.
- Bjornsson, H.T. (2015) The Mendelian disorders of the epigenetic machinery. *Genome Res.*, **25**, 1473–1481.
- Deardorff, M.A., Bando, M., Nakato, R., Watrin, E., Itoh, T., Minamino, M., Saitoh, K., Komata, M., Katou, Y., Clark, D. et al. (2012) HDAC8 mutations in Cornelia de Lange syndrome affect the cohesin acetylation cycle. *Nature*, **489**, 313–317.
- Pistocchi, A., Fazio, G., Cereda, A., Ferrari, L., Bettini, L.R., Messina, G., Cotelli, F., Biondi, A., Selicorni, A. and Massa, V. (2013) Cornelia de Lange syndrome: NIPBL haploinsufficiency downregulates canonical Wnt pathway in zebrafish embryos and patients fibroblasts. *Cell Death Dis.*, **4**, e866.
- Fazio, G., Gaston-Massuet, C., Bettini, L.R., Graziola, F., Scagliotti, V., Cereda, A., Ferrari, L., Mazzola, M., Cazzaniga, G., Giordano, A. et al. (2016) Cyclin D1 down-regulation and increased apoptosis are common features of cohesinopathies. *J. Cell. Physiol.*, **231**, 613–622.
- Yan, W., Liu, S., Xu, E., Zhang, J., Zhang, Y., Chen, X. and Chen, X. (2013) Histone deacetylase inhibitors suppress mutant p53 transcription via histone deacetylase 8. *Oncogene*, doi: 10.1038/onc.2012.81.
- Qi, J., Singh, S., Hua, W.K., Cai, Q., Chao, S.W., Li, L., Liu, H., Ho, Y., McDonald, T., Lin, A., et al. (2015) HDAC8 inhibition specifically targets inv(16) acute myeloid leukemic stem cells by restoring p53 acetylation. *Cell Stem Cell*, doi: 10.1016/j.stem.2015.08.004.
- Wu, J., Du, C., Lv, Z., Ding, C., Cheng, J., Xie, H., Zhou, L. and Zheng, S. (2013) The up-regulation of histone deacetylase 8 promotes proliferation and inhibits apoptosis in hepatocellular carcinoma. *Dig. Dis. Sci.*, doi: 10.1007/s10620-013-2867-7.
- Hua, W.K., Qi, J., Cai, Q., Carnahan, E., Ayala Ramirez, M., Li, L., Marucci, G. and Kuo, Y.H. (2017) HDAC8 regulates long-term hematopoietic stem-cell maintenance under stress by modulating p53 activity. *Blood*, doi:10.1182/blood-2017-03-771386.
- Hutchins, J.B. and Barger, S.W. (1998) Why neurons die: cell death in the nervous system. *Anat. Rec.*, **253**, 79–90.
- Dekkers, M.P.J., Nikolettou, V. and Barde, Y.A. (2013) Death of developing neurons: new insights and implications for connectivity. *J. Cell Biol.*, **203**, 385–393.
- Broad, K.D., Curley, J.P. and Keverne, E.B. (2009) Increased apoptosis during neonatal brain development underlies the adult behavioral deficits seen in mice lacking a functional paternally expressed gene 3 (Peg3). *Dev. Neurobiol.*, **69**, 314–325.
- Martin, C.A., Murray, J.E., Carroll, P., Leitch, A., Mackenzie, K.J., Halachev, M., Fetit, A.E., Keith, C., Bicknell, L.S., Fluteau, A. et al. (2016) Mutations in genes encoding condensin complex proteins cause microcephaly through decatenation failure at mitosis. *Genes Dev.*, **30**, 2158–2172.
- Horsfield, J.A., Anagnostou, S.H., Hu, J.K., Cho, K.H., Geisler, R., Lieschke, G., Crosier, K.E. and Crosier, P.S. (2007) Cohesin-dependent regulation of Runx genes. *Development*, **134**, 2639–2649.

24. Rhodes, J.M., Bentley, F.K., Print, C.G., Dorsett, D., Misulovin, Z., Dickinson, E.J., Crosier, K.E., Crosier, P.S. and Horsfield, J.A. (2010) Positive regulation of c-Myc by cohesin is direct, and evolutionarily conserved. *Dev. Biol.*, doi: 10.1016/j.ydbio.2010.05.493.
25. Schuster, K., Leeke, B., Meier, M., Wang, Y., Newman, T., Burgess, S. and Horsfield, J.A. (2015) A neural crest origin for cohesinopathy heart defects. *Hum. Mol. Genet.*, doi: 10.1093/hmg/ddv402.
26. Tortelote, G.G., Reis, R.R., de Almeida Mendes, F. and Abreu, J.G. (2017) Complexity of the Wnt/ $\beta$ -catenin pathway: searching for an activation model. *Cell. Signal.*, **40**, 30–43.
27. Barker, N., Morin, P.J. and Clevers, H. (2000) The yin-yang of TCF/ $\beta$ -catenin signaling. *Adv. Cancer Res.*, **77**, 1–24.
28. Shtutman, M., Zhurinsky, J., Simcha, I., Albanese, C., D'Amico, M., Pestell, R. and Ben-Ze'ev, A. (1999) The cyclin D1 gene is a target of the  $\beta$ -catenin/LEF-1 pathway. *Proc. Natl. Acad. Sci. U.S.A.*, **96**, 5522–5527.
29. Lange, C., Huttner, W.B. and Calegari, F. (2009) Cdk4/CyclinD1 overexpression in neural stem cells shortens G1, delays neurogenesis, and promotes the generation and expansion of basal progenitors. *Cell Stem Cell*, **5**, 320–331.
30. Salomoni, P. and Calegari, F. (2010) Cell cycle control of mammalian neural stem cells: putting a speed limit on G1. *Trends Cell Biol.*, **20**, 233–243.
31. Artegiani, B., Lange, C. and Calegari, F. (2012) Expansion of embryonic and adult neural stem cells by in utero electroporation or viral stereotaxic injection. *J. Vis. Exp.*, doi: 10.3791/4093.
32. Dasgupta, T., Antony, J., Braithwaite, A.W. and Horsfield, J.A. (2016) HDAC8 inhibition blocks SMC3 deacetylation and delays cell cycle progression without affecting cohesin-dependent transcription in MCF7 cancer cells. *J. Biol. Chem.*, doi: 10.1074/jbc.M115.704627.
33. Waltregny, D., De Leval, L., Glénisson, W., Ly Tran, S., North, B.J., Bellahcène, A., Weidle, U., Verdin, E. and Castronovo, V. (2004) Expression of histone deacetylase 8, a class I histone deacetylase, is restricted to cells showing smooth muscle differentiation in normal human tissues. *Am. J. Pathol.*, **165**, 553–564.
34. Murko, C., Lagger, S., Steiner, M., Seiser, C., Schoefer, C. and Pusch, O. (2010) Expression of class I histone deacetylases during chick and mouse development. *Int. J. Dev. Biol.*, **54**, 1525–1535.
35. Yang, Y., Zhang, Z., Wang, R., Ma, W., Wei, J. and Li, G. (2013) siRNA-mediated knockdown of SMC1A expression suppresses the proliferation of glioblastoma cells. *Mol. Cell. Biochem.*, doi: 10.1007/s11010-013-1704-9.
36. Fazio, G., Bettini, L.R., Rigamonti, S., Meta, D., Biondi, A., Cazzaniga, G., Selicorni, A. and Massa, V. (2017) Impairment of retinoic acid signaling in Cornelia de Lange syndrome fibroblasts. *Birth Defects Res.*, **109**, 1268–1276.
37. Avagliano, L., Grazioli, P., Mariani, M., Bulfamante, G.P., Selicorni, A. and Massa, V. (2017) Integrating molecular and structural findings: Wnt as a possible actor in shaping cognitive impairment in Cornelia de Lange syndrome. *Orphanet J. Rare Dis.*, **12**.
38. Avagliano, L., Bulfamante, G.P. and Massa, V. (2017) Cornelia de Lange syndrome: to diagnose or not to diagnose in utero? *Birth Defects Res.*, **109**, 771–777.
39. Bettini, L.R., Graziola, F., Fazio, G., Grazioli, P., Scagliotti, V., Pasquini, M., Cazzaniga, G., Biondi, A., Larizza, L., Selicorni, A., Gaston-Massuet, C. and Massa, V. (2018) Rings and bricks: expression of cohesin components is dynamic during development and adult life. *Int. J. Mol. Sci.*, **19**.
40. Gelain, F., Bottai, D., Vescovi, A. and Zhang, S. (2006) Designer self-assembling peptide nanofiber scaffolds for adult mouse neural stem cell 3-dimensional cultures. *PLoS One*, **1**, e119.
41. Henry, G.R., Heise, A., Bottai, D., Formenti, A., Gorio, A., Di Giulio, A.M. and Koning, C.E. (2008) Acrylate end-capped poly(ester-carbonate) and poly(ether-ester)s for polymer-on-multielectrode array devices: synthesis, photocuring, and biocompatibility. *Biomacromolecules*, **9**, 867–878.
42. Adami, R., Pagano, J., Colombo, M., Platonova, N., Recchia, D., Chiamonte, R., Bottinelli, R., Canepari, M. and Bottai, D. (2018) Reduction of movement in neurological diseases: effects on neural stem cells characteristics. *Front. Neurosci.*, doi: 10.3389/fnins.2018.00336.
43. Bottai, D., Scesa, G., Cigognini, D., Adami, R., Nicora, E., Abrignani, S., Di Giulio, A.M. and Gorio, A. (2014) Third trimester NG2-positive amniotic fluid cells are effective in improving repair in spinal cord injury. *Exp. Neurol.*, doi: 10.1016/j.expneurol.2014.01.015.
44. Kimmel, C.B., Ballard, W.W., Kimmel, S.R., Ullmann, B. and Schilling, T.F. (1995) Stages of embryonic development of the zebrafish. *Dev. Dyn.*, **203**, 253–310.
45. Thisse, C., Thisse, B., Schilling, T.F. and Postlethwait, J.H. (1993) Structure of the zebrafish *snail1* gene and its expression in wild-type, spadetail and no tail mutant embryos. *Development*, **119**, 1203–1215.
46. Ferrari, L., Bragato, C., Brioschi, L., Spreafico, M., Esposito, S., Pezzotta, A., Pizzetti, F., Moreno-Fortuny, A., Bellipanni, G., Giordano, A. et al. (2018) HDAC8 regulates canonical Wnt pathway to promote differentiation in skeletal muscles. *J. Cell. Physiol.*, **1**.
47. Nasevicius, A. and Ekker, S.C. (2000) Effective targeted gene 'knockdown' in zebrafish. *Nat. Genet.*, **26**, 216–220.

## **3.2 HDAC8 regulates canonical Wnt pathway to promote differentiation in skeletal muscle**

In our previous work we identified defects of tail structure in zebrafish embryos following *hdac8* knockdown. Indeed, such alterations might be due not only to the reported impairment of CNS development, but also to defects in other tissues, such as skeletal muscle. Since we observed *hdac8* expression in zebrafish muscle tissue, we sought to assess a possible involvement of HDAC8 in the development of skeletal muscle tissue. To test this hypothesis, in this work we characterized HDAC8 expression in the skeletal muscle tissue and assessed the effect of its inhibition by PCI on skeletal muscle development using both *in vivo* (zebrafish) and *in vitro* (C2C12 immortalized murine myoblasts) models.

# HDAC8 regulates canonical Wnt pathway to promote differentiation in skeletal muscles

Luca Ferrari<sup>1\*</sup> | Cinzia Bragato<sup>2,3\*</sup> | Loredana Brioschi<sup>1\*</sup> | Marco Spreafico<sup>1</sup> |  
Simona Esposito<sup>1</sup> | Alex Pezzotta<sup>1</sup> | Fabrizio Pizzetti<sup>4</sup> | Artal Moreno-Fortuny<sup>5,6</sup> |  
Gianfranco Bellipanni<sup>7</sup> | Antonio Giordano<sup>7,8</sup> | Paola Riva<sup>1</sup> | Flavia Frabetti<sup>4</sup> |  
Paola Viani<sup>1</sup> | Giulio Cossu<sup>5</sup> | Marina Mora<sup>2</sup> | Anna Marozzi<sup>1</sup> | Anna Pistocchi<sup>1</sup> 

<sup>1</sup>Dipartimento di Biotecnologie Mediche e Medicina Traslationale, Università degli Studi di Milano, Milano, Italy

<sup>2</sup>Neuromuscular Diseases and Neuroimmunology Unit, Fondazione IRCCS Istituto Neurologico C. Besta, Milano, Italy

<sup>3</sup>PhD Program in Neuroscience, University of Milano-Bicocca, Milano, Italy

<sup>4</sup>Department of Experimental, Diagnostic and Specialty Medicine, University of Bologna, Bologna, Italy

<sup>5</sup>Division of Cell Matrix Biology and Regenerative Medicine, Faculty of Biology, Medicine and Health, University of Manchester, Manchester, UK

<sup>6</sup>Developmental Genetics, Department of Biomedicine, University of Basel, Basel, Switzerland

<sup>7</sup>Sbarro Institute for Cancer Research and Molecular Medicine, Department of Biology, Center for Biotechnology, College of Science and Technology, Temple University, Philadelphia

<sup>8</sup>Department of Medicine, Surgery & Neuroscience, University of Siena, Siena, Italy

## Correspondence

Anna Pistocchi, Dipartimento di Biotecnologie Mediche e Medicina Traslationale, L.I.T.A. Via Fratelli Cervi 93, Segrate, Università degli Studi di Milano 20090, Italy.  
Email: anna.pistocchi@unimi.it

## Funding information

Associazione Italiana per la Ricerca sul Cancro, Grant/Award Number: MFAG 2016 18714

## Abstract

Histone deacetylase 8 (HDAC8) is a class 1 histone deacetylase and a member of the cohesin complex. HDAC8 is expressed in smooth muscles, but its expression in skeletal muscle has not been described. We have shown for the first time that HDAC8 is expressed in human and zebrafish skeletal muscles. Using RD/12 and RD/18 rhabdomyosarcoma cells with low and high differentiation potency, respectively, we highlighted a specific correlation with HDAC8 expression and an advanced stage of muscle differentiation. We inhibited HDAC8 activity through a specific PCI-34051 inhibitor in murine C2C12 myoblasts and zebrafish embryos, and we observed skeletal muscles differentiation impairment. We also found a positive regulation of the canonical Wnt signaling by HDAC8 that might explain muscle differentiation defects. These findings suggest a novel mechanism through which HDAC8 expression, in a specific time window of skeletal muscle development, positively regulates canonical Wnt pathway that is necessary for muscle differentiation.

## KEYWORDS

histone deacetylase 8 (HDAC8), rhabdomyosarcoma, skeletal muscle, Wnt, zebrafish

## 1 | INTRODUCTION

Skeletal muscle is necessary to accomplish fundamental functions such as the maintenance of the body structure, motility, and metabolism by storing and consuming energy. Skeletal muscle

\*Luca Ferrari, Cinzia Bragato, and Loredana Brioschi have contributed equally to this study.



development is a multistep process in which myogenic cells are committed to proliferating myogenic precursors, which differentiate into myoblasts and myocytes that fuse to form a multinucleated myotube. Several signals are essential for the regulation of skeletal muscle differentiation involving transcription factors, signaling molecules, transduction pathways, and epigenetic modifications. Among these, the histone deacetylases (HDACs) are frequently a part of the regulatory elements of muscle genes (Sincennes, Brun, & Rudnicki, 2016). The HDAC family comprises at least 18 different enzymes classified in four classes in mammals and has been originally identified for histone deacetylation activity and nucleosome stability. Recent evidence pinpoints their role in deacetylation also of nonhistone targets such as p53 and alpha-tubulin (de Leval et al., 2006), as well as in gene transcription (Grunstein, 1997; Megee, Morgan, Mittman, & Smith, 1990).

HDAC8 is the last cloned and characterized member of class I HDACs (Buggy et al., 2000; Van den Wyngaert et al., 2000), it diverges from other class I enzymes as the C-terminal protein-binding domain is not present, probably indicating a functional specialization during evolution (Gregoretto, Lee, & Goodson, 2004; Somoza et al., 2004). HDAC8 is ubiquitously expressed and can localize to either the nucleus or the cytoplasm interacting with nonhistone proteins such as the cohesin protein SMC3, estrogen receptor  $\alpha$  (ERR $\alpha$ ), p53, inv(16) fusion protein (Deardorff et al., 2012; Durst, Lutterbach, Kummalu, Friedman, & Hiebert, 2003; Wilson, Tremblay, Deblois, Sylvain-Drolet, & Giguère, 2010; Wu et al., 2013). Moreover, in normal human tissues HDAC8 is expressed by smooth muscle including vascular and visceral smooth muscle cells, myoepithelial cells, and myofibroblasts (Durst et al., 2003; Wu et al., 2013), where interacts with cortical actin-binding protein cortactin and smooth muscle actin (SMA) and regulates smooth muscle contraction (Buggy et al., 2000; Li et al., 2014; Olson et al., 2014).

In this study, we describe for the first time a specific HDAC8 expression in murine C2C12 myoblasts and human and zebrafish (*Danio rerio*) skeletal muscles. In particular, we have analyzed the time course of HDAC8 expression during skeletal muscle differentiation in murine C2C12 myoblasts and zebrafish. We noticed that HDAC8 is mainly expressed when differentiation is already started; moreover, in rhabdomyosarcoma derived cell lines RD/12 and RD/18 with low and high differentiation potency, respectively, the increment of HDAC8 expression during the differentiation is prominent in RD/18 than in RD/12 cell line. We also demonstrate that HDAC8 promotes muscle differentiation in vitro and in vivo, as the pharmacological block of its deacetylase activity inhibits myogenesis in the C2C12 cellular model and in zebrafish. We showed that this function is accomplished through the canonical Wnt pathway that is downregulated when HDAC8 activity is inhibited. However, according to the dual role of HDAC8 in the nuclei and in the cytosol, other mechanisms involving HDAC8 might regulate skeletal muscle differentiation acting both on histone or nonhistone targets or regulating different pathways. Therefore, further analyses on acetylome profile are needed to identify both nuclear and cytosolic HDAC8 targets. Our results link for the first time the HDAC8 activity to broad aspects of skeletal muscle development and open new possibilities in the use of

HDAC8-specific inhibitors (i.e., PCI-34051; Balasubramanian et al., 2008) for therapeutic intervention on skeletal muscle diseases.

## 2 | MATERIALS AND METHODS

### 2.1 | Animals

Zebrafish (*D. rerio*) embryos were raised and maintained under standard conditions and national guidelines (Italian decree March 4, 2014, n. 26). All experimental procedures were approved by IACUC (Institutional Animal Care and Use Committee). Zebrafish AB strains obtained from the Wilson Laboratory, University College London, London, United Kingdom, were maintained at 28°C on a 14-hr light/10-hr dark cycle. Embryos were collected by natural spawning, staged according to Kimmel, Ballard, Kimmel, Ullmann, and Schilling (1995) and raised at 28°C in fish water (instant ocean, 0.1% methylene blue in petri dishes), according to established techniques. We express the embryonic ages in hours post fertilization (hpf) and days post fertilization (dpf). After 24 hpf, to prevent pigmentation, 0.003% 1-phenyl-2-thiourea (Sigma-Aldrich, Saint Louis, MO) was added to the fish water. Embryos were washed, dechorionated, and anaesthetized with 0.016% tricaine (ethyl 3-aminobenzoate methanesulfonate salt; Sigma-Aldrich), before observations and picture acquisitions. Embryos were fixed overnight in 4% paraformaldehyde (Sigma-Aldrich) in phosphate-buffered saline (PBS) at 4°C, and then dehydrated stepwise to methanol and stored at -20°C.

To activate the canonical Wnt pathway, lithium chloride (LiCl) was added to fish water for 30 min at the 10–12 somite stage at a concentration of 0.3 M at 28°C.

### 2.2 | C2C12 and rhabdomyosarcoma cells

C2C12 cells were maintained in the growth medium, Dulbecco modified Eagle medium (DMEM), supplemented with 10% fetal calf serum (FCS; Euroclone, Pero, Italy), 100 IU/ml penicillin, and 100 µg/ml streptomycin in a humidified incubator at 37°C with 5% CO<sub>2</sub>. After reaching 80–90% confluence, cells were washed in PBS and differentiated in the DMEM medium with horse serum 2% (Thermo Fisher Scientific, Waltham, MS). The medium was changed every 48 hr and cultured up to 9 days of differentiation.

RD/12 and RD/18 cell lines were two different clones originally isolated from the human embryonal rhabdomyosarcoma cell lines RD by Lollini et al. (1991). Cells were cultured in DMEM supplemented with 100 IU/mL penicillin, 100 µg/mL streptomycin, and either 10% FCS or 2% horse serum. The culture medium was renewed every 48–72 hr up to 11 days of culture in the differentiation medium.

### 2.3 | Reverse transcription and quantitative real-time PCR (qRT-PCRs)

Total RNAs were isolated from C2C12, RD/12, RD/18 cells, and zebrafish embryos at different developmental stages using Trizol reagent (Life Technologies, Carlsbad, CA) according to the producer's instructions. After treatment with DNase I RNase-free (Roche, Basel,

Switzerland) to avoid possible genomic contamination, 1 µg of RNA was reverse-transcribed (RT) using the "ImProm-II™ Reverse Transcription System" (Promega, Madison, WI) and a mixture of oligo (dT) and random primers according to manufacturer's instructions. Quantitative real-time polymerase chain reactions (qRT-PCR) on C2C12 and rhabdomyosarcoma RNAs were carried out in a total volume of 20 µl containing 1X SsoAdv Universal SYBR Green Super Mix (Bio-Rad, Hercules, CA), using proper amount of the RT reaction. qRT-PCRs were performed using the CFX-96 TM (Bio-Rad). Relative expression of *HDAC8* was normalized with different reference genes, in particular TATA-box binding protein and glyceraldehyde-3-phosphate dehydrogenase were used for C2C12 cell line whereas actin and beta-2-microglobulin for rhabdomyosarcoma cell lines.

qRT-PCRs in zebrafish were carried out in a total volume of 20 µl containing 1X iQ SYBR Green Super Mix (Promega), using proper amount of the RT reaction. qRT-PCRs were performed using the Bio-Rad iCycler iQ real-time detection system (Bio-Rad). For normalization purposes, *rpl8* expression levels were tested in parallel with the gene of interest. The primer list is given in Supporting Information Table S1.

## 2.4 | In situ hybridization, histological analysis, and immunohistochemistry

Whole mount in situ hybridization (WISH) experiments were carried out as described by Thisse and Thisse (2008). Antisense riboprobes were previously in vitro labeled with modified nucleotides (i.e. digoxigenin, fluorescein; Roche). *hdac8* probe was cloned in our laboratory. The primer list is given in Supporting Information Table S1. WISH experiments were done at least in three batches of embryos (minimum 30 embryos for each category). Immunohistochemistry analysis was carried out on 6-µm-thick cryosections from human skeletal muscle biopsy. The muscle biopsy was performed after an informed consent; human biological samples were provided by EuroBioBank and Telethon Network of Genetic Biobanks (GTB12001F to M. Mora), snap-frozen in isopentane/liquid nitrogen and maintained in liquid nitrogen. Cryosections were permeabilized in cold methanol (MeOH) 50% for 1 min and MeOH 100% for 1 min. Cryosections were hydrated with PBS and then blocked for 30 min at room temperature in normal goat serum 1X and incubated with primary and secondary antibodies. Primary antibodies were anti-HDAC8 (1:100; polyclonal clone [H-145]; sc-11405; Santa Cruz Biotechnology, Inc., Santa Cruz, CA) and anti-Lamin B (1:100; monoclonal clone; Novocastra/YLEM, Newcastle upon Tyne, UK). Secondary antibodies were Alexa 488-conjugated goat anti-mouse IgG or Alexa 546-conjugated goat anti-rabbit IgG, (Invitrogen Life Technologies, Carlsbad, CA), both diluted in 1:2,000. As control, sections were incubated either with isotype-specific IgG or the primary antibody was omitted. Sections were examined either under a Zeiss fluorescence microscope. Immunohistochemistry in zebrafish was carried out as described by Pistocchi, Gaudenzi et al. (2013). The primary antibody was mouse anti-sarcomeric (MF20, DSHB, Iowa City, IA, dilution 1:4). The secondary antibody was EnVision+ System- horseradish peroxidase (HRP) labeled polymer anti-mouse (Dako, Glostrup, Denmark). Images of embryos and sections were acquired using a microscope equipped with a digital camera with LAS leica imaging

software (Leica, Wetzlar, Germany). Images were processed using the Adobe Photoshop software and, when necessary, different focal images planes of the same image were taken separately and later merged in a single image.

## 2.5 | PCI-34051 treatment

For C2C12 cells, HDAC8 inhibitor PCI-34051 (PCI; Cayman Chemical, Ann Arbor, MI) was administrated at 25 µM together with the differentiating medium; negative controls were treated with the solvent dimethyl sulfoxide (DMSO). The PCI was changed every 24 hr until myogenic differentiation. Zebrafish embryos after the shield developmental stage (6 hpf) were treated with 150 µM PCI added to the fish water at 28°C kept in the dark. As a control DMSO was used at the same concentration. The PCI was changed every 24 hr and the embryos were grown until the desired developmental stage. For dose-dependent assays in zebrafish, the PCI was administrated at 50, 100, 150, and 250 µM.

## 2.6 | Western blotting

Human biological samples were provided by EuroBioBank and Telethon Network of Genetic Biobanks (GTB12001F to M. Mora). The juvenile muscle was of an 8-year-old child; the adult muscle was of a man of 42 years. For zebrafish, at least 30 zebrafish embryos were used for protein preparation, the yolk was previously removed from embryos to avoid yolk protein contamination.

Protein extracts were classically prepared in the radioimmunoprecipitation assay buffer (50 mM Tris-HCl pH 7.4, 1% NP-40, 150 mM NaCl, 0.25% sodium deoxycholate, 1 mM ethylenediaminetetraacetic acid, 1 mM phenylmethylsulfonyl fluoride, and protease inhibitors Roche; 2 µl/embryo or 1 µl/tail). The protein concentration was determined using a Quantum Micro BCA protein assay kit according to the manufacturer's instructions (Euroclone). Each sample (30–40 µg) was loaded onto a 7.5% or 10% polyacrylamide gels and subjected to electrophoresis. The proteins were then transferred onto polyvinylidene fluoride membranes that were blocked using a blocking solution at room temperature for 1 hr before incubation with the primary antibodies listed in Supporting Information Table S2. After incubation with the HRP-conjugated secondary antibodies for 1 hr at room temperature (secondary antibodies are listed in Supporting Information Table S2), the protein bands were detected using enhanced chemiluminescence (ECL) detection systems. Imaging acquisition has been done with the Alliance MINI HD9 AUTO Western Blot Imaging System (UVitec Limited, Cambridge) and analyzed with the related software (Bellipanni, Murakami, & Weinberg, 2010).

## 3 | RESULTS

### 3.1 | HDAC8 is expressed in the skeletal muscle and its expression correlates with an advanced state of muscle differentiation

Several expression profiles of HDAC8 suggested that it has a ubiquitous expression in human tissues, with higher expression in



particular organs such as the brain, pancreas, kidney, prostate, liver, and smooth muscles. HDAC8 transcript and protein have been detected both in the nucleus and cytosol, suggesting that HDAC8 might have a variable localization within the cell, depending on the cell type and its posttranslational modifications such as phosphorylation (Buggy et al., 2000; Hu et al., 2000; de Ruijter, van Gennip, Caron, Kemp, & van Kuilenburg, 2003;

Waltregny et al., 2004). Using immunofluorescence assays we detected for the first time an expression of HDAC8 in normal human skeletal muscle with a predominant nuclear localization of the protein, as shown by the co-localization of HDAC8 and Lamin B (Figure 1a-c). Moreover, by western blot analyses, we observed the expression of HDAC8 both in juvenile and adult skeletal muscles (Figure 1d).

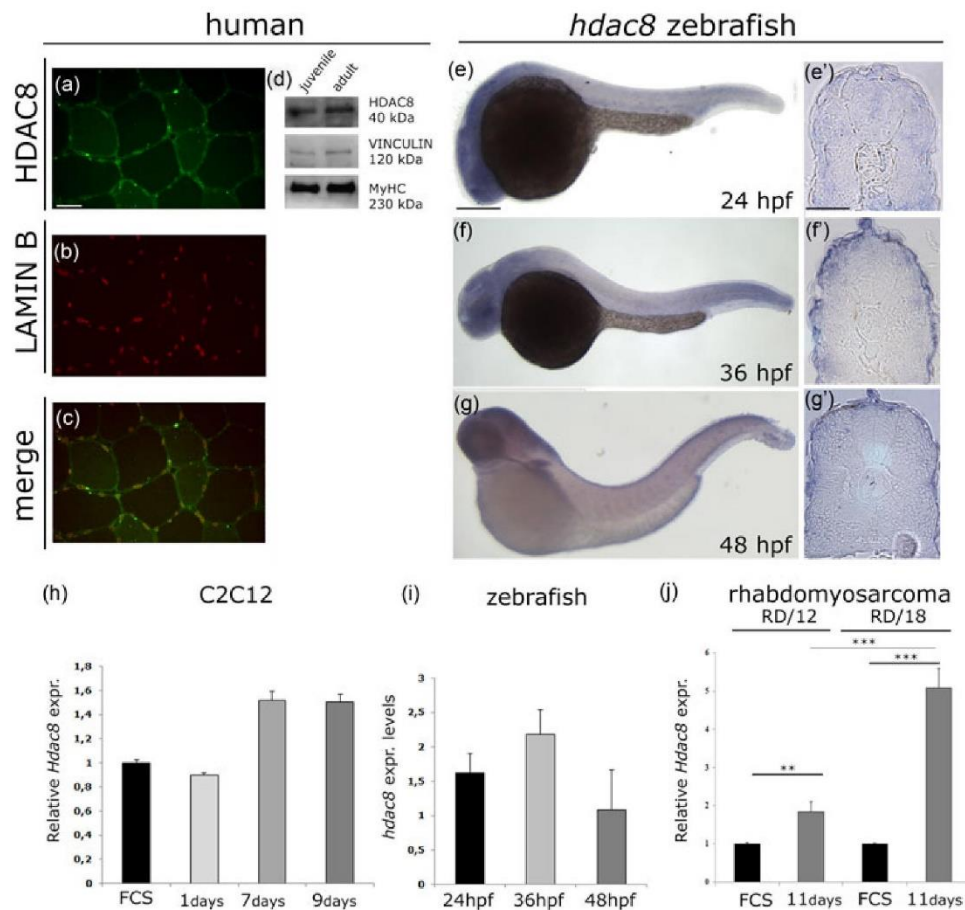


**FIGURE 1** HDAC8 is expressed in human, murine, and zebrafish skeletal muscles, and its expression correlates with differentiation potency. (a–c) HDAC8 protein expression in normal human skeletal muscles. Immunofluorescence staining of HDAC8 (a), lamin B (b), and merge of the two signals (c). The localization of HDAC8 in human skeletal muscle is predominantly nuclear as shown by the colocalization with the Lamin B protein. (d) Western blot analyses of HDAC8, vinculin, and all myosins expression in juvenile and adult skeletal muscles. (e–g) *hdac8* mRNA expression in zebrafish. WISH analyses of *hdac8* transcript localization in skeletal muscle of zebrafish embryos at 24 hpf (e), 36 hpf (f), and 48 hpf (g). Transverse histological sections of the previously hybridized embryos show the localization of *hdac8* transcript in the myotome (e', f', g'). (h) *Hdac8* qRT-PCR analyses on murine C2C12 myoblasts at different stages of differentiation. *Hdac8* expression is increased at 7–9 days after the induction of the differentiation, when differentiation is accomplished. (i) *hdac8* qRT-PCR analyses on RNA from 24, 36, and 48 hpf zebrafish embryos. *hdac8* expression is increased at 36 hpf when the first myogenic wave is completed. (j) HDAC8 qRT-PCR analyses on RD/12 and RD/18 rhabdomyosarcoma cells. At 11 days after the induction of differentiation, HDAC8 is more expressed in RD/18 cells that are able to fully differentiate in comparison to RD/12 cells. Scale bar represents 50  $\mu\text{m}$  in (a–c) and 100  $\mu\text{m}$  (e'–g'). Asterisks represent \*\* $p < 0.01$ , \*\*\* $p < 0.001$ , Student t test. FCS: fetal calf serum; HDAC8: histone deacetylase 8; hpf: hours post fertilization; mRNA: messenger RNA; qRT-PCR: quantitative reverse transcription polymerase reaction; WISH: whole mount in situ hybridization

In parallel, we cloned the zebrafish ortholog of human *HDAC8* (Chr 7: 51,656,099-51,710,015), and, by WISH analyses, we showed the expression of *hdac8* in skeletal muscle of zebrafish embryos at different developmental stages (Figure 1e–g). In zebrafish, the expression of *hdac8* varied among the developmental stages analyzed (24, 36, and 48 hpf) and was increased at 36 hpf when the first myogenic wave had already occurred (Stellabotte, Dobbs-McAuliffe, Fernandez, Feng, & Devoto, 2007; Figure 1e–g). We therefore investigated a possible correlation between *HDAC8* expression and skeletal muscle differentiation progression. We first examined its expression in murine C2C12 skeletal myogenic cells, which represent a highly suitable model for analysis of myogenic differentiation. C2C12 myoblasts proliferate in the growth medium with a high serum concentration (10% FCS) until they reach confluence, whereas a differentiation into multinucleated myotubes is triggered shifting to a differentiation medium with low-serum concentration (2% horse serum). *Hdac8* transcript, analyzed by qRT-PCR techniques, was present in C2C12 cells in the growth medium and in differentiation medium at Day 1 but its expression was significantly increased at Days 7 and 9 of differentiation (Figure 1h). In zebrafish, the expression of *hdac8* analyzed by qRT-PCR techniques confirmed the results previously shown by WISH, as the transcript is increased after the first myogenic wave when the differentiation was accomplished, with an expression peak at 36 hpf (Figure 1i). To further confirm the correlation between *HDAC8* expression and an advanced stage of differentiation, we chose two different subclones of the rhabdomyosarcoma cell line RD, which differ in the differentiation potency: the RD/18 cells are able to reach a terminal differentiation, whereas the RD/12 cells do not fully differentiate (Lollini et al., 1991). The expression of *HDAC8* was significantly increased at 11 days of differentiation with an increment of fourfold in RD/18 and about onefold in RD/12 (Figure 1j).

### 3.2 | HDAC8 activity regulates skeletal muscle differentiation in zebrafish and C2C12 myoblasts

To investigate a possible function of HDAC8 in differentiating skeletal muscles, we took advantage of the well-characterized PCI inhibitor that blocks the HDAC8 deacetylase activity (Balasubramanian et al., 2008). We administrated PCI to zebrafish embryos *in vivo* and C2C12 cells *in vitro*. Zebrafish embryos were treated with a concentration of 150  $\mu$ M of PCI from the 50% stage of epiboly, a developmental stage in which the mesodermal layer, from which skeletal muscle derives, is positioning in the gastrula. At 48 hpf, zebrafish embryos presented morphological defects in the central nervous system (CNS) and muscles, the regions where *hdac8* transcript was more expressed, as shown in Figure 1. PCI-treated embryos were divided in three phenotypical classes based on the severity of the CNS and muscle phenotypes: Class I showed a phenotype comparable to the control embryos treated with the solvent DMSO, Class II presented a mild phenotype, and Class III presented a severe phenotype (Figure 2a–d, class quantification in e). We performed a dose–response assay demonstrating that the observed phenotypes were correlated to the doses of PCI treatment (Supporting Information Figure S1). The sarcomeric myosins, which are expressed in differentiated and functional muscle, were diminished in PCI-treated embryos in comparison to controls, as demonstrated by immunohistochemistry and western blot techniques (Figure 2f–i). Interestingly, same morphological defects and myosin reduction were obtained in zebrafish embryos injected with the *hdac8* morpholino that blocks *Hdac8* protein production. These data indicate that the skeletal muscle differentiation impairment was specific because of the *Hdac8* loss-of-function (Supporting Information Figure S2). Moreover, at 24 hpf the

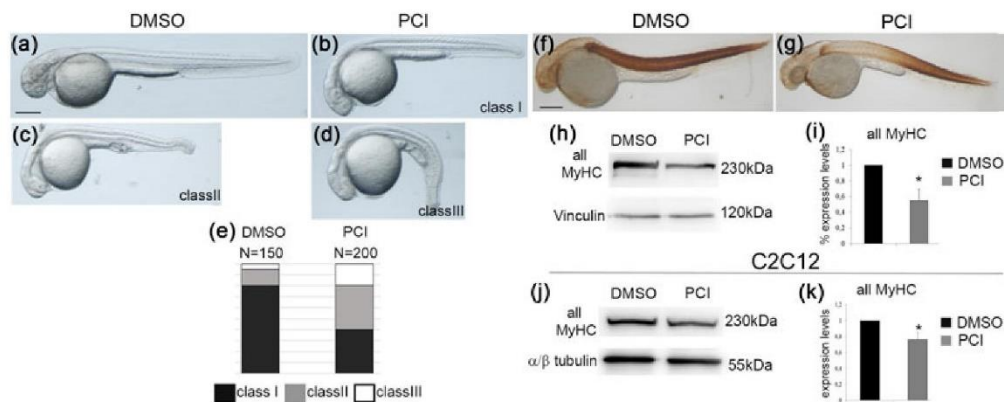


**FIGURE 2** Inhibition of HDAC8 activity reduces skeletal muscle differentiation in zebrafish embryos and murine C2C12 myoblasts. (a–e) *In vivo* treatment of zebrafish embryos with DMSO or PCI. Different phenotypical classes with increased severity (b–d; quantification in e) with PCI treatment compared to the control embryos treated with the DMSO (a). (f,g) Immunohistochemical staining (IHC) and (h,i) western blot analyses of sarcomeric myosins. Sarcomeric myosins were reduced in PCI-treated embryos at 48 hpf (g) in comparison to controls (f). Western blot analyses (h; quantification in i) confirmed all MyHCs reduction in PCI-treated embryos in comparison to controls. (j,k) Inhibition of HDAC8 activity impaired C2C12 differentiation. Western blot analyses (j; quantification in k) confirmed all MyHC reduction in PCI-treated C2C12 cells in comparison with DMSO-treated ones. Scale bars indicate 100  $\mu$ m in (a–d) and (f,g). Asterisks represent \* $p$  < 0.05, Student *t* test. DMSO: dimethyl sulfoxide; HDAC8: histone deacetylase 8; hpf: hours post fertilization

embryos treated with PCI did not present myogenic impairment confirming that Hdac8 activity is not necessary during early skeletal muscle differentiation (Supporting Information Figure S3).

Also in vitro, PCI treatment blocked the differentiation of C2C12 myoblasts in comparison to DMSO-treated cells. Under differentiating conditions, wild-type C2C12 cells fused into multinucleated myotubes. By contrast, when challenged to differentiate in the low-serum medium in the presence of PCI, C2C12 cells remained mononucleated and maintained an undifferentiated phenotype. We assessed that the differentiation of PCI-treated cells was impaired in

comparison with DMSO-treated cells as the levels of sarcomeric myosins, analyzed by the western blot techniques, were diminished (Figure 2j–k).

### 3.3 | HDAC8 regulates skeletal muscle differentiation through the activation of the canonical Wnt pathway

To gain mechanistic insights into how HDAC8 regulates skeletal muscle differentiation, we hypothesized that it modulates the

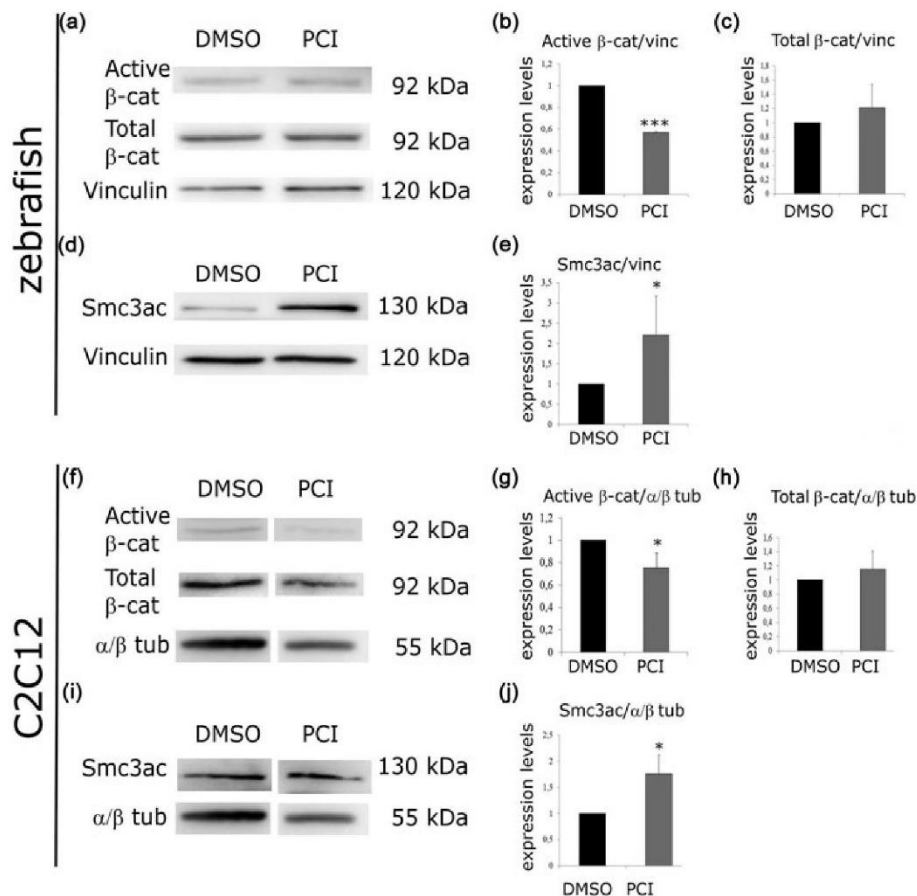


**FIGURE 3** : HDAC8 activates canonical Wnt signaling. (a–c) Canonical Wnt signaling was decreased with the PCI treatment in zebrafish embryos. (a) Active β-catenin was decreased in PCI-treated embryos in comparison to DMSO controls, whereas total β-catenin was increased by western blot analyses and relative quantifications (b–c). (d,e) The efficacy of PCI treatment was verified by the acetylation status of the Hdac8 target Smc3. (d) Smc3ac levels were increased in PCI-treated embryos in comparison with DMSO controls, quantification in (e). (f–h) Canonical Wnt signaling was decreased with the PCI treatment in C2C12 cells in the differentiation medium. (f) Active β-catenin was decreased in PCI-treated C2C12 cells in comparison with those treated with DMSO, whereas total β-catenin was increased by western blot analyses and relative quantifications (g,h). (i,j) The efficacy of PCI treatment in the C2C12 was verified by the acetylation status of the Hdac8 target Smc3. (i) Smc3ac levels were increased in PCI-treated C2C12 in comparison to DMSO treated controls, quantification in (j). Asterisks represent \* $p < 0.05$ , \*\*\* $p < 0.001$ , Student  $t$  test. DMSO: dimethyl sulfoxide; HDAC8: histone deacetylase 8



canonical Wnt pathway, a well-known regulator of skeletal muscle development and differentiation (Rudnicki & Williams, 2015). Indeed, in a hepatocellular model, it has been demonstrated that HDAC8 positively regulates the  $\beta$ -catenin/TCF (T-Cell Factor) signaling acting in concert with enhancer of zeste homolog 2 (EZH2) to epigenetically repress Wnt antagonists (Tian et al., 2015). Therefore, we analyzed the activation status of the canonical Wnt pathway in zebrafish embryos and C2C12 myoblasts treated with PCI. The phosphorylated and active form of  $\beta$ -catenin was diminished, as demonstrated by western blot analyses, in PCI-treated zebrafish embryos in comparison to controls treated with DMSO. In contrast, the levels of total  $\beta$ -catenin were even increased (Figure 3a, quantification in b and c). This last result is not surprising because we have seen similar upregulation of  $\beta$ -catenin in zebrafish embryos with impaired activity of the canonical Wnt pathway (Valenti et al., 2015). To verify the efficiency of the PCI-mediated Hdac8 inhibition that is responsible for the Wnt pathway downregulation, we analyzed the acetylation status of Smc3, a known Hdac8 target (Deardorff et al., 2012). Acetylated Smc3 (Smc3ac) levels were increased following the PCI treatment of the embryos, confirming the block of Hdac8 activity (Figure 3d, quantification in e). Same results were obtained in the C2C12 cells in the differentiation medium treated with PCI: western blot analyses confirmed the lower expression of active  $\beta$ -catenin in comparison with total  $\beta$ -catenin (Figure 3f, quantification in g and h) and increased levels of Smc3ac following the PCI treatment (Figure 3i, quantification in j).

The Wnt pathway in zebrafish can be activated through chemical treatments such as LiCl (Pistocchi, Fazio et al., 2013). Therefore, to further demonstrate that skeletal muscle differentiation impairment, observed with PCI-mediated Hdac8 inhibition, was specifically due to Wnt pathway downregulation, we reactivated the pathway adding

LiCl in PCI-treated zebrafish embryos. The morphological defects presented by PCI-treated embryos at 36 hpf (embryos with morphological defects: 50/70) were partially rescued by LiCl addition (embryos with morphological defects: 20/70; Figure 4a–c). Moreover, the levels of sarcomeric myosins analyzed by western blot techniques were rescued in embryos treated with PCI + LiCl in comparison to embryos treated only with PCI (Figure 4d, quantification in e). We also verify the efficiency of LiCl treatment by measuring the active  $\beta$ -catenin levels (Figure 4d, quantification in f).

#### 4 | DISCUSSION

In previous works, HDAC8 was shown to be expressed in smooth muscle cells in association with SMA and cortactin (Li et al., 2014), and its silencing by the RNA interference impairs the contraction of smooth muscle cultured cells (Waltregny et al., 2005). However, the role and mechanism of HDAC8 action in smooth muscle tissues are largely unknown. In this study, we described for the first time the expression and role of HDAC8 in the skeletal muscles. First, we demonstrated that *HDAC8* is expressed in human and zebrafish skeletal muscles. Then we analyzed the expression of *HDAC8* during muscle differentiation in the murine C2C12 skeletal muscle cells, during zebrafish muscle development and in two types of rhabdomyosarcoma cells with various degrees of invasiveness correlating to their ability to differentiate (RD/12 and RD/18). We decided to include these cells in the expression analyses as it has been reported that histone deacetylase inhibitor (HDACi) synergize with current anticancer drugs to induce apoptosis in rhabdomyosarcoma (Vleeshouwer-Neumann et al., 2015; Di Pompo et al., 2015).

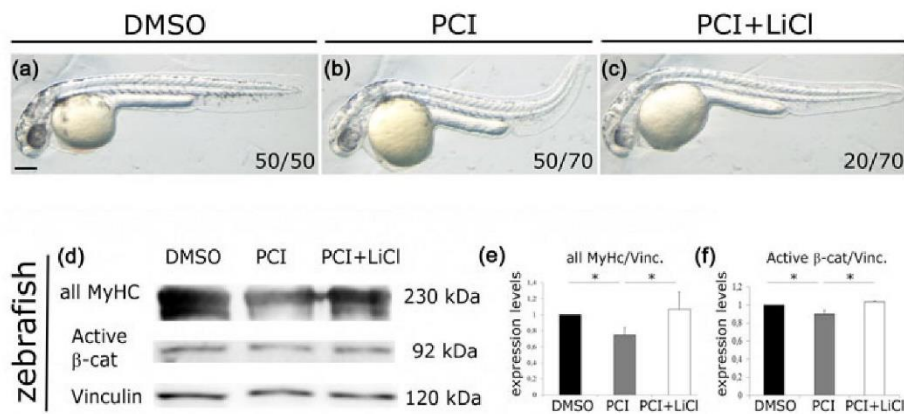


**FIGURE 4** : The HDAC8-mediated positive regulation of Wnt signaling is responsible for the skeletal muscle differentiation. (a–c) Morphological defect presented by PCI-treated embryos was rescued by LiCl addition. (d–f) Skeletal muscle differentiation was rescued when the Wnt pathway was restored by LiCl administration in PCI-treated zebrafish embryos. (d) Sarcomeric myosins, analyzed by western blot techniques, decreased in PCI-treated embryos and returned comparable with those treated with DMSO when Wnt pathway was rescued adding LiCl (quantification in e). The efficacy of LiCl treatment was verified by measuring the active  $\beta$ -catenin by western blot techniques (quantification in f). Asterisks represent  $*p < 0.05$ , Student *t* test. DMSO: dimethyl sulfoxide; HDAC8: histone deacetylase 8

Interestingly, we correlated the expression of *HDAC8* with an advanced differentiation state of skeletal muscles. Indeed, both in C2C12 cells and zebrafish, *HDAC8* expression is weak in the initial phases and increases later during the muscle differentiation process. These data are even more striking in the rhabdomyosarcoma cells, where the RD/18 cell line cultured in the differentiation medium for 11 days shows a greater increase in the *HDAC8* expression compared to the RD/12 cell line maintained in the same conditions. The *HDAC8* increased expression increase correlates with the differentiation capacity of the two cell lines.

For functional analyses, we treated the C2C12 cells and the zebrafish embryos with the *HDAC8* inhibitor PCI-34051. In zebrafish embryos, we performed the *Hdac8* inhibition by adding the PCI-34051 after the shield stage (6 hpf) to prevent gross morphological defects in the initial phase of gastrulation, when mesoderm is defined. We also performed loss-of-function studies in zebrafish by injecting the oligonucleotide antisense morpholino designed against *hdac8* to compare and confirm the results obtained with the PCI-34051 treatment. Both in the cellular and zebrafish models with reduced *HDAC8* activity, we observed an impairment in muscle differentiation following the initial myoblast commitment, in line with the kinetic of *HDAC8* expression previously analyzed. In the C2C12 cells, myoblasts were formed but failed to fuse in myotubes and to express the markers of differentiation; in zebrafish, the levels of functional myosins were reduced after 24 hpf but the myogenic program started, as demonstrated by the proper expression of the myogenic regulatory factors (MRFs) *MyoD* and *Myog* and by the presence of myosin proteins. Interestingly, Iezzi, Cossu, Nervi, Sartorelli, and Puri (2002) demonstrated that the levels of myogenin were not affected by myoblast exposure to HDACi, suggesting that HDACi selectively activate late muscle markers. Previous studies reported that HDACi have different effects by promoting or inhibiting myogenesis (Steinbach, Wolffe, & Rupp, 1997), and this discrepancy might be explained by the stage-specific effects of HDACi exposure.

We also demonstrated that the block on muscle differentiation observed after *HDAC8* inhibition is correlated with the downregulation of the canonical Wnt pathway. Several works demonstrate that the formation of skeletal muscle is tightly modulated by Wnt signaling for self-renewal and muscle differentiation and its dysregulation leads to perturbation of muscle fibers. Chemical activation of the Wnt/ $\beta$ -catenin pathway in differentiating myoblasts using LiCl, increases both the number and size of C2C12 myotubes, whereas inhibition of Wnt/ $\beta$ -catenin signaling results in a significant decrease in myotube length (Abraham, 2016). Indeed, the Wnt target  $\beta$ -catenin interacts directly with *MyoD*, enhancing its binding to E box elements and its transcriptional activity of muscle-specific genes. This transactivation is inhibited when  $\beta$ -catenin is deficient or the interaction between *MyoD* and  $\beta$ -catenin is disrupted (Kim, Neiswender, Baik, Xiong, & Mei, 2008). We demonstrated that the reduction of myosins observed in PCI-34051 treated embryos was caused by a decrease in activated  $\beta$ -catenin levels. A mechanism by which *HDAC8* regulates the canonical Wnt pathway has been recently described in human non-alcoholic

fatty liver disease (NAFLD)-associated hepatocellular carcinoma by Tian, Mok, Yang, and Cheng (2016). *HDAC8* physically interacts with the polycomb protein EZH2 and contributes to the activation of Wnt/ $\beta$ -catenin signaling. Further analyses are necessary to demonstrate whether this mechanism is conserved also in skeletal muscle and for the identification of other mechanisms related to *HDAC8* activity and muscle differentiation. Indeed, while we were preparing this manuscript, Tsai et al. (2018) published that the cohesin complex has to be recruited to the chromatin for the activation of myogenin. The authors showed that the differentiation of C2C12 myoblasts was prevented if the cohesin complex activity was impaired. Because *HDAC8* regulates the residency of the cohesin complex onto the DNA and chromatin accessibility via the acetylation of the cohesin component SMC3, the PCI-mediated inhibition of *HDAC8* might also block this process and impair C2C12 differentiation. Moreover, according to the dual activity of *HDAC8* as nuclear or cytosolic protein, acetylome profile studies following PCI inhibition both in vitro and in vivo models may uncover *HDAC8*-related targets.

Disregulation of canonical Wnt signaling has been reported in different pathologies, such as Duchenne muscular dystrophy (DMD; Trensz, Haroun, Cloutier, Richter, & Grenier, 2010; Barbarino et al., 2018), facioscapulohumeral muscular dystrophy (Block et al., 2013), and oculopharyngeal muscular dystrophy (Abu-Baker et al., 2013). Inhibition of canonical Wnt signaling in a mouse model for DMD (*mdx*) was shown to reduce fibrosis (Trensz et al., 2010). HDACi have recently emerged as potential pharmacological strategies for cancer treatment, and several of them are already approved by the International Drug Administration agencies. The increasing interest and use of HDACi has led to the development of class-specific inhibitors, such as the PCI-34051, which helps us to uncover the functional role of *HDAC8* in skeletal muscle differentiation and, in the future, might ameliorate the phenotype in pathological conditions. On the basis of the numerous beneficial effects of HDACi in skeletal muscle under pathological conditions, we believe that they are promising therapeutic agents.

#### ACKNOWLEDGMENTS

We thank P. L. Lollini, University of Bologna, for providing rhabdomyosarcoma cell lines. This study was supported by the AIRC, Associazione Italiana per la Ricerca sul Cancro (MFAG 2016 #18714). The funders had no role in study design, data collection, and interpretation, or the decision to submit the work for publication. We thank the EuroBioBank and Telethon Network of Genetic Biobanks (GTB12001F to M. Mora) for providing human biological samples.

#### CONFLICTS OF INTEREST

All authors declare that they have no conflict of interest.

#### AUTHOR CONTRIBUTIONS

Conceived and designed the experiments: A. Pistocchi, A. Marozzi, and P. Viani. Performed the experiments on human samples: C. Bragato and



M. Mora. Performed the experiments on a zebrafish: M. Spreafico, S. Esposito, L. Brioschi, A. Pezzotta, A. Pistocchi, and L. Ferrari. Performed the experiments on C2C12 cells: L. Ferrari, A. Moreno-Fortuny, F. Pizzetti, and F. Frabetti. Performed the experiments on rhabdomyosarcoma cells: F. Pizzetti and F. Frabetti. Analyzed data on a human sample: C. Bragato, M. Mora. Analyzed data on a zebrafish: M. Spreafico, S. Esposito, L. Brioschi, A. Pezzotta, A. Pistocchi, L. Ferrari, P. Riva, A. Giordano, and G. Bellipanni. Analyzed data on C2C12 cells: L. Ferrari, P. Riva, F. Pizzetti, F. Frabetti, A. Moreno-Fortuny, and G. Cossu. Wrote the paper: A. Pistocchi. Supervised paper drafting: A. Pistocchi, A. Giordano, and G. Bellipanni. Supervised the research project: A. Pistocchi.

#### ORCID

Anna Pistocchi  <http://orcid.org/0000-0001-9467-2542>

#### REFERENCES

- Abraham, S. T. (2016). A role for the Wnt3a/ $\beta$ -catenin signaling pathway in the myogenic program of C2C12 cells. *In Vitro Cellular and Developmental Biology—Animal*, 52(9), 935–941. <https://doi.org/10.1007/s11626-016-0058-5>
- Abu-Baker, A., Laganiera, J., Gaudet, R., Rochefort, D., Brais, B., Neri, C., ... Rouleau, G. A. (2013). Lithium chloride attenuates cell death in oculopharyngeal muscular dystrophy by perturbing Wnt/ $\beta$ -catenin pathway. *Cell Death & Disease*, 4(10), e821. <https://doi.org/10.1038/cddis.2013.342>
- Balasubramanian, S., Ramos, J., Luo, W., Sirisawad, M., Verner, E., & Buggy, J. J. (2008). A novel histone deacetylase 8 (HDAC8)-specific inhibitor PCI-34051 induces apoptosis in T-cell lymphomas. *Leukemia*, 22(5), 1026–1034. <https://doi.org/10.1038/leu.2008.9>
- Barbarino, M., Cesari, D., Intruglio, R., Indovina, P., Namagerdi, A., Bertolino, F. M., ... Giordano, A. (2018). Possible repurposing of pyriminium pamoate for the treatment of mesothelioma: A pre-clinical assessment. *J Cell Physiol*, 233(9), 7391–7401. <https://doi.org/10.1002/jcp.26579>
- Bellipanni, G., Murakami, T., & Weinberg, E. S. (2010). Molecular dissection of Otx1 functional domains in the zebrafish embryo. *Journal of Cellular Physiology*, 222(2), 286–293. <https://doi.org/10.1002/jcp.21944>
- Block, G. J., Narayanan, D., Amell, A. M., Petek, L. M., Davidson, K. C., Bird, T. D., ... Miller, D. G. (2013). Wnt/ $\beta$ -catenin signaling suppresses DUX4 expression and prevents apoptosis of FSHD muscle cells. *Human Molecular Genetics*, 22(23), 4661–4672. <https://doi.org/10.1093/hmg/ddt314>
- Buggy, J. J., Sideris, M. L., Mak, P., Lorimer, D. D., McIntosh, B., & Clark, J. M. (2000). Cloning and characterization of a novel human histone deacetylase, HDAC8. *The Biochemical Journal*, 350(Pt 1), 199–205. <https://doi.org/10.1042/BJ3500199>
- de Leval, L., Waltregny, D., Boniver, J., Young, R. H., Castronovo, V., & Oliva, E. (2006). Use of histone deacetylase 8 (HDAC8), a new marker of smooth muscle differentiation, in the classification of mesenchymal tumors of the uterus. *The American Journal of Surgical Pathology*, 30(3), 319–327. <https://doi.org/10.1097/O1.pas.0000188029.63706.31>
- de Ruijter, A. J. M., van Gennip, A. H., Caron, H. N., Kemp, S., & van Kuilenburg, A. B. P. (2003). Histone deacetylases (HDACs): Characterization of the classical HDAC family. *The Biochemical Journal*, 370(Pt 3), 737–749. <https://doi.org/10.1042/BJ20021321>
- Deardorff, M. A., Bando, M., Nakato, R., Watrin, E., Itoh, T., Minamino, M., ... Shirahige, K. (2012). HDAC8 mutations in cornelia de lange syndrome affect the cohesin acetylation cycle. *Nature*, 489(7415), 313–317. <https://doi.org/10.1038/nature11316>
- Di Pompo, G., Salerno, M., Rotili, D., Valente, S., Zwergel, C., Avnet, S., ... Mai, A. (2015). Novel histone deacetylase inhibitors induce growth arrest, apoptosis, and differentiation in sarcoma cancer stem cells. *Journal of Medicinal Chemistry*, 58(9), 4073–4079. <https://doi.org/10.1021/acs.jmedchem.5b00126>
- Durst, K. L., Lutterbach, B., Kummalu, T., Friedman, A. D., & Hiebert, S. W. (2003). The *inv(16)* fusion protein associates with corepressors via a smooth muscle myosin heavy-chain domain. *Molecular and Cellular Biology*, 23(2), 607–619. <https://doi.org/10.1128/MCB.23.2.607-619.2003>
- Gregoret, I., Lee, Y. M., & Goodson, H. V. (2004). Molecular evolution of the histone deacetylase family: Functional implications of phylogenetic analysis. *Journal of Molecular Biology*, 338(1), 17–31. <https://doi.org/10.1016/j.jmb.2004.02.006>
- Grunstein, M. (1997). Histone acetylation in chromatin structure and transcription. *Nature*, 389(6649), 349–352. <https://doi.org/10.1038/38664>
- Hu, E., Chen, Z., Fredrickson, T., Zhu, Y., Kirkpatrick, R., Zhang, G. F., ... Winkler, J. (2000). Cloning and characterization of a novel human class I histone deacetylase that functions as a transcription repressor. *Journal of Biological Chemistry*, 275(20), 15254–15264. <https://doi.org/10.1074/jbc.M908988199>
- Iezzi, S., Cossu, G., Nervi, C., Sartorelli, V., & Puri, P. L. (2002). Stage-specific modulation of skeletal myogenesis by inhibitors of nuclear deacetylases. *Proceedings of the National Academy of Sciences of the United States of America*, 99(11), 7757–7762. <https://doi.org/10.1073/pnas.112218599>
- Kim, C.-H., Neiswender, H., Baik, E. J., Xiong, W. C., & Mei, L. (2008). Beta-catenin interacts with MyoD and regulates its transcription activity. *Molecular and Cellular Biology*, 28(9), 2941–2951. <https://doi.org/10.1128/MCB.01682-07>
- Kimmel, C. B., Ballard, W. W., Kimmel, S. R., Ullmann, B., & Schilling, T. F. (1995). Stages of embryonic development of the zebrafish. *Developmental Dynamics*, 203(3), 253–310. <https://doi.org/10.1002/aja.1002030302>
- Li, J., Chen, S., Cleary, R. A., Wang, R., Gannon, O. J., Seto, E., & Tang, D. D. (2014). Histone deacetylase 8 regulates cortactin deacetylation and contraction in smooth muscle tissues. *American Journal of Physiology: Cell Physiology*, 307(3), C288–C295. <https://doi.org/10.1152/ajpcell.00102.2014>
- Lollini, P. L., De Giovanni, C., Landuzzi, L., Nicoletti, G., Scottandi, K., & Nanni, P. (1991). Reduced metastatic ability of in vitro differentiated human rhabdomyosarcoma cells. *Invasion & Metastasis*, 11(2), 116–124. Retrieved from <http://www.ncbi.nlm.nih.gov/pubmed/1917385>
- Megee, P., Morgan, B., Mittman, B., & Smith, M. (1990). Genetic analysis of histone H4: Essential role of lysines subject to reversible acetylation. *Science*, 247(4944), 841–845. <https://doi.org/10.1126/science.2106160>
- Olson, D. E., Udeshi, N. D., Wolfson, N. A., Pitcairn, C. A., Sullivan, E. D., Jaffe, J. D., ... Holson, E. B. (2014). An unbiased approach to identify endogenous substrates of "histone" deacetylase 8. *ACS Chemical Biology*, 9(10), 2210–2216. <https://doi.org/10.1021/cb500492r>
- Pistocchi, A., Fazio, G., Cereda, A., Ferrari, L., Bettini, L. R., Messina, G., ... Massa, V. (2013). Cornelia de lange syndrome: NIPBL haploinsufficiency downregulates canonical Wnt pathway in zebrafish embryos and patients fibroblasts. *Cell Death and Disease*, 4(10), e866–e866. <https://doi.org/10.1038/cddis.2013.371>
- Pistocchi, A., Gaudenzi, G., Foglia, E., Monteverde, S., Moreno-Fortuny, A., Pianca, A., & Messina, G. (2013). Conserved and divergent functions of Nfix in skeletal muscle development during vertebrate evolution. *Development*, 140(7), 1528–1536. <https://doi.org/10.1242/dev.076315>
- Rudnicki, M. A., & Williams, B. O. (2015). Wnt signaling in bone and muscle. *Bone*, 80, 60–66. <https://doi.org/10.1016/j.bone.2015.02.009>

- Sincennes, M.-C., Brun, C. E., & Rudnicki, M. A. (2016). Concise review: Epigenetic regulation of myogenesis in health and disease. *Stem Cells Translational Medicine*, 5(3), 282–290. <https://doi.org/10.5966/sctm.2015-0266>
- Somoza, J. R., Skene, R. J., Katz, B. A., Mol, C., Ho, J. D., Jennings, A. J., ... Tari, L. W. (2004). Structural snapshots of human HDAC8 provide insights into the class I histone deacetylases. *Structure*, 12(7), 1325–1334. <https://doi.org/10.1016/j.str.2004.04.012>
- Steinbach, O. C., Wolffe, A. P., & Rupp, R. A. W. (1997). Somatic linker histones cause loss of mesodermal competence in xenopus. *Nature*, 389(6649), 395–399. <https://doi.org/10.1038/38755>
- Stellabotte, F., Dobbs-McAuliffe, B., Fernandez, D. A., Feng, X., & Devoto, S. H. (2007). Dynamic somite cell rearrangements lead to distinct waves of myotome growth. *Development*, 134(7), 1253–1257. <https://doi.org/10.1242/dev.000067>
- Thisse, C., & Thisse, B. (2008). High-resolution in situ hybridization to whole-mount zebrafish embryos. *Nature Protocols*, 3(1), 59–69. <https://doi.org/10.1038/nprot.2007.514>
- Tian, Y., Mok, M., Yang, P., & Cheng, A. (2016). Epigenetic activation of Wnt/ $\beta$ -catenin signaling in NAFLD-associated hepatocarcinogenesis. *Cancers*, 8(8), 76. <https://doi.org/10.3390/cancers8080076>
- Tian, Y., Wong, V. W. S., Wong, G. L. H., Yang, W., Sun, H., Shen, J., ... Chan, H. L. Y. (2015). Histone deacetylase HDAC8 promotes insulin resistance and  $\beta$ -catenin activation in NAFLD-associated hepatocellular carcinoma. *Cancer Research*, 75(22), 4803–4816. <https://doi.org/10.1158/0008-5472.CAN-14-3786>
- Trensz, F., Haroun, S., Cloutier, A., Richter, M. V., & Grenier, G. (2010). A muscle resident cell population promotes fibrosis in hindlimb skeletal muscles of mdx mice through the Wnt canonical pathway. *American Journal of Physiology-Cell Physiology*, 299(5), C939–C947. <https://doi.org/10.1152/ajpcell.00253.2010>
- Tsai, P. F., Dell'Orso, S., Rodriguez, J., Vivanco, K. O., Ko, K. D., Jiang, K., ... Sartorelli, V. (2018). A muscle-specific enhancer RNA mediates cohesin recruitment and regulates transcription in trans. *Molecular Cell*, 71(1), 129–141. <https://doi.org/10.1016/j.molcel.2018.06.008>
- Valenti, F., Ibetti, J., Komiya, Y., Baxter, M., Lucchese, A. M., Derstine, L., ... Bellipanni, G. (2015). The increase in maternal expression of *axin1* and *axin2* contribute to the zebrafish mutant *ichabod* ventralized phenotype. *Journal of Cellular Biochemistry*, 116(3), 418–430. <https://doi.org/10.1002/jcb.24993>
- Van den Wyngaert, I., de Vries, W., Kremer, A., Neefs, J., Verhasselt, P., Luyten, W. H., & Kass, S. U. (2000). Cloning and characterization of human histone deacetylase 8. *FEBS Letters*, 478(1–2), 77–83. [https://doi.org/10.1016/S0014-5793\(00\)01813-5](https://doi.org/10.1016/S0014-5793(00)01813-5)
- Vleeshouwer-Neumann, T., Phelps, M., Bammler, T. K., MacDonald, J. W., Jenkins, I., & Chen, E. Y. (2015). Histone deacetylase inhibitors antagonize distinct pathways to suppress tumorigenesis of embryonal rhabdomyosarcoma. *PLoS One*, 10(12), e0144320. <https://doi.org/10.1371/journal.pone.0144320>
- Waltregny, D., De Leval, L., Glénisson, W., Ly Tran, S., North, B. J., Bellahcène, A., ... Castronovo, V. (2004). Expression of histone deacetylase 8, a class I histone deacetylase, is restricted to cells showing smooth muscle differentiation in normal human tissues. *The American Journal of Pathology*, 165(2), 553–564. [https://doi.org/10.1016/S0002-9440\(10\)63320-2](https://doi.org/10.1016/S0002-9440(10)63320-2)
- Waltregny, D., Glénisson, W., Tran, S. L., North, B. J., Verdin, E., Colige, A., & Castronovo, V. (2005). Histone deacetylase HDAC8 associates with smooth muscle  $\alpha$ -actin and is essential for smooth muscle cell contractility. *FASEB Journal*, 19(8), 966–968. <https://doi.org/10.1096/fj.04-2303fje>
- Wilson, B. J., Tremblay, A. M., Deblois, G., Sylvain-Drolet, G., & Giguère, V. (2010). An acetylation switch modulates the transcriptional activity of estrogen-related receptor  $\alpha$ . *Molecular Endocrinology*, 24(7), 1349–1358. <https://doi.org/10.1210/me.2009-0441>
- Wu, J., Du, C., Lv, Z., Ding, C., Cheng, J., Xie, H., ... Zheng, S. (2013). The up-regulation of histone deacetylase 8 promotes proliferation and inhibits apoptosis in hepatocellular carcinoma. *Digestive Diseases and Sciences*, 58(12), 3545–3553. <https://doi.org/10.1007/s10620-013-2867-7>

## SUPPORTING INFORMATION

Additional supporting information may be found online in the Supporting Information section at the end of the article.

**How to cite this article:** Ferrari L, Bragato C, Brioschi L, et al. HDAC8 regulates canonical Wnt pathway to promote differentiation in skeletal muscles. *J Cell Physiol*. 2018;1–10. <https://doi.org/10.1002/jcp.27341>

1 **Supplementary materials**

2

3 ***Morpholino injections***

4 Injections were carried out on 1- to 2-cell stage embryos; the dye tracer rhodamine dextran was also  
5 co-injected. To repress *hdac8* mRNA translations, one morpholino was synthesized (Gene Tools  
6 LLC, Philomath OR, USA) targeting *hdac8*-ATG, and used at the concentration of 1 pmole/embryo  
7 in 1x Danieau buffer (pH 7,6). A standard control morpholino oligonucleotide (ctrl-MO) was injected  
8 in parallel (Nasevicius & Ekker, 2000).

9 ATG-*hdac8*-MO: 5'-CATTACTGTCGCTTTTTTCACTCAT-3'.

10 **Supplementary References**

11

12 Nasevicius, a, & Ekker, S. C. (2000). Effective targeted gene “knockdown” in zebrafish. *Nature Genetics*,  
13 26(2), 216–20. <https://doi.org/10.1038/79951>

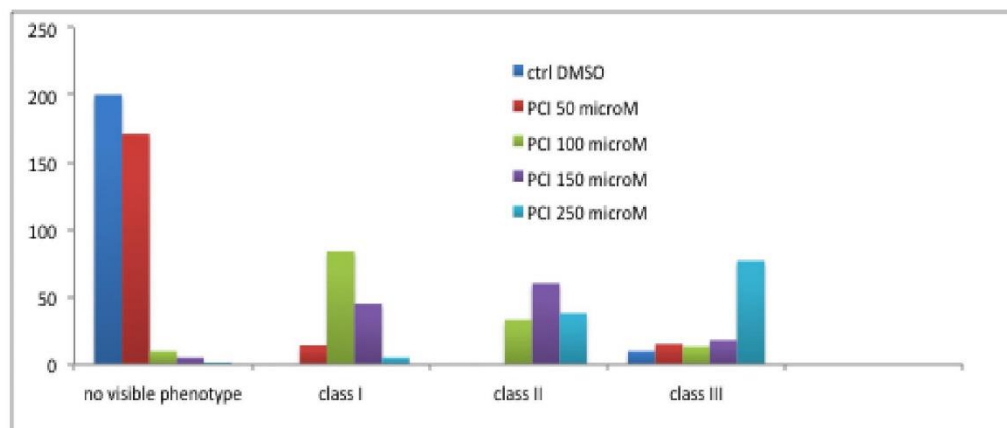
14

15

16 **Supplementary Figures**

17

18



19

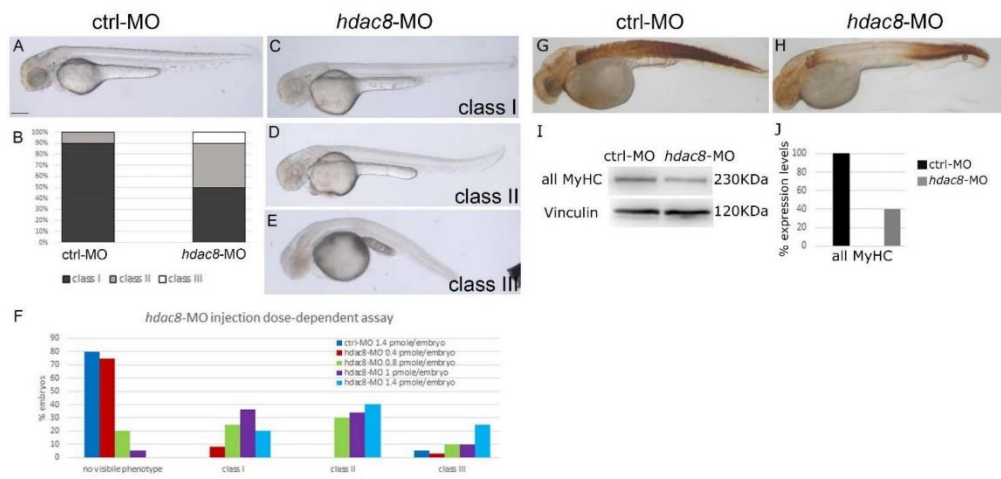
20 **Suppl. Figure S1: PCI-34051 dose response.** Zebrafish embryos were treated with different concentrations  
21 of PCI ranging from 50  $\mu$ M to 250  $\mu$ M. By increasing the concentration of PCI, morphological defects  
22 presented by the embryos were increased. Control embryos were treated with DMSO (250  $\mu$ M). Embryo were  
23 divided into three phenotypical classes with increased severity: class I with low morphological defects, class

1



1 II with more severe defects and class III with the most evident morphological phenotype. The Y axis indicated  
 2 the number of embryos analysed.

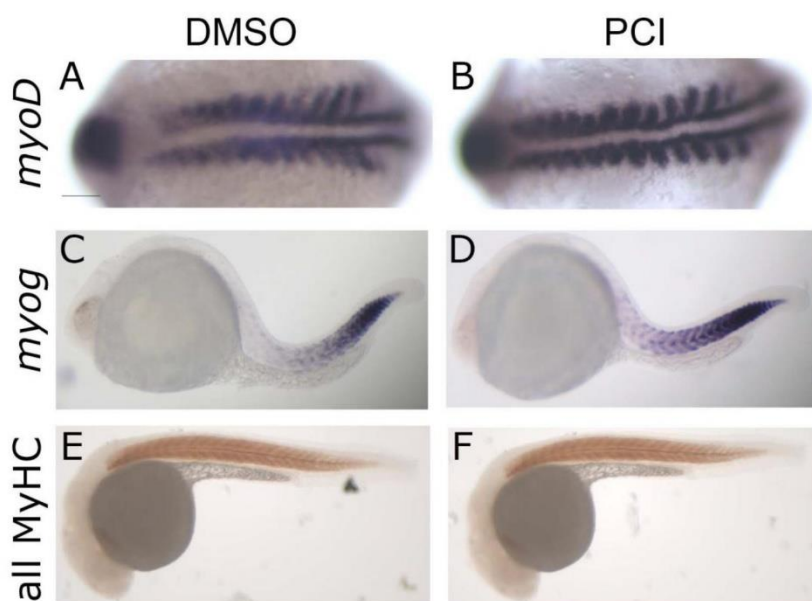
3  
 4  
 5



6

7 **Suppl. Figure S2: *hdac8*-MO injection in zebrafish embryos reduces skeletal muscle differentiation.**  
 8 Different phenotypical classes of zebrafish embryos injected with *hdac8*-MO (C-E) and control-MO (A);  
 9 quantification in (B). (F) Dose-dependent assay for *hdac8*-MO injection. The percentage of embryos exhibiting  
 10 a phenotype specific for each class was dependent to the injected dose of *hdac8*-MO. (G-J) Sarcomeric  
 11 myosins reduction (H) in *hdac8*-MO 48 hpf embryos in comparison to controls (G) with IHC staining analyses.  
 12 Western blot analyses (I; quantification in J) confirmed all MyHC reduction in 48 hpf zebrafish embryos  
 13 injected with the *hdac8*-MO. Scale bar indicates 100  $\mu$ m.

14



1  
2

3 **Suppl. Figure S3: Hdac8 activity is not necessary during early skeletal muscle differentiation.**  
 4 (A-B) WISH analysis of *myoD* expression was comparable in DMSO (A) and PCI treated (B) embryos at 20  
 5 somites. (C-D) WISH analysis of *myog* expression was comparable in DMSO (C) and PCI treated (D) embryos  
 6 at 24 hpf. (E-F) IHC analysis of all MyHC levels was comparable in DMSO (E) and PCI treated (F) embryos  
 7 at 24 hpf. Scale bar indicates 100  $\mu$ m.

8

9 **Supplementary Table 1**

<i>Zf-hdac8 qPCR ff</i>	5'-GGGACAATGATGACCCTCAG-3'
<i>Zf-hdac8 qPCR rev</i>	5'-GCAGCCGCGTAATCAAAA-3'
<i>Zf-rpl8 qPCR ff</i>	5'-CTCCGTCTTCAAAGCCCATGT-3'
<i>Zf-rpl8 qPCR rev</i>	5'-TCCTTCACGATCCCCTTGATG-3'
<i>Zf-hdac8 probe ff</i>	5'-ACATGAGGGTCGTGAAGCCT-3'
<i>Zf-hdac8 probe rev</i>	5'-ACCGCGTCATTCACATAACA-3'
<i>m-Hdac8 qPCR ff</i>	5'-TAGGTTATGACTGCCAGCC-3'
<i>m-Hdac8 qPCR rev</i>	5'-ACCCTCCAGACCAGTTGATG-3'
<i>m-Gapdh qPCR ff</i>	5'-GCTCACTGGCATGGCCTTC-3'
<i>m-Gapdh qPCR rev</i>	5'-CCTTCTTGATGTCATCATACTTGGC-3'

10  
11  
12

3

1 **Supplementary Table S2**

2

<b>Proteins</b>	<b>Polyacrylamide concentration</b>	<b>Blotting</b>	<b>Blocking solution</b>	<b>Primary Antibody dilution (in Blocking solution)</b>	<b>Secondary Antibody dilution (in 5% Skim milk in TBS-T 0.1%)</b>	<b>ECL detection system</b>
<b>All MyHC</b>	7.5%	30 V const. O.N. 4°C	5% Skim milk in TBS-T 0.1%	1:6	Anti-Mouse 1:4000	LiteAblot PLUS Euroclone
<b>Smc3ac</b>	10%	100 V const 2h 4°C	5% BSA in TBS-T 0.1%	1:500	Anti-Mouse 1:4000	ETA C ULTRA 2.0 Cyanagen
<b>Vinculin</b>	7.5%/10%	30V const. O.N. 4°C/ 100V const 2h 4°C	5% Skim milk in TBS-T 0.1%	1:6000	Anti-Mouse 1:4000	LiteAblot PLUS Euroclone
<b>Active <math>\beta</math>-catenin</b>	10%	100 V const 2h 4°C	5% BSA in TBS-T 0.1%	1:500	Anti-Mouse 1:8000	ETA C ULTRA 2.0 Cyanagen
<b>Total <math>\beta</math>-catenin</b>	10%	100 V const 2h 4°C	5% BSA in TBS-T 0.1%	1:1000	Anti-Rabbit 1:5000	ETA C ULTRA 2.0 Cyanagen
<b>A<math>\beta</math>-tubulin</b>	10%	100V const 2h 4°C	5% BSA in TBS-T 0.1%	1:1000	Anti-Rabbit 1:5000	LiteAblot PLUS Euroclone

4

### **3.3 HDAC8: a promising therapeutic target for acute myeloid leukemia**

Previous works reported HDAC8 overexpression in CD34<sup>+</sup> haematopoietic stem cells (HSC) from AML patients and indicated that HDAC8 modulation of p53 activity is crucial in promoting survival of both healthy and leukemic HSCs. Moreover, HDAC8 inhibition was shown to be particularly effective in abrogating leukemic HSC survival in a subset of AML patients carrying the inversion of chromosome 16 (inv(16)). These data suggested that HDAC8 may sustain AML progression and that its inhibition could be a potential treatment for this malignancy. To test this hypothesis, in this paper we took advantage of the zebrafish model in order to evaluate the haematopoietic phenotype following *hdac8* overexpression. We also evaluated the feasibility of HDAC8 inhibition as a pharmacological approach for AML both in *hdac8*-overexpressing zebrafish and in AML cell lines.



# HDAC8: A Promising Therapeutic Target for Acute Myeloid Leukemia

Marco Spreafico<sup>1†</sup>, Alicja M. Gruszka<sup>2†</sup>, Debora Valli<sup>2</sup>, Mara Mazzola<sup>1</sup>, Gianluca Deflorian<sup>3</sup>, Arianna Quintè<sup>3</sup>, Maria Grazia Totaro<sup>3</sup>, Cristina Battaglia<sup>1</sup>, Myriam Alcalay<sup>2,4</sup>, Anna Marozzi<sup>1</sup> and Anna Pistocchi<sup>1\*</sup>

<sup>1</sup> Dipartimento di Biotecnologie Mediche e Medicina Traslazionale, Università degli Studi di Milano, Milan, Italy, <sup>2</sup> Dipartimento di Oncologia Sperimentale, Istituto Europeo di Oncologia IRCCS, Milan, Italy, <sup>3</sup> Cogentech, Società Benefit, Milan, Italy, <sup>4</sup> Dipartimento di Oncologia ed Emato-Oncologia, Università degli Studi di Milano, Milan, Italy

## OPEN ACCESS

### Edited by:

Charlotta Boiers,  
Lund University, Sweden

### Reviewed by:

Patompon Wongtrakongate,  
Mahidol University, Thailand  
Borhane Guezguez,  
German Cancer Research Center  
(DKFZ), Germany

### \*Correspondence:

Anna Pistocchi  
anna.pistocchi@unimi.it

<sup>†</sup> These authors have contributed  
equally to this work

### Specialty section:

This article was submitted to  
Stem Cell Research,  
a section of the journal  
Frontiers in Cell and Developmental  
Biology

Received: 14 May 2020

Accepted: 06 August 2020

Published: 04 September 2020

### Citation:

Spreafico M, Gruszka AM, Valli D,  
Mazzola M, Deflorian G, Quintè A,  
Totaro MG, Battaglia C, Alcalay M,  
Marozzi A and Pistocchi A (2020)  
HDAC8: A Promising Therapeutic  
Target for Acute Myeloid Leukemia.  
*Front. Cell Dev. Biol.* 8:844.  
doi: 10.3389/fcell.2020.00844

Histone deacetylase 8 (HDAC8), a class I HDAC that modifies non-histone proteins such as p53, is highly expressed in different hematological neoplasms including a subtype of acute myeloid leukemia (AML) bearing inversion of chromosome 16 [inv(16)]. To investigate HDAC8 contribution to hematopoietic stem cell maintenance and myeloid leukemic transformation, we generated a zebrafish model with Hdac8 overexpression and observed an increase in hematopoietic stem/progenitor cells, a phenotype that could be reverted using a specific HDAC8 inhibitor, PCI-34051 (PCI). In addition, we demonstrated that AML cell lines respond differently to PCI treatment: HDAC8 inhibition elicits cytotoxic effect with cell cycle arrest followed by apoptosis in THP-1 cells, and cytostatic effect in HL60 cells that lack p53. A combination of cytarabine, a standard anti-AML chemotherapeutic, with PCI resulted in a synergistic effect in all the cell lines tested. We, then, searched for a mechanism behind cell cycle arrest caused by HDAC8 inhibition in the absence of functional p53 and demonstrated an involvement of the canonical WNT signaling in zebrafish and in cell lines. Together, we provide the evidence for the role of HDAC8 in hematopoietic stem cell differentiation in zebrafish and AML cell lines, suggesting HDAC8 inhibition as a therapeutic target in hematological malignancies. Accordingly, we demonstrated the utility of a highly specific HDAC8 inhibition as a therapeutic strategy in combination with standard chemotherapy.

**Keywords:** HDAC8, AML, PCI-34051, zebrafish, p53, WNT

## INTRODUCTION

Acute myeloid leukemia (AML) is a group of heterogeneous malignant hematological disorders underlain by genetic and epigenetic changes in hematopoietic stem cells (HSCs) and myeloid progenitors causing an imbalance between survival, proliferation and differentiation. The net effect of all changes is the accumulation of unfunctional myeloid cells, termed blasts, in the bone marrow. AML is the most frequent acute leukemia type in adults and, currently, it is curable in 35–40% of patients under 60 years of age and only in 5–15% of patients older than 60 years (Döhner et al., 2015).

Histone deacetylase 8 (HDAC8) is a ubiquitously expressed class I HDAC (Buggy et al., 2000; Hu et al., 2000; Van Den Wyngaert et al., 2000). Unlike other class I HDACs, it localizes both in the nucleus and in the cytoplasm (Li et al., 2014), lacks the C-terminal protein-binding domain



(Somoza et al., 2004) and is characterized by a peculiar negative regulation of its activity by cAMP-dependent protein kinase (PKA) (Lee et al., 2004), which suggests a functional specialization. HDAC8 has been demonstrated to target non-histone proteins, such as the structural maintenance of chromosome 3 (SMC3) cohesin protein, retinoic acid induced 1 (RAI1) and p53, thus regulating diverse processes (Deardorff et al., 2012; Wu et al., 2013; Olson et al., 2014). HDAC8 is either overexpressed or dysregulated in cancers, such as neuroblastoma, breast cancer, colon cancer (Nakagawa et al., 2007; Oehme et al., 2009; Park et al., 2011) and hematological malignancies. In particular, HDAC8 expression was found to be increased in primary cells from childhood acute lymphoblastic leukemia patients (Moreno et al., 2010), in adult T cell leukemia/lymphoma (Higuchi et al., 2013) and human myeloma cell lines (Mithraprabhu et al., 2014). HDAC8 was demonstrated to interact with CBF $\beta$ -SMMHC fusion protein, resulting from the inversion of chromosome 16 [inv(16)] (Durst et al., 2003). The interaction of both HDAC8 and p53 with inv(16) fusion protein leads to increased deacetylation and consequent inhibition of p53, which promotes survival and proliferation of inv(16)+ AML CD34+ cells (Qi et al., 2015). Interestingly, high HDAC8 expression was detected not only in inv(16)+ AML CD34+ cells, but also in non-inv(16)+ AML CD34+ cells, suggesting a more general involvement of HDAC8 in AML development (Qi et al., 2015). The role of HDAC8 in AML onset is further supported by a recent finding of it playing a crucial role in maintaining long-term HSC under stress condition by inhibiting p53 (Hua et al., 2017).

Histone deacetylase inhibitors (HDACi) possess an anticancer activity through the induction of apoptosis and cell cycle arrest (Eckschlager et al., 2017) in solid and hematological tumors (Ceccacci and Minucci, 2016; Imai et al., 2016). However, the use of HDACi is still limited due to the safety issues as side effects, including fatigue, diarrhea and thrombocytopenia, have been observed following their administration (Subramanian et al., 2010). Such toxicity is most likely related to the lack of selectivity of most of these drugs that act as pan-HDACi. In order to improve the outcome of the therapy and reduce side effects, compounds targeting specific HDAC isoforms are needed.

The distinctive structure of HDAC8, in comparison to others class I HDAC family members, allowed the development of high specific HDAC8 inhibitor PCI-34051 (hereafter PCI) (Balasubramanian et al., 2008), previously tested in T-cell lymphoma (Balasubramanian et al., 2008) and AML (Qi et al., 2015). The aim of this project was to explore the feasibility of HDAC8 inhibition as a therapeutic approach in AML. To this end, we generated a zebrafish (*Danio rerio*) model for Hdac8 overexpression that displayed a hematopoietic phenotype characterized by an increase in the hematopoietic stem/progenitor cells (HSPCs) population that could be rescued by PCI treatment. In parallel, we assessed the response of AML cell lines (OCI-AML5, HL60, PLB985, THP-1, and AML193) to PCI. We observed that PCI elicits apoptosis in THP-1 cell line and in the zebrafish embryos overexpressing Hdac8, while it induces cell cycle arrest in p53-null HL60 cells, prompting a search of alternative mechanisms explaining PCI action in the absence of p53. We, thus, demonstrated an involvement of the canonical

Wnt signaling. Our results suggest that selective inhibition of HDAC8 by PCI may be a valuable therapeutic approach for the treatment of AML patients.

## MATERIALS AND METHODS

### Zebrafish Embryos

Zebrafish (*D. rerio*) were maintained at the University of Milan, Via Celoria 26 – 20133 Milan, Italy (Autorizzazione Protocollo n. 295/2012-A – December 20, 2012) and Cogentech s.c.a.r.l. via Adamello 16 – 20139 Milan, Italy (Autorizzazione Protocollo n. 007894 – May 29, 2018). Zebrafish strains AB, Tg(*CD41:GFP*), Tg(*TOPdGFP*) and p53<sup>M214K</sup> (Dorsky et al., 2002; Berghmans et al., 2005; Lin et al., 2005) were maintained according to international (EU Directive 2010/63/EU) and national guidelines (Italian decree No 26 of the 4th of March 2014). Embryos were staged and used until 5 days post fertilization, a time windows in which zebrafish is not considered an animal model according to national guidelines (Italian decree No 26 of the 4th of March 2014). Embryos were staged as described in Kimmel et al. (1995) and raised in fish water (Instant Ocean, 0.1% Methylene Blue) at 28°C in Petri dishes, according to established techniques. Embryonic ages are expressed in hours post fertilization (hpf) and days post fertilization (dpf). To prevent pigmentation, 0.003% 1-phenyl-2-thiourea (PTU, Sigma-Aldrich, St. Louis, MI, United States) was added to the fish water. Embryos were anesthetized with 0.016% tricaine (Ethyl 3-aminobenzoate methanesulfonate salt, Sigma-Aldrich) before proceeding with experimental protocols.

### Zebrafish Microinjection and Treatment

Injections were carried out on 1- to 2-cell stage embryos. Zebrafish *hdac8* full-length mRNA was injected at the concentration of 500 pg/embryo as previously described (Bottai et al., 2019). As a control the membrane red fluorescent protein (*mrfp*) coding mRNA was injected at the same concentration. Alternatively, in double immunofluorescence staining analyses, we injected water as a control. For canonical Wnt inhibition, zebrafish *dkk1b* mRNA was injected at the concentration of 50 pg/embryo (Mazzola et al., 2019). PCI treatment were done in 24-well plates, 30 embryos/well. PCI was added to fish water at the concentration of 150  $\mu$ M PCI and embryos were kept at 28°C in the dark for 24 h. Equal concentration of DMSO was used as a control.

### FACS Analysis in Zebrafish

Embryos dissociation was achieved as described in Bresciani et al. (2018). FACS analysis were performed on Tg(*CD41:GFP*) zebrafish embryos at 3 dpf as previously described (Ma et al., 2011; Mazzola et al., 2019). We used Attune NxT (Thermo Fisher Scientific, Waltham, MA, United States) instrument equipped with software Kaluza (Beckman Coulter, Brea, CA, United States) for the analysis. AB wild-type embryos were used to set the gate to exclude auto-fluorescence of cells. The gate for GFP low/high cells was set on control Tg(*CD41:GFP*) embryos to distinguish a GFP<sub>low</sub> population representing around 0.2% of total cells, as

previously reported (Mazzola et al., 2019), and applied to all categories analyzed.

### Immunofluorescence

Embryos were fixed overnight in 4% paraformaldehyde (Sigma-Aldrich) in PBS at 4°C. For single-color staining, we used rabbit anti-GFP 1:500 (NC9589665, Torrey Pines Biolab, Houston, TX, United States) as primary antibody and Alexa Fluor 488-conjugated goat anti-rabbit IgG 1:400 (A11008, Invitrogen Life Technologies, Carlsbad, CA, United States) as secondary antibody. For dual staining, we took advantage of mouse anti-GFP 1:2000 (MAB3580, Merck-Millipore, Burlington, MA, United States), rabbit anti-histone H3 (phospho S10) 1:200 (ab5176, Abcam, Cambridge, United Kingdom), and rabbit anti-cleaved caspase 3 1:100 (9664, Cell Signaling Technologies, Danvers, MA, United States) as primary antibodies and Alexa Fluor 488-conjugated goat anti-mouse IgG and Alexa 546-conjugated goat anti-rabbit IgG 1:400 (A11001 and A11010, Invitrogen Life Technologies) as secondary antibodies. Embryos were equilibrated and mounted in 85% glycerol solution in PBS and imaged using a "TCS-SP2" confocal microscope (Leica, Wetzlar, Germany), with 20× oil immersion 9 objective, 488 nm argon ion and 405 nm diode lasers. Single stack images were acquired for each sample. Images were processed using Adobe Photoshop software. Quantification was performed by using the ImageJ software. For dual staining, we counted the total number of both GFP<sup>+</sup> cells and double positive cells. The percentage of double positive cells was calculated as the ratio of double positive/total GFP<sup>+</sup>.

### Reverse Transcription and Real-Time Quantitative PCR

Total RNA was extracted from cells or zebrafish whole embryos (at least 30 embryos) with NucleoZOL reagent (Macherey-Nagel, Düren, Germany), according to the manufacturer's instructions and treated with RQ1 RNase-free DNase (Promega, Madison, WI, United States). cDNA was synthesized using the GoScript Reverse Transcription Kit (Promega), as specified by the manufacturer's instructions. qPCR analyses were performed with the GoTaq qPCR Master Mix (Promega) on the Bio-Rad iQ5 Real Time Detection System (Bio-Rad, Hercules, CA, United States) and Quantum Studio 5 (Thermo Fisher). Gene expression changes were calculated with the  $\Delta\Delta C_t$  method. We used *GAPDH* for AML cells and *rpl8* and  $\beta$ -*actin* for zebrafish as internal control. Primer sequences are listed in **Supplementary Table 1**.

### Cell Lines PCI Treatment

OCI-AML5, HL60, PLB985, THP-1, and AML193 cell lines were originally obtained from ATCC/DSMZ repositories and since stored at the internal cell line bank at the Department of Experimental Oncology, IEO. Cell lines undergo regular authentication and mycoplasma testing. Cells were seeded at 10<sup>4</sup> cells/well in 96-well plates in 100  $\mu$ l of growth medium and allowed to grow for 24 h prior to treatment commencement. PCI was dissolved in DMSO, diluted in the appropriate culture medium and added into plates, as indicated. The concentration

range of PCI has been determined based on published data and ranged between 3.12 and 50  $\mu$ M (Balasubramanian et al., 2008; Qi et al., 2015). Seventy-two hours later, CellTiter-Glo assay (Promega) was performed as indicated in the manufacturer's instructions and read on GloMax (Promega) plate reader. Cells treated with DMSO (0.2% in appropriate medium) were used as a control.

### In vitro Proliferation

Cells were seeded in duplicate at 10<sup>5</sup> cells/ml and allowed to grow for 24 h at 37°C, 5% CO<sub>2</sub>, 95% humidity. Then cells were treated with 50  $\mu$ M PCI or with 0.2% DMSO (control). At 12, 24, 48, and 72 h, both viable and dead cells were counted under an inverted-light microscope (Leica) following 0.4% trypan blue staining.

### Cell Cycle Analysis

Cells were seeded at 10<sup>5</sup> cells/ml and then treated with DMSO or with 50  $\mu$ M of PCI for 48 h. One-million of viable cells were harvested after 12, 24, and 48 h, washed once with cold PBS, fixed in 70% of ice-cold ethanol dropwise and kept on ice for 30 min. Next, cells were washed in 1% BSA in PBS and stained overnight with DNA staining solution containing 250  $\mu$ g/ml of RNase and 5  $\mu$ g/ml propidium iodide (PI) at 4°C. Data analysis was done using flow cytometry (FACSCelesta, FlowJo10 software).

### Apoptosis Assay

Cells were seeded at 10<sup>5</sup> cells/ml and then treated with DMSO or with 50  $\mu$ M of PCI for 72 h. A total of 50 × 10<sup>4</sup> cells were harvested after 72 h, washed once with cold PBS and then with annexin buffer. Cells were resuspended in 100  $\mu$ l annexin-APC diluted 1:50 in annexin buffer and incubated 1 h at room temperature in the dark. Next, cells were washed once with annexin buffer and resuspended in 1 × PBS. Cells were stained for maximum 5 min with PI solution. Data analysis was done using flow cytometry (FACSCelesta, FlowJo10 software).

### Combination Treatment

Cells were seeded at 10<sup>4</sup> cells/well in 96-well plates and allowed to grow for 24 h prior to treatment commencement. Drug concentrations ranged from 0.78 to 100  $\mu$ M and from 0.078 to 10  $\mu$ M for PCI and cytarabine, respectively. Cells were treated with all concentrations of single agents and in combination setting, in which decreasing concentrations of each compound were used together (**Supplementary Figure 5**). The combination index (CI), based on the Bliss Independence model, was calculated as  $CI = \frac{E_A + E_B - E_{AB}}{E_A E_B}$ , where  $E_A$  indicates the effect of compound A,  $E_B$  indicates the effect of compound B and  $E_{AB}$  the effect of the combination of both compounds.  $CI < 1$  indicates synergism;  $CI = 1$  indicates an additive effect, while  $CI > 1$  indicates antagonism (Fouquier and Guedj, 2015).

### Statistical Analysis

Each experiment was performed at least twice (biological replicates). A minimum number of 15 embryos was analyzed in each imaging experiment, while RNA was extracted from a minimum of 30 animals. PCI treatment outcome was assessed



on at least 30 zebrafish embryos. For qPCR analysis on zebrafish, experiments were performed on at least three different independent experiments (batches of embryos deriving from different matings). The statistical significance was determined using two-sided Student's *t*-test when comparing two groups and one-way ANOVA test followed by Tukey *post hoc* correction when comparing three groups. One-sample *t*-test was used when control group was set to a defined value of 1. Data were considered significant if  $p < 0.05$ .

## RESULTS

### Hdac8 Overexpression in Zebrafish Leads to HSPCs Expansion and Its Inhibition Elicits Apoptosis and Rescues the Phenotype

CD34+ cells derived from inv(16)+ AML patients express high levels of HDAC8 (Qi et al., 2015). We generated a zebrafish model for Hdac8 overexpression by injecting embryos with the full-length zebrafish *hdac8* mRNA (500 pg/embryo) to assess whether HDAC8 upregulation would alter hematopoietic phenotype *in vivo*. The injection of the *hdac8*-mRNA, although increasing the *hdac8* transcript and protein levels (Supplementary Figures S1A,B), did not alter the general morphology of the embryo or organ size (Supplementary Figures S1C–E) but specifically impact on the hematopoietic phenotype. In this regard, to obtain an easy read-out of the hematopoietic phenotype, we performed *hdac8* overexpression in the *Tg(CD41:GFP)* transgenic line that expresses GFP protein in HSPCs, Lin et al. (2005); Supplementary Figures S1F,G, and we assessed the expression of the HSC transcription factor markers *c-Myb*, *gata2b* and *Runx1*, and of the immature myeloid cells *pu.1* that resulted upregulated following Hdac8 ectopic expression (Supplementary Figures 1H,I). Confocal images of the caudal hematopoietic tissue (CHT) in 3 dpf embryos (Figure 1A), showed an increase in HSPC population upon Hdac8 overexpression in comparison to controls (Figures 1B–C). This effect was specific, as we obtained a significant reduction of HSPCs in *hdac8* mRNA-injected embryos treated with PCI (Figure 1D). We then quantified HSPC number by enumerating GFP<sub>low</sub>-HSPCs in the three categories of embryos by flow cytometry (Ma et al., 2011; Mazzola et al., 2019). GFP<sub>low</sub>-HSPCs were significantly increased in *hdac8*-injected embryos compared to controls and were reduced when treated with PCI (Figures 1E–H). We also evaluated the effect of PCI on zebrafish HSPCs in the absence of Hdac8 overexpression as a control. Immunofluorescence and FACS analyses for the HSPCs in the *Tg(CD41:GFP)* line and gene expression analyses for the HSC marker *cmyb* indicated a decrease of HSPCs in PCI-treated embryos compared to control embryos (Supplementary Figures 2A–F). To assess whether the expansion in HSPCs population following Hdac8 ectopic expression is indicative to a pre-leukemic state and if these cells possess higher self-renewal ability compared to their differentiated counterparts,

we performed dual immunofluorescence with GFP (in green) and phospho-histone H3 (PH3, in red) in the *Tg(CD41:GFP)* embryos at 3 dpf. The ectopic expression of Hdac8 induced an increased proliferation of HSPCs in comparison to controls, that was reduced following PCI treatment (Figures 1I–L).

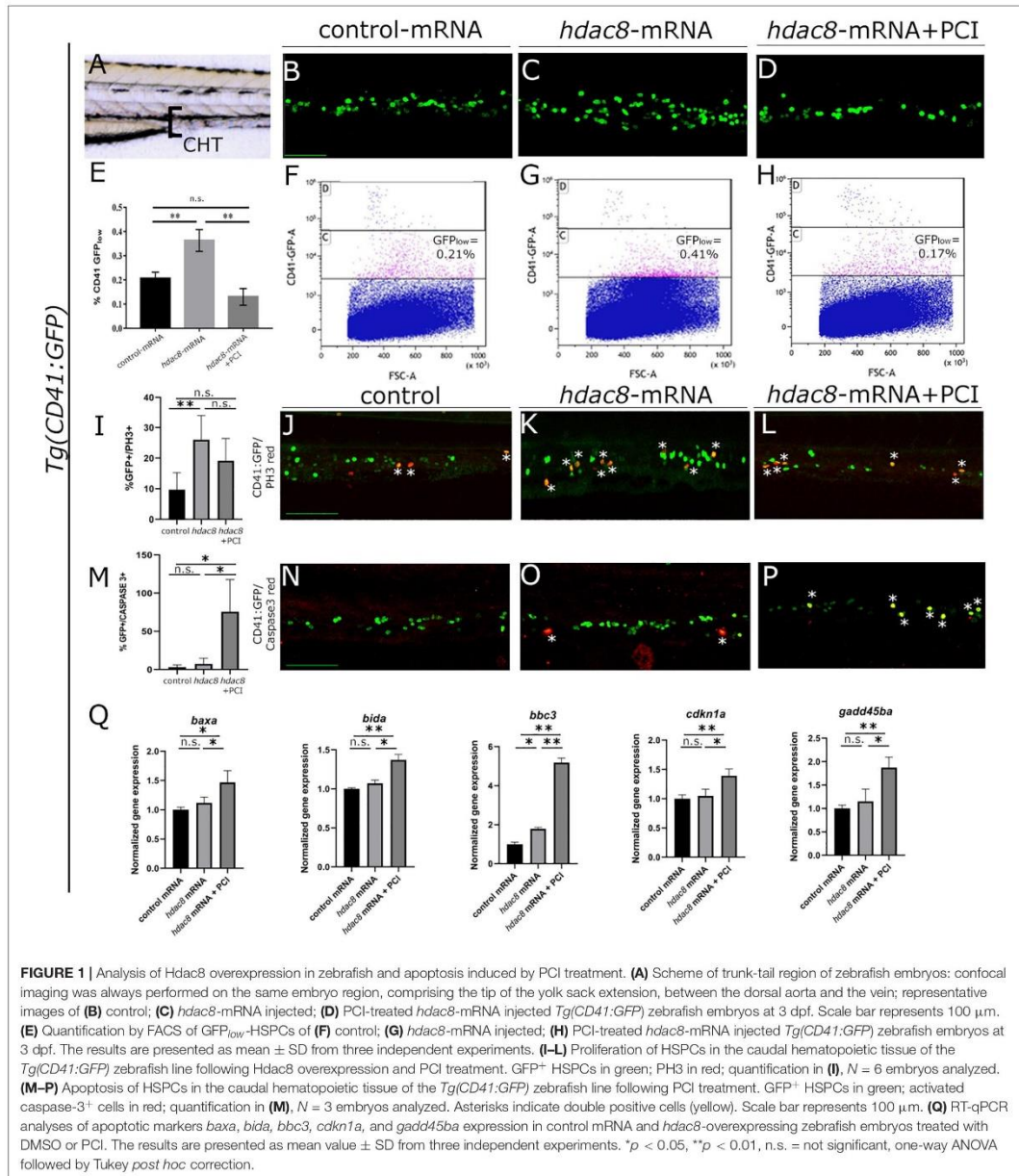
Since p53 is a target of HDAC8 and studies indicate that PCI treatment determines cell cycle arrest and induction of apoptosis in *in vivo* (Oehme et al., 2009) and *in vitro* (Rettig et al., 2015) models, we verified whether PCI treatment determines apoptosis also in zebrafish (Supplementary Figures 2G,H). Thus, to assess PCI-mediated apoptosis specifically in the HSPC population which was expanded following *hdac8*-overexpression, we evaluated caspase-3 activation by dual immunofluorescence in Hdac8-overexpressing *Tg(CD41:GFP)* zebrafish embryos at 3 dpf treated or not with PCI. We observed an increase of caspase-3<sup>+</sup>/GFP<sup>+</sup> HSPCs in PCI-treated *hdac8*-mRNA injected embryos compared to *hdac8*-mRNA-injected and control embryos (Figures 1M–P). This result was confirmed by the significant increase of expression levels of the p53 target genes (*baxa*, *bida*, *bbc3*, *cdkn1a*, and *gadd45ba*) by RT-qPCR in PCI-treated *hdac8*-mRNA injected embryos compared to both control mRNA- and *hdac8*-mRNA-injected embryos (Figure 1Q; Qi et al., 2015). Taken together, these results indicate that Hdac8 overexpression in zebrafish determines an expansion of HSPC population and that PCI treatment induces a block in cell expansion activating p53-mediated apoptosis.

### PCI Exerts Cytostatic and Cytotoxic Effect on AML Cell Lines

To evaluate the effects of HDAC8 inhibition also in human myeloid cells, we selected five AML cell lines expressing HDAC8 (OCI-AML5, HL60, PLB985, THP-1, and AML193). We treated them once for 72 h with decreasing concentrations of PCI and evaluated the viability using CTG luminescence assay, an indicator of metabolically active cells. PCI decreased the viability of HL60, PLB985, THP-1, and AML193 cell lines while OCI-AML5 seemed less sensitive to the treatment (Figure 2A).

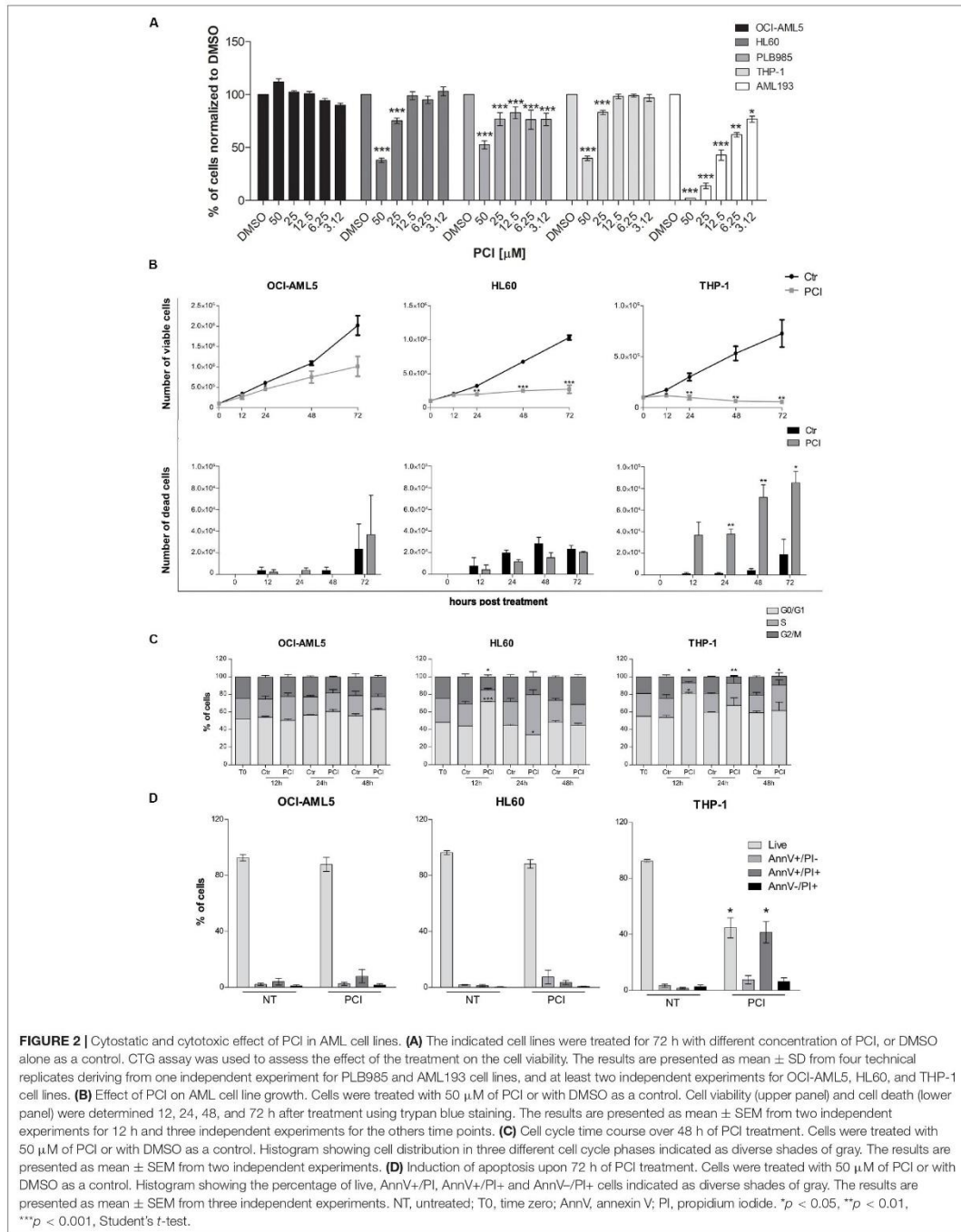
We excluded from further analyses the PLB985 cell line since it is a sub-clone of HL60 and AML193 childhood AML cell line as all the other cell lines derive from adult AML patients. We validated HDAC8 expression levels by means of RT-qPCR and western blot analyses. HL60 and THP-1 expressed significantly higher HDAC8 mRNA than OCI-AML5 by RT-qPCR (Supplementary Figure 3A). Western blot analysis also indicated higher HDAC8 protein levels in HL60 and THP-1 than in OCI-AML5 (Supplementary Figure 3B). To determine whether PCI elicits cytostatic or cytotoxic effect, we treated the selected cell lines with 50 μM of PCI or with DMSO as a control for 12, 24, 48, and 72 h and counted daily following trypan blue staining. No significant effect on cell growth was observed in the less-PCI-sensitive OCI-AML5 cell line (Figure 2B), although PCI treatment increased the levels of acetylated SMC3 (ac-SMC3), a specific HDAC8 target (Supplementary Figure 3C). By contrast, PCI exerted a cytostatic effect in HL60 cell line and caused cell death in THP-1 cells, as indicated by viable and dead cell





count (Figure 2B), which spurred us to investigate how PCI treatment impacted cell cycle. To this end, we treated AML cell lines with 50  $\mu$ M PCI for 12, 24, and 48 h and analyzed DNA content by PI staining. At 12 h PCI treatment resulted in a

block in the G0–G1 phase of over 70 and 80% of HL60 and THP-1 cells, respectively, while we did not detect any variations between untreated and treated OCI-AML5 samples (Figure 2C). Cell cycle arrest following PCI treatment in HL60 and THP-1



cell lines was underlain by a decrease in *CyclinD1* (*CCND1*) and *CMYC* expression (Supplementary Figure 4). Next, we evaluated apoptosis induction using Annexin V/PI staining and we demonstrated that PCI treatment induces apoptosis only in THP-1 cells as attested by increased percentages of Annexin V<sup>+</sup>/PI<sup>+</sup> positive population corresponding to late apoptotic cells at 72 h. Indeed, the HL60 cells responded to PCI inhibition but cannot undergo apoptosis lacking functional p53 (Wolff and Rotter, 1985; Figure 2D).

Taken together, these data indicate that PCI treatment impacts on AML cell survival causing cell cycle arrest followed by apoptosis when p53 is functional.

### PCI Synergizes With Cytarabine in AML Cell Lines

Combination therapy allows for dose reduction, lowers the incidence and severity of side effects and prevents the development of resistance. We treated AML cell lines with cytarabine, an agent used at the frontline of AML treatment, alone or together with PCI to assess whether their combination resulted in synergy, additivity or antagonism as an *in vitro* indicator of a potential advantage of combination over single-agent treatment. OCI-AML5, HL60, and THP-1 cells were treated for 72 h with cytarabine at concentrations ranging from 0.078 to 10  $\mu$ M and PCI at concentration range of 0.78–100  $\mu$ M alone or together mixing decreasing concentrations of each compound (Supplementary Figure 5). Based on CI, a synergistic effect was observed for all AML cell lines when combining 0.35  $\mu$ M cytarabine with 25  $\mu$ M PCI. The combination of cytarabine and PCI resulted in an effect that was greater than the sum of single treatment outcomes in OCI-AML5 and HL60 cell lines, whilst showing a dramatic combination effect in THP-1 cell line at a concentration of cytarabine that alone had no effect. In detail, in THP-1 cell line the combination resulted in 47% of cell death compared to 0% of cytarabine and 23.5% of PCI in single-agent setting (Figure 3).

These results might suggest that cytarabine doses can be reduced in combination therapy while eliciting the same inhibitory effect on cell proliferation.

### HDAC8 Inhibition Downregulates Canonical Wnt Pathway

We wished to identify a mechanism of action responsible for PCI-induced growth arrest in HL60 cells that responded to PCI inhibition without undergoing apoptosis being p53-null. Recently, we and others demonstrated that HDAC8 activates canonical Wnt pathway (Tian et al., 2015; Ferrari et al., 2019), which is frequently dysregulated in AML (Gruszka et al., 2019). We investigated whether Wnt signaling was affected by HDAC8 inhibition in AML cell line. We analyzed by RT-qPCR the expression levels of canonical Wnt pathway inhibitors *NKD1* and *PPP2R2B*, previously reported to be downregulated by forced *HDAC8* expression and upregulated following PCI treatment (Tian et al., 2015). We observed that the expression levels of both *NKD1* and *PPP2R2B* increased following PCI treatment in PCI sensitive cell lines HL60 and THP-1, indicating

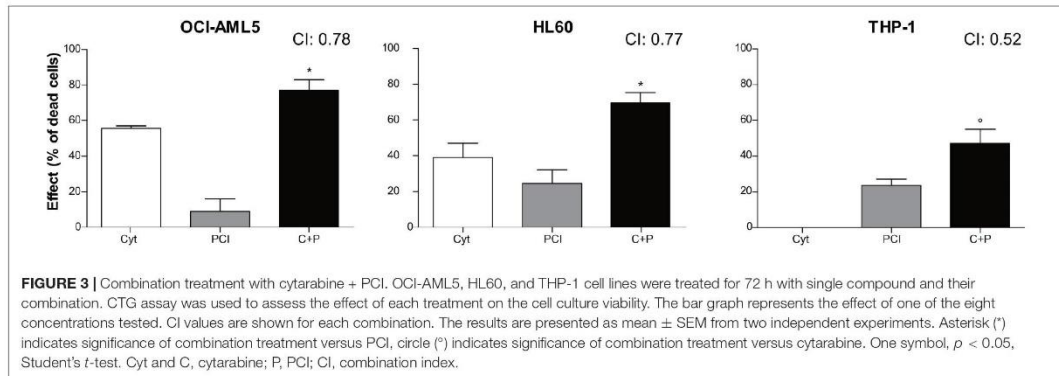
that HDAC8-mediated downregulation of the canonical Wnt signaling could be the cause of cell cycle arrest in these cell lines. Interestingly, the Wnt pathway was not modulated in the less-sensitive OCI-AML5 cells, confirming the specificity of HDAC8 inhibition on Wnt regulation (Figure 4A).

To verify that the downregulation of the Wnt pathway is p53-independent, we assessed Wnt pathway modulation in p53 mutant zebrafish embryos, which mimicked the p53-null HL60 condition. Thus, we took advantage of a homozygous zebrafish p53<sup>M214K</sup> mutant line, which lacks functional p53 (Berghmans et al., 2005), and we observed that, although the expression of the apoptotic markers *bida* and *cdkn1a* was not affected as expected in a p53 null background, a decrease of the expression of Wnt inhibitors *axin2*, *nkd1*, and *ppp2r2b* was observed in Hdac8-overexpressed mutant embryos compared to controls while PCI treatment restored the expression of Wnt inhibitors (Figure 4B). To further demonstrate that Hdac8 modulates Wnt signaling, we evaluated the regulation of canonical Wnt signaling by assessing the levels of active- and total- $\beta$  catenin by western blot techniques (Supplementary Figure 6), and we used a zebrafish canonical Wnt reporter transgenic line *Tg(TOPdGFP)* (Dorsky et al., 2002). Following *hdac8* overexpression, canonical Wnt signaling was increased also in the HSPCs in the CHT region, while it was switched off following PCI administration (Figure 4C and Supplementary Figure 7). Interestingly, a similar reduction in the HSPCs in the CHT region of *Tg(TOPdGFP)* or *Tg(CD41:GFP)* zebrafish embryos was achieved following inhibition of the canonical Wnt signaling in *hdac8*-mRNA-injected embryos by means of co-injection of the *dkk1b* transcript (50 pg/embryo) (Mazzola et al., 2019; Figure 4D,E and Supplementary Figure 7). Taken together, these data demonstrate that HDAC8 activates canonical Wnt pathway that, in turns, regulates hematopoietic cell proliferation (Richter et al., 2017; Mazzola et al., 2019). PCI administration downregulates Wnt signaling and reduces HSPCs, an important finding as Wnt downregulation is a clinical treatment currently in use for AML patients.

## DISCUSSION

Aberrations in epigenetic regulators contribute to cancer, including leukemia insurgence, hence, the use of epigenetic modifiers may comprise a promising therapeutic approach (Nakagawa et al., 2007; Zhang et al., 2012). Epigenetic defects are generally reversible, as opposed to genetic changes, providing a strong rationale for a pharmaceutical intervention. Low level of acetylation due to high expression of HDACs (Nakagawa et al., 2007; Wang et al., 2016) is one of the most frequent epigenetic modifications found in cancer cells. HDACs are more expressed in hematological malignancies including AML than in normal hematopoietic cells (Bradbury et al., 2005; Marquard et al., 2009), and we demonstrated that forced expression of Hdac8 in zebrafish embryos induced an increase in HSPC number that can be rescued with the use of a specific HDAC8 inhibitor. HDACi have been used as therapeutic agents in AML, myelodysplastic syndromes, lymphoma, and chronic lymphoblastic leukemia (Melnick and Licht, 2002; Altucci and Minucci, 2009; Gloghini et al., 2009);





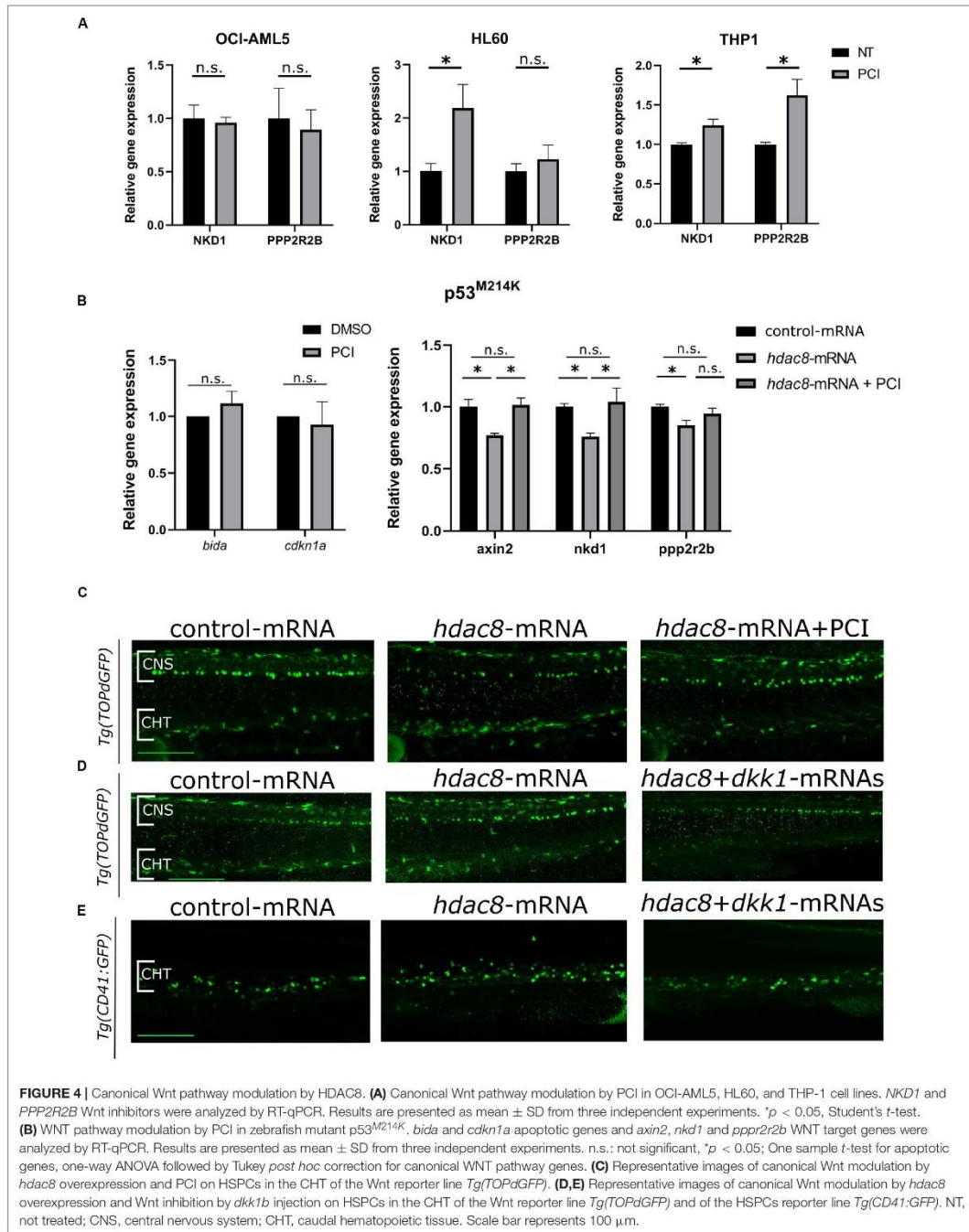
however, monotherapy elicits modest effects. There are several possible reasons behind this failure. For example, HDACi exert different outcomes depending on timing of administration and differentiation stage of the tumor (Kuendgen et al., 2011; Garcia-Manero et al., 2012; Novotny-Diermayr et al., 2012; Romanski et al., 2012; Xie et al., 2012; Candelaria et al., 2017; Huang and Zong, 2017; Young et al., 2017). In addition, the vast majority of preclinical and clinical studies deploying HDACi for anti-cancer treatment involved unselective inhibitors targeting all HDACs (pan-HDACi) with broad spectrum of side effects and toxicity, thus calling for exploitation of agents that specifically block individual HDACs. PCI is a specific small molecule inhibitor endowed with 200-fold higher selectivity for HDAC8 than for other HDACs; it is more effective and less toxic than pan-HDACi (Balasubramanian et al., 2008).

We demonstrated that HSPCs are sensitive to selective HDAC8 inhibition both in a zebrafish embryological context as well as in adult derived-AML cell lines. This is in agreement with findings of Qi et al. (2015) that showed that leukemic cells bearing *inv(16)* linked to high expression levels of HDAC8 (5–12 times that of CD34+ cells from healthy donors) were particularly responsive to treatment with PCI, although also non-*inv(16)* AML blasts showed a degree of sensitivity. Since the hierarchy of HSPCs is finely tuned during development until adulthood and subjected to different regulatory cues, our demonstration that the HDAC8 inhibition is effective on HSPCs during embryogenesis and in the adult, provides a common mechanism against HSPCs self-renewal and amplification and an attractive therapeutic treatment for the future.

We found that PCI elicits cytostatic or cytotoxic effect in AML sensitive cell lines. Mechanistically, sensitive cells undergo cell cycle arrest, followed by apoptosis when expressing p53. Cell cycle arrest in the G0/G1 phase and induction of p21WAF1/CIP1 expression was previously observed in neuroblastoma cells upon HDAC8 silencing, while an increase of cells in G2/M phase of the cell cycle was reported in hepatocellular cancer cells treated with PCI (Tian et al., 2016). p53 is a known HDAC8 target and its aberrant deacetylation by HDAC8 disables p53 function and promotes leukemic transformation (Wu et al., 2013). HDAC8

knockout or pharmacological inhibition effectively restores p53 acetylation and activity inducing apoptosis in *inv(16)*<sup>+</sup> AML CD34<sup>+</sup> cells (Qi et al., 2015). Similarly, we observed p53-dependent apoptosis specifically in CD41-GFP<sup>+</sup> hematopoietic compartment following PCI treatment of zebrafish embryos overexpressing Hdac8. This population was increased in zebrafish embryos upon Hdac8 overexpression. Our findings are consistent with literature data demonstrating that HDAC8 regulates HSPC survival under hematopoietic stress by modulating p53 activity (Liu et al., 2009; Asai et al., 2011, 2012). Our experiments show that THP-1 cells underwent apoptosis, while the p53-null HL60 cell line remained blocked in the G0/G1 phase of the cell cycle. This led us to consider alternative mechanisms of growth arrest elicited by PCI treatment. Studies show that canonical WNT signaling is activated by HDAC8 (Tian et al., 2015; Ferrari et al., 2019). We now show that canonical Wnt pathway is significantly downregulated both in cell lines and in zebrafish embryos following HDAC8 inhibition. Downregulation of canonical Wnt pathway by PCI has been described in a model of hepatocellular cancer, in which HDAC8 physically interacts with chromatin modifier EZH2 to repress Wnt antagonists, activating Wnt pathway. PCI treatment, instead, reduced active  $\beta$ -catenin and *cyclin D1* expression in this system. We showed that PCI downregulates Wnt signaling independently of p53 status; however, it does not kill cells unless p53 is functional (Tian et al., 2016).

We explored the possibility of performing combination treatment and combined cytarabine with PCI. The two compounds synergize in all cell lines treated, including the less-PCI-sensitive OCI-AML5 cells. Although we failed to reduce the concentration of PCI, in THP-1 cell line the synergy was observed when combining a dose of cytarabine that alone elicits no effect. This may indicate that AML patients with high HDAC8 and functional p53 may particularly benefit from this combination. Indeed, a recent study reported the efficacy of HDAC8 inhibition in combination with FLT3 inhibitor in suppressing FLT3-ITD<sup>+</sup> AML cells, thus sustaining the potential of combination treatment employing HDACi and standard chemotherapy (Long et al., 2020). Phase II and III



clinical trial results confirm that HDACi act more efficiently when combined with conventional chemotherapy. However, more studies are needed to understand the precise mechanism of action of the combination.

Taken together, our study validates the preclinical potential of specific inhibition of HDAC8 as a potent therapeutic approach in AML.

## DATA AVAILABILITY STATEMENT

The original contributions presented in the study are included in the article/Supplementary Material, further inquiries can be directed to the corresponding authors.

## AUTHOR CONTRIBUTIONS

AP, AM, CB, AG, and MA conceived and designed the experiments. MS, MM, and GD performed the experiments on zebrafish. AG and DV performed the experiments on AML cells. AQ and MT performed the FACS analyses on zebrafish. MS, MM, GD, and AP analyzed the data on zebrafish. AG, DV, and CB analyzed the data on AML cells. MS, AG, DV, and AP wrote the manuscript. AP, AM, and AG supervised the manuscript drafting.

## REFERENCES

- Altucci, L., and Minucci, S. (2009). Epigenetic therapies in haematological malignancies: searching for true targets. *Eur. J. Cancer* 45, 1137–1145. doi: 10.1016/j.ejca.2009.03.001
- Asai, T., Liu, Y., Bae, N., and Nimer, S. D. (2011). The p53 tumor suppressor protein regulates hematopoietic stem cell fate. *J. Cell. Physiol.* 226, 2215–2221. doi: 10.1002/jcp.22561
- Asai, T., Liu, Y., Di Giandomenico, S., Bae, N., Ndiaye-Lobry, D., Deblasio, A., et al. (2012). Necdin, a p53 target gene, regulates the quiescence and response to genotoxic stress of hematopoietic stem/progenitor cells. *Blood* 120, 1601–1612. doi: 10.1182/blood-2011-11-393983
- Balasubramanian, S., Ramos, J., Luo, W., Sirisawad, M., Verner, E., and Buggy, J. J. (2008). A novel histone deacetylase 8 (HDAC8)-specific inhibitor PCI-34051 induces apoptosis in T-cell lymphomas. *Leukemia* 22, 1026–1034. doi: 10.1038/leu.2008.9
- Berghmans, S., Murphey, R. D., Wienholds, E., Neubergh, D., Kutok, J. L., Fletcher, C. D. M., et al. (2005). Tp53 mutant zebrafish develop malignant peripheral nerve sheath tumors. *Proc. Natl. Acad. Sci. U.S.A.* 102, 407–412. doi: 10.1073/pnas.0406252102
- Bottai, D., Spreafico, M., Pistocchi, A., Fazio, G., Adami, R., Grazioli, P., et al. (2019). Modeling Cornelia de Lange syndrome in vitro and in vivo reveals a role for cohesin complex in neuronal survival and differentiation. *Hum. Mol. Genet.* 28, 64–73. doi: 10.1093/hmg/ddy329
- Bradbury, C. A., Khanim, F. L., Hayden, R., Bunce, C. M., White, D. A., Drayson, M. T., et al. (2005). Histone deacetylases in acute myeloid leukaemia show a distinctive pattern of expression that changes selectively in response to deacetylase inhibitors. *Leukemia* 19, 1751–1759. doi: 10.1038/sj.leu.24.03910
- Bresciani, E., Broadbridge, E., and Liu, P. (2018). An efficient dissociation protocol for generation of single cell suspension from zebrafish embryos and larvae. *MethodsX* 10, 1287–1290. doi: 10.1016/j.mex.2018.10.009
- Buggy, J. J., Sideris, M. L., Mak, P., Lorimer, D. D., McIntosh, B., and Clark, J. M. (2000). Cloning and characterization of a novel human histone deacetylase, HDAC8. *Biochem. J.* 350(Pt 1), 199–205. doi: 10.1042/0264-6021:3500199

AP supervised the research project. All authors contributed to the article and approved the submitted version.

## FUNDING

This work was supported by the Associazione Italiana per la Ricerca sul Cancro (AIRC) (MFAG#18714) and Piano Sostegno alla Ricerca PSR20119\_MAROZZI. The funders had no role in the study design, data collection and interpretation, or the decision to submit the work for publication.

## ACKNOWLEDGMENTS

We thank Alex Pezzotta, Ilaria Gentile, Marco Cafora, and Alessia Brix (University of Milan) for their priceless support in experimental procedures.

## SUPPLEMENTARY MATERIAL

The Supplementary Material for this article can be found online at: <https://www.frontiersin.org/articles/10.3389/fcell.2020.00844/full#supplementary-material>

- Candelaria, M., Burgos, S., Ponce, M., Espinoza, R., and Dueñas-Gonzalez, A. (2017). Encouraging results with the compassionate use of hydralazine/valproate (TRANSKRIP™) as epigenetic treatment for myelodysplastic syndrome (MDS). *Ann. Hematol.* 96, 1825–1832. doi: 10.1007/s00277-017-3103-x
- Ceccacci, E., and Minucci, S. (2016). Inhibition of histone deacetylases in cancer therapy: lessons from leukaemia. *Br. J. Cancer* 114, 605–611. doi: 10.1038/bjc.2016.36
- Deardorff, M. A., Bando, M., Nakato, R., Watrin, E., Itoh, T., Minamino, M., et al. (2012). HDAC8 mutations in Cornelia de Lange syndrome affect the cohesin acetylation cycle. *Nature* 489, 313–317. doi: 10.1038/nature11316
- Döhner, H., Weisdorf, D. J., and Bloomfield, C. D. (2015). Acute myeloid leukemia. *N. Engl. J. Med.* 373, 1136–1152. doi: 10.1056/NEJMra1406184
- Dorsky, R. I., Sheldahl, L. C., and Moon, R. T. (2002). A transgenic Lef1/β-catenin-dependent reporter is expressed in spatially restricted domains throughout zebrafish development. *Dev. Biol.* 241, 229–237. doi: 10.1006/dbio.2001.0515
- Durst, K. L., Lutterbach, B., Kummalue, T., Friedman, A. D., and Hiebert, S. W. (2003). The inv(16) fusion protein associates with corepressors via a smooth muscle myosin heavy-chain domain. *Mol. Cell. Biol.* 23, 607–619. doi: 10.1128/MCB.23.2.607-619.2003
- Eckschlager, T., Plch, J., Stiborova, M., and Hrabeta, J. (2017). Histone deacetylase inhibitors as anticancer drugs. *Int. J. Mol. Sci.* 18, 1–25. doi: 10.3390/ijms18071414
- Ferrari, L., Bragato, C., Brioschi, L., Spreafico, M., Esposito, S., Pezzotta, A., et al. (2019). HDAC8 regulates canonical Wnt pathway to promote differentiation in skeletal muscles. *J. Cell. Physiol.* 234, 6067–6076. doi: 10.1002/jcp.27341
- Fouquier, J., and Guedj, M. (2015). Analysis of drug combinations: current methodological landscape. *Pharmacol. Res. Perspect.* 3:e00149. doi: 10.1002/prp2.149
- Garcia-Manero, G., Tambaro, F. P., Bekele, N. B., Yang, H., Ravandi, F., Jabbour, E., et al. (2012). Phase II trial of vorinostat with idarubicin and cytarabine for patients with newly diagnosed acute myelogenous leukemia or myelodysplastic syndrome. *J. Clin. Oncol.* 30, 2204–2210. doi: 10.1200/JCO.2011.38.3265



- Gloghini, A., Buglio, D., Khaskhely, N. M., Georgakis, G., Orłowski, R. Z., Neelapu, S. S., et al. (2009). Expression of histone deacetylases in lymphoma: implication for the development of selective inhibitors. *Br. J. Haematol.* 147, 515–525. doi: 10.1111/j.1365-2141.2009.07887.x
- Gruszka, A. M., Valli, D., and Alcalay, M. (2019). Wnt signalling in acute myeloid leukaemia. *Cells* 8:1403. doi: 10.3390/cells8111403
- Higuchi, T., Nakayama, T., Arai, T., Nishio, K., and Yoshie, O. (2013). SOX4 is a direct target gene of FRA-2 and induces expression of HDAC8 in adult T-cell leukemia/lymphoma. *Blood* 121, 3640–3649. doi: 10.1182/blood-2012-07-441022
- Hu, E., Chen, Z., Fredrickson, T., Zhu, Y., Kirkpatrick, R., Zhang, G. F., et al. (2000). Cloning and characterization of a novel human class I histone deacetylase that functions as a transcription repressor. *J. Biol. Chem.* 275, 15254–15264. doi: 10.1074/jbc.M908988199
- Hua, W. K., Qi, J., Cai, Q., Carnahan, E., Ramirez, M. A., Li, L., et al. (2017). HDAC8 regulates long-term hematopoietic stem-cell maintenance under stress by modulating p53 activity. *Blood* 130, 2619–2630. doi: 10.1182/blood-2017-03-771386
- Huang, R., and Zong, X. (2017). Aberrant cancer metabolism in epithelial/mesenchymal transition and cancer metastasis: mechanisms in cancer progression. *Crit. Rev. Oncol. Hematol.* 115, 13–22. doi: 10.1016/j.critrevonc.2017.04.005
- Imai, Y., Maru, Y., and Tanaka, J. (2016). Action mechanisms of histone deacetylase inhibitors in the treatment of hematological malignancies. *Cancer Sci.* 107, 1543–1549. doi: 10.1111/cas.13062
- Kimmel, C. B., Ballard, W. W., Kimmel, S. R., Ullmann, B., and Schilling, T. F. (1995). Stages of embryonic development of the zebrafish. *Dev. Dyn.* 203, 253–310. doi: 10.1002/aja.1002030302
- Kuendgen, A., Bug, G., Ottmann, O. G., Haase, D., Schanz, J., Hildebrandt, B., et al. (2011). Treatment of poor-risk myelodysplastic syndromes and acute myeloid leukemia with a combination of 5-azacytidine and valproic acid. *Clin. Epigenet.* 2, 389–399. doi: 10.1007/s13148-011-0031-9
- Lee, H., Rezaei-Zadeh, N., and Seto, E. (2004). Negative regulation of histone deacetylase 8 activity by cyclic AMP-Dependent protein Kinase A. *Mol. Cell Biol.* 24, 765–773. doi: 10.1128/mcb.24.2.765-773.2004
- Li, J., Chen, S., Cleary, R. A., Wang, R., Gannon, O. J., Seto, E., et al. (2014). Histone deacetylase 8 regulates cortactin deacetylation and contraction in smooth muscle tissues. *Am. J. Physiol. Cell Physiol.* 307, 288–295. doi: 10.1152/ajpcell.00102.2014
- Lin, H. F., Traver, D., Zhu, H., Dooley, K., Paw, B. H., Zon, L. I., et al. (2005). Analysis of thrombocyte development in CD41-GFP transgenic zebrafish. *Blood* 106, 3803–3810. doi: 10.1182/blood-2005-01-0179
- Liu, Y., Elf, S. E., Miyata, Y., Sashida, G., Liu, Y., Huang, G., et al. (2009). p53 regulates hematopoietic stem cell quiescence. *Cell Stem Cell* 4, 37–48. doi: 10.1016/j.stem.2008.11.006
- Long, J., Jia, M.-Y., Fang, W.-Y., Chen, X.-J., Mu, L.-L., Wang, Z.-Y., et al. (2020). FLT3 inhibition upregulates HDAC8 via FOXO to inactivate p53 and promote maintenance of FLT3-ITD+ acute myeloid leukemia. *Blood* 135, 1472–1483. doi: 10.1182/blood.2019003538
- Ma, D., Zhang, J., Lin, H. F., Italiano, J., and Handin, R. I. (2011). The identification and characterization of zebrafish hematopoietic stem cells. *Blood* 118, 289–297. doi: 10.1182/blood-2010-12-327403
- Marquard, L., Poulsen, C. B., Gjerdrum, L. M., De Nully Brown, P., Christensen, I. J., Jensen, P. B., et al. (2009). Histone deacetylase 1, 2, 6 and acetylated histone H4 in B- and T-cell lymphomas. *Histopathology* 135, 1472–1483. doi: 10.1111/j.1365-2559.2009.03290.x
- Mazzola, M., Defflorian, G., Pezzotta, A., Ferrari, L., Fazio, G., Bresciani, E., et al. (2019). NIPBL: a new player in myeloid cell differentiation. *Haematologica* 104, 1332–1341. doi: 10.3324/haematol.2018.200899
- Melnick, A., and Licht, J. D. (2002). Histone deacetylases as therapeutic targets in hematologic malignancies. *Curr. Opin. Hematol.* 9, 322–332. doi: 10.1097/00062752-200207000-00010
- Mithraprabhu, S., Kalf, A., Chow, A., Khong, T., and Spencer, A. (2014). Dysregulated Class I histone deacetylases are indicators of poor prognosis in multiple myeloma. *Epigenetics* 9, 1511–1520. doi: 10.4161/15592294.2014.983367
- Moreno, D. A., Scrideli, C. A., Cortez, M. A. A., De Paula Queiroz, R., Valera, E. T., Da Silva Silveira, V., et al. (2010). Differential expression of HDAC3, HDAC7 and HDAC9 is associated with prognosis and survival in childhood acute lymphoblastic leukaemia: research paper. *Br. J. Haematol.* 150, 665–673. doi: 10.1111/j.1365-2141.2010.08301.x
- Nakagawa, M., Oda, Y., Eguchi, T., Aishima, S. I., Yao, T., Hosoi, F., et al. (2007). Expression profile of class I histone deacetylases in human cancer tissues. *Oncol. Rep.* 18, 769–774. doi: 10.3892/or.18.4.769
- Novotny-Diermayr, V., Hart, S., Goh, K. C., Cheong, A., Ong, L. C., Hentze, H., et al. (2012). The oral HDAC inhibitor pracinostat (SB939) is efficacious and synergistic with the JAK2 inhibitor pacritinib (SB1518) in preclinical models of AML. *Blood Cancer J.* 2:e69. doi: 10.1038/bcj.2012.14
- Oehme, I., Deubzer, H. E., Wegener, D., Pickert, D., Linke, J. P., Hero, B., et al. (2009). Histone deacetylase 8 in neuroblastoma tumorigenesis. *Clin. Cancer Res.* 15, 91–99. doi: 10.1158/1078-0432.CCR-08-0684
- Olson, D. E., Udeshi, N. D., Wolfson, N. A., Pitcairn, C. A., Sullivan, E. D., Jaffe, J. D., et al. (2014). An unbiased approach to identify endogenous substrates of “histone” deacetylase 8. *ACS Chem. Biol.* 9, 2210–2216. doi: 10.1021/cb500492r
- Park, S. Y., Jun, J. I. A. E., Jeong, K. J., Heo, H. J., Sohn, J. S., Lee, H. Y., et al. (2011). Histone deacetylases 1, 6 and 8 are critical for invasion in breast cancer. *Oncol. Rep.* 25, 1677–1681. doi: 10.3892/or.2011.1236
- Qi, J., Singh, S., Hua, W. K., Cai, Q., Chao, S. W., Li, L., et al. (2015). HDAC8 inhibition specifically targets Inv(16) acute myeloid leukemic stem cells by restoring p53 acetylation. *Cell Stem Cell* 17, 597–610. doi: 10.1016/j.stem.2015.08.004
- Rettig, I., Koeneke, E., Trippel, F., Mueller, W. C., Burhenne, J., Kopp-Schneider, A., et al. (2015). Selective inhibition of HDAC8 decreases neuroblastoma growth in vitro and in vivo and enhances retinoic acid-mediated differentiation. *Cell Death Dis.* 6:e1657. doi: 10.1038/cddis.2015.24
- Richter, J., Traver, D., and Willert, K. (2017). The role of Wnt signaling in hematopoietic stem cell development. *Crit. Rev. Biochem. Mol. Biol.* 52, 414–424. doi: 10.1080/10409238.2017.1325828
- Romanski, A., Schwarz, K., Keller, M., Wietbrauk, S., Vogel, A., Roos, J., et al. (2012). Deacetylase inhibitors modulate proliferation and self-renewal properties of leukemic stem and progenitor cells. *Cell Cycle* 11, 3219–3226. doi: 10.4161/cc.21565
- Somoza, J. R., Skene, R. J., Katz, B. A., Mol, C., Ho, J. D., Jennings, A. J., et al. (2004). Structural snapshots of human HDAC8 provide insights into the class I histone deacetylases. *Structure* 12, 1325–1334. doi: 10.1016/j.str.2004.04.012
- Subramanian, S., Bates, S. E., Wright, J. J., Espinoza-Delgado, I., and Piekarz, R. L. (2010). Clinical toxicities of histone deacetylase inhibitors. *Pharmaceuticals* 3, 2751–2767. doi: 10.3390/ph3092751
- Tian, Y., Mok, M., Yang, P., and Cheng, A. (2016). Epigenetic Activation of Wnt/ $\beta$ -Catenin signaling in NAFLD-Associated hepatocarcinogenesis. *Cancers* 8:76. doi: 10.3390/cancers8080076
- Tian, Y., Wong, V. W. S., Wong, G. L. H., Yang, W., Sun, H., Shen, J., et al. (2015). Histone deacetylase HDAC8 promotes insulin resistance and  $\beta$ -catenin activation in NAFLD-associated hepatocellular carcinoma. *Cancer Res.* 75, 4803–4816. doi: 10.1158/0008-5472.CAN-14-3786
- Van Den Wyngaert, I., De Vries, W., Kremer, A., Neefs, J. M., Verhasselt, P., Luyten, W. H. M. L., et al. (2000). Cloning and characterization of human histone deacetylase 8. *FEBS Lett.* 478, 77–83. doi: 10.1016/S0014-5793(00)1813-5
- Wang, Z. T., Chen, Z. J., Jiang, G. M., Wu, Y. M., Liu, T., Yi, Y. M., et al. (2016). Histone deacetylase inhibitors suppress mutant p53 transcription via HDAC8/YY1 signals in triple negative breast cancer cells. *Cell. Signal.* 28, 506–515. doi: 10.1016/j.cellsig.2016.02.006
- Wolf, D., and Rotter, V. (1985). Major deletions in the gene encoding the p53 tumor antigen cause lack of p53 expression in HL-60 cells. *Proc. Natl. Acad. Sci. U.S.A.* 82, 790–794. doi: 10.1073/pnas.82.3.790
- Wu, J., Du, C., Lv, Z., Ding, C., Cheng, J., Xie, H., et al. (2013). The up-regulation of histone deacetylase 8 promotes proliferation and inhibits apoptosis in

- hepatocellular carcinoma. *Dig. Dis. Sci.* 58, 3545–3553. doi: 10.1007/s10620-013-2867-7
- Xie, C., Edwards, H., Lograsso, S. B., Buck, S. A., Matherly, L. H., Taub, J. W., et al. (2012). Valproic acid synergistically enhances the cytotoxicity of clofarabine in pediatric acute myeloid leukemia cells. *Pediatr. Blood Cancer* 59, 1245–1251. doi: 10.1002/pbc.24152
- Young, C. S., Clarke, K. M., Kettle, L. M., Thompson, A., and Mills, K. I. (2017). Decitabine-Vorinostat combination treatment in acute myeloid leukemia activates pathways with potential for novel triple therapy. *Oncotarget* 8, 51429–51446. doi: 10.18632/oncotarget.18009
- Zhang, J., Ding, L., Holmfeldt, L., Wu, G., Heatley, S. L., Payne-Turner, D., et al. (2012). The genetic basis of early T-cell precursor acute lymphoblastic leukaemia. *Nature* 481, 157–163. doi: 10.1038/nature10725
- Conflict of Interest:** GD, AQ, and MT was employed by company Cogentech.
- The remaining authors declare that the research was conducted in the absence of any commercial or financial relationships that could be construed as a potential conflict of interest.
- Copyright © 2020 Spreafico, Gruszka, Valli, Mazzola, DeFlorian, Quintè, Totaro, Battaglia, Alcalay, Marozzi and Pistocchi. This is an open-access article distributed under the terms of the Creative Commons Attribution License (CC BY). The use, distribution or reproduction in other forums is permitted, provided the original author(s) and the copyright owner(s) are credited and that the original publication in this journal is cited, in accordance with accepted academic practice. No use, distribution or reproduction is permitted which does not comply with these terms.



## *Supplementary Material*

### **1 Supplementary Methods**

#### **1.1 Western blot**

Total proteins from zebrafish embryos (at least 30 embryos) were extracted with Laemmli buffer with the addition of protease inhibitor cocktail (Roche), 2  $\mu$ l/embryo. Lysates were incubated 3 min at 95°C and 2 min at 4°C, followed by disaggregation by using insulin syringe. Incubation and disaggregation were repeated twice and then lysates were centrifuged 10 min at 16.000 g at 4°C. The supernatant was recovered and extracts were quantified by using the Quantum Micro protein Assay (EuroClone). 40  $\mu$ g of proteins were loaded in a 10% acrylamide/polyacrilammide gel and subjected to electrophoresis. Total proteins from AML cell lines were extracted with Laemmli sample buffer. 20  $\mu$ l of extracts were loaded in a 10% acrylamide/polyacrilammide gel and subjected to electrophoresis. Proteins were transferred onto polyvinylidene fluoride (PVDF) membranes that were incubated with blocking solution (BS) (5% skimmed powder milk in TBS containing 0.1% TWEEN-20) for 1h at room temperature before overnight incubation at 4°C with primary antibodies in blocking solution. Membranes were then incubated 1h at room temperature with HRP-conjugated secondary antibodies in blocking solution. Protein bands were detected by using WESTAR ECL detection system (Cyanagen, Bologna, Italy). Images were acquired with the Alliance MINI HD9 AUTO Western Blot Imaging System (UVItec Limited, Cambridge, UK) and analyzed with the related software. Tubulin or vinculin were used as internal control. Antibodies are list in **Supplementary Table 2**.

### **2 Supplementary Figures and Tables**

#### **2.1 Supplementary Figures**

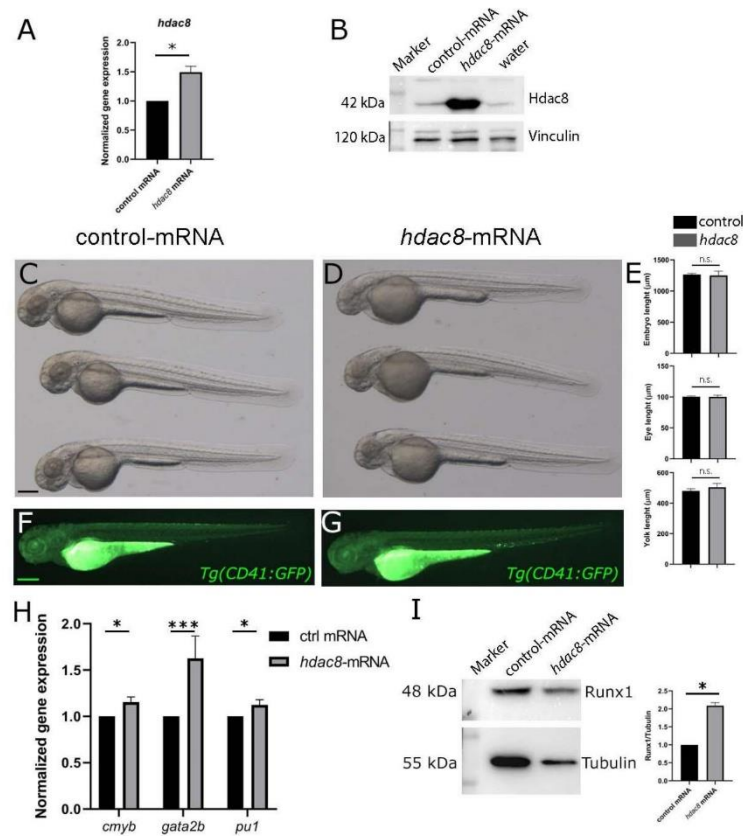


**Figure S1: Effects of Hdac8 ectopic expression in zebrafish**

RT-qPCR analysis (A) and Western blot analysis (B) of HDAC8 expression in control mRNA-, *hdac8* mRNA- and water injected embryos. The results in (A) are presented as mean value  $\pm$  SD from three independent experiments; \* $p < 0.05$ , One sample t test. Morphological phenotypes of control mRNA- (C) and *hdac8* mRNA- (D) injected embryos at 48 hpf. (E) Quantification of 3 dpf embryo length, eye diameter and yolk extension length (N=10). n.s.: non significant, Student's t test. Morphological phenotypes of control mRNA- (F) and *hdac8* mRNA-(G) injected embryos at 3 dpf of the *Tg(CD41:GFP)* transgenic line. Scale bar represents 100  $\mu$ m. (H) *c-Myb*, *gata2b* and *pu.1* expression analysis at 48 hpf by RT-qPCR techniques. Histograms represent mean value  $\pm$  SD from three independent experiments. \* $p < 0.05$ , \*\*\* $p < 0.001$ , One sample t test. (I) Western blot analysis of Runx1 expression at 48 hpf. Histograms represent mean value  $\pm$  SD from two independent experiments. \* $p < 0.05$ , One sample t test.

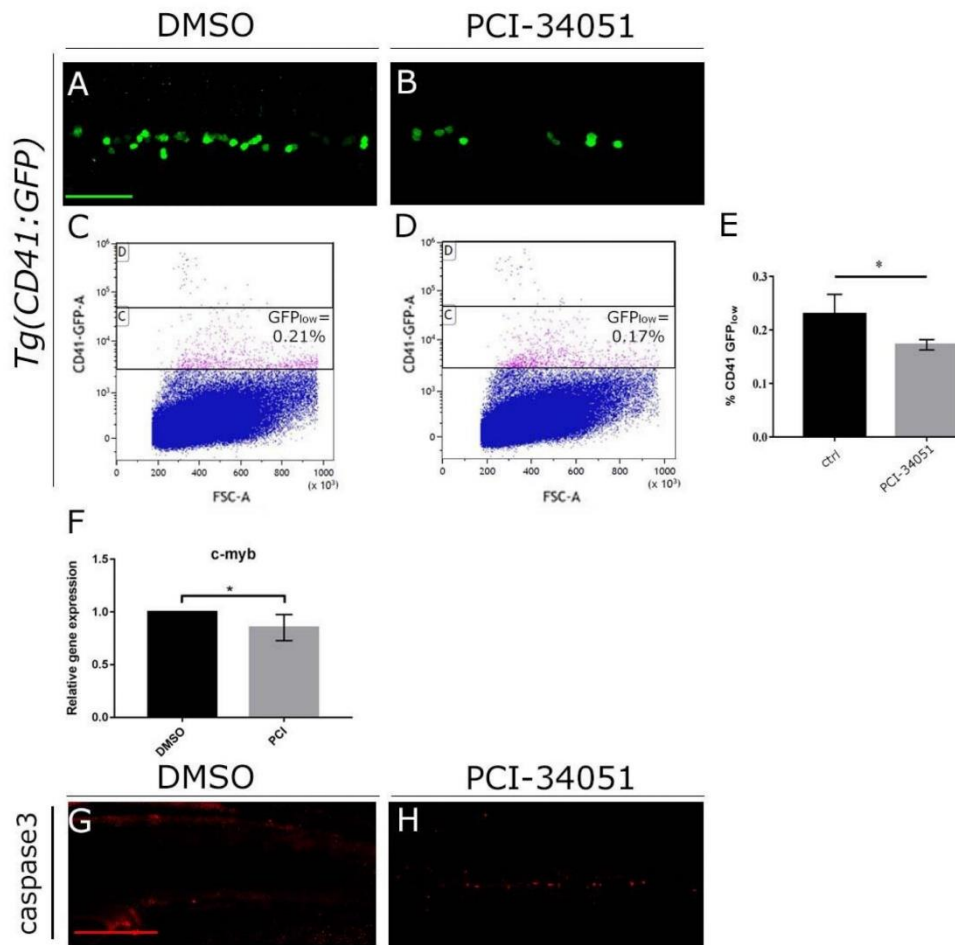


**Figure S2: Effect of PCI treatment in zebrafish**

(A, B) Confocal imaging of CHT of (A) DMSO or (B) PCI-treated *Tg(CD41:GFP)* zebrafish embryos at 3 dpf. (C-D) Quantification by FACS of GFP<sub>low</sub>-HSPCs of (C) DMSO and (D) PCI-treated *Tg(CD41:GFP)* zebrafish embryos at 3 dpf, quantification in (E). The results in (E) are presented as mean value  $\pm$  SD from four independent experiments; \*  $p < 0.05$ , Student's t test. (F) RT-qPCR quantification of the HSCs marker *c-myb* in DMSO- and PCI-treated zebrafish embryos. Histograms represent mean value  $\pm$  SD from four independent experiments; \*  $p < 0.05$ , One sample t test. (G, H) Confocal imaging of CHT of (A) DMSO or (B) PCI-treated zebrafish embryos at 3 dpf stained with caspase3 antibody to detect apoptosis. Scale bar in A, B, G, H represents 100  $\mu$ m.

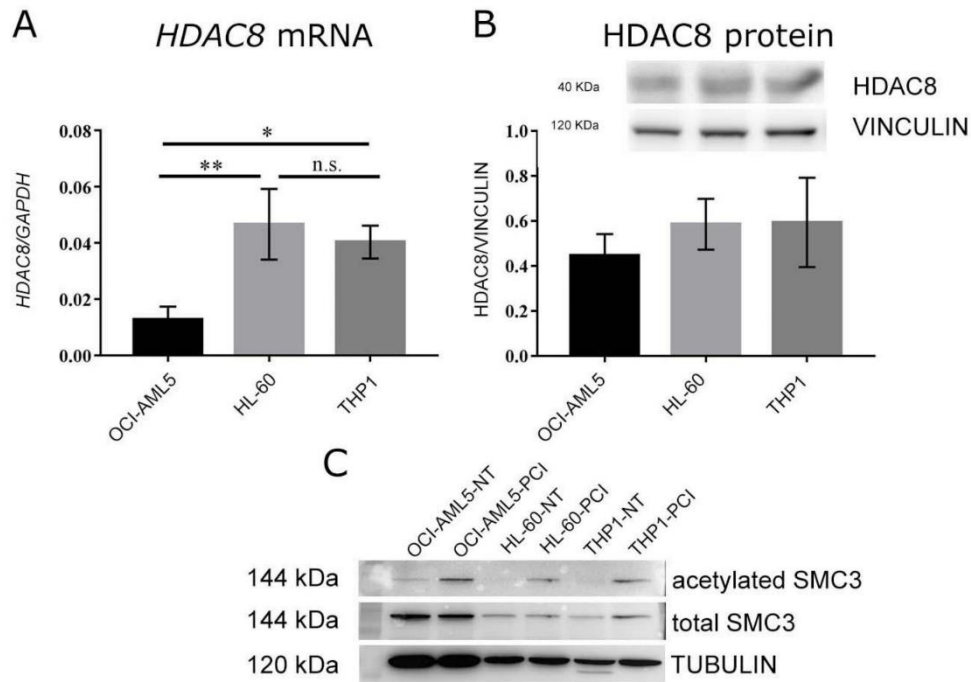


**Figure S3: Assessment of HDAC8 expression and PCI efficacy in OCI-AML5, HL-60 and THP1 AML cell lines.**

RT-qPCR analysis (A) and Western blot analysis (B) of HDAC8 expression. The results are presented as mean value  $\pm$  SD from three independent experiments; \* $p < 0.05$ , \*\* $p < 0.01$ , ns: not significant, ANOVA One-Way followed by Tukey post-hoc correction. (C) Western blot analyses of SMC3 acetylation status in control untreated (NT) and PCI-treated AML cell lines.

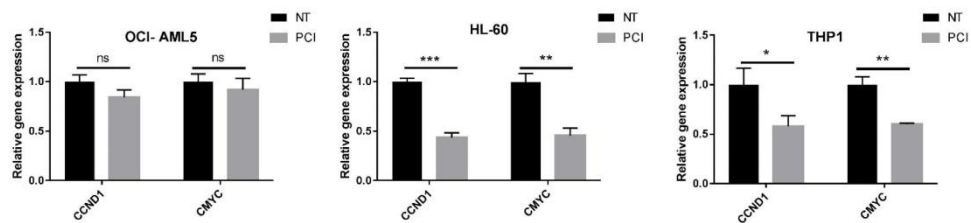


**Figure S4: PCI blocks cell cycle progression in AML cell lines**

RT-qPCR analyses of *CCND1* and *CMYC* gene expression in control untreated (NT) and PCI-treated OCI-AML5, HL-60 and THP1 AML cell lines. The results are presented as mean value  $\pm$  SD from three independent experiments. ns: not significant, \* $p < 0.05$ , \*\* $p < 0.01$ , \*\*\* $p < 0.001$ ; Student's t test.

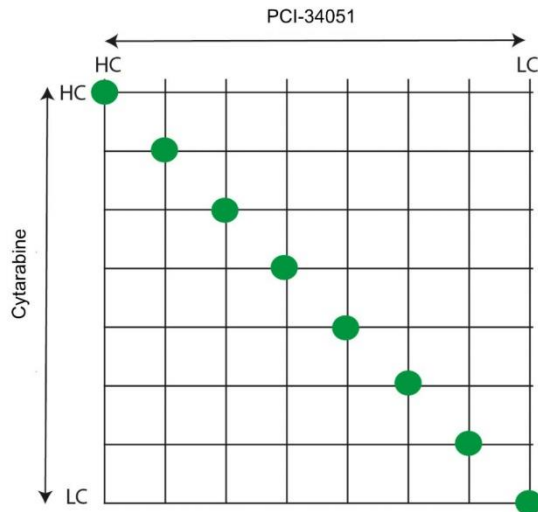


**Figure S5: Combination treatment setting**

Cells were exposed to the indicated drugs at decreasing concentration for 72h. Dots on the lines indicate data points used to determine the cytotoxicity effects. HC, highest concentration; LC, lowest concentration.

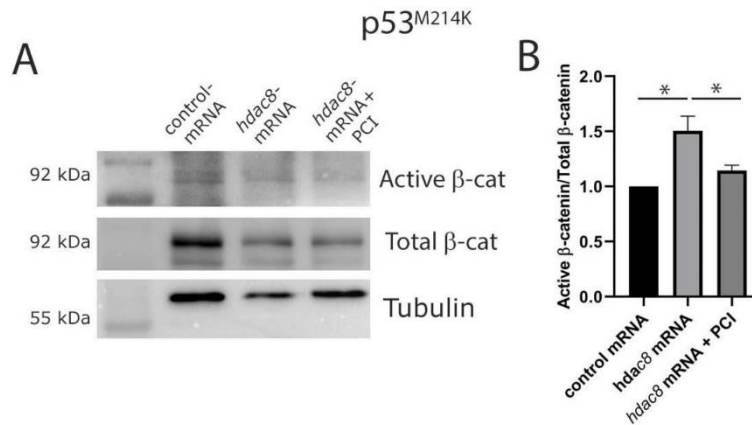


**Figure S6:  $\beta$ -catenin activation in zebrafish p53<sup>M214K</sup> embryos**

(A-B) Western blot analyses of  $\beta$ -catenin activation status in control-mRNA, *hdac8*- and *hdac8*-injected PCI-treated embryos at 3 dpf. Histograms represent mean value  $\pm$  SD from two independent experiments. \* $p < 0.05$ , ANOVA One-Way followed by Tukey post-hoc correction.

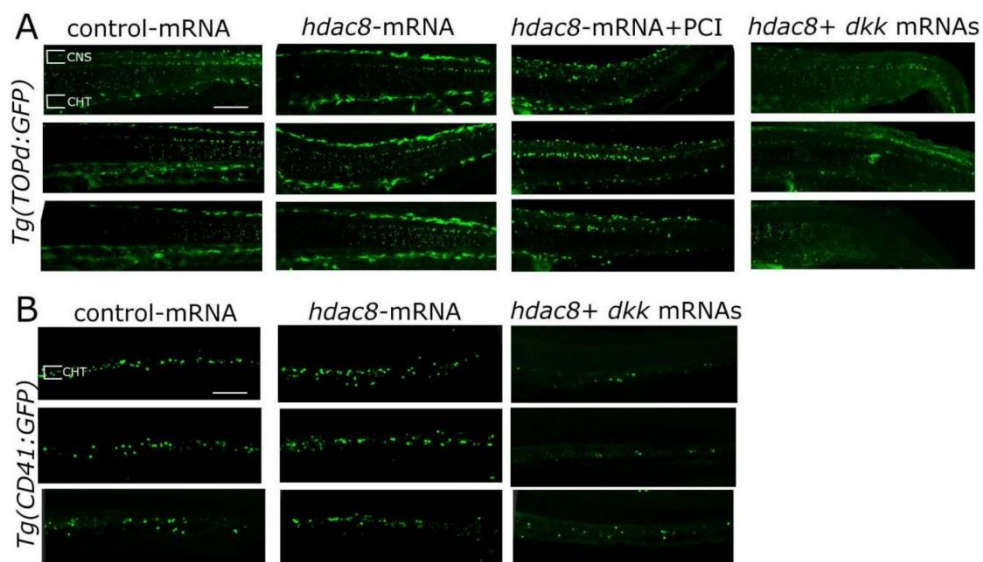


**Figure S7: Canonical Wnt pathway modulation by HDAC8**

(A) Representative images of canonical Wnt pathway modulation by *hdac8* overexpression, *dkk1b* injection and PCI treatment on HSPCs in the CHT of the Wnt reporter line Tg(TOPdGFP). (B)



Representative images of canonical Wnt pathway modulation by *hdac8* overexpression and Wnt inhibition by PCI on HSPCs in the CHT of the reporter line *Tg(CD41:GFP)*. Scale bar represents 100  $\mu$ m.

## 2.2 Supplementary tables

### Supplementary Table 1

#### Primer list

<b>Primers human</b>	<b>Sequence 5'- 3'</b>
<i>CCND1</i> FW	GAAGATCGTCGCCACCTG
<i>CCND1</i> REV	GACCTCCTCCTCGCACTTCT
<i>CMYC</i> FW	CACCAGCAGCGACTCTGA
<i>CMYC</i> REV	GATCCAGACTCTGACCTTTTGC
<i>GAPDH</i> FW	CAACGACCACTTTGTCAAGC
<i>GAPDH</i> REV	CTGTGAGGAGGGGAGATTCA
<i>NKD1</i> FW	TCGCCGGGATAGAAACTACA
<i>NKD1</i> REV	CAGTTCTGACTTCTGGGCCAC
<i>PPP2R2B</i> FW	CCTCATTCGGCCAGGCTC
<i>PPP2R2B</i> REV	ATCCATGATCCCTCCCCGCA
<b>Primers zebrafish</b>	<b>Sequence 5'- 3'</b>
<i>axin2</i> FW	GGCCACTGTAGTGGGTCTGT
<i>axin2</i> REV	ATTAGGATTTCCGGGGTCAC
<i><math>\beta</math>-actin</i> FW	CCGTGACATCAAGGAGAAG

## Supplementary Material

<i>β-actin</i> REV	ATACCGCAAGATTCCATACC
<i>baxa</i> FW	CAACTGGGGAAGAGTTGTGG
<i>baxa</i> REV	ACCCTGGTTGAAATAGCCTTG
<i>bbc3</i> FW	CCCACATCCCCTCACATGAT
<i>bbc3</i> REV	TCTGTTCCCTGAATTGTCCCTG
<i>bida</i> FW	CAGCGACCTACAGAGACCTT
<i>bida</i> REV	GCCTCTTCTGCATTGACTGA
<i>cdkn1a</i> FW	CCTGAGGAGATCTGAAACCC
<i>cdkn1a</i> REV	TGTGACAATATGTTTTGAGCTTCT
<i>cmyb</i> FW	GACACAAAGCTGCCAGTTG
<i>cmyb</i> REV	GCTCTTCCGTCTTCCCACAA
<i>gadd45ba</i> FW	TGCATCCCTCGTCACTAACTCT
<i>gadd45ba</i> REV	CAACGGCTCTCCTCACAGTA
<i>gata2b</i> FW	TCTGCTCGGAAACATGACGA
<i>gata2b</i> REV	ATTTACACATTCACGTCCCGAG
<i>nkd1</i> FW	ACACATCCCGCTTTGGAACA
<i>nkd1</i> REV	AACGGGTGGCGTGGGTAGGT
<i>ppp2r2b</i> FW	GTCTTCCAGAGAGAGCAGGAG
<i>ppp2r2b</i> REV	GCTCGTGGGTCTGGAAGGTCTT
<i>spi1b</i> FW	GCCATTTTCATGGACCCAGG

<i>spi1b</i> REV	ACACCGATGTCCGGGGCAA
<i>rpl8</i> FW	CTCCGTCTTCAAAGCCCATGT
<i>rpl8</i> REV	TCCTTCACGATCCCCTTGATG

## Supplementary Table 2

### Antibodies for western blot analyses

Primary antibody and catalogue number	Dilution	Company
anti-total-SMC3 (rabbit) SAB2701720	1:500	Sigma Aldrich, St. Louis, Missouri, US
anti-acetyl-SMC3 (mouse) MABE1073	1:500	Merck-Millipore, Burlington, Massachusetts, US
anti-HDAC8 (rabbit) sc-11405	1:500	Santa Cruz Biotechnology, Dallas, Texas, US
anti-active $\beta$ -catenin (mouse), clone 8E7 05-665	1:500	Merck-Millipore
anti-total $\beta$ -catenin (rabbit) 8480	1:1000	Cell Signaling Technology, Danvers, Massachusetts, US
anti-vinculin (mouse) V9131	1:6000	Sigma-Aldrich
anti-tubulin (mouse) T9026	1:2500	Merck-Millipore
Anti-RUNX1 (rabbit) PB9157	1:1000	Boster Biological Technology, Pleasanton, California, US
Secondary antibody	Dilution	Company

Supplementary Material

HRP-conjugated goat anti-rabbit 7074	1:5000	Cell Signaling Technology
HRP-conjugated horse anti-mouse 7076	1:4000	Cell Signaling Technology



## **4. RESULTS: SUBMITTED PAPERS**

### **4.1 Targeting HDAC8 to ameliorate skeletal muscle differentiation in Duchenne muscular dystrophy**

HDAC inhibitors (HDACi) are currently under study as a possible therapeutic approach for Duchenne muscular dystrophy (DMD) and pan-HDACi Givinostat is currently under phase III clinical trial. However, HDACi use is still hampered by several side effects associated with them. As we observed HDAC8 involvement in skeletal muscle development, in this work we sought to investigate its possible involvement in DMD and its inhibition as a possible therapeutic approach. Also, we performed acetylome profiling to identify new HDAC8 substrates.



## **AUTHORS**

Spreafico Marco<sup>1\*</sup>, Cafora Marco<sup>1\*</sup>, Bragato Cinzia<sup>2,3\*</sup>, Capitanio Daniele<sup>4,5</sup>, Marasca Federica<sup>6</sup>, Bodega Beatrice<sup>6</sup>, Mora Marina<sup>3</sup>, Gelfi Cecilia<sup>4,5</sup>, Marozzi Anna<sup>1\*</sup>, Pistocchi Anna<sup>1\*</sup>

## **AFFILIATIONS**

<sup>1</sup> Dipartimento di Biotecnologie Mediche e Medicina Traslazionale, Università degli Studi di Milano, Italy.

<sup>2</sup> PhD program in Neuroscience, Università degli studi di Milano-Bicocca, Monza, Italy

<sup>3</sup> Fondazione IRCCS Istituto Neurologico C. Besta, Milano, Italy.

<sup>4</sup> Dipartimento di Scienze Biomediche per la Salute, Università degli Studi di Milano, Italy

<sup>5</sup> IRCCS Istituto ortopedico Galeazzi, Milano, Italy

<sup>6</sup> Istituto Nazionale di Genetica Molecolare "Romeo ed Enrica Invernizzi" (INGM), Milan, Italy.

\*These authors equally contributed to the work

## **ABSTRACT**

Duchenne muscular dystrophy (DMD) causes progressive skeletal muscle degeneration and currently lacks an effective therapeutic treatment. Histone deacetylases (HDACs) play key roles in myogenesis and the therapeutic approach targeting HDACs in DMD is presently used although limited by adverse reactions. The unique structure of HDAC8 allows the development of highly specific inhibitors that might increase the effectiveness and reduce the side effect of pan-HDACs inhibitors. Here, we showed that the expression of HDAC8 was increased in DMD patients and zebrafish, and that the treatment with the HDAC8 inhibitor PCI-34051 rescued skeletal muscle defects in both human DMD myoblasts and zebrafish embryos. Through acetylation profile of zebrafish with HDAC8 dysregulation, we identified new HDAC8 targets involved in cytoskeleton organization such as tubulin that, when acetylated, is a marker of stable microtubules. Together, our results demonstrated that the specific HDAC8 inhibition is efficient in the rescue of damaged skeletal muscle both *in vitro* and *in vivo*. Since HDAC8 inhibitors are currently under study for cancer treatment, they might be rapidly introduced for the treatment of DMD patients.

## INTRODUCTION

Duchenne muscular dystrophy (DMD) is a severe X linked disorder generated by mutations in the *DMD* gene, encoding for dystrophin, [1] that causes rapid degeneration of heart and skeletal muscle, eventually leading to respiratory or hearth failure and consequent death [2]. In the last years, advancement in medical management and therapies have improved quality and life expectancy of DMD patients who can now live to experience their 40th birthday and beyond [3]. However, a cure is still not available and the standard of care for DMD patients is represented by corticosteroids treatment, which efficiently delays the progression of the pathology but shows differences in responsiveness among patients and causes several side effects such as weight gain, osteoporosis and Cushingoid appearance [4]. Therefore, there is a compelling need to find more efficacious and safer therapies.

Histone deacetylases (HDACs) are a large family of enzymes involved in several cellular processes, as they are responsible for the removal of acetyl moieties from lysines on both histone and non-histone proteins. Studies have revealed a crucial role for HDACs in the epigenetic regulation of myogenesis [5] and their inhibition has been proven to favour myoblasts fusion and myogenic differentiation [6,7]. These findings led to an increasing interest in using HDAC inhibitors (HDACi) for the treatment of skeletal muscle disorders, including DMD. Pan-HDACi have already been demonstrated to display effectiveness in the treatment of dystrophies *in vivo* [8–10] and Givinostat is currently in Phase III clinical trial. In comparison to other HDACi, which use is still hampered due to their side effects [11], phase II clinical trial (NCT01761292) demonstrated that Givinostat is well tolerated by DMD patients, presenting mild adverse events. Nevertheless, the use of more specific HDACi instead of pan-HDACi may improve current therapeutic strategy. For instance, HDAC8 possesses a unique structure among HDACs, as the C-terminal (aa 50–111) protein-binding domain is not present and the L1 loop in the proximity of the active site is particularly flexible and capable to accommodate different substrates trough conformational changes [12]. This distinctive structure allowed the development of high specific

HDAC8 inhibitors (such as the PCI-34051 and meta-sulfamoyl N-hydroxybenzamides) [13,14], which are already being studied as a therapeutic approach for a broad range of human diseases, such as acute myeloid leukemia (AML) [15], breast cancer [16], malignant peripheral nerve sheath tumour (MPNST) [17], T-cell lymphoma [13] and nonalcoholic fatty liver disease (NAFLD) associated hepatocellular carcinoma (HCC) [18].

HDAC8 involvement in muscle tissues dynamics has already been reported in smooth muscle tissue, as it binds to smooth muscle  $\alpha$ -actin ( $\alpha$ -SMA) and regulates contraction through acetylation of cortactin [19,20]. Moreover, we recently demonstrated that HDAC8 is also involved in the development of skeletal muscle both *in vitro* and *in vivo*, suggesting that HDAC8 modulation might be a possible pharmacological approach in the treatment of skeletal muscle diseases [21]. In this work we sought to investigate the potential of HDAC8 inhibition by PCI-34051 as a treatment for DMD both *in vitro*, in myotubes cultures from DMD patients, and *in vivo*, in a zebrafish DMD model. In both models we observed a higher expression of *HDAC8* compared to controls and we demonstrated that the PCI-34051-mediated HDAC8 inhibition rescued the DMD phenotype. Moreover, through comparison of acetylome profiles of zebrafish embryos with normal or pharmacological inhibited HDAC8 activity, we identified new HDAC8 targets involved in skeletal muscle dynamics, such as tubulins and skeletal muscle actin- $\alpha$ 1. We also demonstrated that HDAC8 inhibition increased  $\alpha$ -tubulin acetylation levels in dystrophic zebrafish and rescued cytoskeleton organization in myotubes derived from DMD patients.

Our results suggest that HDAC8 specific inhibition could represent a promising approach for the treatment of DMD patients.

## **MATERIALS AND METHODS**

### **Zebrafish embryo maintenance**

Zebrafish (*Danio rerio*) AB strains were maintained under standard conditions at the zebrafish fish facility of the University of Milan, Via Celoria 26 - 20133 Milan, Italy (Aut. Prot, n. 295/2012-A

- 20/12/2012). Zebrafish embryos were raised and maintained according to international (EU Directive 2010/63/EU) and national guidelines (Italian decree No 26 of the 4th of March 2014). Embryos were collected by natural spawning, staged according to Kimmel and colleagues [22] and raised at 28°C in fish water (Instant Ocean, 0.1% Methylene Blue) in Petri dishes, according to established techniques. We express the embryonic ages in hours post fertilization (hpf) and days post fertilization (dpf). After 24 hpf, to prevent pigmentation, 0.003% 1-phenyl-2-thiourea (PTU, Sigma-Aldrich, St. Louis, Missouri, US) was added to the fish water. Embryos were washed, dechorionated and anaesthetized with 0.016% tricaine (Ethyl 3-aminobenzoate methanesulfonate salt, Sigma-Aldrich) before proceeding with experimental protocols.

### **Microinjections and HDACi treatment**

Morpholino (MO, GeneTools LLC, Oregon, USA) and zebrafish *hdac8* full-length mRNA injections were carried out on 1- to 2-cells stage embryos. *dmd*-MOs were used as described in [23]: *dmd*-MO1 5'-TTGAGTCCTTTAATCCTACAATTTT-3'; *dmd*-MO6 5'-GCCATGACATAAGATCCAAGCCAAC-3'. MOs were co-injected at the concentration of 0.6 (*dmd*-MO1) and 1 (*dmd*-MO6) pmol/embryo, as described by [10], in 1X Danieau buffer (pH = 7.6). A standard control morpholino (ctrl-MO) was injected in parallel. Zebrafish *hdac8* full-length mRNA was injected at the concentration of 500 pg/embryo.

For PCI-34051 (PCI) and Givinostat (Sigma-Aldrich) treatment, 24 hpf embryos were put in 24-wells plate, 15 embryos/well, and PCI or Givinostat was added to fish water at the concentration of 37.5 µM. After 24 hours, fish water was changed, fresh PCI or Givinostat was added at the concentration of 12.5 µM and embryos were raised until they reached the 72 hpf stage. Embryos were kept at 28°C in the dark for the whole duration of the treatment. Equal concentrations of DMSO were used as a control.

### **Cell culture**

Patient specimens were collected from the Muscle Cell Biobank present at the Foundation IRCCS Neurological Institute Carlo Besta. Written, informed consent was obtained from the subjects or their parents/legal guardians. Control muscle cell cultures derived from healthy patients but who had normal muscle on biopsies and no DMD mutations. Primary myoblasts were developed directly from biopsied material by culturing in Dulbecco's modified Eagle's medium (DMEM; Lonza Group Ltd, Basel, Switzerland) containing 20% heat-inactivated calf bovine serum (CBS) (Gibco Life Technologies), 1% penicillin-streptomycin (Lonza), L-glutamine (Lonza), 10 µg/ml insulin (Sigma Aldrich, St. Louis, MO), 2.5 ng/ml basic fibroblast growth factor (bFGF) (Gibco Life Technologies), and 10 ng/ml epidermal growth factor (EGF) (Gibco). The medium was changed twice weekly and the cultures examined by inverted-phase microscopy. At 70% confluence they were dissociated enzymatically with trypsin-EDTA (Sigma) and seeded for immediate propagation. In order to obtain myotubes, the myoblasts were seeded into 35 mm dishes in DMEM proliferating medium. At 70% confluence, proliferating medium was changed to differentiating medium (DMEM, 1% penicillin-streptomycin, L-glutamine and insulin, without FCS or growth factors) and the myoblasts were allowed to differentiate into myotubes up to 10 days [24].

### **PCI treatment**

DMD- and control-derived myotubes were treated with 10 µM PCI or DMSO, the latter used as negative control. Treatment with both, PCI and DMSO, was made after inducing differentiation, starting from the day two (MT2 stage). Every 48 hours, fresh PCI or DMSO was added to the culture medium until the cells reached the day ten (MT10 stage).

### **Immunofluorescence and fusion index**

Cells were seeded at 25,000 cells/cm<sup>2</sup>, in triplicate wells for fusion index determination. Once the myoblast reached 90% confluence, they were treated with differentiation medium. Cells were fixed



with 4% paraformaldehyde, stained with Alexa-Fluor 488 phalloidin (1:10; Life Technologies) for 40 minutes, and DAPI (1:10000; Life Technologies) for 10 minutes.

Fusion index is defined as the number of nuclei in myotubes expressing myosin heavy chain divided by the total number of nuclei in a field, and was used to assess myoblast differentiation efficacy.

Primitive myotubes with 3–4 myonuclei and mature myotubes with  $\geq 5$  myonuclei were quantified.

For the fusion index of treated and not treated myotubes, 3 biological replicates were performed.

Myonuclei were counted on images taken at 40X under a Zeiss Axioplan2 microscope, by the use of Microscope Software AxioVision Release 4.8.2 (Zeiss, Oberkochen, Germany).

### **Confocal microscopy and Fiji analyses**

Control and DMD myotubes, treated or not with PCI, were investigated after performing the Alexa-Fluor 488 phalloidin staining. The microtubule structure around the multinucleated portion was examined on images taken at 63X under a Leica SP8 microscope (Leica). The maximum average width of segment presenting  $\geq 5$  myonuclei was measured by NIH Fiji software in 3 biological replicates.

### **Reverse transcription and real-time quantitative PCR**

Total RNA was extracted from cells or tails of zebrafish embryos at 3 dpf by using NucleoZOL reagent (Macherey-Nagel, Düren, Germany), according to the manufacturer's instructions. Concentration and purity of RNA were measured using the Nanodrop spectrophotometer (ThermoFisher Scientific, Waltham, Massachusetts, US). DNase reaction was performed on 1  $\mu$ g of RNA using RQ1 RNase-free DNase (Promega, Madison, Wisconsin, USA) and then cDNA was synthesized with the GoScript Reverse Transcription Kit (Promega), according to the manufacturer's instructions. qPCR analyses were performed with the GoTaq qPCR Master Mix (Promega) on the BioRad iQ5 Real Time Detection System (Biorad, Hercules, California, US).

The calculation of gene expression was based on the  $\Delta\Delta C_t$  method. GAPDH and *rpl8* were used as the internal control in qPCR on human cells and zebrafish cDNAs, respectively. Primer sequences are list in **Supplementary Table 1**.

### **Western blot**

Total proteins from human cells were extracted in lysis buffer (7M urea, 2M thiourea, 4% CHAPS, 30mM Tris, 1mM PMSF) with the addition of protease inhibitor cocktail (Roche). Lysates were sonicated at 20 Hz, kept on ice for 15 min and then centrifuged 15 min at 16.000 g at 4°C. The supernatant was recovered and quantified by using the 2-D Quant Kit (GE Healthcare, Life Sciences). Total proteins were extracted with Laemmli buffer from at least 40 zebrafish embryo tails at 3 dpf, with the addition of protease inhibitor cocktail (Roche), 1 $\mu$ l/tail. Lysates were incubated 3 min at 95°C and 2 min at 4°C, followed by disaggregation by using insulin syringe. Incubation and disaggregation were repeated twice and then lysates were centrifuged 10 min at 16.000 g at 4°C. The supernatant was recovered and extracts were quantified by using the Quantum Micro protein Assay (EuroClone). 40  $\mu$ g of proteins were loaded in a 10% acrylamide/polyacrilammide gel and subjected to electrophoresis. Proteins were transferred onto polyvinylidene fluoride (PVDF) membranes that were incubated with blocking solution (5% skimmed powder milk in TBS containing 0.1% TWEEN-20) for 1h at room temperature before overnight incubation at 4°C with primary antibodies diluted in blocking solution. Membranes were then incubated 1h at room temperature with HRP-conjugated secondary antibodies diluted in blocking solution. Protein bands were detected by using WESTAR ECL detection system (Cyanagen, Bologna, Italy). Images were acquired with the Alliance MINI HD9 AUTO Western Blot Imaging System (UVItec Limited, Cambridge, UK) and analysed with the related software. Vinculin was used as the internal control in determining HDAC8 levels. Primary antibodies were rabbit anti-HDAC8 (1:500, Santa Cruz Biotechnology, Dallas, Texas, US), rabbit anti-total tubulin (1:1000, Cell Signaling), mouse anti-acetylated tubulin (1:1000, Merck), and mouse anti-vinculin

(1:6000, Sigma Aldrich). Secondary antibodies were HRP-conjugated goat anti-rabbit (1:5000, Cell Signalling Technologies, Danvers, Massachusetts, US) and HRP-conjugated horse anti-mouse (1:4000, Cell Signalling Technologies).

### **Acetylome analysis**

Total protein from at least 100 zebrafish embryos tails at 3 dpf were extracted in lysis buffer (7M urea, 2M thiourea, 4% CHAPS, 30mM Tris, 1mM PMSF) with the addition of protease inhibitor cocktail (Roche) and 20 mM deacetylation inhibition cocktail (Santa Cruz Biotechnology), 1  $\mu$ l/tail. Lysates were sonicated at 20 Hz and centrifuged 15 min at 16.000 g at 4°C. The supernatant was recovered and quantified by using the 2-D Quant Kit (GE Healthcare).

2-D immunoblotting was carried out by subjecting each sample (120  $\mu$ g) to isoelectrofocusing in triplicate on 13 cm, 3–10 pH-gradient IPG strips (GE Healthcare), with a voltage gradient ranging from 200 to 8000 V, for a total of 55000 Vh, using an IPGphor electrophoresis unit (GE Healthcare). After focusing, proteins were reduced and alkylated. The second dimension was carried out in 14x15 cm<sup>2</sup>, 12% polyacrylamide gels at 20 °C. After transfer, PVDF membranes were stained with SYPRO Ruby Protein Blot Stain (ThermoFisher Scientific) for total protein content quantitation, then blots were incubated with a 1:1 mixture of rabbit anti-Acetylated-Lysine (Ac-K2-100) 1:1000 (Cell Signaling Technology, #9814) and anti-Acetylated-Lysine 1:1000 (Cell Signaling Technology, #9441) primary antibodies. After washing, membranes were incubated with anti-rabbit HRP-conjugated (GE Healthcare) secondary antibody (1:10000). Signals were visualized by chemiluminescence using the ECL Prime (GE Healthcare) detection kit and the Image Quant LAS 4000 (GE Healthcare) analysis system. Spot quantification was performed using the Image Quant TL (Molecular Dynamics) software. Acetylated spot intensity was normalised against the corresponding spot in the total stain image and the ratio of PCI sample intensities over controls was calculated. Only spots with intensity ratios above 1 showed increased acetylation levels.

To identify proteins, three 18 cm, 3–10 pH-gradient IPG strips were loaded with 200 µg protein extract per strip; electrophoretic conditions were the same as 2-D immunoblotting. Semi-preparative gels were stained with a total-protein fluorescent stain (Krypton, ThermoFisher Scientific). Image acquisition was performed using a Typhoon 9200 laser scanner. Spots of interest were excised from gel using the Ettan spot picker robotic system (GE Healthcare), destained in 50% methanol/50 mM ammonium bicarbonate (AMBIC) and incubated with 30 µl of 6 ng/ml trypsin (Promega) dissolved in 10 mM AMBIC for 16 hours at 37 °C. Released peptides were subjected to reverse phase chromatography (Zip-Tip C18 micro, Millipore), eluted with 50% acetonitrile/0,1% trifluoroacetic acid. Peptides mixture (1 µl) was diluted in an equal volume of 10 mg/ml  $\alpha$ -cyano-4-hydroxycinnamic acid matrix dissolved in 70% acetonitrile/30% citric acid and processed on a Ultraflex III MALDI-ToF/ToF (Bruker Daltonics) mass spectrometer. Mass spectrometry was performed at an accelerating voltage of 20 kV and spectra were externally calibrated using Peptide Mix calibration mixture (Bruker Daltonics); 1000 laser shots were taken per spectrum. Spectra were processed by FlexAnalysis software v. 3.0 (Bruker Daltonics) setting the signal to noise threshold value to 6 and search was carried out by correlation of uninterpreted spectra to *Danio rerio* entries in NCBIprot database. The significance threshold was set at a p-value < 0.05. No mass and pI constraints were applied and trypsin was set as enzyme. One missed cleavage per peptide was allowed and carbamidomethylation was set as fixed modification while methionine oxidation as variable modification. Mass tolerance was set at 30 ppm for MS spectra. To confirm protein identification, an MS/MS spectrum was collected by Ultraflex III MALDI-ToF/ToF (Bruker Daltonics) mass spectrometer, as acceptance criterium. Spectra were searched against the database using BioTools v. 3.2 (Bruker Daltonics) interfaced to the on-line MASCOT software, which utilizes a robust probabilistic scoring algorithm. The significance threshold was set at a p-value < 0.05. One missed cleavage per peptide was allowed and carbamidomethylation was set as fixed modification while methionine oxidation as variable modification. Mass tolerance was set at 30 ppm and 0.5 Da for peptide and MS/MS fragment ion respectively.

## **Muscle lesions imaging**

Muscle lesions in zebrafish embryos were assessed by birefringence as described by [25]. Images of embryos and sections were acquired using a microscope equipped with a digital camera with LAS Leica Imaging software (Leica, Wetzlar, Germany). Images were processed using Adobe Photoshop software.

## **Statistical analysis**

Each experiment was performed at least three times. Histograms represent the mean value and bars indicate standard deviation. Statistical significance was determined by Student's t test when comparing two groups and by One-way ANOVA followed by Tukey post-hoc correction when comparing more than two groups. Data were considered significant if  $p < 0.05$ .

## **RESULTS**

### ***HDAC8* expression is increased in DMD and its inhibition ameliorates DMD phenotype**

Inhibition of HDACs has been proven to be efficient in the treatment of DMD [8–10]. However, the use of more specific HDACi could offer new possibilities in DMD treatment. As HDAC8 presents a peculiar structure that allows the development of more specific and selective inhibitors compared to the other HDACs, we investigated its expression in the context of DMD. We assessed *HDAC8* expression in myoblasts and myotubes from DMD patients and controls. *HDAC8* expression was evaluated by means of RT-qPCR at different stages of differentiation: undifferentiated myoblasts (MB) and myotubes at 2 days (MT2) and 7 days (MT7) of differentiation. The analysis revealed a significantly higher expression of *HDAC8* during the differentiation of DMD-myoblast cells compared to those of controls at all the developmental stages considered (**Figure 1A**). Then, to evaluate whether HDAC8 inhibition could rescue the DMD phenotype, we assessed the efficiency of the highly-specific HDAC8 inhibitor PCI-34051



[13]. We treated DMD myotubes with 10  $\mu$ M PCI from the second day after differentiation induction (MT2), until the day ten (MT10). To evaluate the degree of cell differentiation, we performed immunofluorescence experiments assessing both the expression of myosins and the fusion index of the cultured myotubes. Cell morphology was determined by phalloidin staining (green) whereas anti-myosin antibody (red) and DAPI (blue) were used to visualise sarcomeric myosin and nuclei, respectively. Immunofluorescence analysis revealed an increase of myosin content in DMD patients-derived myotubes following PCI treatment, compared to DMSO-treated cells (**Figure 1B**). As a further evidence of enhanced myogenic differentiation of cells, DMD myotubes from all three patients showed a significant increase ( $p < 0.05$  in patients 1 and 3,  $p < 0.01$  in patient 2) of the fusion index following PCI treatment (**Figure 1C**). These results were also confirmed by quantification of myosin expression in myotubes by RT-qPCR analysis. Expression levels of myosins were significantly lower ( $p < 0.001$ ) in untreated DMD myotubes in comparison to myotubes derived from controls and were recovered, although not completely, following PCI treatment ( $p < 0.01$ ) (**Figure 1D**).

In parallel, we also investigated Hdac8 expression *in vivo*, in a zebrafish DMD model. Zebrafish embryos were co-injected with two *dmd*-MOs as previously described [10] and Hdac8 levels were assessed at the stage of 48 hpf by RT-qPCR and at 72 hpf by Western blot analyses. We observed an increase of both Hdac8 mRNA (**Figure 1E**) and protein levels (**Figure 1F**) in *dmd*-MO injected embryos, compared to control embryos. To evaluate the efficiency of HDAC8 inhibition *in vivo*, we treated *dmd*-MO injected zebrafish embryos with PCI from the stage of 24 hpf, when the first myogenic wave is already completed [26], and assessed the extent of muscles lesions by birefringence at the stage of 3 dpf [25]. The lesions presented by untreated *dmd*-MO injected embryos were partially rescued by PCI treatment. Interestingly, the extent of the rescue was comparable to muscle lesions recovery observed in zebrafish embryos treated with pan-HDACi Givinostat, currently in phase III clinical trial for DMD treatment (**Figure 1G**). To further support this result, we quantified expression levels of *myl2* (fast fiber myosin) by RT-qPCR and we

observed a rescue of *mylz2* mRNA in *dmd*-MO injected embryos following PCI treatment. This rescue was comparable to the one determined by Givinostat treatment (**Figure 1H**).

Taken together, these results confirm an upregulation of *HDAC8* expression in the DMD phenotype, thus supporting the hypothesis of its involvement in the pathology, and suggest that PCI-mediated HDAC8 inhibition represents a valuable approach in treating DMD phenotype.

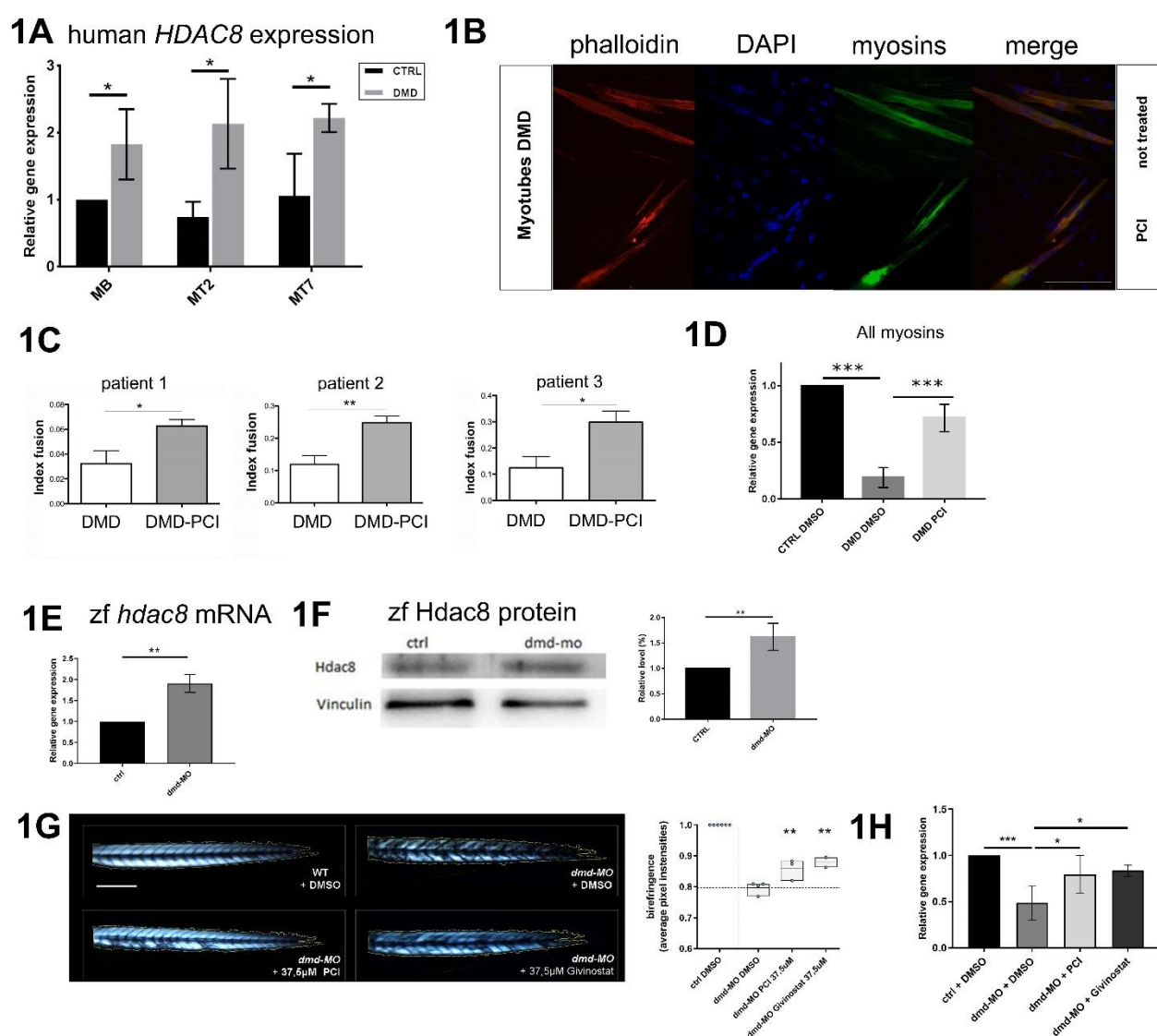


**Figure 1.** (A) RT-qPCR analysis of *HDAC8* expression in DMD patients- and controls-derived myoblasts (MB) and myotubes at 2 (MT2) and 7 days (MT7) of differentiation. (B) Myosins (red), DAPI (blue) and phalloidin (green) staining of DMD-derived myotubes untreated or treated with PCI. Scale bar = 20  $\mu$ m. (C) Fusion index of three DMD-derived myotubes untreated or treated with PCI. (D) RT-qPCR analysis of myosin expression in myotubes from controls, DMD and DMD+PCI patients. (E) RT-qPCR analysis of *hdac8* expression in *dmd*-MO and control zebrafish embryos. (F) Western blot analysis of Hdac8 expression in *dmd*-MO and control zebrafish

embryos. (G) Skeletal muscle lesions imaging by birefringence in control, *dmd*-MO, *dmd*-MO injected and PCI- or Givinostat-treated zebrafish embryos at 72 hpf. Scale bar = 100  $\mu$ m. (H) RT-qPCR quantification of fast-myosin *mylz2* expression in control, *dmd*-MO injected and *dmd*-MO injected DMSO-, PCI- or Givinostat-treated zebrafish embryos. \*  $p < 0.05$ , \*\*  $p < 0.01$ , \*\*\*  $p < 0.001$ .

### **HDAC8 targets proteins involved with cytoskeleton organization and skeletal muscle dynamic**

To gain more insight into how HDAC8 is involved in skeletal muscle differentiation and function, we compared global acetylation changes in control and PCI treated zebrafish embryos. In order to enrich skeletal muscle tissue proteins, the analysis was performed only with tails of zebrafish embryos at 3 dpf. We performed 2D-electrophoresis and then membranes were incubated with an anti-acetylated lysins antibody cocktail to visualize acetylated proteins (**Figure 2A**). Next, differentially acetylated peptides were identified by mass spectrometry (MS). Several cytoskeleton proteins differently acetylated in PCI-treated embryos, in comparison to untreated, were identified: four proteoforms of Krt4 protein (*krt4*, AAH66728.1); Type I cyokeratin enveloping layer (*cyt1*, AAH65653.1); Tubulin  $\alpha$  chain (*tuba2*, AAH60904.1); Tubulin  $\beta$  chain (*tubb4b*, AAQ97859.1); Actin  $\alpha 1$  skeletal muscle (*actc1b*, AAH45406.1); Vitellogenin 5 (*vtg5*, AAW56969.1); Vtg1 protein (*vtg1*, AAH94995.1) (**Figure 2B**).

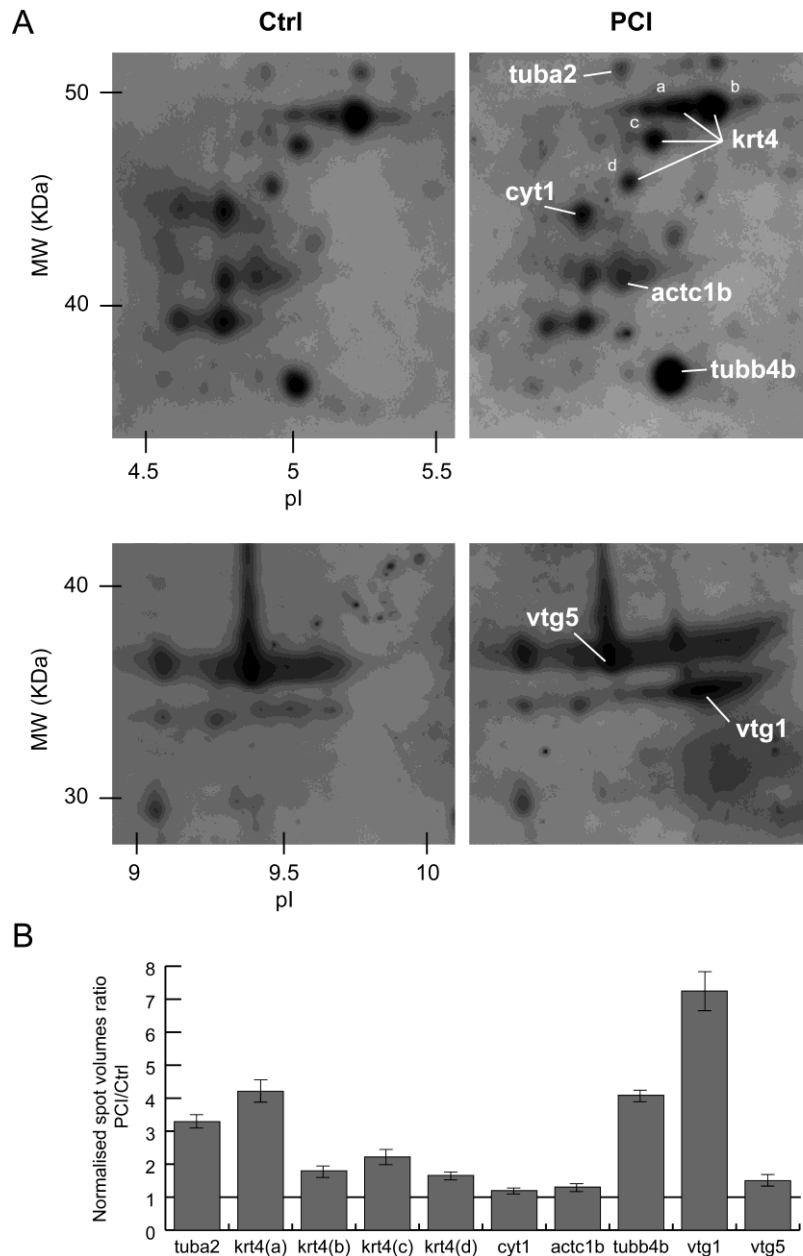


**Figure 2.** HDAC8 targets identification. (A) 2D-immunoblotting representative close-ups of acetylated protein extracted from the tails of control and PCI-treated zebrafish embryos at 3 dpf. (B) Histograms showing increasing acetylation levels of identified proteins in PCI-treated embryos compared to control.

### HDAC8 inhibition impacts on microtubule architecture in DMD

Our acetylome analysis identified tubulin as HDAC8 target. Since it has been reported that microtubule organization is severely impaired in DMD [27], we decided to deepen HDAC8 correlation with microtubule structure. First, to confirm that HDAC8 overexpression can modify  $\alpha$ -tubulin acetylation status, we decided to analyse acetylome profile also in *hdac8* overexpressing

embryos. To analyse whether increased *HDAC8* overexpression could modify the acetylation status of zebrafish proteins even in absence of the DMD phenotype, we injected embryos with full-length zebrafish *hdac8* mRNA (500 pg/embryo) and acetylome profile was assessed by 2-D electrophoresis. Comparison with 2-D electrophoresis from *hdac8* mRNA, control and PCI-treated embryos confirmed differential acetylation of two of the previously identified HDAC8 acetylation targets, tubulin- $\alpha$ 2 and krt4 protein (**Figure 3A**).

We next assessed  $\alpha$ -tubulin acetylation levels in *dmd*-MO injected embryos. By Western blot analysis we observed a reduction of acetylated-tubulin in *dmd*-MO injected embryos, compared to controls while PCI treatment partially rescued  $\alpha$ -tubulin acetylation status (**Figure 3B**). The acetylation levels of krt4 cannot be assessed due to the lack of an antibody for the acetylated form of this protein.

The evidence of  $\alpha$ -tubulin acetylation regulation by HDAC8 prompted us to investigate whether HDAC8 inhibition could have an effect on cytoskeleton. To this aim, we decided to evaluate microtubules architecture in myoblasts from DMD human patients and in those treated with PCI. Phalloidin staining [28] revealed a significant increase in maximum average width in DMD myotubes, compared to controls (DMD myotubes:  $32.21 \pm 1.370$ , vs Ctrl myotubes:  $13.06 \pm 0.6937$ ,  $p < 0.0001$ ), and to DMD myotubes treated with PCI (DMD myotubes:  $32.21 \pm 1.370$ , vs DMD myotubes treated with PCI:  $18.06 \pm 1.983$ ,  $p < 0.0001$ ). The HDAC8 inhibition rescued the cytoskeleton organization of DMD myotubes although not fully recovering the maximum average width of controls (DMD myotubes treated with PCI:  $18.06 \pm 1.983$ , vs Ctrl myotubes:  $13.06 \pm 0.6937$ ,  $p = 0.0223$ ) (**Figure 3C-D**).



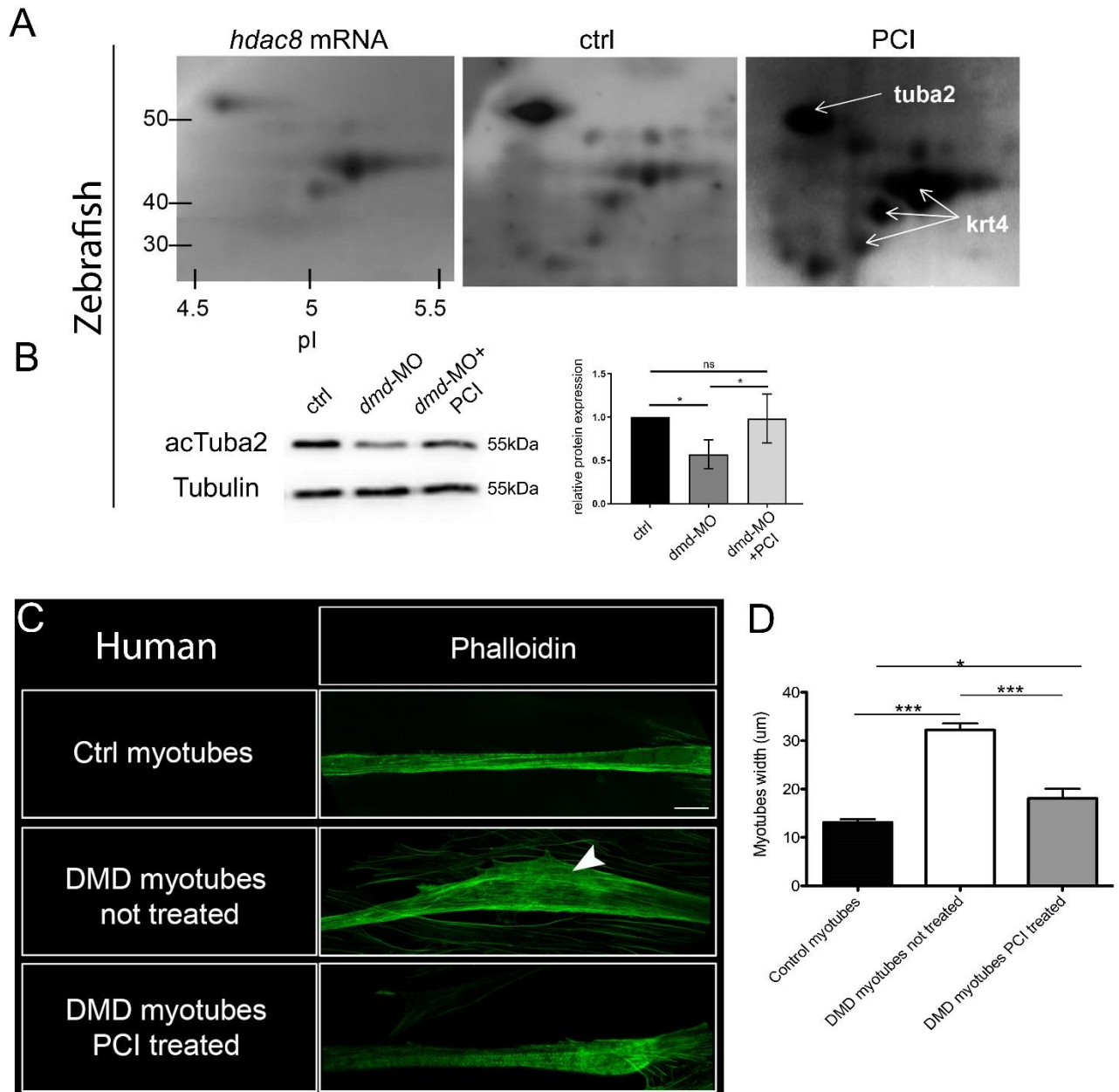


**Figure 3.** HDAC8 and cytoskeleton architecture. (A) 2D-immunoblotting of protein extracted from the tails of *hdac8*-injected, control, and PCI-treated zebrafish embryos at 3 dpf. (B) Western blot analysis of  $\alpha$ -tubulin acetylation in control, *dmd*-MO and *dmd*-MO/PCI-treated zebrafish embryos at 3 dpf. (C) Illustrative images taken at 63X of human control and DMD myotubes, treated or not treated with PCI. Scale bar = 30  $\mu$ m. (D) Graph reporting the maximum average width measures \* $p < 0.05$ , \*\*\* $p < 0.001$ , n.s. = not significant.

## DISCUSSION

Pharmacological treatment of muscular dystrophies is rapidly obtaining interest as an immediate and more efficient approach than gene and cell therapy-based strategies, which are still hindered by several hurdles [29]. In particular, HDACi are a class of drugs which have been shown to display a very promising efficiency in the treatment of DMD phenotype. However, pan-HDACi treatment is associated with several side effects, ranging from nausea and thrombocytopenia to more severe events, such as cardiac and metabolic disfunctions [11]. Indeed, pan-HDACi Givinostat was demonstrated to be safer and better tolerated by DMD patients, in comparison to other pan-HDACi, thus receiving approval for phase III clinical trial. Nevertheless, the use of isoform-specific HDACi could offer an alternative therapeutical strategy for DMD treatment. Such an approach would require an extensive knowledge of the role of individual HDAC isoforms in skeletal muscle and their possible implication in DMD progression. By using both *in vitro* (human myotubes) and *in vivo* (zebrafish embryos) DMD models, we demonstrated a possible involvement of HDAC8 in DMD pathogenesis. First, we highlighted an increased HDAC8 expression in DMD patient-derived myotubes and *dmd*-MO injected zebrafish embryos. To our knowledge, this is the first evidence of HDAC8 overexpression in DMD, both in human and in the zebrafish model. In this regard, a previous study indicated a higher activity of class I HDACs in muscles from dystrophin-deficient *Mdx* mice, but only HDAC2 was found to be more expressed compared to wild-type mice [9]. This discrepancy might be due to the differences between mouse and humans. Indeed, *Mdx* mouse is known to develop a milder DMD phenotype, compared to human and zebrafish DMD models [30].

Studies have revealed that HDAC8 possess a peculiar structure [12], which allows development of high specific inhibitors. Such a possibility makes HDAC8 specific inhibition a new potential therapeutic approach for DMD. To test this hypothesis, we assessed the effect of HDAC8 blocking by using the highly specific HDAC8-inhibitor PCI-34051 [13]. Following PCI treatment, we observed a rescue of DMD phenotype, in terms of increased fusion index in human myoblasts and

reduced lesion extent in zebrafish embryos. Also, in both DMD models PCI treatment rescued myosin expression to a level comparable to wild-type controls. These results are in accordance with previous works demonstrating that HDACi ameliorate the phenotype of DMD models by restoring morphology and promoting regeneration of skeletal muscle tissue [8–10,31]. Noticeably, PCI efficiency *in vivo* was comparable to the rescue determined by Givinostat treatment in *dmd*-MO injected embryos. This is of great interest, as it indicates that inhibition of a single HDAC isoform might be *per se* sufficient to determine an amelioration of DMD phenotype, thereby sustaining the use of highly specific HDACi as an alternative to pan-HDACi. Indeed, in addition to efficacy, safety of HDAC8 specific inhibitors requires evaluation as well and future studies will have to be addressed to this aim.

Molecular mechanisms underlying HDAC8 inhibition efficacy could be multiple. We have recently described a mainly nuclear localization of HDAC8 in human skeletal muscle [21], which could imply an active role in transcription modulation. Indeed, by deacetylation of SMC3, HDAC8 is known to modulate recycling of the cohesin complex [32], which has been recently proven to regulate chromatin accessibility at the *Myogenin* locus [33]. Moreover, several studies demonstrated that HDACs inhibition enhances the expression and the activity of factors promoting skeletal muscle differentiation, myogenesis and regeneration, such as MyoD and follistatin [6,7,34,35]. Moreover, by acetylome profiling we identified cytoskeleton proteins as HDAC8 targets such as tubulin- $\alpha$ 2 and  $\beta$ 2. This result is supported by a recent work, in which Vanaja and colleagues demonstrated that HDAC8 deacetylates  $\alpha$ -tubulin in different cervical cancer cell lines, with a predominant role in HeLa cells [36]. Alterations of microtubules have been reported in dystrophic mice [27] as a consequence of loss of dystrophin [37], and their destabilization has been shown to contribute to DMD progression by multiple mechanisms [38,39]. Interestingly, tubulin acetylation is considered a marker of stable microtubules, although it is still debated whether it contributes to or is a consequence of microtubule stabilization [40]. Thus, the regulation of microtubule dynamics by modulating tubulin acetylation could represent an interesting approach

to DMD treatment. Moreover, previous studies indicated that  $\alpha$ -tubulin acetylation is increased at a late stage of myogenesis, thus suggesting this modification to be a crucial event during terminal differentiation of skeletal muscle cells [41,42]. Notably, tubulin post-translational modifications have already been demonstrated to influence skeletal muscle development, as inhibition of tubulin deetyrosination affects myoblasts differentiation and myotubes fusion [43]. Whether tubulin acetylation can affect muscle cell differentiation is not known but the possibility of promoting both renewal and stabilization of myofibers by inhibiting a single HDAC isoform would be very fascinating.

As a further evidence of HDAC8 involvement in cytoskeleton function, we identified  $\alpha$ 1 skeletal muscle actin as a HDAC8 target by proteomic analyses in zebrafish embryos. Although co-immunoprecipitation experiments already reported HDAC8 and actin to directly interact in smooth muscle tissue [19], our results are the first evidence of skeletal muscle actin deacetylation by HDAC8. Interestingly, Li and colleagues [20] demonstrated that HDAC8 activity on cortactin in smooth muscle tissue is crucial in contraction modulation. The precise effect of actin acetylation/deacetylation is not known, but our results open the interesting possibility that HDAC8 might play a role in contraction modulation, opening new perspectives toward pharmacological approach for DMD patients. Although studies to unveil the precise mechanism of HDAC8 action in the skeletal muscle and in DMD pathogenesis and progression are needed, our work provides the first evidence of HDAC8 overexpression in DMD patients and zebrafish and support its specific inhibition as a new valuable therapeutic approach in the treatment of this pathology.

## REFERENCES

- [1] E.P. Hoffman, R.H. Brown, L.M. Kunkel, Dystrophin: The protein product of the duchenne muscular dystrophy locus, *Cell*. (1987). [https://doi.org/10.1016/0092-8674\(87\)90579-4](https://doi.org/10.1016/0092-8674(87)90579-4).
- [2] B. Wu, C. Cloer, P. Lu, S. Milazi, M. Shaban, S.N. Shah, L. Marston-Poe, H.M. Moulton, Q.L. Lu, Exon skipping restores dystrophin expression, but fails to prevent disease progression in later stage dystrophic dko mice, *Gene Ther*. 21 (2014) 785–793. <https://doi.org/10.1038/gt.2014.53>.
- [3] E. Landfeldt, R. Thompson, T. Sejersen, H.J. McMillan, J. Kirschner, H. Lochmüller, *Life*

- expectancy at birth in Duchenne muscular dystrophy: a systematic review and meta-analysis, *Eur. J. Epidemiol.* (2020). <https://doi.org/10.1007/s10654-020-00613-8>.
- [4] N. Goemans, G. Buyse, Current treatment and management of dystrophinopathies, *Curr. Treat. Options Neurol.* 16 (2014). <https://doi.org/10.1007/s11940-014-0287-4>.
- [5] M.-C. Sincennes, C.E. Brun, M.A. Rudnicki, Concise Review: Epigenetic Regulation of Myogenesis in Health and Disease, *Stem Cells Transl. Med.* (2016). <https://doi.org/10.5966/sctm.2015-0266>.
- [6] S. Iezzi, G. Cossu, C. Nervi, V. Sartorelli, P.L. Puri, Stage-specific modulation of skeletal myogenesis by inhibitors of nuclear deacetylases, *Proc. Natl. Acad. Sci. U. S. A.* 99 (2002) 7757–7762. <https://doi.org/10.1073/pnas.112218599>.
- [7] S. Iezzi, M. Di Padova, C. Serra, G. Caretti, C. Simone, E. Maklan, G. Minetti, P. Zhao, E.P. Hoffman, P.L. Puri, V. Sartorelli, Deacetylase inhibitors increase muscle cell size by promoting myoblast recruitment and fusion through induction of follistatin, *Dev. Cell.* 6 (2004) 673–684. [https://doi.org/10.1016/S1534-5807\(04\)00107-8](https://doi.org/10.1016/S1534-5807(04)00107-8).
- [8] G.C. Minetti, C. Colussi, R. Adami, C. Serra, C. Mozzetta, V. Parente, S. Fortuni, S. Straino, M. Sampaolesi, M. Di Padova, B. Illi, P. Gallinari, C. Steinkühler, M.C. Capogrossi, V. Sartorelli, R. Bottinelli, C. Gaetano, P.L. Puri, Functional and morphological recovery of dystrophic muscles in mice treated with deacetylase inhibitors, *Nat. Med.* 12 (2006) 1147–1150. <https://doi.org/10.1038/nm1479>.
- [9] C. Colussi, C. Mozzetta, A. Gurtner, B. Illi, J. Rosati, S. Straino, G. Ragone, M. Pescatori, G. Zaccagnini, A. Antonini, G. Minetti, F. Martelli, G. Piaggio, P. Gallinari, C. Steinkühler, E. Clementi, C. Dell’Aversana, L. Altucci, A. Mai, M.C. Capogrossi, P.L. Puri, C. Gaetano, HDAC2 blockade by nitric oxide and histone deacetylase inhibitors reveals a common target in Duchenne muscular dystrophy treatment, *Proc. Natl. Acad. Sci. U. S. A.* 105 (2008) 19183–19187. <https://doi.org/10.1073/pnas.0805514105>.
- [10] N.M. Johnson, G.H. Farr, L. Maves, The HDAC Inhibitor TSA Ameliorates a Zebrafish Model of Duchenne Muscular Dystrophy, *PLoS Curr.* (2013). <https://doi.org/10.1371/currents.md.8273cf41db10e2d15dd3ab827cb4b027>.
- [11] S. Subramanian, S.E. Bates, J.J. Wright, I. Espinoza-Delgado, R.L. Piekarczyk, Clinical toxicities of histone deacetylase inhibitors, *Pharmaceuticals.* 3 (2010) 2751–2767. <https://doi.org/10.3390/ph3092751>.
- [12] J.R. Somoza, R.J. Skene, B.A. Katz, C. Mol, J.D. Ho, A.J. Jennings, C. Luong, A. Arvai, J.J. Buggy, E. Chi, J. Tang, B.C. Sang, E. Verner, R. Wynands, E.M. Leahy, D.R. Dougan, G. Snell, M. Navre, M.W. Knuth, R. V. Swanson, D.E. McRee, L.W. Tari, Structural snapshots of human HDAC8 provide insights into the class I histone deacetylases, *Structure.* 12 (2004) 1325–1334. <https://doi.org/10.1016/j.str.2004.04.012>.
- [13] S. Balasubramanian, J. Ramos, W. Luo, M. Sirisawad, E. Verner, J.J. Buggy, A novel histone deacetylase 8 (HDAC8)-specific inhibitor PCI-34051 induces apoptosis in T-cell lymphomas, *Leukemia.* 22 (2008) 1026–1034. <https://doi.org/10.1038/leu.2008.9>.
- [14] C. Zhao, J. Zang, Q. Ding, E.S. Inks, W. Xu, C.J. Chou, Y. Zhang, Discovery of meta-sulfamoyl N-hydroxybenzamides as HDAC8 selective inhibitors, *Eur. J. Med. Chem.* 150 (2018) 282–291. <https://doi.org/10.1016/j.ejmech.2018.03.002>.
- [15] J. Qi, S. Singh, W.K. Hua, Q. Cai, S.W. Chao, L. Li, H. Liu, Y. Ho, T. McDonald, A. Lin, G. Marcucci, R. Bhatia, W.J. Huang, C.I. Chang, Y.H. Kuo, HDAC8 Inhibition Specifically Targets Inv(16) Acute Myeloid Leukemic Stem Cells by Restoring p53 Acetylation, *Cell Stem Cell.* 17 (2015) 597–610. <https://doi.org/10.1016/j.stem.2015.08.004>.
- [16] M.W. Chao, P.C. Chu, H.C. Chuang, F.H. Shen, C.C. Chou, E.C. Hsu, L.E. Himmel, H.L. Huang, H.J. Tu, S.K. Kulp, C.M. Teng, C.S. Chen, Non-epigenetic function of HDAC8 in regulating breast cancer stem cells by maintaining Notch1 protein stability, *Oncotarget.* 7 (2016) 1796–1807. <https://doi.org/10.18632/oncotarget.6427>.



- [17] G. Lopez, K.L.J. Bill, H.K. Bid, D. Braggio, D. Constantino, B. Prudner, A. Zewdu, K. Batte, D. Lev, R.E. Pollock, HDAC8, A potential therapeutic target for the treatment of malignant peripheral nerve sheath tumors (MPNST), *PLoS One*. 10 (2015) 1–12. <https://doi.org/10.1371/journal.pone.0133302>.
- [18] Y. Tian, V.W.S. Wong, G.L.H. Wong, W. Yang, H. Sun, J. Shen, J.H.M. Tong, M.Y.Y. Go, Y.S. Cheung, P.B.S. Lai, M. Zhou, G. Xu, T.H.M. Huang, J. Yu, K.F. To, A.S.L. Cheng, H.L.Y. Chan, Histone deacetylase HDAC8 promotes insulin resistance and  $\beta$ -catenin activation in NAFLD-associated hepatocellular carcinoma, *Cancer Res*. 75 (2015) 4803–4816. <https://doi.org/10.1158/0008-5472.CAN-14-3786>.
- [19] D. Waltregny, W. Glénisson, S.L. Tran, B.J. North, E. Verdin, A. Colige, V. Castronovo, Histone deacetylase HDAC8 associates with smooth muscle  $\alpha$ -actin and is essential for smooth muscle cell contractility, *FASEB J*. 19 (2005) 966–968. <https://doi.org/10.1096/fj.04-2303fje>.
- [20] J. Li, S. Chen, R.A. Cleary, R. Wang, O.J. Gannon, E. Seto, D.D. Tang, Histone deacetylase 8 regulates cortactin deacetylation and contraction in smooth muscle tissues, *Am. J. Physiol. - Cell Physiol*. 307 (2014) 288–295. <https://doi.org/10.1152/ajpcell.00102.2014>.
- [21] L. Ferrari, C. Bragato, L. Brioschi, M. Spreafico, S. Esposito, A. Pezzotta, F. Pizzetti, A. Moreno-Fortuny, G. Bellipanni, A. Giordano, P. Riva, F. Frabetti, P. Viani, G. Cossu, M. Mora, A. Marozzi, A. Pistocchi, HDAC8 regulates canonical Wnt pathway to promote differentiation in skeletal muscles, *J. Cell. Physiol*. 234 (2019) 6067–6076. <https://doi.org/10.1002/jcp.27341>.
- [22] C.B. Kimmel, W.W. Ballard, S.R. Kimmel, B. Ullmann, T.F. Schilling, Stages of embryonic development of the zebrafish, *Dev. Dyn*. 203 (1995) 253–310. <https://doi.org/10.1002/aja.1002030302>.
- [23] J.R. Guyon, A.N. Mosley, Y. Zhou, K.F. O'Brien, X. Sheng, K. Chiang, A.J. Davidson, J.M. Volinski, L.I. Zon, L.M. Kunkel, The dystrophin associated protein complex in zebrafish, *Hum. Mol. Genet.* (2003). <https://doi.org/10.1093/hmg/ddg071>.
- [24] S. Zanotti, S. Saredi, A. Ruggieri, M. Fabbri, F. Blasevich, S. Romaggi, L. Morandi, M. Mora, Altered extracellular matrix transcript expression and protein modulation in primary Duchenne muscular dystrophy myotubes, *Matrix Biol*. 26 (2007) 615–624. <https://doi.org/10.1016/j.matbio.2007.06.004>.
- [25] G. Kawahara, J.R. Guyon, Y. Nakamura, L.M. Kunkel, Zebrafish models for human FKRP muscular dystrophies, *Hum. Mol. Genet*. 19 (2009) 623–633. <https://doi.org/10.1093/hmg/ddp528>.
- [26] F. Stellabotte, B. Dobbs-McAuliffe, D.A. Fernández, X. Feng, S.H. Devoto, Dynamic somite cell rearrangements lead to distinct waves of myotome growth, *Development*. 134 (2007) 1253–1257. <https://doi.org/10.1242/dev.000067>.
- [27] J.M. Percival, P. Gregorevic, G.L. Odom, G.B. Banks, J.S. Chamberlain, S.C. Froehner, rAAV6-Microdystrophin rescues aberrant Golgi complex organization in mdx skeletal muscles, *Traffic*. 8 (2007) 1424–1439. <https://doi.org/10.1111/j.1600-0854.2007.00622.x>.
- [28] H. Cao, D. Yu, X. Yan, B. Wang, Z. Yu, Y. Song, L. Sheng, Hypoxia destroys the microstructure of microtubules and causes dysfunction of endothelial cells via the PI3K / Stathmin1 pathway, *Cell Biosci.* (2019) 1–10. <https://doi.org/10.1186/s13578-019-0283-1>.
- [29] S. Consalvi, V. Saccone, L. Giordani, G. Minetti, C. Mozzetta, P.L. Puri, Histone deacetylase inhibitors in the treatment of muscular dystrophies: Epigenetic drugs for genetic diseases, *Mol. Med*. 17 (2011) 457–465. <https://doi.org/10.2119/molmed.2011.00049>.
- [30] L. Maves, Recent advances using zebrafish animal models for muscle disease drug discovery, *Expert Opin. Drug Discov.* (2014). <https://doi.org/10.1517/17460441.2014.927435>.

- [31] C. Mozzetta, S. Consalvi, V. Saccone, M. Tierney, A. Diamantini, K.J. Mitchell, G. Marazzi, G. Borsellino, L. Battistini, D. Sassoon, A. Sacco, P.L. Puri, Fibroadipogenic progenitors mediate the ability of HDAC inhibitors to promote regeneration in dystrophic muscles of young, but not old Mdx mice, *EMBO Mol. Med.* 5 (2013) 626–639. <https://doi.org/10.1002/emmm.201202096>.
- [32] M.A. Deardorff, M. Bando, R. Nakato, E. Watrin, T. Itoh, M. Minamino, K. Saitoh, M. Komata, Y. Katou, D. Clark, K.E. Cole, E. De Baere, C. Decroos, N. Di Donato, S. Ernst, L.J. Francey, Y. Gyftodimou, K. Hirashima, M. Hullings, Y. Ishikawa, C. Jaulin, M. Kaur, T. Kiyono, P.M. Lombardi, L. Magnaghi-Jaulin, G.R. Mortier, N. Nozaki, M.B. Petersen, H. Seimiya, V.M. Siu, Y. Suzuki, K. Takagaki, J.J. Wilde, P.J. Willems, C. Prigent, G. Gillessen-Kaesbach, D.W. Christianson, F.J. Kaiser, L.G. Jackson, T. Hirota, I.D. Krantz, K. Shirahige, HDAC8 mutations in Cornelia de Lange syndrome affect the cohesin acetylation cycle, *Nature*. (2012). <https://doi.org/10.1038/nature11316>.
- [33] P.F. Tsai, S. Dell’Orso, J. Rodriguez, K.O. Vivanco, K.D. Ko, K. Jiang, A.H. Juan, A.A. Sarshad, L. Vian, M. Tran, D. Wangsa, A.H. Wang, J. Perovanovic, D. Anastasakis, E. Ralston, T. Ried, H.W. Sun, M. Hafner, D.R. Larson, V. Sartorelli, A Muscle-Specific Enhancer RNA Mediates Cohesin Recruitment and Regulates Transcription In trans, *Mol. Cell.* 71 (2018) 129–141.e8. <https://doi.org/10.1016/j.molcel.2018.06.008>.
- [34] N. Kobayashi, K. Goto, K. Horiguchi, M. Nagata, M. Kawata, K. Miyazawa, M. Saitoh, K. Miyazono, c-Ski activates MyoD in the nucleus of myoblastic cells through suppression of histone deacetylases, *Genes to Cells*. (2007). <https://doi.org/10.1111/j.1365-2443.2007.01052.x>.
- [35] V. Saccone, S. Consalvi, L. Giordani, C. Mozzetta, I. Barozzi, M. Sandoná, T. Ryan, A. Rojas-Muñoz, L. Madaro, P. Fasanaro, G. Borsellino, M. De Bardi, G. Frigè, A. Termanini, X. Sun, J. Rossant, B.G. Bruneau, M. Mercola, S. Minucci, P.L. Puri, HDAC-regulated myomiRs control BAF60 variant exchange and direct the functional phenotype of fibro-adipogenic progenitors in dystrophic muscles, *Genes Dev.* (2014). <https://doi.org/10.1101/gad.234468.113>.
- [36] G.R. Vanaja, H.G. Ramulu, A.M. Kalle, Overexpressed HDAC8 in cervical cancer cells shows functional redundancy of tubulin deacetylation with HDAC6, *Cell Commun. Signal.* (2018). <https://doi.org/10.1186/s12964-018-0231-4>.
- [37] K.W. Prins, J.L. Humston, A. Mehta, V. Tate, E. Ralston, J.M. Ervasti, Dystrophin is a microtubule-associated protein, *J. Cell Biol.* 186 (2009) 363–369. <https://doi.org/10.1083/jcb.200905048>.
- [38] R.J. Khairallah, G. Shi, F. Sbrana, B.L. Prosser, C. Borroto, M.J. Mazaitis, E.P. Hoffman, A. Mahurkar, F. Sachs, Y. Sun, Y.W. Chen, R. Raiteri, W.J. Lederer, S.G. Dorsey, C.W. Ward, Microtubules underlie dysfunction in duchenne muscular dystrophy, *Sci. Signal.* (2012). <https://doi.org/10.1126/scisignal.2002829>.
- [39] S.R. Iyer, S.B. Shah, A.P. Valencia, M.F. Schneider, E.O. Hernández-Ochoa, J.P. Stains, S.S. Blemker, R.M. Lovering, Altered nuclear dynamics in MDX myofibers, *J. Appl. Physiol.* 122 (2017) 470–481. <https://doi.org/10.1152/jappphysiol.00857.2016>.
- [40] L. Li, X.J. Yang, Tubulin acetylation: Responsible enzymes, biological functions and human diseases, *Cell. Mol. Life Sci.* 72 (2015) 4237–4255. <https://doi.org/10.1007/s00018-015-2000-5>.
- [41] G.G. Gundersen, S. Khawaja, J.C. Bulinski, Generation of a stable, posttranslationally modified microtubule array is an early event in myogenic differentiation, *J. Cell Biol.* 109 (1989) 2275–2288. <https://doi.org/10.1083/jcb.109.5.2275>.
- [42] M. Conacci-Sorrell, C. Ngouenet, R.N. Eisenman, Myc-nick: A cytoplasmic cleavage product of Myc that promotes  $\alpha$ -tubulin acetylation and cell differentiation, *Cell.* 142 (2010) 480–493. <https://doi.org/10.1016/j.cell.2010.06.037>.
- [43] W. Chang, D.R. Webster, A.A. Salam, D. Gruber, A. Prasad, J.P. Eiserich, J. Chloë

Bulinski, Alteration of the C-terminal amino acid of tubulin specifically inhibits myogenic differentiation, *J. Biol. Chem.* 277 (2002) 30690–30698.  
<https://doi.org/10.1074/jbc.M204930200>.

**SUPPLEMENTARY TABLE 1**

<b>Primers human</b>	<b>Sequence 5'- 3'</b>
<i>GAPDH</i> FW	CAACGACCACTTTGTCAAGC
<i>GAPDH</i> REV	CTGTGAGGAGGGGAGATTCA
<i>HDAC8</i> FW	GGTGCATTCTTTGATTGAAGCA
<i>HDAC8</i> REV	AAGCATCAGTGTGGAAGGTG
<i>ALL-MYOSIN</i> FW	TCGCCGGGATAGAAAACACTACA
<i>ALL-MYOSIN</i> REV	CAGTTCTGACTTCTGGGCCAC
<b>Primers zebrafish</b>	<b>Sequence 5'- 3'</b>
<i>rpl8</i> FW	CTCCGTCTTCAAAGCCCATGT
<i>rpl8</i> REV	TCCTTCACGATCCCCTTGATG
<i>mylz2</i> FW	CCACTCAGTGCGACAGGTT
<i>mylz2</i> REV	AACATTGCCAGCCACATCT

## **4.2 The genome-wide impact of *nipblb* loss-of-function on zebrafish gene expression**

*NIPBL* is one of the most frequently mutated gene in CdLS patients. It is responsible for cohesin loading onto DNA and it is also involved in regulation of gene expression at genome-wide level. Since CdLS is characterized by several developmental alterations, in this study we performed RNA-seq analyses in zebrafish embryos at two different stages of development (24 hpf and 3 dpf) following *nipblb* knockdown in order to evaluate its impact on whole-genome gene expression.

1 Article

## 2 The genome-wide impact of *nipblb* loss-of-function 3 on zebrafish gene expression

4 Marco Spreafico<sup>1\*</sup>, Eleonora Mangano<sup>2\*</sup>, Mara Mazzola<sup>1</sup>, Clarissa Consolandi<sup>2</sup>, Roberta Bordoni<sup>2</sup>,  
5 Cristina Battaglia<sup>1</sup>, Silvio Bicciato<sup>3</sup>, Anna Marozzi<sup>1,‡</sup>, Anna Pistocchi<sup>1,‡</sup>

6 <sup>1</sup> Dip. Biotecnologie Mediche e Medicina Traslazionale, Università degli Studi di Milano, LITA, Via Fratelli  
7 Cervi 93, 20090, Segrate, Milano, Italy; [marco.spreafico@unimi.it](mailto:marco.spreafico@unimi.it), [mara.mazzola@unimi.it](mailto:mara.mazzola@unimi.it),  
8 [cristina.battaglia@unimi.it](mailto:cristina.battaglia@unimi.it), [anna.marozzi@unimi.it](mailto:anna.marozzi@unimi.it), [anna.pistocchi@unimi.it](mailto:anna.pistocchi@unimi.it)

9 <sup>2</sup> Institute of Biomedical Technologies, Italian National Research Council (ITB-CNR), Via Fratelli Cervi 93,  
10 20090, Segrate, Milano, Italy; [eleonora.mangano@itb.cnr.it](mailto:eleonora.mangano@itb.cnr.it), [clarissa.consolandi@itb.cnr.it](mailto:clarissa.consolandi@itb.cnr.it),  
11 [roberta.bordoni@itb.cnr.it](mailto:roberta.bordoni@itb.cnr.it)

12 <sup>3</sup> Dep. of Life Sciences, University of Modena and Reggio-Emilia, Via G. Campi 287, 41125 Modena, Italy

13 \* Correspondence: [anna.pistocchi@unimi.it](mailto:anna.pistocchi@unimi.it)

14 <sup>‡</sup> the authors equally contributed to the work

15 Received: date; Accepted: date; Published: date

16 **Abstract:** Transcriptional changes normally occur during development but also underlie differences  
17 between healthy and pathological conditions. Transcription factors or chromatin modifiers are  
18 involved in orchestrating gene activity, such as the cohesin genes and their regulator NIPBL. In our  
19 previous studies, using a zebrafish model for *nipblb* knock-down, we described the effect of *nipblb*  
20 loss-of-function in specific contexts such as central nervous system development and  
21 hematopoiesis. However, the genome-wide transcriptional impact of *nipblb* loss-of-function in  
22 zebrafish embryos at diverse developmental stages remains under investigated. By RNA-seq  
23 analyses in zebrafish embryos at 24 hours and 3 days post fertilization, we examined genome-wide  
24 effects of *nipblb* haploinsufficiency on transcriptional programs. Differential gene expression  
25 analysis revealed that *nipblb* loss-of-function has a major impact on gene expression at 24 hours post  
26 fertilization, and that this massive transcriptional dysregulation is rescued by specific back-up  
27 mechanisms that counteract the transcriptional patterns induced by *nipblb* silencing. Moreover, we  
28 unraveled a connection between *nipblb*-dependent differential expression and gene expression  
29 patterns of hematological cell populations and AML subtypes, enforcing our previous evidences on  
30 the involvement of NIPBL-related transcriptional dysregulation in hematological malignancies.

31 **Keywords:** NIPBL, RNA sequencing, zebrafish, gene expression regulation, Acute Myeloid  
32 Leukemia

### 34 1. Introduction

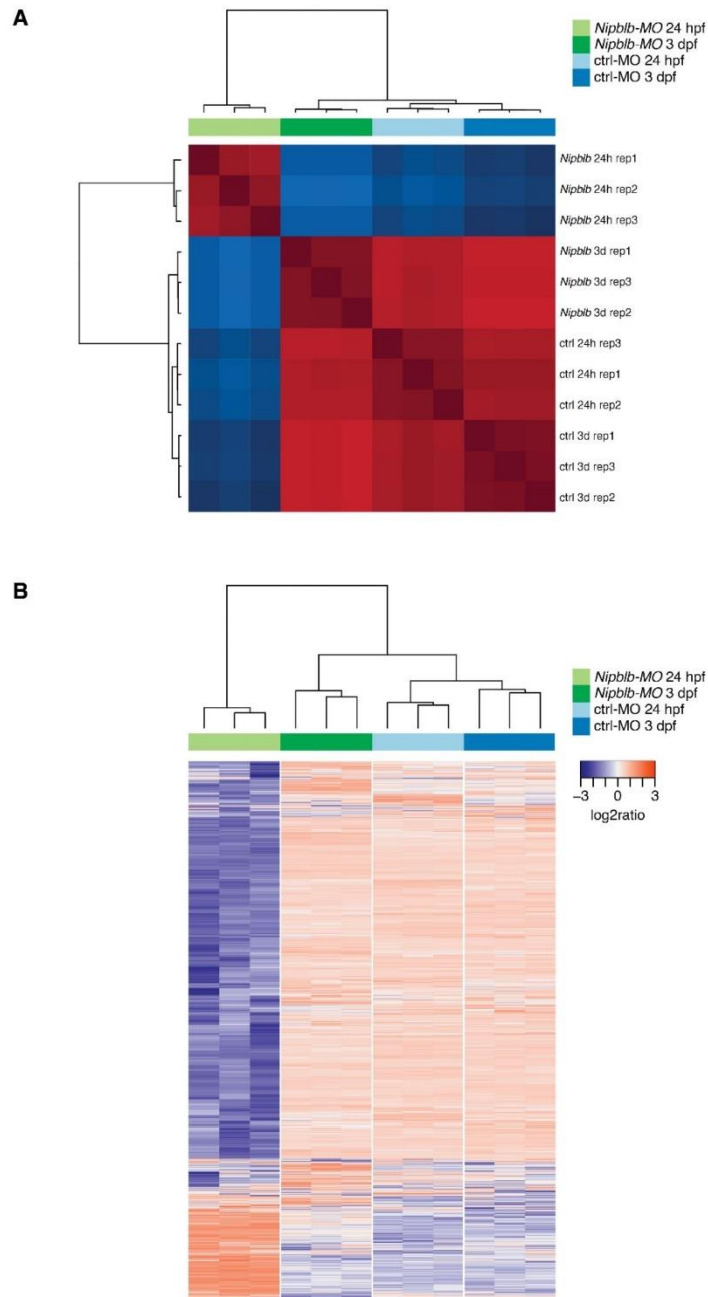
35 The capability of regulating gene expression is a key feature of cells and is implicated in all cellular  
36 processes. Thousands of genes are differentially transcribed within diverse cell types and whole-  
37 genome changes in gene expression constitutively occur during organism development and tissue  
38 differentiation. This transcriptional specificity depends on several regulatory proteins, such as  
39 transcription factors and chromatin modifiers, which determine time- and tissue-specific gene  
40 expression patterns through activation and repression of genes at genome-wide level. Diverse  
41 transcriptional patterns characterize not only physiological conditions but are also a distinct hallmark  
42 of pathological states. Thus, unrevealing factors involved in gene expression regulation and  
43 identifying their target genes might not only improve the knowledge of physiological development  
44 and tissue differentiation but also be exploited to design new therapeutic approaches for pathologies.

45 Cohesin is a ring-shaped multiprotein complex, which was initially identified as a key regulator of  
46 sister chromatid cohesion, segregation during mitosis [1] and for genome stability maintenance  
47 during DNA repair [2]. The core structure of the cohesin complex is formed by the structural  
48 maintenance of chromosomes (SMC) subunits SMC1 and SMC3, by the  $\alpha$ -kleisin subunit RAD21 and  
49 by a stromal antigen (SA) subunit, either SA1 or SA2. In addition, several proteins, such as ESCO1/2  
50 acetylases and histone deacetylase 8 (HDAC8), are associated with the complex and regulate its  
51 function. In particular, the Nipped B-like (NIPBL) loading factor is required for cohesin loading onto  
52 the DNA. In fact, even though the complex itself is capable of binding the DNA [3], cohesin loading  
53 onto chromosomes requires NIPBL to be efficient. Apart from its aforementioned role, cohesin has  
54 recently emerged as an epigenetic regulator of gene expression. Studies have revealed that cohesin  
55 mediates long-range chromatin interactions between enhancers and promoters [4–6] and a recent  
56 work highlighted its role in the formation and stabilization of Topologically Associating Domains  
57 (TADs) [7]. In addition, there is evidence of cohesin-mediated regulation of gene expression, either  
58 positive or negative, through interaction with RNA polymerase II [8–10].  
59 Since NIPBL is involved in mediating cohesin function, it also regulates cohesin-mediated gene  
60 expression. In particular, NIPBL co-localizes with cohesin and mediator at transcriptionally active  
61 sites [4]. Interestingly, NIPBL is also found to bind at the promoters of active genes in the absence of  
62 cohesin and its knockdown results in reduced gene expression of these genes [11]. Thus, NIPBL seems  
63 to play an even greater role than cohesin in regulating genome-wide gene expression. Indeed,  
64 previous works using different models highlighted NIPBL importance in transcriptional regulation  
65 during development and its deregulation was reported to alter the whole genome transcription and  
66 induce pathological defects, particularly in the Cornelia de Lange Syndrome (CdLS) models.  
67 Mutations in the Nipped-B gene, the *Drosophila melanogaster* ortholog of NIPBL, caused  
68 developmental defects in mutant flies [12] and NIPBL<sup>+/-</sup> mice displayed alteration of multiple organs,  
69 including heart, bone and fatty tissue [13]. Also, both NIPBL deficiency and haploinsufficiency  
70 impaired pectoral fin and limb development in zebrafish and mouse, respectively, through the  
71 downregulation of several *Hox* genes [14]. In lymphoblastoid cell lines (LCLs) derived from CdLS  
72 patients carrying NIPBL mutations, cohesin-binding sites were reduced by approximately 30%,  
73 leading to transcription deregulation of more than 300 genes [15]. Similarly, transcriptome analysis  
74 revealed hundreds of deregulated genes, either downregulated or overexpressed, both in iPSCs and  
75 cardiomyocytes derived from NIPBL<sup>+/-</sup> CdLS patients [16] and another study identified whole-  
76 genome changes in gene expression in both LCLs derived from NIPBL-mutated CdLS patients and  
77 mouse embryonic fibroblasts (MEFs) derived from *Nipbl*<sup>+/-</sup> mice [17].  
78 Other works associated NIPBL alterations to tumors. For example, the loss of NIPBL reduces  
79 sensitivity to chemotherapy in gastrointestinal cancers [18] and its mutation was found in acute  
80 megakarioblastic leukemia associated with Down syndrome (DS-AMKL) [19]. Interestingly, we have  
81 observed a modulation of the canonical Wnt pathway in zebrafish embryos at different  
82 developmental stages upon *nipblb* loss-of-function: at 24 hours post fertilization (hpf) we reported a  
83 reduction of canonical Wnt pathway genes [20] that was recovered starting from 2 days post  
84 fertilization (dpf) [21]. This evidence raises the possibility that *nipblb* haploinsufficiency primes a  
85 series of back-up mechanisms that counteract the transcriptional patterns induced by its silencing.  
86 In this work, we further analyze the transcriptional role of *nipblb* loss-of-function zebrafish embryos  
87 broadening the analyses to the whole transcriptome through RNAseq analyses. In this regard, we  
88 consider a possible role of *nipblb* during development choosing to compare wild-type and *nipblb*-  
89 haploinsufficient embryos at both 24 hpf and 3 dpf. The experiments allowed the identification of a  
90 strong *nipblb*-mediated modulation of transcriptional events in the early development, until 24 hpf,  
91 that was mostly recovered at 3 dpf by other factors than *nipblb*. In addition, we confirmed our  
92 previous findings highlighting the role of NIPBL in the regulation of pathways common to  
93 hematopoiesis and mutated *NPM1*.

## 94 95 2. Results

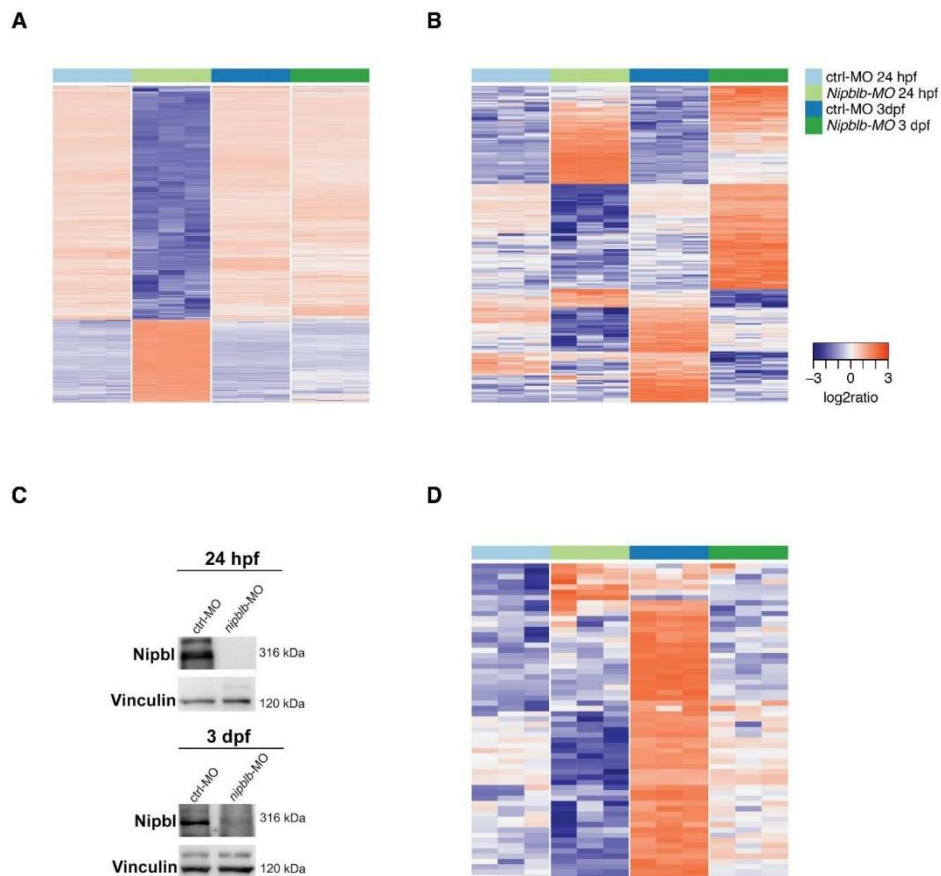


96 NIPBL has emerged as a major player in gene expression regulation at the genome-wide level and its  
97 alterations have been reported to underlie substantial transcriptional changes, particularly in CdLS.  
98 In this work we studied the role of the *NIPBL* orthologue in zebrafish, *nipblb* (Ch 10: 36,475,860-  
99 36,547,128), in transcriptional activation relatively to a specific developmental stage. To assess the  
100 global *nipblb* impact on the whole-genome transcription during zebrafish development, we  
101 performed RNA-seq analysis on three replicates of control- and *nipblb*-morpholino (MO, Gene Tools)  
102 injected embryos at 24 hpf (ctrl-MO 24h and *nipblb*-MO 24h) and 3 dpf (ctrl-MO 3d and *nipblb*-MO  
103 3d). For the generated 12 libraries, we obtained approximately 80 million reads for each sample, with  
104 a range from 95 to 97% of reads mapped onto zebrafish genome (**Table S1**). We chose these  
105 developmental stages since at 24 hpf the overall structure of the body has already been completed  
106 and the three main axes assessed following gastrulation and somitogenesis. At 3 dpf, more specific  
107 differentiation of tissues and organs have been accomplished, such as definitive hematopoiesis [22],  
108 second myogenesis [23], activation of innate immunity [24], and thymus specification [25]. The  
109 unsupervised analysis highlighted that the gene expression data were highly reproducible among  
110 the various biological replicates (**Figure 1A**) and that only *nipblb*-MO injected embryos at 24 hpf were  
111 characterized by a completely distinct transcriptional pattern as compared to both control and *nipblb*-  
112 MO injected embryos at 3 dpf (**Figure 1B**).  
113



114  
 115 **Figure 1.** (A) Sample correlation matrix using gene-wise standardized expression values of 1,999  
 116 highly variable genes. (B) Unsupervised hierarchical clustering of wild-type and *nipblb*-MO injected  
 117 embryos at 24 hpf and 3 dpf based on the standardized gene expression values of 1,999 highly  
 118 variable genes. Each column represents one separated biological sample.  
 119

120 To explore the molecular changes underlying loss of *nipblb* in early and late developmental  
 121 stages and the interplay between *nipblb* loss-of-function and development, we compared the  
 122 transcriptional profiles of zebrafish embryos from all 4 conditions (Table S2). Differential gene  
 123 expression analysis returned 5,691 genes differentially expressed in the comparison between *nipblb*-  
 124 MO and control embryos at 24 hpf (false discovery rate  $FDR \leq 1\%$  and absolute fold change  $\geq 3$ ; Figure  
 125 2A). Among them, 1,486 genes were up-regulated and 4,205 were down-regulated. Surprisingly, as  
 126 suggested by the unsupervised analysis of Figure 2B, only a small set of 223 genes (143 overexpressed  
 127 and 80 down-regulated) were differentially expressed when comparing *nipblb*-MO injected and  
 128 control embryos at 3 dpf ( $FDR \leq 1\%$  and absolute fold change  $\geq 3$ ). Since the effects of *nipblb* silencing  
 129 were still effective (Figure 2C) and the differential gene expression between 24 hpf and 3 dpf in a  
 130 normal condition (control embryos) is limited ( $FDR \leq 1\%$  and absolute fold change  $\geq 3$ ; Figure 2D), we  
 131 hypothesized that the rescue of the differential expression induced by *nipblb*-haploinsufficiency at 3  
 132 dpf has to be ascribed to mechanisms counteracting *nipblb* loss-of-function rather than to the loss of  
 133 morpholino perdurance or to the effect of normal development processes. For instance, the paralog  
 134 *nipbla* (Ch 5: 8,005,911-8,096,232) might exert a compensative effect as its expression resulted  
 135 increased, although not drastically, at 24 hpf ( $FDR \leq 1\%$  and absolute fold change=2.36; Table S2).  
 136

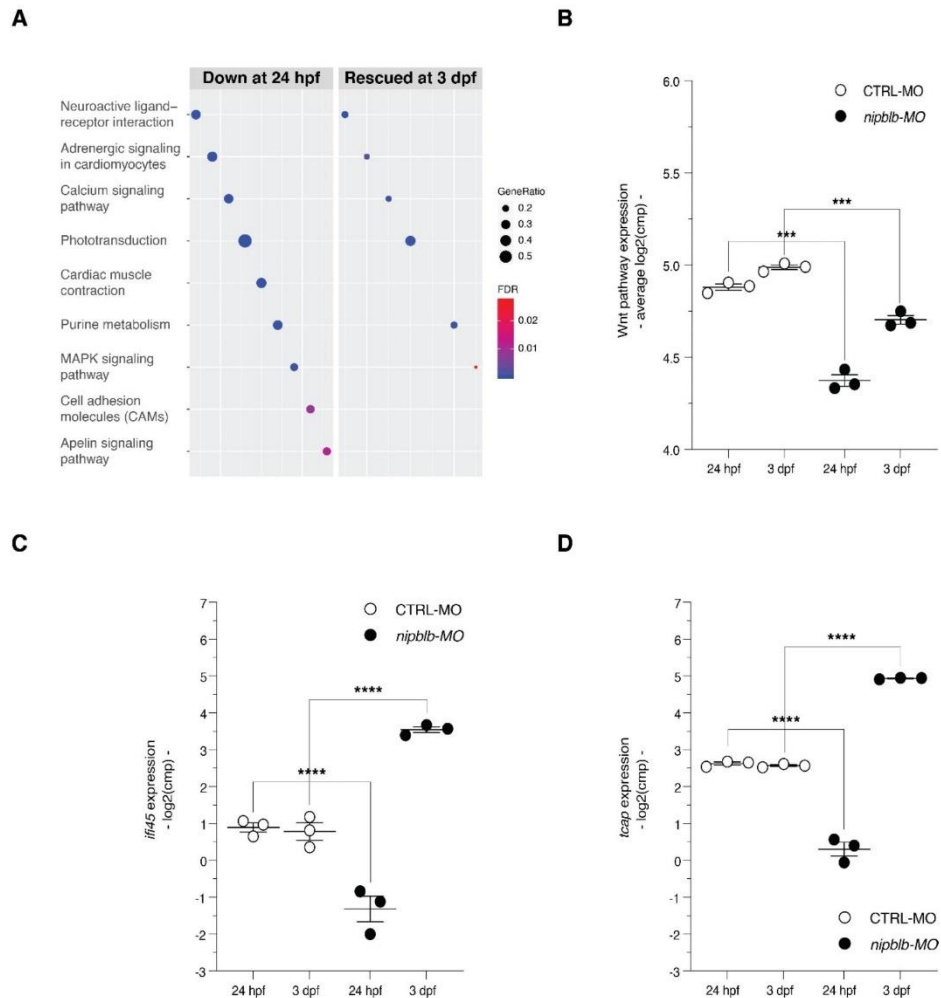


137  
 138  
 139  
 140

141 **Figure 2.** (A) Supervised hierarchical clustering of wild-type and *nipblb*-MO injected embryos based  
142 on the standardized gene expression values of 5,691 genes differentially expressed in the comparison  
143 between *nipblb*-MO and wild-type embryos at 24 hpf. Each column represents one separated  
144 biological sample. (B) Same as in (A) based on the set of 223 genes differentially expressed when  
145 comparing *nipblb*-MO injected and control embryos at 3 dpf. (C) Western blot analyses of Nipbl  
146 protein expression in control-MO and *nipblb*-MO injected embryos at 24 hpf and 3 dpf. Vinculin  
147 marker was used for normalization. (D) Same as in (A) using the 60 differentially expressed genes in  
148 the comparison between control samples at 24 hpf and 3 dpf.

149  
150

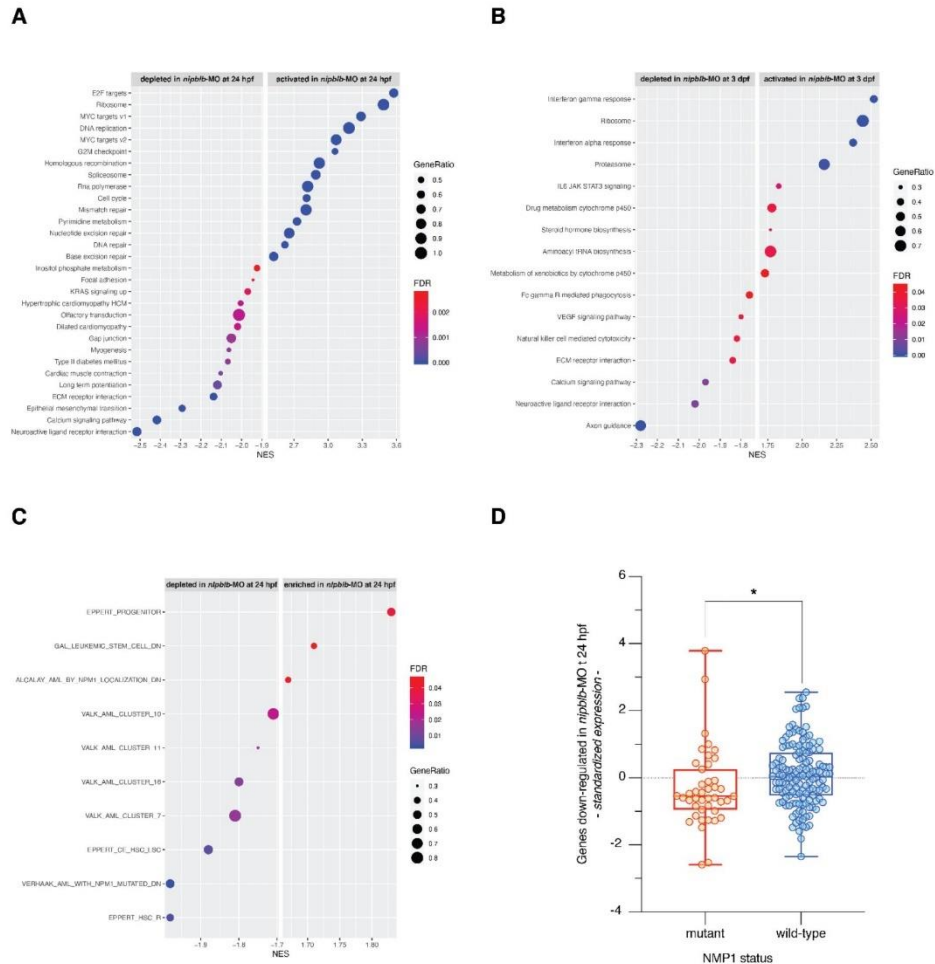
151 Overall, more than 60% of the 5,691 genes differentially expressed in *nipblb*-MO embryos at 24  
152 hpf returned, in *nipblb*-MO embryos at 3 dpf, to the same expression levels of the control embryos.  
153 Functionally, this corresponded to restoring the gene expression levels of pathways related to  
154 receptors and ligands associated with intracellular and extracellular signaling, phototransduction,  
155 purine metabolism, and MAPK signaling that were all repressed in *nipblb*-haploinsufficient embryos  
156 at 24 hpf (**Figure 3A**). As we previously showed, *nipblb* loss-of-function determined, at 24 hpf, a  
157 significant reduction ( $p=1 \times 10^{-4}$ ) in the overall activation of the Wnt canonical pathway [20,21] that  
158 was almost recovered at 3 dpf ( $p=4 \times 10^{-4}$ ; **Figure 3B**). Conversely, 44 and 17 genes remained up- and  
159 down-regulated respectively, in *nipblb*-MO embryos at 3 dpf compared to their respective controls.  
160 Interestingly, 29 genes down-regulated by *nipblb* silencing at 24 hpf resulted up-regulated in *nipblb*-  
161 MO at 3 dpf. Among these genes, the interferon alpha inducible protein (*ifl45*), involved in apoptotic  
162 signaling pathway, and the *titin-cap* (*telethonin*, *tcap*), implicated in T-tubule organization and heart  
163 contraction, were oppositely regulated at 24 hpf and 3 dpf (**Figure 3C-D**).



164  
 165 **Figure 3.** (A) Dot plot of the KEGG gene sets significantly enriched in the 4,205 down-regulated genes  
 166 by *nipblb* loss-of-function at 24 hpf and in the 2,558 genes that returned, in *nipblb*-MO embryos at 3  
 167 dpf, to the same expression levels of the wild-type embryos at both developmental stages. Dot color  
 168 indicates statistical significance of the enrichment (false discovery rate FDR); dot size represents the  
 169 fraction of genes annotated to each term. Gene sets are ranked in increasing order based on the FDR  
 170 value. (B) Average expression of all KEGG Wnt canonical pathway genes in sample subgroups (\*\*\*,  
 171  $p \leq 0.001$  in unpaired t-test). (C) Gene expression of *ifi45* in sample subgroups (\*\*\*\*,  $FDR \leq 0.0001$  in  
 172 edgeR exactTest). (D) Gene expression of *tcap* in sample subgroups (\*\*\*\*,  $FDR \leq 0.0001$  in edgeR  
 173 exactTest).  
 174

175 Functional annotation using GSEA and gene sets from the MSigDB Hallmark and KEGG  
 176 collections highlighted that *nipblb* loss-of-function activated, at 24 hpf, gene sets related to cell cycle,  
 177 MYC signaling, DNA replication, RNA polymerase, and ribosome metabolism while repressed gene  
 178 sets associated to receptors and ligands involved in the intracellular and extracellular signaling, EMT,  
 179 ECM, motility and function of the cardiac muscle, MAPK signaling pathway, and cell-matrix  
 180 adhesion (Table S3 and Figure 4A). Differently, at 3 dpf, in *nipblb*-haploinsufficiency, activated genes  
 181 sets connected to interferon response, JAK-STAT signaling, the proteasome, and the metabolisms of

182 ribosome and cytochrome p450 while repressing gene sets related to receptors and ligands involved  
 183 in cell signaling, cytotoxicity and phagocytosis, ECM interactions, and VEGF signaling (Table S4 and  
 184 Figure 4B).  
 185



186 **Figure 4.** (A) Dot plot of the top 10 significantly enriched (normalized enrichment score NES>0  
 187 and FDR≤0.05) and depleted (normalized enrichment score NES<0 and FDR≤0.05) gene sets from  
 188 Gene Set Enrichment Analysis of *nipblb*-MO at 24 hpf as compared to their wild-type counterpart.  
 189 Dot color indicates statistical significance of the enrichment (false discovery rate FDR); dot size  
 190 represents the fraction of genes annotated to each term. Gene sets are ranked in increasing order  
 191 based on the NES value. (B) Same as in (A) for all the significantly enriched (normalized enrichment  
 192 score NES>0 and FDR≤0.05) and depleted (normalized enrichment score NES<0 and FDR≤0.05) gene  
 193 sets from Gene Set Enrichment Analysis of *nipblb*-MO at 3 dpf as compared to their wild-type  
 194 counterpart. (C) Dot plot of the significantly enriched (normalized enrichment score NES>0 and  
 195 FDR≤0.05) and depleted (normalized enrichment score NES<0 and FDR≤0.05) myeloid differentiation  
 196 and AML-related gene sets from Gene Set Enrichment Analysis of *nipblb*-MO at 24 hpf as compared  
 197 to their wild-type counterpart. (D) Average expression in NMP1 mutant and wild-type AMLs of 4,205  
 198 genes down-regulated by *nipblb* loss-of-function at 24 hpf (\*, p=0.019 in unpaired t-test)  
 199  
 200



201 Since NIPBL has emerged as a potential player in myeloid cell differentiation and in the  
202 insurgence of hematological malignancies [21,26,27], we performed the functional enrichment  
203 analysis also using a collection of gene sets related to myeloid differentiation and acute myeloid  
204 leukemia (AML; **Table S5**). Interestingly, we found that a set of genes up-regulated in human  
205 hematopoietic lineage committed progenitor cells, as compared to hematopoietic stem cells (HSC)  
206 and mature cells, were significantly activated in *nipblb* embryos at 24 hpf. Conversely, we found  
207 depleted sets of genes up-regulated in HSC enriched populations and in AML stem cell (LSC; **Figure**  
208 **4C**). In addition, *nipblb* loss-of-function downregulated genes active in AML patients with wild-type  
209 *NPM1*, thus suggesting that *nipblb*-haploinsufficiency phenocopies the transcriptional effects induced  
210 by *NPM1* mutations in AMLs. We next sought to determine the expression patterns of genes  
211 downregulated by *nipblb* loss-of-function in a cohort of AML patients with mutant and wild-type  
212 *NPM1* [28] and verified that the transcriptional program repressed by *nipblb*-haploinsufficiency is  
213 indeed repressed also in AMLs with mutant *NPM1* (**Figure 4D**). No gene sets associated to myeloid  
214 differentiation and AML resulted significantly modulated in *nipblb* embryos at 3 dpf.  
215

### 216 3. Discussion

217 The Nipped B-like protein (NIPBL) is the factor that allows the loading of the cohesin complex  
218 on the DNA during the G2 phase of the cell cycle [29]. In addition to its canonical role, NIPBL was  
219 also identified as a transcription factor and architect of the chromatin, independently to its  
220 interactions with the cohesin complex. For instance, Hi-C data showed that *Nipbl* deletion in  
221 hepatocytes strongly impacts on genome organization, while few changes were reported following  
222 cohesin depletion [5,30,31]. Moreover, ChIP-sequencing analyses in human HB2 cells revealed that  
223 the binding sites of NIPBL to the genome were independent to those of cohesin or CTCF [11],  
224 suggesting that NIPBL may have a direct role in gene expression. Indeed, in HB2 cells NIPBL was  
225 shown to localize preferentially to active promoters rich in CpG islands, and near the RNA Pol II  
226 binding sites [11]. Also in *D. melanogaster* genome, Nipped-B and cohesin preferentially bind to  
227 transcribed regions, frequently overlapping with RNA polymerase II binding sites [8]. In human ES  
228 cells, ChIP-Seq data revealed an association between NIPBL and the enhancer and core promoter  
229 region sites bound by mediator and cohesin in actively transcribed genes [4].

230 NIPBL has been linked to gene expression regulation in different models such as *Cut* and  
231 *Ultrabithorax* in *D. melanogaster* [32], adipogenic differentiation genes such as *Cebpb* and *Ebf1* in  
232 murine embryonic fibroblasts [13], endodermal differentiation and left-right axis genes such as *sox32*,  
233 *sox17*, *foxa2*, *gata5*, *spaw*, *lefty2*, and *dnah9* in zebrafish [33], histone deacetylases HDAC1 and HDAC3  
234 [34] and heterochromatin protein 1 in human [35].

235 Here, we used RNA-seq analyses in *nipblb*-haploinsufficient zebrafish embryos at 24 hours and  
236 3 days post fertilization to investigate the genome-wide effect of *nipblb* loss-of-function on zebrafish  
237 transcriptional programs during development. Our findings revealed a significant gene inactivation  
238 following down-regulation of *nipblb* in zebrafish embryos, as already described in *D. melanogaster* [8].  
239 Indeed, as compared to their control samples, *nipblb*-haploinsufficient embryos at 24 hpf showed a  
240 down-regulation of 4,205 genes while only 1,486 genes were up-regulated. Interestingly, the massive  
241 transcriptional impact of *nipblb* loss-of-function was abundantly recovered during development  
242 resulting in the minor transcriptional changes observed at 3 dpf upon *nipblb* silencing. Although the  
243 technique of oligo morpholino injection used to block *Nipblb* protein production has been  
244 demonstrated to drop down during the first 120 hpf of development [36], the absence of *Nipblb*  
245 protein observed at 3 dpf let hypothesizing that the rescue of the differential expression induced by  
246 *nipblb*-haploinsufficiency was associated to specific mechanisms counteracting *nipblb* loss-of-function  
247 during development and not to a loss of *nipblb* silencing. Since in zebrafish NIPBL is present in two  
248 paralogs, *nipblb* (Ch 10: 36,475,860-36,547,128) and *nipbla* (Ch 5: 8,005,911-8,096,232), one possible  
249 explanation for the recovery could be related to the compensatory action of *nipbla*. Indeed, it has been  
250 previously suggested both *nipbl* paralogs have similar functions in zebrafish [14] and we showed that

251 the knock-down of *nipblb* slightly increase the expression of *nipbla*. However, although the role of  
252 *nipblb* seemed preponderant as the knock-down of *nipblb* determined a most severe phenotype in the  
253 early developmental stages than the *nipbla* knock-down, Muto and colleagues also demonstrated that  
254 *nipbla* silencing did not affect the expression of endodermal gene such as *nipblb* reduction, suggesting  
255 functional specialization in gene regulation between the two paralog [14].

256 Among the down-regulated genes, we identified genes that could be correlated with phenotypes  
257 presented by CdLS patients with *NIPBL* mutation. For instance, we described down-regulation of  
258 genes associated to receptors and ligands involved in the intracellular and extracellular signaling,  
259 EMT, ECM, cardiac muscle motility and function, MAPK signaling pathway and cell-matrix  
260 adhesion. In a murine model of *Nipbl*-haploinsufficiency, genes involved in neural differentiation,  
261 such as *MAP2K1* and *MAP4K1*, and heart development, such as *BMP2*, were also described [13]. To  
262 note, differences in gene expression were also described in iPSCs and cardiomyocytes derived from  
263 CdLS *NIPBL*<sup>+/-</sup> patients, suggesting a role for *NIPBL* in transcriptional regulation of cardiac cells [16].  
264 The functional enrichment of differentially expressed genes resulted also in pathways that were up-  
265 regulated following *nipblb*-haploinsufficiency, such as MYC and JAK-STAT signaling pathways, and  
266 genes sets connected to interferon and immune response. Noticeably, the up-regulation of stress-  
267 induced immune response has been described also in *Nipbl*<sup>+/-</sup> MEF cells as a consequence of the down-  
268 regulation of RNA-processing genes and aberrant RNA biogenesis [17].

269 In recent years, dysregulation of *NIPBL* has been associated with tumor insurgence, in particular  
270 in hematological malignancies [21,26,27]. To further verify this association, we used a collection of  
271 gene sets related to myeloid differentiation and AML in the functional enrichment analysis of the  
272 gene expression pattern induced by *nipblb* loss-of-function. Interestingly, we found that genes  
273 activated by *nipblb*-haploinsufficiency are associated to the hematopoietic lineage committed  
274 progenitor cells while genes repressed by the loss of *nipblb* are expressed by HSC enriched  
275 populations and in AML stem cell (LSC). In addition, the downregulation induced by *nipblb* loss-of-  
276 function resembles the transcriptional pattern induced by *NMP1* mutations in AMLs, as verified by  
277 the functional annotation and by the expression level of genes downregulated by *nipblb* loss-of-  
278 function in the transcriptomes of AML patients with mutant and wild-type NPM1.

279 Taken together, these data provide new insights into the role of *NIPBL* in regulating zebrafish  
280 gene expression. In particular, our analysis reveals that *nipblb* loss-of-function has a major impact on  
281 gene expression in the early development, until 24 hpf, and that this massive transcriptional  
282 dysregulation is significantly recovered later during development by compensative mechanisms that  
283 need further identification analyses. Moreover, by unraveling a connection between *nipblb*-  
284 dependent differential expression and genes sets related to different hematological cell populations  
285 and AML subtypes, we shed light on the possible involvement of *NIPBL*-related transcriptional  
286 dysregulation in hematological malignancies.

287

#### 288 4. Materials and Methods

##### 289 *Zebrafish embryos*

290 Zebrafish (*Danio rerio*) were maintained at the University of Milan, Via Celoria 26 - 20133 Milan, Italy  
291 (Autorizzazione Protocollo n. 295/2012-A - 20/12/2012). Zebrafish AB strains were maintained  
292 according to international (EU Directive 2010/63/EU) and national guidelines (Italian decree n. 26 of the  
293 4th of March 2014). Embryos were staged and used until 5 days post fertilization, a time window in  
294 which zebrafish is not considered an animal model according to national guidelines (Italian decree n.  
295 26 of the 4th of March 2014). Embryos were staged according to Kimmel and colleagues [37] and raised  
296 in fish water (Instant Ocean, 0.1% Methylene Blue) at 28°C in Petri dishes, according to established  
297 techniques. Embryonic ages are expressed in hours post fertilization (hpf) and days post fertilization  
298 (dpf) and the embryos used in this work were younger than 5 dpf. To prevent pigmentation, 0.003% 1-  
299 phenyl-2-thiourea (PTU, Sigma-Aldrich, St. Louis, Missouri, US) was added to the fish water. Embryos  
300 were anaesthetized with 0.016% tricaine (Ethyl 3-aminobenzoate methanesulfonate salt, Sigma-  
301 Aldrich) before proceeding with experimental protocols.

302

303 *Injections*

304 Injections were carried out on one- to two-cell stage embryos. Details of concentration and sequence of  
305 *nipblb* morpholino (*nipblb*-MO, LLC, Philomath OR, USA) are described in [21]. In all experiments, MO-  
306 injected embryos were compared to embryos at the same developmental stage injected with the same  
307 amount of a ctrl-MO that has no target in zebrafish (Gene Tools).

308  
309 *RNA extraction*

310 Total RNA was extracted from at least 30 embryos at the desired developmental stage (24 hpf or 72 hpf)  
311 by TRIzol reagent (ThermoFisher Scientific, MA, USA) and chloroform (Carlo Erba, Milan, Italy),  
312 followed by phenol-chloroform separation and isopropanol precipitation. The pellet was resuspended  
313 by adding 30  $\mu$ l of RNase-free water. Following RNA isolation, DNase treatment was performed using  
314 Turbo DNase (Life Technology, Carlsbad, California, USA). After purification, RNA yield, quality and  
315 size of isolated RNAs were assessed using Nanodrop spectrophotometer (ThermoFisher) and  
316 TapeStation instrument (Agilent Technologies, Santa Clara, CA, USA). Total RNA concentration from  
317 each biological sample ranged from 0.3 to 1.2  $\mu$ g/ $\mu$ l and the RNA Integrity Number (RIN) values were  
318 between 5.7 and 6.9.

319  
320 *RNA-Seq and bioinformatics analyses*

321 Total RNA was isolated from ctrl-MO and *nipblb*-MO embryos at 24 hpf and 3 dpf using the Illumina  
322 TruSeq Stranded mRNA Library Prep Kit, according to manufacturer's instructions. Before sequencing,  
323 libraries were analyzed with the TapeStation instrument and quantified by Nanodrop  
324 spectrophotometer with the use of the fluorescent dye PicoGreen® to verify the length and  
325 concentration of the inserts. RNA libraries were then diluted at 2 nM concentration and normalized  
326 using standard library quantification and quality control procedures as recommended by the Illumina  
327 protocol. RNA sequencing was carried out in triplicates on an Illumina HiSeq4000 with a 2x150bp run.  
328 Raw reads of NGS data are available in NCBI Short-read Archive (SRA,  
329 <https://www.ncbi.nlm.nih.gov/sra/>) under accession number PRJNA675020. Read quality was accessed  
330 using fastQC (v. 0.11.3; <http://www.bioinformatics.babraham.ac.uk/projects/fastqc/>). Raw reads were  
331 trimmed for adapters and for length at 100 bp with Trimmomatic [38] and subsequently aligned to the  
332 zebrafish reference genome (GRCz11.97) using STAR (v.020201) [39]. Raw gene counts were obtained  
333 using htseq-count (v.0.6.0 options: --stranded=reverse) [40] with the Ensembl annotation file  
334 GRCz11.97.gtf as a reference. Raw counts were normalized to counts per million mapped reads (cpm)  
335 using the *edgeR* package [41]; only genes with a cpm greater than 1 in at least 1 sample were further  
336 retained for differential analysis. Global unsupervised clustering was performed using the function  
337 *hclust* of R *stats* package with Pearson correlation as distance metric and average agglomeration method.  
338 Gene expression heatmaps have been generated using the function *heatmap.2* of R *gplots* package after  
339 row-wise standardization of the expression values. Before unsupervised clustering, to reduce the effect  
340 of noise from non-varying genes, we removed those probe sets with a coefficient of variation smaller  
341 than the 90<sup>th</sup> percentile of the coefficients of variation in the entire dataset. The filter retained 1,999 genes  
342 that are more variable (highly variable genes) across samples in any of the 4 subsets (i.e., ctrl-MO and  
343 *nipblb*-MO at 24 hpf and 3 dpf). Differential gene expression analysis was performed using the *exactTest*  
344 function of the *edgeR* package [41]. Genes were considered significantly differently expressed at False  
345 Discovery Rate (FDR)  $\leq 0.01$  and absolute fold-change  $\geq 3$ . Functional annotation of the differentially  
346 expressed genes was performed using gProfiler (<https://biit.cs.ut.ee/gprofiler>) and the gene sets of the  
347 KEGG biological pathways. Functional over-representation analysis was performed using Gene Set  
348 Enrichment Analysis (GSEA; <http://software.broadinstitute.org/gsea/index.jsp>) and curated gene sets  
349 of the Molecular Signatures Database (MSigDB). In particular, we used the Hallmark gene sets, the  
350 KEGG subset of canonical pathways (MSigDB C2), and a collection of 80 gene sets related to myeloid  
351 differentiation and AML (Table S5). Prior to GSEA analysis, we converted zebrafish Entrez IDs into  
352 the corresponding human orthologues genes using the HUGO Gene Nomenclature Committee  
353 (HGNC) Orthology Predictions Search (HCOP; <https://www.genenames.org/cgi-bin/hcop>). Gene sets  
354 were considered significantly enriched at false discovery rate (FDR)  $\leq 0.05$  when using Signal2Noise as



355 metric and 1.000 permutations of gene sets. The dot plots showing the most significantly enriched and  
356 depleted gene sets were generated using the *ggplot* function of the *ggplot2* R package.

357 Gene expression data of AML patients were measured on Affymetrix arrays and have been  
358 downloaded from NCBI Gene Expression Omnibus (GEO, <http://www.ncbi.nlm.nih.gov/geo/>)  
359 GSE10358 along with annotations on the mutational status of NMP1. Since raw data (.CEL files) were  
360 available for all samples, the integration, normalization and summarization of gene expression signals  
361 has been obtained converting probe level signals to expression values using the robust multi-array  
362 average procedure RMA [42] of the Bioconductor *affy* package.

363 Average signature expression has been calculated as the standardized average expression of all  
364 signature genes in all 184 samples with NMP1 annotation.

365 All analyses were performed using R 3.6.2 and publicly available packages explicitly cited in the  
366 manuscript. No custom functions were written for the analysis.

#### 367 *Western blot*

368 At least 30 zebrafish embryos were used for protein preparation and the yolk was previously removed  
369 from embryos to avoid yolk protein contamination. Total proteins were extracted with RIPA buffer  
370 (50 mM Tris-HCl pH 7.4, 1% NP-40, 150 mM NaCl, 0.25% sodium deoxycholate, 1mM EDTA, 1mM  
371 PMSF,) with the addition of protease inhibitor cocktail (Roche). Lysates were incubated 3 min at 95°C  
372 and 2 min at 4°C, followed by disaggregation by using insulin syringe. Incubation and disaggregation  
373 were repeated twice and then lysates were centrifuged 10 min at 16.000 g at 4°C. The supernatant was  
374 recovered and extracts were quantified by using the Quantum Micro protein Assay (EuroClone). 50 µg  
375 of proteins were loaded in a 6.5% acrylamide/polyacrilamide gel and subjected to electrophoresis.  
376 Protein transfer onto polyvinylidene fluoride (PVDF) membrane was performed at 30 V for 16 hours at  
377 4°C. Membranes were incubated with blocking solution (5% skimmed powder milk in TBS containing  
378 0.1% TWEEN-20) for 1h at room temperature before overnight incubation at 4°C with primary  
379 antibodies in blocking solution. Membranes were then incubated 1h at room temperature with HRP-  
380 conjugated secondary antibodies in blocking solution. Protein bands were detected by using WESTAR  
381 ECL detection system (Cyanagen, Bologna, Italy). Images were acquired with the Alliance MINI HD9  
382 AUTO Western Blot Imaging System (UVIttec Limited, Cambridge, UK) and analyzed with the related  
383 software. Vinculin were used as internal control. Primary antibodies were mouse anti-vinculin 1:6000  
384 (V9131, Sigma-Aldrich) and rabbit anti-NIPBL 1:200 (NB100-93320, Novus Biologicals, Littleton,  
385 Colorado, USA) Secondary antibody were HRP-conjugated goat anti-rabbit 1:5000 (7074, Cell Signaling  
386 Technology, Danvers, Massachusetts, US) and HRP-conjugated horse anti-mouse 1:4000 (7076, Cell  
387 Signaling Technology).

388  
389

390 **Supplementary Materials:** Supplementary materials can be found at [www.mdpi.com/xxx/s1](http://www.mdpi.com/xxx/s1).

391 **Author Contributions:** “Conceptualization, A.P. and A.M.; methodology, A.P, M.M., C.B., S.B., C.C., R.B. and  
392 E.M.; software, S.B. and E.M.; validation, M.M. and M.S; formal analysis, S.B., A.P, M.S., A.M. and E.M;  
393 investigation, A.P., M.S. and A.M.; resources, S.B., A.M and E.M.; data curation, S.B., A.P., A.M. and E.M.;  
394 writing—original draft preparation, A.P, C.C. and M.S; writing—review and editing, A.P, A.M, C.B., S.B, and  
395 C.C.; project administration, A.P. and A.M.; funding acquisition, A.P. All authors have read and agreed to the  
396 published version of the manuscript.

397 **Funding:** This research was funded by the Associazione Italiana per la Ricerca sul Cancro (AIRC)  
398 (MFAG#18714). The funders had no role in the study design, data collection and interpretation, or the decision  
399 to submit the work for publication.

400 **Acknowledgments:** We thank Alex Pezzotta and Marco Cafora (University of Milan) for their priceless support  
401 in experimental procedures, and Chiara Priami (Istituto Europeo di Oncologia, Milan) for experimental help in  
402 RNA extraction and sample library preparation and Tania Camboni (ITB-CNR) for technical support in RNA-  
403 Seq library preparation.

404 **Conflicts of Interest:** The authors declare no conflict of interest.

405 **Abbreviations**

NIPBL	Nipped B-like
MO	Morpholino
RNA-seq	RNA sequencing
EMT	Epithelial–Mesenchymal Transition
ECM	Extra-Cellular Matrix
AML	Acute Myeloid Leukemia
HSC	Hematopoietic Stem Cells
LSC	Leukemia Stem Cells
FDR	False Discovery Rate
GSEA	Gene Set Enrichment Analysis
NES	Normalized Enrichment Score

406

407 **References**

- 408 1. Michaelis, C.; Ciosk, R.; Nasmyth, K. Cohesins: Chromosomal proteins that prevent premature  
409 separation of sister chromatids. *Cell* **1997**, doi:10.1016/S0092-8674(01)80007-6.
- 410 2. Watrin, E.; Peters, J.M. The cohesin complex is required for the DNA damage-induced G2/M checkpoint  
411 in mammalian cells. *EMBO J.* **2009**, doi:10.1038/emboj.2009.202.
- 412 3. Gligoris, T.G.; Scheinost, J.C.; Bürmann, F.; Petela, N.; Chan, K.L.; Uluocak, P.; Beckouët, F.; Gruber, S.;  
413 Nasmyth, K.; Löwe, J. Closing the cohesin ring: Structure and function of its Smc3-kleisin interface.  
414 *Science (80-. )*. **2014**, doi:10.1126/science.1256917.
- 415 4. Kagey, M.H.; Newman, J.J.; Bilodeau, S.; Zhan, Y.; Orlando, D.A.; Van Berkum, N.L.; Ebmeier, C.C.;  
416 Goossens, J.; Rahl, P.B.; Levine, S.S.; et al. Mediator and cohesin connect gene expression and chromatin  
417 architecture. *Nature* **2010**, doi:10.1038/nature09380.
- 418 5. Seitan, V.C.; Faure, A.J.; Zhan, Y.; McCord, R.P.; Lajoie, B.R.; Ing-Simmons, E.; Lenhard, B.; Giorgetti, L.;  
419 Heard, E.; Fisher, A.G.; et al. Cohesin-Based chromatin interactions enable regulated gene expression  
420 within preexisting architectural compartments. *Genome Res.* **2013**, doi:10.1101/gr.161620.113.
- 421 6. Lyu, X.; Rowley, M.J.; Corces, V.G. Architectural Proteins and Pluripotency Factors Cooperate to  
422 Orchestrate the Transcriptional Response of hESCs to Temperature Stress. *Mol. Cell* **2018**,  
423 doi:10.1016/j.molcel.2018.07.012.
- 424 7. Bernardi, G. The formation of chromatin domains involves a primary step based on the 3-D structure of  
425 DNA. *Sci. Rep.* **2018**, doi:10.1038/s41598-018-35851-0.
- 426 8. Misulovin, Z.; Schwartz, Y.B.; Li, X.Y.; Kahn, T.G.; Gause, M.; MacArthur, S.; Fay, J.C.; Eisen, M.B.;  
427 Pirrotta, V.; Biggin, M.D.; et al. Association of cohesin and Nipped-B with transcriptionally active  
428 regions of the *Drosophila melanogaster* genome. *Chromosoma* **2008**, doi:10.1007/s00412-007-0129-1.
- 429 9. Fay, A.; Misulovin, Z.; Li, J.; Schaaf, C.A.; Gause, M.; Gilmour, D.S.; Dorsett, D. Cohesin selectively binds  
430 and regulates genes with paused RNA polymerase. *Curr. Biol.* **2011**, doi:10.1016/j.cub.2011.08.036.
- 431 10. Downen, J.M.; Bilodeau, S.; Orlando, D.A.; Hübner, M.R.; Abraham, B.J.; Spector, D.L.; Young, R.A.  
432 Multiple structural maintenance of chromosome complexes at transcriptional regulatory elements. *Stem*  
433 *Cell Reports* **2013**, doi:10.1016/j.stemcr.2013.09.002.
- 434 11. Zuin, J.; Franke, V.; van Ijcken, W.F.J.; van der Sloot, A.; Krantz, I.D.; van der Reijden, M.I.J.A.; Nakato,  
435 R.; Lenhard, B.; Wendt, K.S. A Cohesin-Independent Role for NIPBL at Promoters Provides Insights in  
436 CdLS. *PLoS Genet.* **2014**, doi:10.1371/journal.pgen.1004153.
- 437 12. Rollins, R.A.; Morcillo, P.; Dorsett, D. Nipped-B, a *Drosophila* homologue of chromosomal adherins,

- 438 participates in activation by remote enhancers in the cut and Ultrabithorax genes. *Genetics* **1999**.
- 439 13. Kawauchi, S.; Calof, A.I.; Santos, R.; Lopez-Burks, M.E.; Young, C.M.; Hoang, M.P.; Chua, A.; Lao, T.;  
440 Lechner, M.S.; Daniel, J.A.; et al. Multiple organ system defects and transcriptional dysregulation in the  
441 Nipbl<sup>+/-</sup> mouse, a model of Cornelia de Lange syndrome. *PLoS Genet.* **2009**,  
442 doi:10.1371/journal.pgen.1000650.
- 443 14. Muto, A.; Ikeda, S.; Lopez-Burks, M.E.; Kikuchi, Y.; Calof, A.I.; Lander, A.D.; Schilling, T.F. Nipbl and  
444 Mediator Cooperatively Regulate Gene Expression to Control Limb Development. *PLoS Genet.* **2014**,  
445 doi:10.1371/journal.pgen.1004671.
- 446 15. Liu, J.; Zhang, Z.; Bando, M.; Itoh, T.; Deardorff, M.A.; Clark, D.; Kaur, M.; Tandy, S.; Kondoh, T.;  
447 Rappaport, E.; et al. Transcriptional Dysregulation in NIPBL and Cohesin Mutant Human Cells. *PLoS*  
448 *Biol.* **2009**, doi:10.1371/journal.pbio.1000119.
- 449 16. Mills, J.A.; Herrera, P.S.; Kaur, M.; Leo, L.; McEldrew, D.; Tintos-Hernandez, J.A.; Rajagopalan, R.;  
450 Gagne, A.; Zhang, Z.; Ortiz-Gonzalez, X.R.; et al. NIPBL<sup>+/-</sup> haploinsufficiency reveals a constellation of  
451 transcriptome disruptions in the pluripotent and cardiac states. *Sci. Rep.* **2018**, doi:10.1038/s41598-018-  
452 19173-9.
- 453 17. Yuen, K.C.; Xu, B.; Krantz, I.D.; Gerton, J.I. NIPBL Controls RNA Biogenesis to Prevent Activation of  
454 the Stress Kinase PKR. *Cell Rep.* **2016**, doi:10.1016/j.celrep.2015.12.012.
- 455 18. Liu, T.; Han, Y.; Yu, C.; Ji, Y.; Wang, C.; Chen, X.; Wang, X.; Shen, J.; Zhang, Y.; Lang, J.Y. MYC  
456 predetermines the sensitivity of gastrointestinal cancer to antifolate drugs through regulating TYMS  
457 transcription. *EBioMedicine* **2019**, doi:10.1016/j.ebiom.2019.10.003.
- 458 19. Yoshida, K.; Toki, T.; Okuno, Y.; Kanezaki, R.; Shiraishi, Y.; Sato-Otsubo, A.; Sanada, M.; Park, M.J.;  
459 Terui, K.; Suzuki, H.; et al. The landscape of somatic mutations in Down syndrome-related myeloid  
460 disorders. *Nat. Genet.* **2013**, doi:10.1038/ng.2759.
- 461 20. Pistocchi, A.; Fazio, G.; Cereda, A.; Ferrari, L.; Bettini, L.R.; Messina, G.; Cotelli, F.; Biondi, A.; Selicorni,  
462 A.; Massa, V. Cornelia de Lange Syndrome: NIPBL haploinsufficiency downregulates canonical Wnt  
463 pathway in zebrafish embryos and patients fibroblasts. *Cell Death Dis.* **2013**, doi:10.1038/cddis.2013.371.
- 464 21. Mazzola, M.; Deflorian, G.; Pezzotta, A.; Ferrari, L.; Fazio, G.; Bresciani, E.; Saitta, C.; Ferrari, L.;  
465 Fumagalli, M.; Parma, M.; et al. NIPBL: a new player in myeloid cell differentiation. *Haematologica*  
466 **2019**, doi:10.3324/haematol.2018.200899.
- 467 22. Davidson, A.J.; Zon, L.I. The "definitive" (and 'primitive') guide to zebrafish hematopoiesis. *Oncogene*  
468 **2004**.
- 469 23. Pistocchi, A.; Gaudenzi, G.; Foglia, E.; Monteverde, S.; Moreno-Fortuny, A.; Pianca, A.; Cossu, G.; Cotelli,  
470 F.; Messina, G. Conserved and divergent functions of Nfix in skeletal muscle development during  
471 vertebrate evolution. *Dev.* **2013**, doi:10.1242/dev.076315.
- 472 24. Renshaw, S.A.; Trede, N.S. A model 450 million years in the making: Zebrafish and vertebrate immunity.  
473 *DMM Dis. Model. Mech.* **2012**.
- 474 25. Willett, C.E.; Zapata, A.G.; Hopkins, N.; Steiner, L.A. Expression of zebrafish rag genes during early  
475 development identifies the thymus. *Dev. Biol.* **1997**, doi:10.1006/dbio.1996.8446.
- 476 26. Dang, J.; Nance, S.; Ma, J.; Cheng, J.; Walsh, M.P.; Vogel, P.; Easton, J.; Song, G.; Rusch, M.; Gedman,  
477 A.L.; et al. AMKL chimeric transcription factors are potent inducers of leukemia. *Leukemia* **2017**,  
478 doi:10.1038/leu.2017.51.
- 479 27. Mazzola, M.; Pezzotta, A.; Fazio, G.; Rigamonti, A.; Bresciani, E.; Gaudenzi, G.; Pelleri, M.C.; Saitta, C.;  
480 Ferrari, L.; Parma, M.; et al. Dysregulation of NIPBL leads to impaired RUNX1 expression and



- 481 haematopoietic defects. *J. Cell. Mol. Med.* **2020**, doi:10.1111/jcmm.15269.
- 482 28. Tomasson, M.H.; Xiang, Z.; Walgren, R.; Zhao, Y.; Kasai, Y.; Miner, T.; Ries, R.E.; Lubman, O.; Fremont,  
483 D.H.; McLellan, M.D.; et al. Somatic mutations and germline sequence variants in the expressed tyrosine  
484 kinase genes of patients with de novo acute myeloid leukemia. *Blood* **2008**, doi:10.1182/blood-2007-09-  
485 113027.
- 486 29. Nasmyth, K.; Haering, C.H. Cohesin: Its Roles and Mechanisms. *Annu. Rev. Genet.* **2009**,  
487 doi:10.1146/annurev-genet-102108-134233.
- 488 30. Zuin, J.; Dixon, J.R.; Van Der Reijden, M.I.J.A.; Ye, Z.; Kolovos, P.; Brouwer, R.W.W.; Van De Corput,  
489 M.P.C.; Van De Werken, H.J.G.; Knoch, T.A.; Van Ijcken, W.F.J.; et al. Cohesin and CTCF differentially  
490 affect chromatin architecture and gene expression in human cells. *Proc. Natl. Acad. Sci. U. S. A.* **2014**,  
491 doi:10.1073/pnas.1317788111.
- 492 31. Sofueva, S.; Yaffe, E.; Chan, W.C.; Georgopoulou, D.; Vietri Rudan, M.; Mira-Bontenbal, H.; Pollard,  
493 S.M.; Schroth, G.P.; Tanay, A.; Hadjur, S. Cohesin-mediated interactions organize chromosomal domain  
494 architecture. *EMBO J.* **2013**, doi:10.1038/emboj.2013.237.
- 495 32. Rollins, R.A.; Korom, M.; Aulner, N.; Martens, A.; Dorsett, D. Drosophila Nipped-B Protein Supports  
496 Sister Chromatid Cohesion and Opposes the Stromalin/Scs3 Cohesion Factor To Facilitate Long-Range  
497 Activation of the cut Gene. *Mol. Cell. Biol.* **2004**, doi:10.1128/mcb.24.8.3100-3111.2004.
- 498 33. Muto, A.; Calof, A.L.; Lander, A.D.; Schilling, T.F. Multifactorial origins of heart and gut defects in  
499 Nipbl-deficient zebrafish, a model of cornelia de Lange Syndrome. *PLoS Biol.* **2011**,  
500 doi:10.1371/journal.pbio.1001181.
- 501 34. Jahnke, P.; Xu, W.; Wülling, M.; Albrecht, M.; Gabriel, H.; Gillesen-Kaesbach, G.; Kaiser, F.J. The  
502 Cohesin loading factor NIPBL recruits histone deacetylases to mediate local chromatin modifications.  
503 *Nucleic Acids Res.* **2008**, doi:10.1093/nar/gkn688.
- 504 35. Lechner, M.S.; Schultz, D.C.; Negorev, D.; Maul, G.G.; Rauscher, F.J. The mammalian heterochromatin  
505 protein 1 binds diverse nuclear proteins through a common motif that targets the chromoshadow  
506 domain. *Biochem. Biophys. Res. Commun.* **2005**, doi:10.1016/j.bbrc.2005.04.016.
- 507 36. Eisen, J.S.; Smith, J.C. Controlling morpholino experiments: Don't stop making antisense. *Development*  
508 **2008**.
- 509 37. Kimmel, C.B.; Ballard, W.W.; Kimmel, S.R.; Ullmann, B.; Schilling, T.F. Stages of embryonic development  
510 of the zebrafish. *Dev. Dyn.* **1995**, *203*, 253–310, doi:10.1002/aja.1002030302.
- 511 38. Bolger, A.M.; Lohse, M.; Usadel, B. Trimmomatic: A flexible trimmer for Illumina sequence data.  
512 *Bioinformatics* **2014**, doi:10.1093/bioinformatics/btu170.
- 513 39. Dobin, A.; Davis, C.A.; Schlesinger, F.; Drenkow, J.; Zaleski, C.; Jha, S.; Batut, P.; Chaisson, M.; Gingeras,  
514 T.R. STAR: Ultrafast universal RNA-seq aligner. *Bioinformatics* **2013**, doi:10.1093/bioinformatics/bts635.
- 515 40. Anders, S.; Pyl, P.T.; Huber, W. HTSeq-A Python framework to work with high-throughput sequencing  
516 data. *Bioinformatics* **2015**, doi:10.1093/bioinformatics/btu638.
- 517 41. Robinson, M.D.; McCarthy, D.J.; Smyth, G.K. edgeR: A Bioconductor package for differential expression  
518 analysis of digital gene expression data. *Bioinformatics* **2009**, doi:10.1093/bioinformatics/btp616.
- 519 42. Irizarry, R.A.; Hobbs, B.; Collin, F.; Beazer-Barclay, Y.D.; Antonellis, K.J.; Scherf, U.; Speed, T.P.  
520 Exploration, normalization, and summaries of high density oligonucleotide array probe level data.  
521 *Biostatistics* **2003**, doi:10.1093/biostatistics/4.2.249.  
522

**Table S1** Summary statistics of RNA-seq profiling and read alignment.

Sample	total_reads	mapped_reads	mapped_reads_pct
CTRL_24h_1	106320197	102654009	96.55
CTRL_24h_2	86519359	83030507	95.97
CTRL_24h_3	82622705	79702889	96.47
CTRL_3d_1	83993616	80332888	95.64
CTRL_3d_2	80608466	77092652	95.64
CTRL_3d_3	86163909	81937501	95.09
Nipblb_24h_1	78683922	75715162	96.23
Nipblb_24h_2	91981783	88171489	95.86
Nipblb_24h_3	58330315	56197319	96.34
Nipblb_3d_1	89482968	86230798	96.37
Nipblb_3d_2	74766515	72119105	96.46
Nipblb_3d_3	74548438	71882596	96.42

**Table S2.** Fold change (FC) and statistical significance (False Discovery Rate, FDR) of differential gene expression in the comparisons of *nipblb*-MO and ctrl-MO samples at 24 hpf and 3 dpf.

[See Table S2.xlsx](#)

**Table S3.** Gene sets of the Hallmark and KEGG collections from the Molecular Signature Database (MSigDB; <https://www.gsea-msigdb.org/gsea/msigdb/collections.jsp>) enriched and depleted in *nipblb*-MO embryos as compared to ctrl-MO samples at 24 hpf (FDR $\leq$ 0.05).

Gene set	Size	NES	FDR	GeneRatio	Effect
E2F TARGETS	170	3.58	0	0.69	Enriched in nipblb-MO
RIBOSOME	74	3.49	0	0.95	Enriched in nipblb-MO
MYC TARGETS V1	173	3.29	0	0.73	Enriched in nipblb-MO
DNA REPLICATION	29	3.18	0	0.97	Enriched in nipblb-MO
MYC TARGETS V2	54	3.07	0	0.85	Enriched in nipblb-MO
G2M CHECKPOINT	156	3.06	0	0.51	Enriched in nipblb-MO
HOMOLOGOUS RECOMBINATION	22	2.92	0	0.91	Enriched in nipblb-MO
SPLICEOSOME	102	2.89	0	0.74	Enriched in nipblb-MO
RNA POLYMERASE	22	2.82	0	0.91	Enriched in nipblb-MO
CELL CYCLE	94	2.81	0	0.59	Enriched in nipblb-MO
MISMATCH REPAIR	20	2.81	0	0.90	Enriched in nipblb-MO
PYRIMIDINE METABOLISM	72	2.73	0	0.63	Enriched in nipblb-MO
NUCLEOTIDE EXCISION REPAIR	36	2.66	0	0.83	Enriched in nipblb-MO
DNA REPAIR	120	2.62	0	0.56	Enriched in nipblb-MO
BASE EXCISION REPAIR	27	2.52	0	0.70	Enriched in nipblb-MO
RNA DEGRADATION	49	2.33	0	0.55	Enriched in nipblb-MO
PORPHYRIN AND CHLOROPHYLL METABOLISM	21	2.14	4.15E-04	0.43	Enriched in nipblb-MO
UNFOLDED PROTEIN RESPONSE	98	2.10	5.18E-04	0.41	Enriched in nipblb-MO
PROTEASOME	30	2.09	5.49E-04	0.73	Enriched in nipblb-MO
BASAL TRANSCRIPTION FACTORS	26	2.07	7.02E-04	0.69	Enriched in nipblb-MO
PROTEIN EXPORT	20	1.96	0.003	0.90	Enriched in nipblb-MO
AMINOACYL TRNA BIOSYNTHESIS	34	1.90	0.004	0.71	Enriched in nipblb-MO
CYTOSOLIC DNA SENSING PATHWAY	22	1.79	0.010	0.41	Enriched in nipblb-MO
P53 SIGNALING PATHWAY	50	1.75	0.012	0.42	Enriched in nipblb-MO
GLYCOSYLPHOSPHATIDYLINOSITOL GPI ANCHOR BIOSYNTHESIS	22	1.68	0.020	0.50	Enriched in nipblb-MO

NEUROACTIVE LIGAND RECEPTOR INTERACTION	123	-2.52	0	0.68	Enriched in CTRL-MO
CALCIUM SIGNALING PATHWAY	90	-2.42	0	0.64	Enriched in CTRL-MO
EPITHELIAL MESENCHYMAL TRANSITION	127	-2.29	0	0.54	Enriched in CTRL-MO
ECM RECEPTOR INTERACTION	51	-2.14	0	0.57	Enriched in CTRL-MO
LONG TERM POTENTIATION	34	-2.12	3.70E-04	0.65	Enriched in CTRL-MO
CARDIAC MUSCLE CONTRACTION	44	-2.10	6.07E-04	0.43	Enriched in CTRL-MO
TYPE II DIABETES MELLITUS	32	-2.07	7.95E-04	0.47	Enriched in CTRL-MO
MYOGENESIS	134	-2.06	8.16E-04	0.43	Enriched in CTRL-MO
GAP JUNCTION	50	-2.05	9.32E-04	0.72	Enriched in CTRL-MO
DILATED CARDIOMYOPATHY	57	-2.02	0.001	0.54	Enriched in CTRL-MO
OLFACTORY TRANSDUCTION	15	-2.01	0.001	1.00	Enriched in CTRL-MO
HYPERTROPHIC CARDIOMYOPATHY HCM	49	-2.00	0.001	0.47	Enriched in CTRL-MO
KRAS SIGNALING UP	117	-1.97	0.002	0.51	Enriched in CTRL-MO
FOCAL ADHESION	115	-1.94	0.002	0.41	Enriched in CTRL-MO
INOSITOL PHOSPHATE METABOLISM	36	-1.92	0.003	0.50	Enriched in CTRL-MO
PHOSPHATIDYLINOSITOL SIGNALING SYSTEM	47	-1.90	0.004	0.60	Enriched in CTRL-MO
GNRH SIGNALING PATHWAY	50	-1.88	0.004	0.64	Enriched in CTRL-MO
ARRHYTHMOGENIC RIGHT VENTRICULAR CARDIOMYOPATHY ARVC	47	-1.87	0.004	0.45	Enriched in CTRL-MO
CHEMOKINE SIGNALING PATHWAY	86	-1.84	0.006	0.58	Enriched in CTRL-MO
INFLAMMATORY RESPONSE	96	-1.82	0.007	0.36	Enriched in CTRL-MO
MAPK SIGNALING PATHWAY	148	-1.78	0.011	0.41	Enriched in CTRL-MO
INSULIN SIGNALING PATHWAY	82	-1.78	0.011	0.38	Enriched in CTRL-MO
APICAL JUNCTION	117	-1.77	0.011	0.37	Enriched in CTRL-MO
VASCULAR SMOOTH MUSCLE CONTRACTION	60	-1.77	0.010	0.50	Enriched in CTRL-MO
COMPLEMENT AND COAGULATION CASCADES	41	-1.76	0.012	0.66	Enriched in CTRL-MO
TRYPTOPHAN METABOLISM	25	-1.74	0.014	0.44	Enriched in CTRL-MO
ALDOSTERONE REGULATED SODIUM REABSORPTION	22	-1.72	0.016	0.68	Enriched in CTRL-MO
LONG TERM DEPRESSION	35	-1.69	0.024	0.54	Enriched in CTRL-MO
ESTROGEN RESPONSE EARLY	133	-1.68	0.023	0.46	Enriched in CTRL-MO
BILE ACID METABOLISM	82	-1.67	0.025	0.55	Enriched in CTRL-MO
CELL ADHESION MOLECULES CAMS	62	-1.64	0.033	0.37	Enriched in CTRL-MO
UV RESPONSE DN	97	-1.64	0.032	0.55	Enriched in CTRL-MO
AXON GUIDANCE	72	-1.63	0.034	0.65	Enriched in CTRL-MO
KRAS SIGNALING DN	97	-1.61	0.040	0.35	Enriched in CTRL-MO
AMYOTROPHIC LATERAL SCLEROSIS ALS	32	-1.60	0.043	0.44	Enriched in CTRL-MO

**Table S4.** Gene sets of the Hallmark and KEGG collections from the Molecular Signature Database (MSigDB; <https://www.gsea-msigdb.org/gsea/msigdb/collections.jsp>) enriched and depleted in *nipblb*-MO embryos as compared to ctrl-MO samples at 3 dpf (FDR≤0.05).

Gene set	Size	NES	FDR	GeneRatio	Effect
INTERFERON GAMMA RESPONSE	99	2.52	0	0.43	Enriched in nipblb-MO
RIBOSOME	74	2.44	0	0.76	Enriched in nipblb-MO
INTERFERON ALPHA RESPONSE	47	2.37	0	0.43	Enriched in nipblb-MO
PROTEASOME	30	2.16	7.249E-04	0.67	Enriched in nipblb-MO
IL6 JAK STAT3 SIGNALING	46	1.83	0.028	0.33	Enriched in nipblb-MO
DRUG METABOLISM CYTOCHROME P450	20	1.78	0.036	0.50	Enriched in nipblb-MO
AMINOACYL TRNA BIOSYNTHESIS	34	1.77	0.034	0.71	Enriched in nipblb-MO
STEROID HORMONE BIOSYNTHESIS	21	1.77	0.032	0.29	Enriched in nipblb-MO
METABOLISM OF XENOBIOTICS BY CYTOCHROME P450	22	1.73	0.042	0.45	Enriched in nipblb-MO
AXON GUIDANCE	72	-2.28	0	0.63	Enriched in CTRL-MO
NEUROACTIVE LIGAND RECEPTOR INTERACTION	123	-2.02	0.009	0.41	Enriched in CTRL-MO
CALCIUM SIGNALING PATHWAY	90	-1.97	0.011	0.37	Enriched in CTRL-MO
ECM RECEPTOR INTERACTION	51	-1.84	0.036	0.37	Enriched in CTRL-MO
NATURAL KILLER CELL MEDIATED CYTOTOXICITY	36	-1.82	0.037	0.36	Enriched in CTRL-MO
VEGF SIGNALING PATHWAY	31	-1.80	0.037	0.32	Enriched in CTRL-MO
FC GAMMA R MEDIATED PHAGOCYTOSIS	57	-1.76	0.044	0.40	Enriched in CTRL-MO

**Table S5.** Gene sets related to myeloid differentiation and AML derived from the Molecular Signature Database (MSigDB; <https://www.gsea-msigdb.org/gsea/msigdb/collections.jsp>).

[See Table S5.xlsx](#)

**Table S6.** Gene sets related to myeloid differentiation and AML enriched and depleted in nipblb-MO embryos as compared to ctrl-MO samples at 24 hpf (FDR<0.05).

Gene set	Size	NES	FDR	GeneRatio	Effect
EPPERT_PROGENITOR	114	1.83	0.039	0.49	Enriched in nipblb-MO
GAL_LEUKEMIC_STEM_CELL_DN	127	1.71	0.046	0.37	Enriched in nipblb-MO
ALCALAY_AML_BY_NPM1_LOCALIZATION_DN	131	1.67	0.041	0.37	Enriched in nipblb-MO
EPPERT_HSC_R	80	-1.98	0.005	0.44	Enriched in CTRL-MO
VERHAAK_AML_WITH_NPM1_MUTATED_DN	147	-1.98	0.003	0.52	Enriched in CTRL-MO
EPPERT_CE_HSC_LSC	22	-1.88	0.007	0.55	Enriched in CTRL-MO
VALK_AML_CLUSTER_7	15	-1.81	0.016	0.80	Enriched in CTRL-MO
VALK_AML_CLUSTER_16	19	-1.80	0.013	0.53	Enriched in CTRL-MO
VALK_AML_CLUSTER_11	23	-1.75	0.019	0.30	Enriched in CTRL-MO
VALK_AML_CLUSTER_10	21	-1.71	0.023	0.76	Enriched in CTRL-MO

## 5. DISCUSSION

By epigenetic regulation of gene expression and protein modification through deacetylation, HDACs are involved in several biological processes. Therefore HDACs alteration is frequently associated with pathological conditions, in particular with cancer (Patra et al. 2019). In recent years HDAC inhibition has emerged as an attractive potential pharmacological approach for the treatment of different diseases. Indeed, studies showed that HDACi not only possess a promising anti-cancer activity (Ceccacci and Minucci 2016; Imai, Maru, and Tanaka 2016; Eckschlager et al. 2017) but also display therapeutic potential in the treatment of other pathological conditions, such as Duchenne muscular dystrophy (DMD) (Consalvi et al. 2011). However, their use is still hampered by variable efficacy and safety issues. In fact, many side effects are associated with HDACi, ranging from nausea, diarrhoea and thrombocytopenia to cardiac and metabolic disorders (Subramanian et al. 2010). These side effects are due to pan-HDAC inhibitory activity of these drugs, which lack specificity and inhibit multiple HDAC isoforms, thus affecting several biological processes. Inhibition of specific HDACs may improve the outcome of therapy in terms of both efficacy and safety. Such an approach would require both a better in-depth knowledge of specific HDAC involvement in cellular processes and availability of more selective HDACi. In this regard, HDAC8 represents an interesting target, as its peculiar structure among HDACs (Somoza et al. 2004) allowed the development of highly specific inhibitors, such as the PCI-34051 (Balasubramanian et al. 2008).

To examine in depth HDAC8 physiological and pathological roles, we analysed its function and the effect of its inhibition by using both *in vitro* (cell lines) and *in vivo* (zebrafish) models. In particular, we assessed HDAC8 dysregulation in association with HDAC8-related pathologies: acute myeloid leukaemia (AML), (Durst et al. 2003; Qi et al. 2015) Cornelia de Lange syndrome



(CdLS) (Deardorff, Bando, et al. 2012; Kaiser et al. 2014; Feng et al. 2014; X. Gao et al. 2018) and DMD insurgence.

Since HDAC8 was overexpressed in haematopoietic stem cells from AML patients (Qi et al. 2015), we sought to evaluate in the zebrafish model the effect of *hdac8* overexpression on haematopoietic stem and progenitor cells (HSPCs). Firstly, we checked the expression pattern of *hdac8* gene in zebrafish; then, we assessed the haematopoietic phenotype by overexpression of *hdac8* through the injection of *hdac8* full-length mRNA in zebrafish embryos. Our results indicated an expansion of HSPCs following *hdac8* mRNA injection. In particular, in accordance with previous works reporting HDAC8 to promote survival and proliferation of tumour cells (Wu et al. 2013; Qi et al. 2015; Tian et al. 2015), HSPC expansion was underlined by increased proliferation of this cell population. Whether this increased self-renewal capability of HSPCs is accompanied by an impairment of differentiation is currently unknown. To note, by using a Hdac8 conditional knock-out mouse model Hua and colleagues demonstrated that HDAC8 is crucial in the maintenance of long-term haematopoietic stem cells (LT-HSC) survival but seems dispensable in determining lineage differentiation (Hua et al. 2017). Interestingly, we demonstrated that PCI treatment rescued HSPC expansion in *hdac8*-overexpressing embryos and displayed cytostatic and cytotoxic effects in AML cell lines characterized by high HDAC8 levels (HL60 and THP-1). As already shown in other studies (Qi et al. 2015; Rettig et al. 2015; Tian et al. 2015), PCI treatment exerted its effect by cell cycle arrest in G0-G1 phase and induction of p53-dependent apoptosis, which is not surprisingly considering p53 negative modulation by HDAC8 (Wu et al. 2013). Importantly, PCI treatment was effective even in a p53-null context through blocking cell cycle, thus suggesting it may be an interesting approach for the treatment of malignancies for which apoptosis induction is inhibited due to p53 mutations. In addition to single treatment, we also assessed PCI in combination with the standard chemotherapeutical cytarabine and observed a synergistic effect in all tested AML cell lines. This is interesting as double treatment could be done with lower doses of each compound, thus reducing possible dose-dependent side effects. Future studies aimed to

deciphering the molecular mechanisms underlying the synergistic effect of the combination would allow to identify more relevant pathways involved in tumour progression and to adopt a more targeted approach.

Analogously to AML cell lines, we observed reduction of proliferation and apoptosis induction also in murine neural stem cells (NSCs) following either *Hdac8* silencing by siRNA or PCI treatment. Considering the identification of *HDAC8* loss-of-function mutations in CdLS patients (Deardorff, Bando, et al. 2012; Kaiser et al. 2014; Feng et al. 2014; X. Gao et al. 2018), these results suggest that the severe intellectual disability characterizing CdLS (Kline et al. 2018) is likely due to aberrant apoptosis observed during CNS development. To further confirm our data, we assessed HDAC8 loss-of-function *in vivo*, by mean of *hdac8* knockdown in zebrafish embryos through *hdac8*-MO injection. In accordance with our *in vitro* results, *hdac8*-haploinsufficient embryos displayed an impairment of cephalic structure development which was consequence of an increased apoptosis, thus confirming the hypothesis that HDAC8 deficiency impairs CNS development through dysregulation of apoptosis. Indeed, this effect may be at least in part due to p53 hyperactivation following HDAC8 loss. However, HDAC8 dysregulation might also affect cohesin activity, thus impairing its role during mitosis and in DNA repair (Michaelis, Ciosk, and Nasmyth 1997; Watrin and Peters 2009; Jeppsson et al. 2014), eventually leading to cell cycle arrest and apoptosis induction. Consistently with this hypothesis, previous studies in CdLS models showed that defects of other cohesin complex members reduce cell proliferation and induce apoptosis (Pistocchi et al. 2013; Fazio et al. 2016), thus sustaining an important role for cohesin in CNS development. In addition to apoptosis, HDAC8 inhibition determined a strong reduction of NSCs differentiation. In line with these data, it was recently reported that CdLS is characterized by an impairment of retinoic acid (RA) signaling (Fazio et al. 2017), which is a master regulator of neuronal differentiation, thus suggesting HDAC8 to play a role in the modulation of this pathway. Indeed, HDAC8 was reported to be overexpressed in neuroblastoma and its specific

inhibition impaired tumour growth but, differently from our data, promoted RA-mediated differentiation (Rettig et al. 2015).

Previous works highlighted a role for HDAC8 also in smooth muscle tissue (Waltregny et al. 2005; J. Li et al. 2014). In our work, following *hdac8* inhibition in zebrafish embryos, we discovered a still unreported role in skeletal muscle tissue. We assessed HDAC8 expression in human skeletal muscle tissue, rhabdomyosarcoma cell lines, C2C12 murine myoblasts and zebrafish embryos. Our results indicated that HDAC8 is expressed in skeletal muscle and displays a nuclear localization. In particular, we observed that its expression strongly correlated with an advanced stage of muscle differentiation, as it was higher in differentiated C2C12 and rhabdomyosarcoma cells compared to undifferentiated C2C12 and low-differentiating rhabdomyosarcoma cells, respectively. In zebrafish embryos *hdac8* expression showed a peak at 36 hpf, a stage in which the first myogenic wave has already occurred (Stellabotte et al. 2007). These data suggested that HDAC8 could be involved in mediating skeletal muscle differentiation. Consistently with this hypothesis, PCI treatment impaired C2C12 differentiation and caused a reduction of skeletal muscle myosin both in C2C12 and zebrafish embryos. These results prompted us to investigate whether HDAC8 dysregulation could be associated to skeletal muscle disorders such as DMD. Therefore, we assessed HDAC8 expression in myotubes from DMD patients and in a zebrafish DMD model generated by *dmd*-MO injection (J. R. Guyon et al. 2003). Surprisingly, HDAC8 was overexpressed in both DMD models, in comparison to respective controls. To our knowledge, HDAC8 dysregulation in DMD has never been described so far. Indeed, a previous study indicated a higher activity of class I HDACs in muscles from dystrophin-deficient *Mdx* mice, but only HDAC2 was found to be more expressed compared to wild-type mice (Colussi et al. 2008). This discrepancy might be due to the fact that *Mdx* mouse is known to develop a milder DMD phenotype, compared to human and zebrafish DMD models (Maves 2014). Since inhibition of HDACs was demonstrated to ameliorate DMD phenotype (Minetti et al. 2006; Johnson, Farr, and Maves 2013; Mozzetta et al. 2013), we assessed the potential of HDAC8 specific inhibition by

PCI in the treatment of this disorder. PCI treatment was able to increase fusion of human DMD myoblasts into myotubes and to rescue skeletal muscle lesions in *dmd*-MO injected zebrafish embryos, thus raising the possibility that HDAC8 inhibition may represent a valuable approach for DMD treatment. In this regard, HDACi are currently under study as a pharmacological approach for DMD and pan-HDACi Givinostat is currently in phase III clinical trial. Since the possibility to inhibit a specific HDAC isoform could ameliorate the outcome by reducing side effects, selective targeting of HDAC8 is worthy to be studied more in depth in future.

Considering the multiple HDAC8 roles that we observed, we sought to find possible mechanisms underlying HDAC8 activity, other than p53 modulation. A recent work by Tian and colleagues reported HDAC8 as a positive modulator of canonical Wnt pathway in NAFLD-associated hepatocarcinoma (Tian et al. 2015). Thus, we tested WNT activity in several disease models both *in vivo* and *in vitro* obtaining many evidences indicating the involvement of HDAC8 in WNT activation. AML cell lines overexpressing HDAC8 showed high expression of canonical WNT antagonists PPP2R2B and NKD1 after treatment with PCI. Likely, in C2C12 cells the treatment with PCI caused reduction of  $\beta$ -catenin active form. In zebrafish, overexpression of HDAC8 reduced the expression of canonical Wnt inhibitors and increased the pathway activity in the caudal haematopoietic tissue; both effects were rescued by inhibiting HDAC8 with PCI or by co-injection with the canonical Wnt inhibitor *dkk1* full-length mRNA. Also, wild-type embryos treated with PCI showed a reduction of  $\beta$ -catenin activation. Moreover, exposure to the canonical Wnt signaling activator lithium chloride (LiCl) rescued both muscular impairment and apoptosis induction in *Hdac8*-deficient embryos. The involvement of HDAC8 in regulating canonical Wnt pathway represents an interesting possibility for therapeutical intervention in several contexts. Different studies reported downregulation of canonical Wnt pathway in CdLS models and LiCl treatment was already reported to rescue *nipblb*-deficiency phenotype in zebrafish (Pistocchi et al. 2013; Schuster et al. 2015; Fazio et al. 2016). Similarly, as Wnt signaling is involved in myogenesis (Abraham 2016), its induction may be taken into account also for skeletal muscle

diseases. Importantly, the canonical Wnt pathway was reported to be involved in AML insurgence and maintenance of leukemic cells (Gruszka, Valli, and Alcalay 2019; Mazzola et al. 2019). Thus, combination of HDAC8 inhibitors and canonical Wnt pathway antagonist may represent an intriguing approach to be considered in the treatment of AML.

In addition to the characterization of HDAC8 role in the modulation of the canonical Wnt pathway, we also performed acetylome profiling in PCI-treated embryos in order to identify possible other HDAC8 targets. Among differently acetylated proteins, we identified cytoskeleton proteins, namely tubulin- $\alpha$ 2/ $\beta$ 2 and  $\alpha$ 1 skeletal muscle actin. The identification of  $\alpha$ -tubulin as HDAC8 target is supported by a recent work by Vanaja and colleagues who demonstrated that HDAC8 deacetylates  $\alpha$ -tubulin in different cervical cancer cell lines (Vanaja, Ramulu, and Kalle 2018). Since alterations of microtubules have been reported in DMD models (Percival et al. 2007; Khairallah et al. 2012; Iyer et al. 2017), we considered it as a relevant feature to be analysed. We observed a reduction of  $\alpha$ -tubulin acetylation status in *dmd*-MO injected zebrafish embryos, which was rescued by PCI treatment. The precise mechanism by which restoration of  $\alpha$ -tubulin acetylation status rescued cytoskeleton organization is currently unknown, even though we speculate it might favour stabilization of microtubules, as tubulin acetylation is considered a marker of stable microtubules (L. Li and Yang 2015). Although more studies are still needed to better understand HDAC8 functions in order to evaluate its feasibility as a pharmacological target in pathologies characterized by HDAC8 dysregulation, our data support the potential of HDAC8 inhibition in the treatment of DMD.

Lastly, to compare and indirectly validate our findings with HDAC8 mis-regulation, we sought to investigate the impact of the loss-of-function of another modulator of the cohesin complex, *NIPBL*, which is one the most frequently mutated gene in CdLS patients (Krantz et al. 2004; Kline et al. 2018). To assess the effect of NIPBL deficiency on gene expression, we performed the knockdown of the zebrafish ortholog *nipblb* by injecting the *nipblb*-MO and performed RNA-seq analyses on control and *nipblb*-MO embryos at 24 hpf and 3 dpf. Following *nipblb* downregulation at 24 hpf

we observed deregulated expression of 5691 genes, most of which (4205) were reduced. By contrast, at 3 dpf only 223 genes were differentially expressed between *nipblb*-MO and control-MO embryos. As Nipblb protein was still absent at 3 dpf, these data suggested the existence of a mechanism opposing to *nipblb* loss-of-function during development. Possibly, this effect is mediated by the *nipblb* paralog *nipbla*, which expression was increased in *nipblb*-MO injected embryos. Indeed, zebrafish *nipbl* paralogs were suggested to have similar functions, even though with some functional specialization (Muto et al. 2014). Gene set enrichment analyses revealed that the genes downregulated at 24 hpf correlated with CdLS phenotype. For example, we identified genes associated with neural functions, such as neuroactive ligand-receptor interaction, which could underlie CdLS intellectual disability. Also, we observed downregulation of genes involved in MAPK signaling pathway and cardiac muscle contraction, previously identified also in a murine model for *Nipbl*-haploinsufficiency (Kawauchi et al. 2009) and CdLS *NIPBL*<sup>+/-</sup> cardiomyocytes (Mills et al. 2018). Moreover, in line with our previous work, canonical Wnt pathway was downregulated as well (Pistocchi et al. 2013). Conversely, upregulated genes in *nipblb*-haploinsufficient embryos were associated with interferon and immune response. Similar results were obtained by Yuen and colleagues, who showed that in *Nipbl*<sup>+/-</sup> MEF cells upregulation of stress-induced immune response was caused by downregulation of RNA-processing genes and aberrant RNA biogenesis (Yuen et al. 2016).

We also performed functional enrichment analysis using a collection of gene sets related to myeloid differentiation and AML, as recent evidence suggested a role for NIPBL in leukemia insurgence (Dang et al. 2017; Mazzola et al. 2019; 2020). Noticeably, *nipblb*-haploinsufficiency determined upregulation of genes associated with hematopoietic lineage committed progenitor cells and repressed genes expressed by HSC enriched populations and in AML stem cells, thus supporting its role in AML insurgence. Also, *nipblb* loss-of-function determined a transcriptional pattern resembling the one induced by mutation of nucleophosmin 1 (NMP1), a well-known AML-



associated gene. However, more studies are needed to further explore NIPBL role in AML insurgence.

## 6.CONCLUSIONS

In these works, we demonstrated that HDAC8 is implicated in several biological processes and diseases. HDAC8 downregulation triggers apoptosis and inhibits neural differentiation in the CNS as well as it impairs differentiation also in skeletal muscle. Conversely, its overexpression triggers an expansion of HSPCs in zebrafish embryos and is associated with DMD. We showed that HDAC8 specific inhibition by PCI-34051 rescues HSPC expansion and exerts cytostatic and cytotoxic effects in AML cell lines, with a higher efficacy in combination with the standard chemotherapeutical cytarabine. Moreover, PCI treatment ameliorates DMD phenotype both in human myotubes and in zebrafish. We also investigated the pathways modulated by HDAC8 such as cell cycle and apoptosis, canonical Wnt signaling and microtubule arrangement.

In parallel, to further increase the “omics” analyses on HDAC8 and cohesin, we analysed the effect of transcriptional dysregulation following NIPBL loss-of-function in zebrafish. By RNA-seq analyses we observed reduced expression of genes associated with neural differentiation, cardiac development and MAPK signaling and upregulation of genes associated with immune response. Interestingly, as observed for HDAC8 mis-regulation, also NIPBL impairment determined differential expression of genes associated with AML insurgence.

Taken together, our data suggest that HDAC8 and cohesin represent an interesting tool to understand molecular mechanisms behind the insurgence of specific diseases, such as AML, and are promising targets for their treatment.

## REFERENCES

Abraham, S. Thomas. 2016. "A Role for the Wnt3a/ $\beta$ -Catenin Signaling Pathway in the Myogenic Program of C2C12 Cells." *In Vitro Cellular and Developmental Biology - Animal*. <https://doi.org/10.1007/s11626-016-0058-5>.

An, Panpan, Jiexin Li, Linlin Lu, Yingmin Wu, Yuyi Ling, Jun Du, Zhuojia Chen, and Hongsheng Wang. 2019. "Histone Deacetylase 8 Triggers the Migration of Triple Negative Breast Cancer Cells via Regulation of YAP Signals." *European Journal of Pharmacology*. <https://doi.org/10.1016/j.ejphar.2018.12.030>.

Balasubramanian, S., J. Ramos, W. Luo, M. Sirisawad, E. Verner, and J. J. Buggy. 2008. "A Novel Histone Deacetylase 8 (HDAC8)-Specific Inhibitor PCI-34051 Induces Apoptosis in T-Cell Lymphomas." *Leukemia* 22 (5): 1026–34. <https://doi.org/10.1038/leu.2008.9>.

Banerjee, Suvankar, Nilanjan Adhikari, Sk Abdul Amin, and Tarun Jha. 2019. "Histone Deacetylase 8 (HDAC8) and Its Inhibitors with Selectivity to Other Isoforms: An Overview." *European Journal of Medicinal Chemistry*. <https://doi.org/10.1016/j.ejmech.2018.12.039>.

Barbieri, Elisa, Gianluca Deflorian, Federica Pezzimenti, Debora Valli, Marco Saia, Natalia Meani, Alicja M. Gruszka, and Myriam Alcalay. 2016. "Nucleophosmin Leukemogenic Mutant Activates Wnt Signaling during Zebrafish Development." *Oncotarget*. <https://doi.org/10.18632/oncotarget.10878>.

Bassett, David I., Robert J. Bryson-Richardson, David F. Daggett, Philippe Gautier, David G. Keenan, and Peter D. Currie. 2003. "Dystrophin Is Required for the Formation of Stable Muscle Attachments in the Zebrafish Embryo." *Development*. <https://doi.org/10.1242/dev.00799>.

Bennett, Carolyn M., John P. Kanki, Jennifer Rhodes, Ting X. Liu, Barry H. Paw, Mark W.

- Kieran, David M. Langenau, et al. 2001. "Myelopoiesis in the Zebrafish, *Danio Rerio*." *Blood*. <https://doi.org/10.1182/blood.V98.3.643>.
- Bernardi, Giorgio. 2018. "The Formation of Chromatin Domains Involves a Primary Step Based on the 3-D Structure of DNA." *Scientific Reports*. <https://doi.org/10.1038/s41598-018-35851-0>.
- Bertrand, Julien Y., Neil C. Chi, Buyung Santoso, Shutian Teng, Didier Y.R. Stainier, and David Traver. 2010. "Haematopoietic Stem Cells Derive Directly from Aortic Endothelium during Development." *Nature*. <https://doi.org/10.1038/nature08738>.
- Bertrand, Julien Y., Albert D. Kim, Emily P. Violette, David L. Stachura, Jennifer L. Cisson, and David Traver. 2007. "Definitive Hematopoiesis Initiates through a Committed Erythromyeloid Progenitor in the Zebrafish Embryo." *Development*. <https://doi.org/10.1242/dev.012385>.
- Buggy, J. J., M. L. Sideris, P. Mak, D. D. Lorimer, B. McIntosh, and J. M. Clark. 2000. "Cloning and Characterization of a Novel Human Histone Deacetylase, HDAC8." *Biochemical Journal*. <https://doi.org/10.1042/0264-6021:3500199>.
- Canudas, Silvia, and Susan Smith. 2009. "Differential Regulation of Telomere and Centromere Cohesion by the Scc3 Homologues SA1 and SA2, Respectively, in Human Cells." *Journal of Cell Biology*. <https://doi.org/10.1083/jcb.200903096>.
- Ceccacci, Elena, and Saverio Minucci. 2016. "Inhibition of Histone Deacetylases in Cancer Therapy: Lessons from Leukaemia." *British Journal of Cancer* 114 (6): 605–11. <https://doi.org/10.1038/bjc.2016.36>.
- Ciosk, Rafal, Masaki Shirayama, Anna Shevchenko, Tomoyuki Tanaka, Attila Toth, Andrej Shevchenko, and Kim Nasmyth. 2000. "Cohesin's Binding to Chromosomes Depends on a Separate Complex Consisting of Scc2 and Scc4 Proteins." *Molecular Cell*. [https://doi.org/10.1016/S1097-2765\(00\)80420-7](https://doi.org/10.1016/S1097-2765(00)80420-7).
- Colussi, Claudia, Chiara Mozzetta, Aymone Gurtner, Barbara Illi, Jessica Rosati, Stefania

- Straino, Gianluca Ragone, et al. 2008. “HDAC2 Blockade by Nitric Oxide and Histone Deacetylase Inhibitors Reveals a Common Target in Duchenne Muscular Dystrophy Treatment.” *Proceedings of the National Academy of Sciences of the United States of America* 105 (49): 19183–87. <https://doi.org/10.1073/pnas.0805514105>.
- Consalvi, Silvia, Valentina Saccone, Lorenzo Giordani, Giulia Minetti, Chiara Mozzetta, and Pier Lorenzo Puri. 2011. “Histone Deacetylase Inhibitors in the Treatment of Muscular Dystrophies: Epigenetic Drugs for Genetic Diseases.” *Molecular Medicine* 17 (5–6): 457–65. <https://doi.org/10.2119/molmed.2011.00049>.
- Dang, J., S. Nance, J. Ma, J. Cheng, M. P. Walsh, P. Vogel, J. Easton, et al. 2017. “AMKL Chimeric Transcription Factors Are Potent Inducers of Leukemia.” *Leukemia*. <https://doi.org/10.1038/leu.2017.51>.
- Dasgupta, Tanushree, Jisha Antony, Antony W. Braithwaite, and Julia A. Horsfield. 2016. “HDAC8 Inhibition Blocks SMC3 Deacetylation and Delays Cell Cycle Progression without Affecting Cohesin-Dependent Transcription in MCF7 Cancer Cells.” *Journal of Biological Chemistry*. <https://doi.org/10.1074/jbc.M115.704627>.
- Deardorff, Matthew A., Masashige Bando, Ryuichiro Nakato, Erwan Watrin, Takehiko Itoh, Masashi Minamino, Katsuya Saitoh, et al. 2012. “HDAC8 Mutations in Cornelia de Lange Syndrome Affect the Cohesin Acetylation Cycle.” *Nature*. <https://doi.org/10.1038/nature11316>.
- Deardorff, Matthew A., Maninder Kaur, Dinah Yaeger, Abhinav Rampuria, Sergey Korolev, Juan Pie, Concepcion Gil-Rodríguez, et al. 2007. “Mutations in Cohesin Complex Members SMC3 and SMC1A Cause a Mild Variant of Cornelia de Lange Syndrome with Predominant Mental Retardation.” *American Journal of Human Genetics*. <https://doi.org/10.1086/511888>.
- Deardorff, Matthew A., Jonathan J. Wilde, Melanie Albrecht, Emma Dickinson, Stephanie Tennstedt, Diana Braunholz, Maren Mönnich, et al. 2012. “RAD21 Mutations Cause a

Human Cohesinopathy.” *American Journal of Human Genetics*.

<https://doi.org/10.1016/j.ajhg.2012.04.019>.

Decroos, Christophe, Christine M. Bowman, Joe Ann S. Moser, Karen E. Christianson, Matthew A. Deardorff, and David W. Christianson. 2014. “Compromised Structure and Function of HDAC8 Mutants Identified in Cornelia de Lange Syndrome Spectrum Disorders.” *ACS Chemical Biology*. <https://doi.org/10.1021/cb5003762>.

Detrich, H. William, Mark W. Kieran, Fung Yee Chan, Lauren M. Barone, Karen Yee, Jon A. Rundstadler, Steven Pratt, David Ransom, and Leonard I. Zon. 1995. “Intraembryonic Hematopoietic Cell Migration during Vertebrate Development.” *Proceedings of the National Academy of Sciences of the United States of America*.  
<https://doi.org/10.1073/pnas.92.23.10713>.

Dorsky, Richard I., Laird C. Sheldahl, and Randall T. Moon. 2002. “A Transgenic Lef1/ $\beta$ -Catenin-Dependent Reporter Is Expressed in Spatially Restricted Domains throughout Zebrafish Development.” *Developmental Biology* 241 (2): 229–37.  
<https://doi.org/10.1006/dbio.2001.0515>.

Draper, Bruce W., Paul A. Morcos, and Charles B. Kimmel. 2001. “Inhibition of Zebrafish Fgf8 Pre-mRNA Splicing with Morpholino Oligos: A Quantifiable Method for Gene Knockdown.” *Genesis*. <https://doi.org/10.1002/gene.1053>.

Durst, Kristie L, Bart Lutterbach, Tanawan Kummalue, Alan D Friedman, and Scott W Hiebert. 2003. “The Inv(16) Fusion Protein Associates with Corepressors via a Smooth Muscle Myosin Heavy-Chain Domain.” *Molecular and Cellular Biology* 23 (2): 607–19.  
<https://doi.org/10.1128/MCB.23.2.607-619.2003>.

Eckschlager, Tomas, Johana Plch, Marie Stiborova, and Jan Hrabeta. 2017. “Histone Deacetylase Inhibitors as Anticancer Drugs.” *International Journal of Molecular Sciences* 18 (7): 1–25. <https://doi.org/10.3390/ijms18071414>.

Fazio, Grazia, Laura Rachele Bettini, Silvia Rigamonti, Dorela Meta, Andrea Biondi, Giovanni



- Cazzaniga, Angelo Selicorni, and Valentina Massa. 2017. "Impairment of Retinoic Acid Signaling in Cornelia de Lange Syndrome Fibroblasts." *Birth Defects Research*.  
<https://doi.org/10.1002/bdr2.1070>.
- Fazio, Grazia, Carles Gaston-Massuet, Laura Rachele Bettini, Federica Graziola, Valeria Scagliotti, Anna Cereda, Luca Ferrari, et al. 2016. "CyclinD1 Down-Regulation and Increased Apoptosis Are Common Features of Cohesinopathies." *Journal of Cellular Physiology*. <https://doi.org/10.1002/jcp.25106>.
- Feng, Lei, Daizhan Zhou, Zhou Zhang, Yun Liu, and Yabo Yang. 2014. "Exome Sequencing Identifies a de Novo Mutation in HDAC8 Associated with Cornelia de Lange Syndrome." *Journal of Human Genetics*. <https://doi.org/10.1038/jhg.2014.60>.
- Fischer, André, Farahnaz Sananbenesi, Alison Mungenast, and Li Huei Tsai. 2010. "Targeting the Correct HDAC(s) to Treat Cognitive Disorders." *Trends in Pharmacological Sciences*.  
<https://doi.org/10.1016/j.tips.2010.09.003>.
- Gao, Jingxia, Benjamin Siddoway, Qing Huang, and Houhui Xia. 2009. "Inactivation of CREB Mediated Gene Transcription by HDAC8 Bound Protein Phosphatase." *Biochemical and Biophysical Research Communications* 379 (1): 1–5.  
<https://doi.org/10.1016/j.bbrc.2008.11.135>.
- Gao, Xueren, Zhuo Huang, Yanjie Fan, Yu Sun, Huili Liu, Lili Wang, Xue Fan Gu, and Yongguo Yu. 2018. "A Functional Mutation in HDAC8 Gene as Novel Diagnostic Marker for Cornelia de Lange Syndrome." *Cellular Physiology and Biochemistry*.  
<https://doi.org/10.1159/000491613>.
- Gore, Aniket V., Laura M. Pillay, Marina Venero Galanternik, and Brant M. Weinstein. 2018. "The Zebrafish: A Fantastic Model for Hematopoietic Development and Disease." *Wiley Interdisciplinary Reviews: Developmental Biology* 7 (3): 1–17.  
<https://doi.org/10.1002/wdev.312>.
- Gruszka, Alicja M., Debora Valli, and Myriam Alcalay. 2019. "Wnt Signalling in Acute Myeloid

- Leukaemia.” *Cells* 8 (11): 1403. <https://doi.org/10.3390/cells8111403>.
- Guyon, J. R., A. N. Mosley, Y. Zhou, K. F. O’Brien, X. Sheng, K. Chiang, A. J. Davidson, J. M. Volinski, L. I. Zon, and L. M. Kunkel. 2003. “The Dystrophin Associated Protein Complex in Zebrafish.” *Human Molecular Genetics*. <https://doi.org/10.1093/hmg/ddg071>.
- Guyon, Jeffrey R., Julie Goswami, Susan J. Jun, Marielle Thorne, Melanie Howell, Timothy Pusack, Genri Kawahara, Leta S. Steffen, Michal Galdzicki, and Louis M. Kunkel. 2009. “Genetic Isolation and Characterization of a Splicing Mutant of Zebrafish Dystrophin.” *Human Molecular Genetics*. <https://doi.org/10.1093/hmg/ddn337>.
- Higuchi, Tomonori, Takashi Nakayama, Tokuzo Arao, Kazuto Nishio, and Osamu Yoshie. 2013. “SOX4 Is a Direct Target Gene of FRA-2 and Induces Expression of HDAC8 in Adult T-Cell Leukemia/Lymphoma.” *Blood* 121 (18): 3640–49. <https://doi.org/10.1182/blood-2012-07-441022>.
- Hoffman, Eric P., Robert H. Brown, and Louis M. Kunkel. 1987. “Dystrophin: The Protein Product of the Duchenne Muscular Dystrophy Locus.” *Cell*. [https://doi.org/10.1016/0092-8674\(87\)90579-4](https://doi.org/10.1016/0092-8674(87)90579-4).
- Hou, Fajian, and Hui Zou. 2005. “Two Human Orthologues of Eco1/Ctf7 Acetyltransferases Are Both Required for Proper Sister-Chromatid Cohesion.” *Molecular Biology of the Cell*. <https://doi.org/10.1091/mbc.E04-12-1063>.
- Hu, Erding, Zunxuan Chen, Todd Fredrickson, Yuan Zhu, Robert Kirkpatrick, Gui Feng Zhang, Kyung Johanson, Chiu Mei Sung, Ronggang Liu, and James Winkler. 2000. “Cloning and Characterization of a Novel Human Class I Histone Deacetylase That Functions as a Transcription Repressor.” *Journal of Biological Chemistry* 275 (20): 15254–64. <https://doi.org/10.1074/jbc.M908988199>.
- Hua, Wei Kai, Jing Qi, Qi Cai, Emily Carnahan, Maria Ayala Ramirez, Ling Li, Guido Marcucci, and Ya Huei Kuo. 2017. “HDAC8 Regulates Long-Term Hematopoietic Stem-Cell Maintenance under Stress by Modulating P53 Activity.” *Blood* 130 (24): 2619–30.

<https://doi.org/10.1182/blood-2017-03-771386>.

- Hubbert, Charlotte, Amaris Guardiola, Rong Shao, Yoshiharu Kawaguchi, Akihiro Ito, Andrew Nixon, Minoru Yoshida, Xiao Fan Wang, and Tso Pang Yao. 2002. "HDAC6 Is a Microtubule-Associated Deacetylase." *Nature*. <https://doi.org/10.1038/417455a>.
- Iezzi, Simona, Giulio Cossu, Clara Nervi, Vittorio Sartorelli, and Pier Lorenzo Puri. 2002. "Stage-Specific Modulation of Skeletal Myogenesis by Inhibitors of Nuclear Deacetylases." *Proceedings of the National Academy of Sciences of the United States of America* 99 (11): 7757–62. <https://doi.org/10.1073/pnas.112218599>.
- Iezzi, Simona, Monica Di Padova, Carlo Serra, Giuseppina Caretti, Cristiano Simone, Eric Maklan, Giulia Minetti, et al. 2004. "Deacetylase Inhibitors Increase Muscle Cell Size by Promoting Myoblast Recruitment and Fusion through Induction of Follistatin." *Developmental Cell* 6 (5): 673–84. [https://doi.org/10.1016/S1534-5807\(04\)00107-8](https://doi.org/10.1016/S1534-5807(04)00107-8).
- Imai, Yoichi, Yoshiro Maru, and Junji Tanaka. 2016. "Action Mechanisms of Histone Deacetylase Inhibitors in the Treatment of Hematological Malignancies." *Cancer Science* 107 (11): 1543–49. <https://doi.org/10.1111/cas.13062>.
- Ingham, Oscar J., Ronald M. Paranal, William B. Smith, Randolph A. Escobar, Han Yueh, Tracy Snyder, John A. Porco, James E. Bradner, and Aaron B. Beeler. 2016. "Development of a Potent and Selective HDAC8 Inhibitor." *ACS Medicinal Chemistry Letters*. <https://doi.org/10.1021/acsmchemlett.6b00239>.
- Iyer, Shama R., Sameer B. Shah, Ana P. Valencia, Martin F. Schneider, Erick O. Hernández-Ochoa, Joseph P. Stains, Silvia S. Blemker, and Richard M. Lovering. 2017. "Altered Nuclear Dynamics in MDX Myofibers." *Journal of Applied Physiology* 122 (3): 470–81. <https://doi.org/10.1152/jappphysiol.00857.2016>.
- Jeppsson, Kristian, Takaharu Kanno, Katsuhiko Shirahige, and Camilla Sjögren. 2014. "The Maintenance of Chromosome Structure: Positioning and Functioning of SMC Complexes." *Nature Reviews Molecular Cell Biology*. <https://doi.org/10.1038/nrm3857>.

- Johnson, Nathan M., Gist H. Farr, and Lisa Maves. 2013. "The HDAC Inhibitor TSA Ameliorates a Zebrafish Model of Duchenne Muscular Dystrophy." *PLoS Currents*. <https://doi.org/10.1371/currents.md.8273cf41db10e2d15dd3ab827cb4b027>.
- Kagey, Michael H., Jamie J. Newman, Steve Bilodeau, Ye Zhan, David A. Orlando, Nynke L. Van Berkum, Christopher C. Ebmeier, et al. 2010. "Mediator and Cohesin Connect Gene Expression and Chromatin Architecture." *Nature*. <https://doi.org/10.1038/nature09380>.
- Kaiser, Frank J., Morad Ansari, Diana Braunholz, María Concepción Gil-Rodríguez, Christophe Decroos, Jonathan J. Wilde, Christopher T. Fincher, et al. 2014. "Loss-of-Function HDAC8 Mutations Cause a Phenotypic Spectrum of Cornelia de Lange Syndrome-like Features, Ocular Hypertelorism, Large Fontanelle and X-Linked Inheritance." *Human Molecular Genetics*. <https://doi.org/10.1093/hmg/ddu002>.
- Kang, Y., H. Nian, P. Rajendran, W. M. Dashwood, J. T. Pinto, L. A. Boardman, S. N. Thibodeau, et al. 2014. "HDAC8 and STAT3 Repress BMF Gene Activity in Colon Cancer Cells." *Cell Death and Disease*. <https://doi.org/10.1038/cddis.2014.422>.
- Karlsson, Johnny, Jonas Von Hofsten, and Per Erik Olsson. 2001. "Generating Transparent Zebrafish: A Refined Method to Improve Detection of Gene Expression during Embryonic Development." *Marine Biotechnology*. <https://doi.org/10.1007/s1012601-0053-4>.
- Kawauchi, Shimako, Anne L. Calof, Rosaysela Santos, Martha E. Lopez-Burks, Clint M. Young, Michelle P. Hoang, Abigail Chua, et al. 2009. "Multiple Organ System Defects and Transcriptional Dysregulation in the Nipbl<sup>+/-</sup> Mouse, a Model of Cornelia de Lange Syndrome." *PLoS Genetics*. <https://doi.org/10.1371/journal.pgen.1000650>.
- Khairallah, Ramzi J., Guoli Shi, Francesca Sbrana, Benjamin L. Prosser, Carlos Borroto, Mark J. Mazaitis, Eric P. Hoffman, et al. 2012. "Microtubules Underlie Dysfunction in Duchenne Muscular Dystrophy." *Science Signaling*. <https://doi.org/10.1126/scisignal.2002829>.
- Kline, Antonie D., Joanna F. Moss, Angelo Selicorni, Anne Marie Bisgaard, Matthew A. Deardorff, Peter M. Gillett, Stacey L. Ishman, et al. 2018. "Diagnosis and Management of

- Cornelia de Lange Syndrome: First International Consensus Statement.” *Nature Reviews Genetics*. <https://doi.org/10.1038/s41576-018-0031-0>.
- Kobayashi, Norihiko, Kouichiro Goto, Kana Horiguchi, Motoko Nagata, Mikiko Kawata, Keiji Miyazawa, Masao Saitoh, and Kohei Miyazono. 2007. “C-Ski Activates MyoD in the Nucleus of Myoblastic Cells through Suppression of Histone Deacetylases.” *Genes to Cells*. <https://doi.org/10.1111/j.1365-2443.2007.01052.x>.
- Krantz, Ian D., Jennifer McCallum, Cheryl DeScipio, Maninder Kaur, Lynette A. Gillis, Dinah Yaeger, Lori Jukofsky, et al. 2004. “Cornelia de Lange Syndrome Is Caused by Mutations in NIPBL, the Human Homolog of *Drosophila Melanogaster* Nipped-B.” *Nature Genetics*. <https://doi.org/10.1038/ng1364>.
- KrennHrubec, Keris, Brett L. Marshall, Mark Hedglin, Eric Verdin, and Scott M. Ulrich. 2007. “Design and Evaluation of ‘Linkerless’ Hydroxamic Acids as Selective HDAC8 Inhibitors.” *Bioorganic and Medicinal Chemistry Letters*. <https://doi.org/10.1016/j.bmcl.2007.02.064>.
- Kuefer, R., M. D. Hofer, V. Altug, C. Zorn, F. Genze, K. Kunzi-Rapp, R. E. Hautmann, and J. E. Gschwend. 2004. “Sodium Butyrate and Tributyrin Induce in Vivo Growth Inhibition and Apoptosis in Human Prostate Cancer.” *British Journal of Cancer*. <https://doi.org/10.1038/sj.bjc.6601510>.
- Lee, H., N. Rezai-Zadeh, and E. Seto. 2004. “Negative Regulation of Histone Deacetylase 8 Activity by Cyclic AMP-Dependent Protein Kinase A.” *Molecular and Cellular Biology* 24 (2): 765–73. <https://doi.org/10.1128/mcb.24.2.765-773.2004>.
- Lee, Heehyoung, Nilanjan Sengupta, Alejandro Villagra, Natalie Rezai-Zadeh, and Edward Seto. 2006. “Histone Deacetylase 8 Safeguards the Human Ever-Shorter Telomeres 1B (HEST1B) Protein from Ubiquitin-Mediated Degradation.” *Molecular and Cellular Biology*. <https://doi.org/10.1128/mcb.01971-05>.
- Li, Jia, Shu Chen, Rachel A. Cleary, Ruping Wang, Olivia J. Gannon, Edward Seto, and Dale D. Tang. 2014. “Histone Deacetylase 8 Regulates Cortactin Deacetylation and Contraction in

- Smooth Muscle Tissues.” *American Journal of Physiology - Cell Physiology* 307 (3): 288–95. <https://doi.org/10.1152/ajpcell.00102.2014>.
- Li, Lin, and Xiang Jiao Yang. 2015. “Tubulin Acetylation: Responsible Enzymes, Biological Functions and Human Diseases.” *Cellular and Molecular Life Sciences* 72 (22): 4237–55. <https://doi.org/10.1007/s00018-015-2000-5>.
- Li, Mingyu, Liyuan Zhao, Patrick S. Page-McCaw, and Wenbiao Chen. 2016. “Zebrafish Genome Engineering Using the CRISPR–Cas9 System.” *Trends in Genetics*. <https://doi.org/10.1016/j.tig.2016.10.005>.
- Li, Xiao Nan, Qin Shu, Jack Men Feng Su, Laszlo Perlaky, Susan M. Blaney, and Ching C. Lau. 2005. “Valproic Acid Induces Growth Arrest, Apoptosis, and Senescence in Medulloblastomas by Increasing Histone Hyperacetylation and Regulating Expression of P21Cip1, CDK4, and CMYC.” *Molecular Cancer Therapeutics*. <https://doi.org/10.1158/1535-7163.MCT-05-0184>.
- Lieschke, Graham J., Andrew C. Oates, Barry H. Paw, Margaret A. Thompson, Nathan E. Hall, Alister C. Ward, Robert K. Ho, Leonard I. Zon, and Judith E. Layton. 2002. “Zebrafish SPI-1 (PU.1) Marks a Site of Myeloid Development Independent of Primitive Erythropoiesis: Implications for Axial Patterning.” *Developmental Biology*. <https://doi.org/10.1006/dbio.2002.0657>.
- Lin, Hui Feng, David Traver, Hao Zhu, Kimberly Dooley, Barry H. Paw, Leonard I. Zon, and Robert I. Handin. 2005. “Analysis of Thrombocyte Development in CD41-GFP Transgenic Zebrafish.” *Blood* 106 (12): 3803–10. <https://doi.org/10.1182/blood-2005-01-0179>.
- Lombardi, Patrick M., Kathryn E. Cole, Daniel P. Dowling, and David W. Christianson. 2011. “Structure, Mechanism, and Inhibition of Histone Deacetylases and Related Metalloenzymes.” *Current Opinion in Structural Biology*. <https://doi.org/10.1016/j.sbi.2011.08.004>.
- Lopez, Gonzalo, Kate Lynn J. Bill, Hemant Kumar Bid, Danielle Braggio, Dylan Constantino,



- Bethany Prudner, Abeba Zewdu, Kara Batte, Dina Lev, and Raphael E. Pollock. 2015. “HDAC8, A Potential Therapeutic Target for the Treatment of Malignant Peripheral Nerve Sheath Tumors (MPNST).” *PLoS ONE* 10 (7): 1–12.  
<https://doi.org/10.1371/journal.pone.0133302>.
- Lyu, Xiaowen, M. Jordan Rowley, and Victor G. Corces. 2018. “Architectural Proteins and Pluripotency Factors Cooperate to Orchestrate the Transcriptional Response of HESCs to Temperature Stress.” *Molecular Cell*. <https://doi.org/10.1016/j.molcel.2018.07.012>.
- Ma, Dongdong, Jing Zhang, Hui Feng Lin, Joseph Italiano, and Robert I. Handin. 2011. “The Identification and Characterization of Zebrafish Hematopoietic Stem Cells.” *Blood* 118 (2): 289–97. <https://doi.org/10.1182/blood-2010-12-327403>.
- MacRae, Calum A., and Randall T. Peterson. 2015. “Zebrafish as Tools for Drug Discovery.” *Nature Reviews Drug Discovery*. <https://doi.org/10.1038/nrd4627>.
- Marek, Martin, Srinivasaraghavan Kannan, Alexander Thomas Hauser, Marina Moraes Mourão, Stéphanie Caby, Vincent Cura, Diana A. Stolfa, et al. 2013. “Structural Basis for the Inhibition of Histone Deacetylase 8 (HDAC8), a Key Epigenetic Player in the Blood Fluke *Schistosoma Mansoni*.” *PLoS Pathogens*. <https://doi.org/10.1371/journal.ppat.1003645>.
- Maves, Lisa. 2014. “Recent Advances Using Zebrafish Animal Models for Muscle Disease Drug Discovery.” *Expert Opinion on Drug Discovery*.  
<https://doi.org/10.1517/17460441.2014.927435>.
- Mazzola, Mara, Gianluca Deflorian, Alex Pezzotta, Laura Ferrari, Grazia Fazio, Erica Bresciani, Claudia Saitta, et al. 2019. “NIPBL : A New Player in Myeloid Cell Differentiation .” *Haematologica*. <https://doi.org/10.3324/haematol.2018.200899>.
- Mazzola, Mara, Alex Pezzotta, Grazia Fazio, Alessandra Rigamonti, Erica Bresciani, Germano Gaudenzi, Maria Chiara Pelleri, et al. 2020. “Dysregulation of NIPBL Leads to Impaired RUNX1 Expression and Haematopoietic Defects.” *Journal of Cellular and Molecular Medicine*. <https://doi.org/10.1111/jcmm.15269>.

- Michaelis, Christine, Rafal Ciosk, and Kim Nasmyth. 1997. "Cohesins: Chromosomal Proteins That Prevent Premature Separation of Sister Chromatids." *Cell*.  
[https://doi.org/10.1016/S0092-8674\(01\)80007-6](https://doi.org/10.1016/S0092-8674(01)80007-6).
- Mills, Jason A., Pamela S. Herrera, Maninder Kaur, Lanfranco Leo, Deborah McEldrew, Jesus A. Tintos-Hernandez, Ramakrishnan Rajagopalan, et al. 2018. "NIPBL<sup>+/-</sup> Haploinsufficiency Reveals a Constellation of Transcriptome Disruptions in the Pluripotent and Cardiac States." *Scientific Reports*. <https://doi.org/10.1038/s41598-018-19173-9>.
- Minetti, G. C., C. Colussi, R. Adami, C. Serra, C. Mozzetta, V. Parente, S. Fortuni, et al. 2006. "Functional and Morphological Recovery of Dystrophic Muscles in Mice Treated with Deacetylase Inhibitors." *Nature Medicine* 12 (10): 1147–50.  
<https://doi.org/10.1038/nm1479>.
- Mithraprabhu, Sridurga, Anna Kalff, Annie Chow, Tiffany Khong, and Andrew Spencer. 2014. "Dysregulated Class I Histone Deacetylases Are Indicators of Poor Prognosis in Multiple Myeloma." *Epigenetics* 9 (11): 1511–20. <https://doi.org/10.4161/15592294.2014.983367>.
- Moens, Cecilia B., Thomas M. Donn, Emma R. Wolf-Saxon, and Taylur P. Ma. 2008. "Reverse Genetics in Zebrafish by TILLING." *Briefings in Functional Genomics and Proteomics*.  
<https://doi.org/10.1093/bfpg/eln046>.
- Moreno, Daniel Antunes, Carlos Alberto Scrideli, Maria Angélica Abdala Cortez, Rosane De Paula Queiroz, Elvis Terci Valera, Vanessa Da Silva Silveira, José Andres Yunes, Silvia Regina Brandalise, and Luiz Gonzaga Tone. 2010. "Differential Expression of HDAC3, HDAC7 and HDAC9 Is Associated with Prognosis and Survival in Childhood Acute Lymphoblastic Leukaemia: Research Paper." *British Journal of Haematology* 150 (6): 665–73. <https://doi.org/10.1111/j.1365-2141.2010.08301.x>.
- Mozzetta, Chiara, Silvia Consalvi, Valentina Saccone, Matthew Tierney, Adamo Diamantini, Kathryn J. Mitchell, Giovanna Marazzi, et al. 2013. "Fibroblast Progenitors Mediate the Ability of HDAC Inhibitors to Promote Regeneration in Dystrophic Muscles of Young,

- but Not Old Mdx Mice.” *EMBO Molecular Medicine* 5 (4): 626–39.  
<https://doi.org/10.1002/emmm.201202096>.
- Mullins, Mary C., Matthias Hammerschmidt, Pascal Haffter, and Christiane Nüsslein-Volhard. 1994. “Large-Scale Mutagenesis in the Zebrafish: In Search of Genes Controlling Development in a Vertebrate.” *Current Biology*. [https://doi.org/10.1016/S0960-9822\(00\)00048-8](https://doi.org/10.1016/S0960-9822(00)00048-8).
- Musio, Antonio, Angelo Selicorni, Maria Luisa Focarelli, Cristina Gervasini, Donatella Milani, Silvia Russo, Paolo Vezzoni, and Lidia Larizza. 2006. “X-Linked Cornelia de Lange Syndrome Owing to SMC1L1 Mutations.” *Nature Genetics*.  
<https://doi.org/10.1038/ng1779>.
- Muto, Akihiko, Shingo Ikeda, Martha E. Lopez-Burks, Yutaka Kikuchi, Anne L. Calof, Arthur D. Lander, and Thomas F. Schilling. 2014. “Nipbl and Mediator Cooperatively Regulate Gene Expression to Control Limb Development.” *PLoS Genetics*.  
<https://doi.org/10.1371/journal.pgen.1004671>.
- Nakagawa, Masamune, Yoshinao Oda, Takashi Eguchi, Shin Ichi Aishima, Takashi Yao, Fumihito Hosoi, Yuji Basaki, et al. 2007. “Expression Profile of Class I Histone Deacetylases in Human Cancer Tissues.” *Oncology Reports* 18 (4): 769–74.  
<https://doi.org/10.3892/or.18.4.769>.
- Nasevicius, Aidan, and Stephen C. Ekker. 2000. “Effective Targeted Gene ‘knockdown’ in Zebrafish.” *Nature Genetics*. <https://doi.org/10.1038/79951>.
- Nasmyth, Kim. 2011. “Cohesin: A Catenase with Separate Entry and Exit Gates?” *Nature Cell Biology*. <https://doi.org/10.1038/ncb2349>.
- Oehme, Ina, Hedwig E. Deubzer, Dennis Wegener, Diana Pickert, Jan Peter Linke, Barbara Hero, Annette Kopp-Schneider, et al. 2009. “Histone Deacetylase 8 in Neuroblastoma Tumorigenesis.” *Clinical Cancer Research* 15 (1): 91–99. <https://doi.org/10.1158/1078-0432.CCR-08-0684>.

- Olson, David E., Namrata D. Udeshi, Noah A. Wolfson, Carol Ann Pitcairn, Eric D. Sullivan, Jacob D. Jaffe, Tanya Svinkina, et al. 2014. "An Unbiased Approach to Identify Endogenous Substrates of 'Histone' Deacetylase 8." *ACS Chemical Biology* 9 (10): 2210–16. <https://doi.org/10.1021/cb500492r>.
- Paik, Elizabeth J., and Leonard I. Zon. 2010. "Hematopoietic Development in the Zebrafish." *International Journal of Developmental Biology* 54 (6–7): 1127–37. <https://doi.org/10.1387/ijdb.093042ep>.
- Parbin, Sabnam, Swayamsiddha Kar, Arunima Shilpi, Dipta Sengupta, Moonmoon Deb, Sandip Kumar Rath, and Samir Kumar Patra. 2014. "Histone Deacetylases: A Saga of Perturbed Acetylation Homeostasis in Cancer." *Journal of Histochemistry and Cytochemistry*. <https://doi.org/10.1369/0022155413506582>.
- Park, Soon Young, J. I.A.E. Jun, Kang Jin Jeong, Hoi Jeong Heo, Jang Sihm Sohn, Hoi Young Lee, Chang Gyo Park, and Jaeku Kang. 2011. "Histone Deacetylases 1, 6 and 8 Are Critical for Invasion in Breast Cancer." *Oncology Reports* 25 (6): 1677–81. <https://doi.org/10.3892/or.2011.1236>.
- Patra, Srimanta, Debasna P. Panigrahi, Prakash P. Praharaaj, Chandra S. Bhol, Kewal K. Mahapatra, Soumya R. Mishra, Bishnu P. Behera, Mrutyunjay Jena, and Sujit K. Bhutia. 2019. "Dysregulation of Histone Deacetylases in Carcinogenesis and Tumor Progression: A Possible Link to Apoptosis and Autophagy." *Cellular and Molecular Life Sciences*. <https://doi.org/10.1007/s00018-019-03098-1>.
- Percival, Justin M., Paul Gregorevic, Guy L. Odom, Glen B. Banks, Jeffrey S. Chamberlain, and Stanley C. Froehner. 2007. "RAAV6-Microdystrophin Rescues Aberrant Golgi Complex Organization in Mdx Skeletal Muscles." *Traffic* 8 (10): 1424–39. <https://doi.org/10.1111/j.1600-0854.2007.00622.x>.
- Pezzotta, Alex, Mara Mazzola, Marco Spreafico, Anna Marozzi, and Anna Pistocchi. 2019. "Enigmatic Ladies of the Rings: How Cohesin Dysfunction Affects Myeloid Neoplasms

- Insurgence.” *Frontiers in Cell and Developmental Biology* 7 (February): 1–7.  
<https://doi.org/10.3389/fcell.2019.00021>.
- Pistocchi, A., G. Fazio, A. Cereda, L. Ferrari, L. R. Bettini, G. Messina, F. Cotelli, A. Biondi, A. Selicorni, and V. Massa. 2013. “Cornelia de Lange Syndrome: NIPBL Haploinsufficiency Downregulates Canonical Wnt Pathway in Zebrafish Embryos and Patients Fibroblasts.” *Cell Death and Disease*. <https://doi.org/10.1038/cddis.2013.371>.
- Porter, Nicholas J., Nicolas H. Christianson, Christophe Decroos, and David W. Christianson. 2016. “Structural and Functional Influence of the Glycine-Rich Loop G302GGGY on the Catalytic Tyrosine of Histone Deacetylase 8.” *Biochemistry* 55 (48): 6718–29.  
<https://doi.org/10.1021/acs.biochem.6b01014>.
- Porteus, Matthew H., and Dana Carroll. 2005. “Gene Targeting Using Zinc Finger Nucleases.” *Nature Biotechnology*. <https://doi.org/10.1038/nbt1125>.
- Potts, Kathryn S., and Teresa V. Bowman. 2017. “Modeling Myeloid Malignancies Using Zebrafish.” *Frontiers in Oncology*. <https://doi.org/10.3389/fonc.2017.00297>.
- Qi, Jing, Sandeep Singh, Wei Kai Hua, Qi Cai, Shi Wei Chao, Ling Li, Hongjun Liu, et al. 2015. “HDAC8 Inhibition Specifically Targets Inv(16) Acute Myeloid Leukemic Stem Cells by Restoring P53 Acetylation.” *Cell Stem Cell* 17 (5): 597–610.  
<https://doi.org/10.1016/j.stem.2015.08.004>.
- Qiu, Xiaoyan, Xiong Xiao, Nan Li, and Yuemin Li. 2017. “Histone Deacetylases Inhibitors (HDACis) as Novel Therapeutic Application in Various Clinical Diseases.” *Progress in Neuro-Psychopharmacology and Biological Psychiatry*.  
<https://doi.org/10.1016/j.pnpbp.2016.09.002>.
- Rescan, P. Y. 2001. “Regulation and Functions of Myogenic Regulatory Factors in Lower Vertebrates.” *Comparative Biochemistry and Physiology - B Biochemistry and Molecular Biology*. [https://doi.org/10.1016/S1096-4959\(01\)00412-2](https://doi.org/10.1016/S1096-4959(01)00412-2).
- Rettig, I., E. Koeneke, F. Trippel, W. C. Mueller, J. Burhenne, A. Kopp-Schneider, J. Fabian, et

- al. 2015. "Selective Inhibition of HDAC8 Decreases Neuroblastoma Growth in Vitro and in Vivo and Enhances Retinoic Acid-Mediated Differentiation." *Cell Death and Disease* 6 (2). <https://doi.org/10.1038/cddis.2015.24>.
- Richter, Jenna, David Traver, and Karl Willert. 2017. "The Role of Wnt Signaling in Hematopoietic Stem Cell Development." *Critical Reviews in Biochemistry and Molecular Biology*. <https://doi.org/10.1080/10409238.2017.1325828>.
- Rosen, Jonathan N., Michael F. Sweeney, and John D. Mably. 2009. "Microinjection of Zebrafish Embryos to Analyze Gene Function." *Journal of Visualized Experiments*. <https://doi.org/10.3791/1115>.
- Rossi, Giuliana, and Graziella Messina. 2014. "Comparative Myogenesis in Teleosts and Mammals." *Cellular and Molecular Life Sciences*. <https://doi.org/10.1007/s00018-014-1604-5>.
- Rudnicki, Michael A., and Bart O. Williams. 2015. "Wnt Signaling in Bone and Muscle." *Bone*. <https://doi.org/10.1016/j.bone.2015.02.009>.
- Saccone, Valentina, Silvia Consalvi, Lorenzo Giordani, Chiara Mozzetta, Iros Barozzi, Martina Sandoña, Tammy Ryan, et al. 2014. "HDAC-Regulated MyomiRs Control BAF60 Variant Exchange and Direct the Functional Phenotype of Fibro-Adipogenic Progenitors in Dystrophic Muscles." *Genes and Development*. <https://doi.org/10.1101/gad.234468.113>.
- Saito, Shigeki, Yan Zhuang, Takayoshi Suzuki, Yosuke Ota, Marjorie E. Bateman, Ala L. Alkhatib, Gilbert F. Morris, and Joseph A. Lasky. 2019. "Hdac8 Inhibition Ameliorates Pulmonary Fibrosis." *American Journal of Physiology - Lung Cellular and Molecular Physiology*. <https://doi.org/10.1152/ajplung.00551.2017>.
- Sander, Jeffry D., Lindsay Cade, Cyd Khayter, Deepak Reyon, Randall T. Peterson, J. Keith Joung, and Jing Ruey J. Yeh. 2011. "Targeted Gene Disruption in Somatic Zebrafish Cells Using Engineered TALENs." *Nature Biotechnology*. <https://doi.org/10.1038/nbt.1934>.
- Schmidt, Rebecca, Uwe Strähle, and Steffen Scholpp. 2013. "Neurogenesis in Zebrafish - from



- Embryo to Adult.” *Neural Development*. <https://doi.org/10.1186/1749-8104-8-3>.
- Schölz, Christian, Brian T. Weinert, Sebastian A. Wagner, Petra Beli, Yasuyuki Miyake, Jun Qi, Lars J. Jensen, et al. 2015. “Acetylation Site Specificities of Lysine Deacetylase Inhibitors in Human Cells.” *Nature Biotechnology*. <https://doi.org/10.1038/nbt.3130>.
- Schuster, Kevin, Bryony Leeke, Michael Meier, Yizhou Wang, Trent Newman, Sean Burgess, and Julia A. Horsfield. 2015. “A Neural Crest Origin for Cohesinopathy Heart Defects.” *Human Molecular Genetics*. <https://doi.org/10.1093/hmg/ddv402>.
- Seitan, Vlad C., Andre J. Faure, Ye Zhan, Rachel Patton McCord, Bryan R. Lajoie, Elizabeth Ing-Simmons, Boris Lenhard, et al. 2013. “Cohesin-Based Chromatin Interactions Enable Regulated Gene Expression within Preexisting Architectural Compartments.” *Genome Research*. <https://doi.org/10.1101/gr.161620.113>.
- Shabbeer, Shabana, Madeleine S.Q. Kortenhorst, Sushant Kachhap, Nathan Galloway, Ron Rodriguez, and Michael A. Carducci. 2007. “Multiple Molecular Pathways Explain the Anti-Proliferative Effect of Valproic Acid on Prostate Cancer Cells in Vitro and in Vivo.” *Prostate*. <https://doi.org/10.1002/pros.20587>.
- Sincennes, Marie-Claude, Caroline E. Brun, and Michael A. Rudnicki. 2016. “Concise Review: Epigenetic Regulation of Myogenesis in Health and Disease.” *STEM CELLS Translational Medicine*. <https://doi.org/10.5966/sctm.2015-0266>.
- Somoza, John R., Robert J. Skene, Bradley A. Katz, Clifford Mol, Joseph D. Ho, Andy J. Jennings, Christine Luong, et al. 2004. “Structural Snapshots of Human HDAC8 Provide Insights into the Class I Histone Deacetylases.” *Structure* 12 (7): 1325–34. <https://doi.org/10.1016/j.str.2004.04.012>.
- Stellabotte, Frank, Betsy Dobbs-McAuliffe, Daniel A. Fernández, Xuesong Feng, and Stephen H. Devoto. 2007. “Dynamic Somite Cell Rearrangements Lead to Distinct Waves of Myotome Growth.” *Development* 134 (7): 1253–57. <https://doi.org/10.1242/dev.000067>.
- Stickney, Heather L., Michael J.F. Barresi, and Stephen H. Devoto. 2000. “Somite Development

- in Zebrafish.” *Developmental Dynamics*. [https://doi.org/10.1002/1097-0177\(2000\)9999:9999<::AID-DVDY1065>3.0.CO;2-A](https://doi.org/10.1002/1097-0177(2000)9999:9999<::AID-DVDY1065>3.0.CO;2-A).
- Subramanian, Srividya, Susan E. Bates, John J. Wright, Igor Espinoza-Delgado, and Richard L. Piekarz. 2010. “Clinical Toxicities of Histone Deacetylase Inhibitors.” *Pharmaceuticals* 3 (9): 2751–67. <https://doi.org/10.3390/ph3092751>.
- Sun, Xiaojuan, Lei Wei, Qian Chen, and Richard M. Terek. 2009. “HDAC4 Represses Vascular Endothelial Growth Factor Expression in Chondrosarcoma by Modulating RUNX2 Activity.” *Journal of Biological Chemistry*. <https://doi.org/10.1074/jbc.M109.019091>.
- Suzuki, Takayoshi, Nobusuke Muto, Masashige Bando, Yukihiro Itoh, Ayako Masaki, Masaki Ri, Yosuke Ota, et al. 2014. “Design, Synthesis, and Biological Activity of NCC149 Derivatives as Histone Deacetylase 8-Selective Inhibitors.” *ChemMedChem*. <https://doi.org/10.1002/cmdc.201300414>.
- Tian, Yuan, Vincent W.S. Wong, Grace L.H. Wong, Weiqin Yang, Hanyong Sun, Jiayun Shen, Joanna H.M. Tong, et al. 2015. “Histone Deacetylase HDAC8 Promotes Insulin Resistance and  $\beta$ -Catenin Activation in NAFLD-Associated Hepatocellular Carcinoma.” *Cancer Research* 75 (22): 4803–16. <https://doi.org/10.1158/0008-5472.CAN-14-3786>.
- Tonkin, Emma T., Tzu Jou Wang, Steven Lisgo, Michael J. Bamshad, and Tom Strachan. 2004. “NIPBL, Encoding a Homolog of Fungal Scc2-Type Sister Chromatid Cohesion Proteins and Fly Nipped-B, Is Mutated in Cornelia de Lange Syndrome.” *Nature Genetics*. <https://doi.org/10.1038/ng1363>.
- Vaidya, Aditya Sudheer, Raghupathi Neelarapu, Antonett Madriaga, He Bai, Emma Mendonca, Hazem Abdelkarim, Richard B. Van Breemen, Sylvie Y. Blond, and Pavel A. Petukhov. 2012. “Novel Histone Deacetylase 8 Ligands without a Zinc Chelating Group: Exploring an ‘upside-down’ Binding Pose.” *Bioorganic and Medicinal Chemistry Letters*. <https://doi.org/10.1016/j.bmcl.2012.08.104>.
- Vanaja, G. R., Hemalatha Golaconda Ramulu, and Arunasree M. Kalle. 2018. “Overexpressed

- HDAC8 in Cervical Cancer Cells Shows Functional Redundancy of Tubulin Deacetylation with HDAC6.” *Cell Communication and Signaling*. <https://doi.org/10.1186/s12964-018-0231-4>.
- Vega, Hugo, Quinten Waisfisz, Miriam Gordillo, Norio Sakai, Itaru Yanagihara, Minoru Yamada, Djoke Van Gosliga, et al. 2005. “Roberts Syndrome Is Caused by Mutations in ESCO2, a Human Homolog of Yeast ECO1 That Is Essential for the Establishment of Sister Chromatid Cohesion.” *Nature Genetics*. <https://doi.org/10.1038/ng1548>.
- Waltregny, David, Wendy Glénisson, Siv Ly Tran, Brian J. North, Eric Verdin, Alain Colige, and Vincent Castronovo. 2005. “Histone Deacetylase HDAC8 Associates with Smooth Muscle A-actin and Is Essential for Smooth Muscle Cell Contractility.” *The FASEB Journal* 19 (8): 966–68. <https://doi.org/10.1096/fj.04-2303fje>.
- Watrin, Erwan, and Jan Michael Peters. 2009. “The Cohesin Complex Is Required for the DNA Damage-Induced G2/M Checkpoint in Mammalian Cells.” *EMBO Journal*. <https://doi.org/10.1038/emboj.2009.202>.
- Wendt, Kerstin S., Keisuke Yoshida, Takehiko Itoh, Masashige Bando, Birgit Koch, Erika Schirghuber, Shuichi Tsutsumi, et al. 2008. “Cohesin Mediates Transcriptional Insulation by CCCTC-Binding Factor.” *Nature*. <https://doi.org/10.1038/nature06634>.
- Wilson, Brian J., Annie M. Tremblay, Geneviève Deblois, Guillaume Sylvain-Drolet, and Vincent Giguère. 2010. “An Acetylation Switch Modulates the Transcriptional Activity of Estrogen-Related Receptor  $\alpha$ .” *Molecular Endocrinology*. <https://doi.org/10.1210/me.2009-0441>.
- Wu, Jian, Chengli Du, Zhen Lv, Chaofeng Ding, Jun Cheng, Haiyang Xie, Lin Zhou, and Shusen Zheng. 2013. “The Up-Regulation of Histone Deacetylase 8 Promotes Proliferation and Inhibits Apoptosis in Hepatocellular Carcinoma.” *Digestive Diseases and Sciences* 58 (12): 3545–53. <https://doi.org/10.1007/s10620-013-2867-7>.
- Wyngaert, Ilse Van Den, Winfred De Vries, Andreas Kremer, Jean Marc Neefs, Peter

- Verhasselt, Walter H.M.L. Luyten, and Stefan U. Kass. 2000. "Cloning and Characterization of Human Histone Deacetylase 8." *FEBS Letters* 478 (1–2): 77–83.  
[https://doi.org/10.1016/S0014-5793\(00\)01813-5](https://doi.org/10.1016/S0014-5793(00)01813-5).
- Yamauchi, Yohei, Heithem Boukari, Indranil Banerjee, Ivo F. Sbalzarini, Peter Horvath, and Ari Helenius. 2011. "Histone Deacetylase 8 Is Required for Centrosome Cohesion and Influenza A Virus Entry." *PLoS Pathogens*. <https://doi.org/10.1371/journal.ppat.1002316>.
- Yeh, Jing Ruey J., Kathleen M. Munson, Yvonne L. Chao, Quinn P. Peterson, Calum A. MacRae, and Randall T. Peterson. 2008. "AML1-ETO Reprograms Hematopoietic Cell Fate by Downregulating Scl Expression." *Development*.  
<https://doi.org/10.1242/dev.008904>.
- Yuen, Kobe C., Baoshan Xu, Ian D. Krantz, and Jennifer L. Gerton. 2016. "NIPBL Controls RNA Biogenesis to Prevent Activation of the Stress Kinase PKR." *Cell Reports*.  
<https://doi.org/10.1016/j.celrep.2015.12.012>.
- Zhao, Chunlong, Jie Zang, Qin'ge Ding, Elizabeth S. Inks, Wenfang Xu, C. James Chou, and Yingjie Zhang. 2018. "Discovery of Meta-Sulfamoyl N-Hydroxybenzamides as HDAC8 Selective Inhibitors." *European Journal of Medicinal Chemistry* 150: 282–91.  
<https://doi.org/10.1016/j.ejmech.2018.03.002>.
- Zwamborn, Ramona A.J., Clara Snijders, Ning An, Alix Thomson, Bart P.F. Rutten, and Laurence de Nijs. 2018. "Wnt Signaling in the Hippocampus in Relation to Neurogenesis, Neuroplasticity, Stress and Epigenetics." In *Progress in Molecular Biology and Translational Science*. <https://doi.org/10.1016/bs.pmbts.2018.04.005>.